University of Bradford eThesis

This thesis is hosted in Bradford Scholars – The University of Bradford Open Access repository. Visit the repository for full metadata or to contact the repository team

INVESTIGATIONS INTO THE ROLES OF POTASSIUM CHANNELS IN HAIR GROWTH

K. ZEMARYALAI

PhD

2010

INVESTIGATIONS INTO THE ROLES OF POTASSIUM CHANNELS IN HAIR GROWTH

Studies confirming the presence of several ATP-sensitive potassium (K^+_{ATP}) channels in hair follicles and exploring their mechanism of action using molecular biological, cell culture, organ culture and proteomic approaches

Khatera ZEMARYALAI
B.Eng. (Hons) in Medical Engineering

Submitted for the degree
of Doctor of Philosophy

Department of Biomedical Sciences

University of Bradford

2010

Abstract

Investigations into the roles of potassium channels in hair growth

Khatera Zemaryalai

Keywords: Hair follicle, human, K_{ATP} channel, minoxidil, animal model, red deer, SUR1, SUR2B, dermal papilla, hair loss

Hair disorders cause significant distress. The main, but limited, treatment for hair loss is minoxidil, an ATP-sensitive potassium (K_{ATP}) channel opener whose mechanism of stimulation is unclear. The regulatory component of K_{ATP} channels has three forms: SUR1, SUR2A and SUR2B which all respond to different molecules. Minoxidil only opens SUR2B channels, though SUR1 and SUR2B are present in human hair follicles.

To expand our understanding, the red deer hair follicle model was used initially. Deer follicles expressed the same K_{ATP} channel genes as human follicles when growing (anagen), but no channels were detected in resting follicles. This reinforces the importance of K_{ATP} channels in active hair growth and the usefulness of the deer model. To assess whether SUR1 K_{ATP} channels are actually involved in human hair growth, the effects of a selective SUR1 channel opener, NNC55-9216, on scalp follicle growth in organ culture was examined. NNC55-9216 stimulated anagen; its effect was augmented by minoxidil. This creates the potential for more effective pharmaceuticals to treat hair loss via SUR1 channels, either alone or in combination with minoxidil.

The dermal papilla plays a crucial regulatory role in hair follicle activity determining the type of hair produced. Minoxidil had no effect on dermal papilla cell proliferation, but altered the profile of proteins produced when assessed by proteomics. Further research into the roles of K_{ATP} channels and greater understanding of the significance of these protein changes should enhance our knowledge of hair biology and help the development of new, improved therapies for hair pathologies.

Contents

Chapter 4. Proteomics and potassium channels 170

List of figures

Chapter 3- The role of SUR1 containing ATP-sensitive potassium channels in human hair growth

Chapter 4- Proteomics and potassium channels

List of tables

List of abbreviations

A	Anagen
ABC	Adenosine triphosphate-binding cassette
ADP	Adenosine diphosphate
AKR1B1	Aldose reductase
AMV	Avian Myeloblastosis Virus
ANOVA	Analysis of variance
APP	Amyloid beta A4 protein precursor
ARPC4	Actin Related Protein 2/3 Complex subunit 4
ATP	Adenosine triphosphate
ATP_i	Intracellular adenosine triphosphate
bp	Base pair
C	Cortex
Ca^{2+}	Calcium ion
CAMPTF	Cellular assembly, maintenance and protein trafficking functions
cDNA	Complementary deoxyribonucleic acid
CHCA	α-cyano-4-hydroxycinnamic acid
CID	Collision induced disassociation
CO1A1	Collagen, type I, alpha 1
CO1A2	Collagen alpha-2(I) chain
COCA1	Collagen, type XII, alpha 1
CPA	Cyproterone acetate
CTS	Connective tissue sheath
CTSK	Cathepsin K precursor
D	Dermis
DEPC	Diethyl pyrocarbonate
DMEM	Dulbecco's modified eagles medium
DMSO	Dimethyl sulphoxide
DNA	Deoxyribonucleic acid
DNAJC3	DNAJ homolog subfamily C member 3
dNTP	Deoxynucleotide triphosphates
DP	Dermal papilla
DS	Dermal sheath
DTT	Dithiothreitol
E	Epidermis
EDTA	Ethylenediaminetetraacetic acid
FCS	Fetal calf serum
FN1	Fibronectin 1
GGH	Gamma-glutamyl hydrolase precursor
GLUT-4	Glucose transporter 4
HB	Hair bulb
HF	Hair fibre
HM	Hair medulla
HMOX1	Heme oxygenase 1
HNRNPUL1	Heterogeneous Nuclear Ribonucleoprotein U-like 1
HPLC	High performance liquid chromatography
IAA	Iodoacetamide

IPA	Ingenuity pathway analysis
IRS	Inner root sheath
K^+	Potassium ion
K^+_{ATP}	Adenosine triphosphate sensitive potassium channel
Kir6.x	Inwardly rectifying potassium channel
LC	Liquid chromatography
M	Matrix
m/z	Mass to charge ratio
MALDI	Matrix assisted laser desorption ionisation
Mg^{2+}	Magnesium ion
MgADP	Mg^{2+} bound adenosine diphosphate
$MgADP_i$	Intracellular Mg^{2+} bound adenosine diphosphate
$MgCl_2$	Magnesium chloride
mRNA	Messenger ribonucleic acid
MS	Mass spectrometry
MTCH1	Mitochondrial carrier homolog 1
N	Negative control
NBD	Nucleotide binding domain
ORS	Outer root sheath
PBS	Phosphate buffered saline
PCOS	Polycystic ovary syndrome
PCR	Polymerase chain reaction
PD	Primer dimer
PLOD1	Procollagen-lysine 1, 2-oxoglutarate 5-dioxygenase 1 protein 3
RNA	Ribonucleic acid
RPMI	Roswell Park Memorial Institute medium
RS	Root sheath
RT-PCR	Reverse transcription-Polymerase chain reaction
S.E.M.	Standard error of the mean
SD	Standard deviation
SDS PAGE	Sodium dodecyl sulfate polyacrylamide gel electrophoresis
SDS	Sodium dodecyl sulfate
SF	Subcutaneous fat
SG	Sebaceous gland
SILAC	Stable isotope labelling with amino acids in cell culture
SM	Skeletal muscle
SNRPG	Small nuclear ribonucleo protein G
SPSS	Statistical analysis programme
SUR	Sulphonylurea receptor
T	Telogen
TAE	Tris-acetate-EDTA
TFA	Trifluoroacetic acid
TGF-β1	Transforming growth factor-β1
THRAP3	Thyroid hormone receptor-associated
TMD	Transmembrane domains
TOF	Time of flight
VEGF	Vascular endothelial growth factor
WASL	Wiskott-Aldrich syndrome-like

This thesis is dedicated to my family, especially to my father and mother with love and gratitude for the endless love and affection bestowed upon me from the first instance till the gift of the present and the assurance of it in the future.

Robert Frost (1874–1963). Mountain Interval. 1920.

The Road Not Taken

TWO roads diverged in a yellow wood,
And sorry I could not travel both
And be one traveller, long I stood
And looked down one as far as I could
To where it bent in the undergrowth;

Then took the other, as just as fair,
And having perhaps the better claim,
Because it was grassy and wanted wear;
Though as for that the passing there
Had worn them really about the same,

And both that morning equally lay
In leaves no step had trodden black.
Oh, I kept the first for another day!
Yet knowing how way leads on to way,
I doubted if I should ever come back.

I shall be telling this with a sigh
Somewhere ages and ages hence:
Two roads diverged in a wood, and I—
I took the one less travelled by,
And that has made all the difference.

Acknowledgements

First and foremost I thank God.

This work would not have been completed without Professor Randall, who not only guided me as a supervisor but also encouraged and challenged me throughout my academic period at Bradford University. I would like to express my deep and sincere gratitude to my second supervisor, Dr. Thornton, for her steadfast support, for always being there to talk through ideas with me and most importantly for being a wonderful friend.

I must say thank you to Dr. Sutton from The Institute of Cancer Therapeutics, for introducing me to the new world of proteomics. Dr. Picksley for instructing me in molecular biological studies and Professor Tobin for his assistance at the initial stages of my work. Thank you to Mr. Rustogi for being my go-to guy and for having the patience and fortitude to answer all those long winded emails. A special thank you also to Dr. Gledhill and Dr. Singh for their unending kindness and support.

Allow me to say thank you to the following people for their friendship, confidence and laughter: Dr. Vafaee, Dr. Shorter, Mr. Al-waleedi, Mr. Khidhir, Ms. Rahman, Dr. Miranda, Mr. Alkhoury, Ms. Wright, Ms. Kurzawa, Dr. Kauser, Dr. Masoodi and Dr Papageorgiou. I could not have wished for better colleagues and your friendship brightened up the most arduous days.

This research would not have been possible without the kind donations of skin samples made by Farjo Medical Centre, of particular acclamation is Dr. Nilofer Farjo who organised all the sample collections. Thank you also to the Round Green Deer Farm, South Yorkshire for making this venture possible.

Thank you to Dr. Fletcher, Dr. Jones, Dr. Graham, Dr. Porter, Prof. Anderson and Dr. Parkin for making me feel so welcomed. I would further like to mention Ms Tucny, Mrs Dove, Mrs Illingworth, Mrs Keeble, Mrs Mountain, Mr Pearson, Mr Reed and Mr Raza. Their effort and assistance throughout my work has been greatly appreciated.

A group of people who played quite a crucial role in the completion of my work were Lawrence Atwell's Charity, BFWG Charitable Foundation and Sir Richard Stapley Educational Trust. Without their financial backing this thesis would not have been possible. Thank you to Mrs Moorhouse, the Financial Support Manager, who went to great lengths in assisting me.

I am deeply indebted to Mr. Ali for his patience, support, strength and thoughtfulness. Thank you for your endurance through those long excruciating hours of research and moments of uncertainty. I would not have had the courage to complete this journey without you.

Last, but not least, I wish to thank my family: my father, Basir Zemaryalai, and my mother, Alia Zemaryalai, for giving me life, for taking chances with their own lives for my sake and that of my siblings; your life has taught me more than any respected educational institute. My siblings (Arezou, Tamana, Tarana, Parniyan and Ariana), and Shafiq jan and Qais jan for supporting me throughout this venture, for listening to my complaints and frustrations, and for having such deep confidence in me. My sister, Parniyan, maintained throughout this long journey that my work should not only be a source of pride for myself, but should also endeavour to serve a greater purpose for the world of research at large.

Chapter 1

Introduction

1.1   The importance of human hair

Hair plays a vital role in a person's appearance, self-image and communication with other people both in social and sexual contexts throughout life. This provides insight into why it is possible for hair growth disorders to be at the root of serious psychological distress (Girman *et al.*, 1998; Gulec *et al.*, 2004).

The hair follicle, which produces the hair, represents an attractive experimental system because of its accessibility, dispensability, and self-renewal capacity. Owing to its complex, but highly organised architecture, this miniorgan can serve as an excellent model for investigating aspects of stem cell biology, cell lineage specification, cell differentiation, patterning processes, and cell–cell interactions (Schlake, 2007). Its exceptional ability to regenerate is of particular interest to cell and developmental biologists, with its fascinating recapitulation of the steps of embryogenesis (Dry, 1926; Kligman, 1959b). Zoologists are interested in the insulation function of the hair follicle that makes it an essential mammalian characteristic for warm bloodedness and crucial for their evolutionary success (Young, 1957), while endocrinologists perceive the hair follicle as a paradoxical tissue, that can simultaneously stimulate hair growth in one area of the body, like the chin, whilst inhibiting growth in another, such as the scalp, causing balding (Randall, 1994; Randall, 2004).

1.2   Functions of Hair

The most important functions of hair for most mammals are insulation for thermoregulation and hair pigmentation for purposes of camouflage (Flux, 1970). Hair can also be specialised as neuroreceptors in certain mammals, (e.g. whiskers)

and provides a protective physical coating from harmful rays like ultraviolet rays and other factors (Oliver and Jahoda, 1989).

For human beings, however, such functions are almost redundant in light of thousands of years of evolution and technological advances (like clothing and hats), despite the display of hair erection in response to cold and seasonal variations in the rate of hair growth (Orentreich, 1969; Randall and Ebling, 1991; Courtois *et al.*, 1996). Consequently hair plays little vital temperature protective role in human beings; its remaining main functions are that of protection and communication.

In children, the chief function is protection; eyebrows and eyelashes prevent the intrusion of foreign bodies into the eyes, and scalp hair is a defensive layer against direct sunlight, cold and physical damage to the head and neck (Goodhart, 1960; Ebling, 1985). The role scalp hair plays in social communication is also rather fascinating, for abundance of strong healthy hair indicates good health to others, whilst brittle and sparse growth of hair, which can develop through starvation or disease is an indicator of poor health (Bradfield, 1971). Human hair is also a signalling characteristic in sexual communication. The development of pubic and axillary hair in males and females is an indicator of the onset of puberty (Reynolds, 1951; Marshall and Tanner, 1969; Marshall and Tanner, 1970). Growth of hair on the face and chest, upper pubic triangle and limbs are all an indicative exhibition of sexual maturity in men.

Taking into account the noteworthy communication roles hair performs, it is understandable how a defect of its natural form can stimulate serious psychological consequences, and have a negative impact on the quality of life (Girman *et al.*, 1998; Gulec *et al.*, 2004). Examples of this include hirsutism, which

is excessive male pattern hair growth in women and alopecia areata, an autoimmune disease of hair loss, affecting both sexes at all ages (Randall, 2001). Androgenetic alopecia, common balding or male pattern hair loss (Randall, 2005), also causes negative consequences, even amongst sufferers who have chosen not to seek medical consultation (Girman *et al.*, 1998), these are also severe in those who suffer from hair loss as a side effect of chemotherapy. Thus, an understanding of the mechanisms controlling hair growth, leading to control of these conditions is of great interest worldwide.

1.3   Structure of the hair and its follicle

Hairs are greatly variable in colour, length, diameter and cross-sectional shape. Following birth, hairs can be classified into two main types, vellus hairs and terminal hairs. Vellus hairs are defined as small, fine, unpigmented hairs located in regions of the body described as 'hairless', e.g. the cheek (Blume *et al.*, 1991; Randall, 1994). In contrast, terminal hairs are longer, thicker, and deeply pigmented, located in regions such as the scalp, eyebrows and eyelashes (Abell, 1988; Randall, 1994).

Hairs outside the skin are flexible shafts of dead, fully keratinised epithelial cells which are produced by follicles and taper to a point. Hair follicles are continuous with the epidermis and cylindrical epithelial layers grow to various depths downwards into the dermis and in some species project into the subcutaneous adipose layer. The follicle enlarges at the base into the hair bulb surrounding the mesenchyme-derived dermal papilla (Auber, 1952; Montagna and Van Scott, 1958; Oliver and Jahoda, 1989).

The hair and its follicle both unveil a complex structure consisting of various compartments (Figure 1.1). The hair itself consists of three distinct cell lineages, the cuticle, cortex, and medulla. The cortex is composed of bundles of keratin filaments. The medulla, which is only present in terminal hairs, can be both continuous and discontinuous. Hair fibres with a continuous medulla, such as eyelashes, are stiff in character (Forslind, 2000).

The hair follicle is made up of several layers that act to shape the emerging hair. Surrounding the hair fibre is the inner root sheath which is composed of three distinct cell lineages, the Henle and Huxley layers as well as the cuticle, the latter of which is in direct contact with the cuticle of the hair. The inner root sheath surrounds the hair fibre from the bulb up to the level of the sebaceous gland allowing the hair fibre elasticity (Forslind, 2000). The cuticle cells of the hair fibre interconnect/interdigitate with the cuticle cells of the inner root sheath like a zip, consequently fastening the hair fibre to the follicle. The outer root sheath surrounds the inner sheath, and is continuous with the epithelial surface. The outer root sheath is surrounded by the vitreous membrane outside which lies the connective/dermal tissue sheath, which surrounds the whole of the follicle.

Figure 1.1 The structure of the hair follicle

An isometric view of the lower part of a human hair follicle cut away to show component parts (drawn by Richard J. Dew). Reproduced from Randall (1994), with the author's permission.
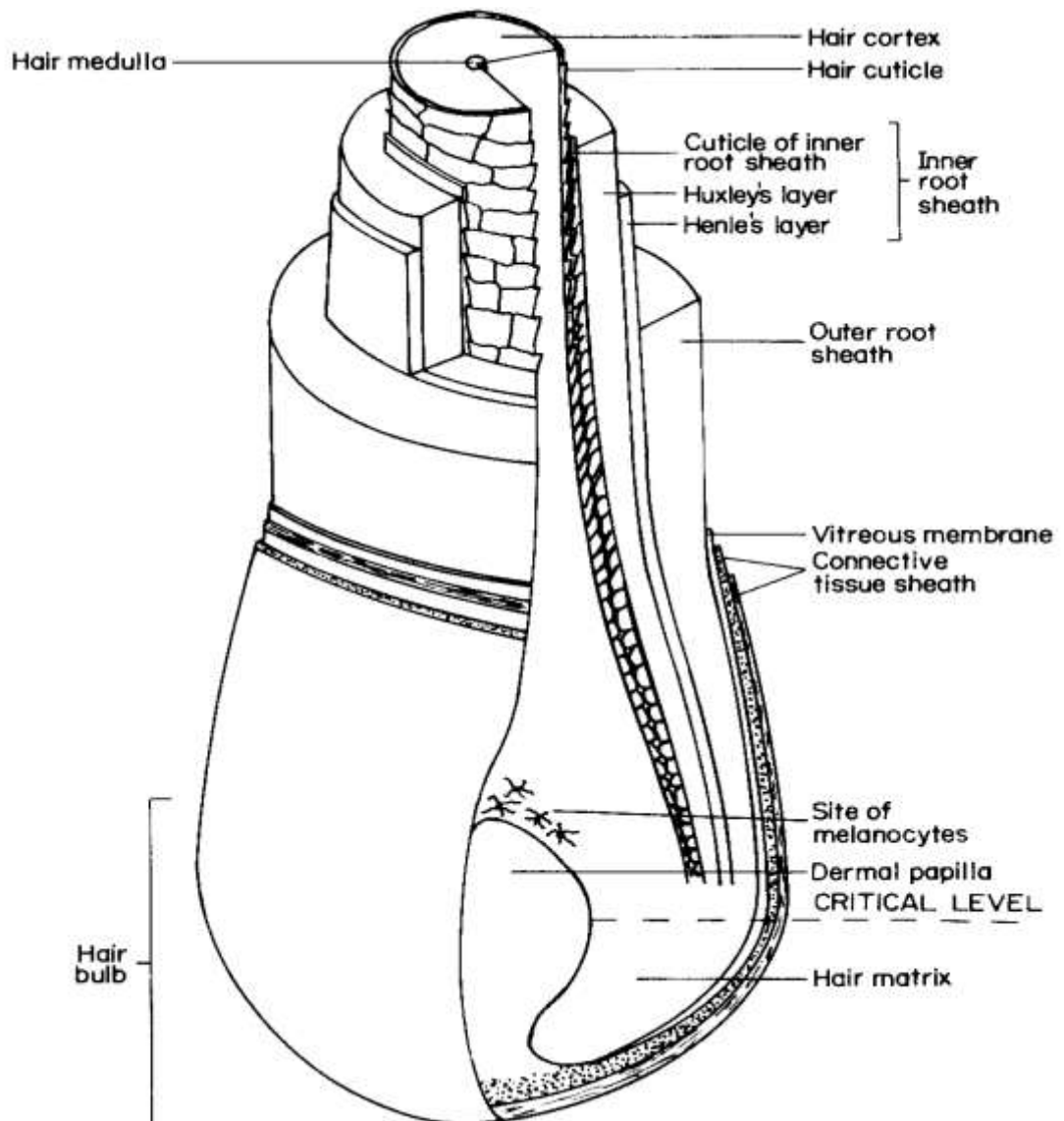
The mesenchyme-derived dermal papilla plays an important role throughout hair follicle development and its life cycle. It contains specialised fibroblast cells called dermal papilla cells and extracellular matrix, within which mucopolysaccharides and basement membrane proteins are present (Couchman, 1986; Couchman *et al.*, 1990; Messenger *et al.*, 1991) as well as blood vessels and nerves. The number of dermal papilla cells is proportional to the size of the hair follicle, and therefore the hair fibre produced (Van Scott and Ekel, 1958; Ibrahim and Wright, 1982; Elliott *et al.*, 1999). The hair matrix almost completely encloses the dermal papilla, with the exception of a gap at the base of the follicle bulb, which permits the entrance of blood vessels and nerves into the papilla. A trilaminar basement membrane efficiently separates the epithelial matrix from the dermal papilla (Nutbrown and Randall, 1995). The hair matrix gives rise to all epithelial compartments except the outer root sheath (Schlake, 2007).

The critical level is a line that can be drawn through the widest part of the follicular bulb, separating the germinative centre of the follicle below from the differentiating cells (upper bulb) of the hair and root sheath above (Auber, 1952). Hair production entails speedy cell division of the epithelial keratinocytes in the hair matrix. Below the critical level the matrix cells are mitotically active and undifferentiated, whilst above the critical level the rate of mitotic activity is decelerated and cells become differentiated into either the inner root sheath or hair fibre cells. The movement of cells from the bulb into the more narrowed part of the follicle elongates the cells, and keratinisation takes place. This process continues as the cells migrate through the follicle, ultimately becoming fully keratinised by the time they reach the surface of the skin.

The hair follicle is often referred to as the pilosebaceous unit, due to its association with the sebaceous gland. Sebaceous glands emit a waxy secretion into the follicle via the sebaceous duct, inducing a waterproof coating over the hair fibre. In some follicles, such as those found in axillae and genital regions, apocrine sweat glands are also present above the sebaceous ducts (Hurley, 2001). The apocrine glands discharge into the superior portion of the hair follicle and are a possible origin of pheromones (Spielman *et al.*, 1995). The follicle is also associated with the arrector pili muscle, a smooth muscle bundle that attaches to the bulge region of the follicle and extends to its superior attachment in the upper dermis. This muscle allows adjustment of the hair for thermoregulation, for example erection of hairs on skin in response to cold temperatures.

1.4 The hair growth cycle

The hair follicle has a unique cyclic regeneration phenomenon, summarized in figure 1.2, originally described fully for the mouse by Dry (1926) and later for human beings by Kilgman (1959). Starting with the growth phase, anagen, the follicle and its shaft pass through the transitional phase, catagen, the resting phase, telogen, and finally exogen (Stenn *et al.*, 1998; Milner *et al.*, 2002; Stenn, 2005; Higgins *et al.,* 2009). All hair follicles undergo this cycle, although the duration of the cycle, individual phases, and length of individual shafts vary significantly from site to site (Trotter, 1924; Saitoh *et al.*, 1970) as well as varying between species (Messenger, 1993).

Figure 1.2 The hair growth cycle

Stages of the hair growth cycle. Reproduced from Randall (1994), with the author's permission.

| Growing phase | Involution phase | Resting phase | Regrowing phase | New growing phase |
| ANAGEN | CATAGEN | TELOGEN | EARLY MID ANAGEN | ANAGEN |
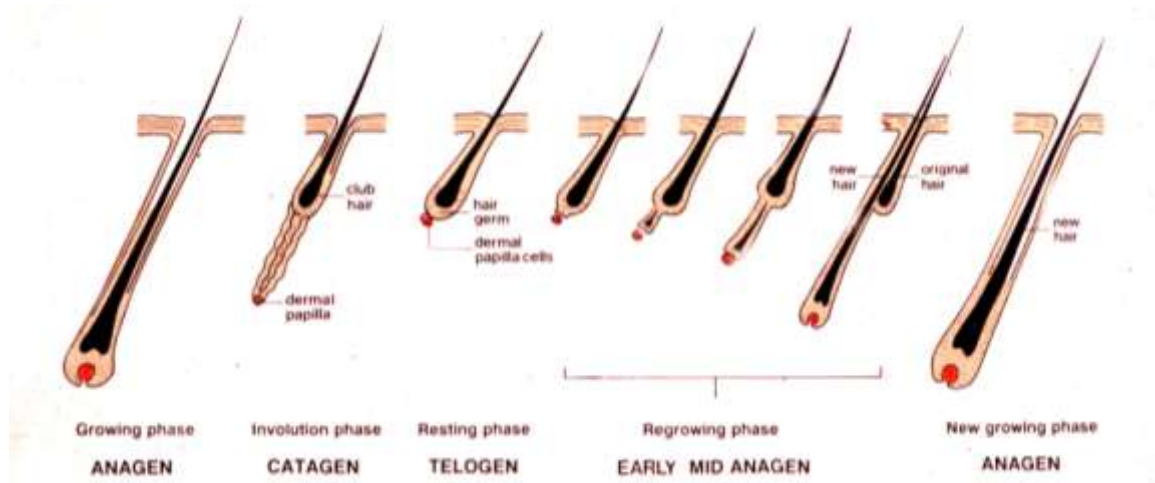
During the anagen phase, the matrix keratinocytes in the hair follicle bulb proliferate rapidly; conversely at the end of anagen, matrix keratinocytes abruptly cease proliferating and pigmentation, and become fully keratinised producing a hair with a "club" shaped, unpigmented end, and the anagen follicle starts the transition into the catagen phase. During the catagen phase the hair stops growing and there is extensive apoptosis, resulting in regression of the lower follicle and the dermal papilla. The hair moves upwards and comes to rest at the base of the sebaceous gland, commonly referred to as the bulge. This phase lasts for about 2-3 weeks in human scalp and leads to the telogen phase, the resting phase of a hair follicle. (Kligman, 1959a). At the end of catagen, if the dermal papilla fails to reach the bulge level, the site of the follicle stem cells, during catagen, the cycle stops and the hair is lost (Paus and Cotsarelis, 1999). A telogen hair has a club-shaped

proximal end, which is surrounded by a thick epithelial sac, lasting around approximately 3 months on the human scalp before re-entering the anagen phase (Kligman, 1959a).

The anagen phase has been divided into six subphases (Chase *et al.*, 1951; Chase, 1954; Paus and Cotsarelis, 1999). Stages I–V of anagen are the developmental stages at which point the follicle regenerates, and the length of these subphases does not differ substantially between follicles from different regions, unlike the last subphase, anagen VI the duration of which dictates the shaft length, (Trotter, 1924; Saitoh *et al.*, 1970).

The initial subphase (I) commences with the activation of the dermal papilla and the onset of mitotic activity in the epithelial cells beneath the bulge region, known as the germ. Following this the germ instigates a downward growth (subphase II), enveloping the dermal papilla and the matrix cells begin differentiation. Subphase (III) follows with the bulb matrix cells showing a differentiation into most follicular components, until the follicle reaches its deepest level. Subsequently the matrix melanocytes activate, and the hair fibre reaches the level of the sebaceous gland; subphase (IV). Upward growth continues until subphase (V) the new shaft emerges from the skin, this may dislodge the telogen hair. The new hair shaft, ultimately at stage VI, proceeds to grow until the follicle re-enters catagen. The length of the hair is proportional to the length of anagen and it differs depending on the location of the follicle (Kligman, 1959a; Saitoh *et al.*, 1970; Paus and Cotsarelis, 1999). The last phase within the hair growth cycle is exogen, an independent and active shedding phase, during which the original hair is enzymatically released and falls out (Stenn *et al.*, 1998; Stenn and Paus, 2001; Milner *et al.*, 2002; Stenn, 2005; Higgins *et al.,* 2009).

1.5   Embryogenesis of the hair follicle

The embryonic development of the hair follicle is initiated as a result of an interaction between epithelial and mesenchymal tissues. The initial event in embryonic development is the formation of the pre-germ that begins as a result of localized thickening of the basal layer of the epidermis and an aggregation of mesenchymal cells at the junction between the epidermis and dermis (Pinkus, 1958; Holbrook and Minami, 1991) (See figure 1.3). Following this epidermal placode formation, epidermal and mesenchymal cells then continue development into the dermis forming the hair germ. The hair germ then elongates and grows deeper into the dermis to form the hair peg.

The proximal end of the peg flattens, forming an elongated concave-shaped structure (bulbous hair peg), which eventually will enclose the mesenchymal cells to form the dermal papilla. The epidermal cells surrounding the dermal papilla form the matrix, which differentiates to form the inner root sheath and hair fibre. The epithelial cells connecting the matrix cells to the interfollicular epidermis form the outer root sheath and mesenchymal cells alongside form a connective/dermal tissue sheath. In addition, two epithelial protrusions develop on the posterior side of the follicle. The uppermost epithelial protrusion will develop into the sebaceous gland and the lower protrusion forms the bulge, at this precise site the arrector pili muscle attaches to the follicle. At some regions of the body (such as the axilla and groin) a third protrusion can develop above the sebaceous gland, developing into the apocrine gland.

The middle cells of the bulbous hair peg degenerate to form the hair canal, whilst the dermal papilla is completely surrounded by epithelial cells. At this stage, the hair follicle components will continue to proliferate, increasing hair fibre

length, until the hair emerges from the epidermis. The follicle will maintain its elongation into the dermis until it reaches its full depth within the skin. Most of the stages identified above are repeated in the early stages of anagen, with the exception of the starting point occurring at the base of the telogen hair follicle rather the actual epidermis (Holbrook and Minami, 1991; Muller *et al.*, 1991; Hardy, 1992; Randall, 1994; Paus *et al.*, 1999; Wu-Kuo and Chuong, 2000).

Figure 1.3 Embryology of the hair follicle

The different stages of hair follicle embryogenesis. Reproduced from Randall (1994), with the author's permission.
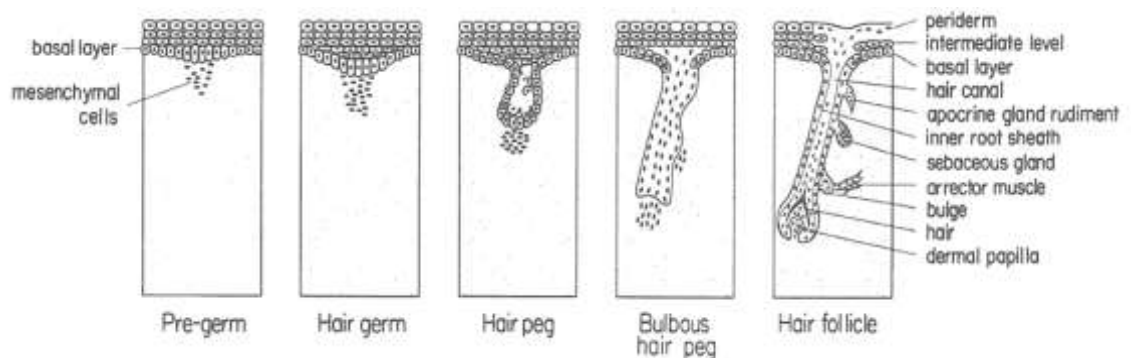
1.6 Hair disorders

1.6.1 *Hirsutism*

Hirsutism refers to excessive and increased hair growth in women, in areas where there is typically only fine hair or no hair at all, for example above the lip, on the chin, chest, and abdomen (Figure 1.4). This growth may be triggered by excess androgen production (male sex hormones). Androgen modifies vellus follicles producing fine hairs to form thick, pigmented hairs. Several different conditions can lead to hirsutism. The two most common causes of hirsutism are polycystic ovary syndrome (PCOS) and idiopathic hirsutism (Bardin and Lipsett, 1967; Franks, 1989; Martin *et al.*, 2008).

Both cosmetic and pharmacological approaches can be taken to treat hirsutism. The pharmacological approach includes antiandrogen drugs, e.g. cyproterone acetate (CPA), which inhibits hirsutism (Hammerstein, 1987) and finasteride which inhibits the enzyme 5α- reductase type 2 preventing androgen action (Randall, 2008). A cosmetic approach employs various methods which physically remove or lighten excess hair to make it less conspicuous; such treatments include shaving, chemical depilation, waxing, and bleaching, electrolysis and laser hair removal.

1.6.2 *Androgenetic alopecia*

Androgenetic alopecia is a common form of hair loss in the region of the scalp for both men and women (Figure 1.4) (Ludwig, 1977). In men, this condition is also known as male-pattern baldness (Hamilton, 1942). This form of disorder entails the gradual transformation of thick, pigmented hairs to thinner, shorter, non pigmented vellus hairs, in both men and women. As the disorder progresses,

the anagen phase shortens with the telogen phase remaining constant. The loss occurs in a precise, distinctive pattern on the scalp, first described by Hamilton (Figure 1.5) (Hamilton, 1951; Norwood, 1975; Randall, 2005). Hamilton highlighted the severity of the hair loss, grading it from prepubertal scalp (type I) through to the progressive recession of the bitemporal hairline and thinning on the vertex (type VII). To improve the grading of the middle balding types, Norwood modified this classification system (Figure 1.4) (Norwood, 1975). Though it is possible for male pattern balding to occur in women, a different pattern of hair loss is more common, described and graded by Ludwig (Ludwig, 1977) as the gradual hair loss in the crown, with preservation of the frontal hair line (Sinclair *et al.*, 1999; Price, 2003).

Figure 1.4 Patterns of human hair growth

Modified from Randall (2000), with the author's permission

Normal child

Normal woman
body hair may increase after menopause

Normal man
body hair increases with age

Normal man with inherited male pattern baldness
as normal male plus gradual decrease in scalp hair

Hirsutism
Male hair distribution

Female androgenetic alopecia
gradual thinning on vertex - retention of frontal hairline
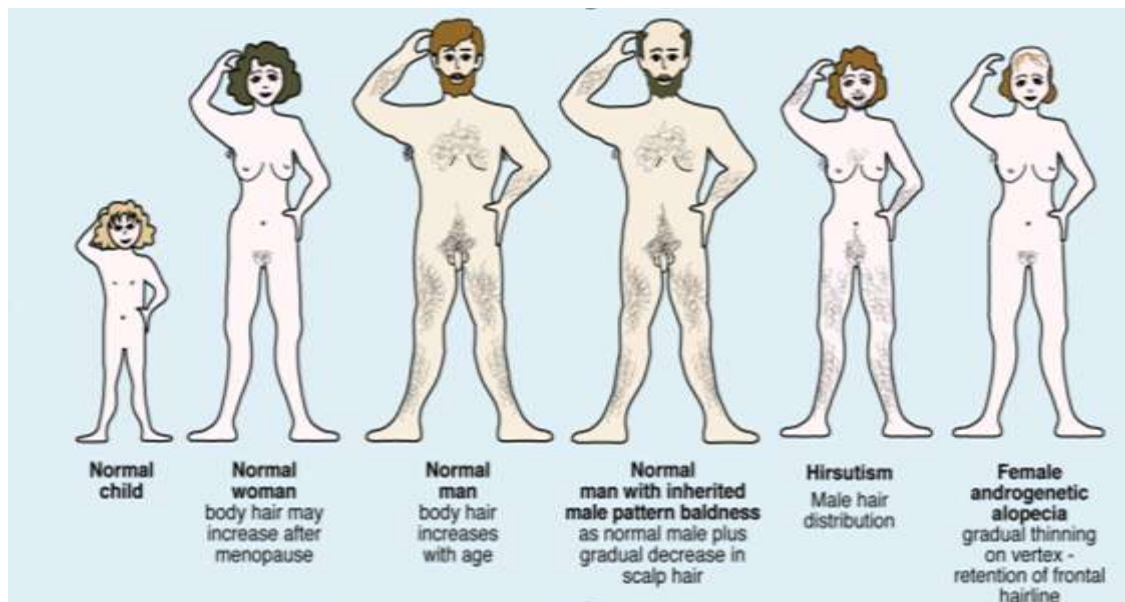
Figure 1.5 The pattern of hair loss in androgenetic alopecia in men

The Hamilton scale (as modified by Norwood) is used to classify the type and extent of common baldness in men.   Reproduced from Randall (2000), with permission.
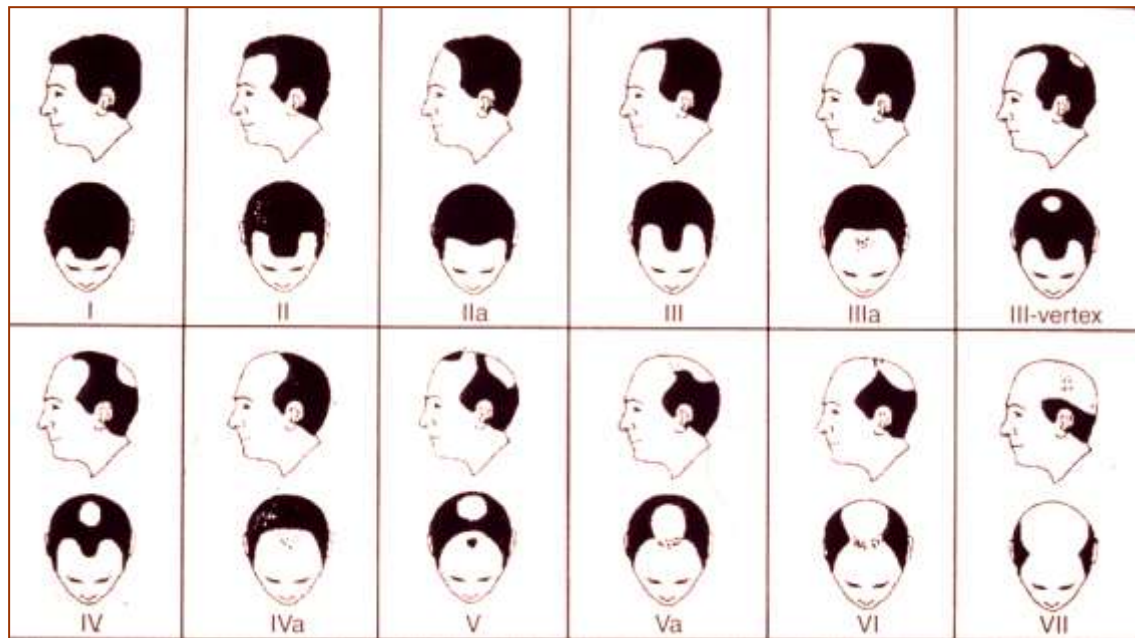
Androgens and genetic disposition are the two main factors in the pathogenesis of androgenetic alopecia.   Research evidence supports the involvement of local androgens in the development of androgenetic alopecia. For example androgenetic alopecia does not occur in men castrated prior to puberty, and for men castrated after puberty baldness ceases to progress (Hamilton, 1942; Hamilton, 1958; Hamilton, 1960).   Although a number of genes have been investigated for an association with androgenetic alopecia, no specific gene or set of genes have been identified (Randall, 2005).

A range of treatments for androgenetic alopecia can be undertaken, such as wigs and hairpieces, surgery, hormonal and non-hormonal therapy. The surgical treatment involves the relocation of follicles from the non-balding areas to the sites that are bald, relying on the intrinsic responses of hair follicles to androgens

(Orentreich and Durr, 1982). Though this treatment endures for a long time, it is expensive and painful; furthermore it may require further surgery as the hair loss develops around the transplanted region.   Hormonal treatments include antiandrogens and 5α-reductase inhibitors. Antiandrogen treatment blocks the androgen binding to the androgen receptor, which has impractical effects on male masculinity.   5α-reductase inhibitors, however, such as finasteride, block the conversion of testosterone to 5α-dihydrotestosterone, which has been found to both slow down gradual hair loss, and promote hair growth in men under 42 years of age with stage II to V hair loss (Figure 1.4) (Kaufman *et al.*, 1998). 5α-reductase inhibitors remain as the main hormonal treatment for hair loss in men, however similar to all hormonal treatments, it is subject to continuation.

The most commonly used non-hormonal treatment is minoxidil, which is a widely used topical treatment for hair loss in men and women. It belongs to a group of drugs known as potassium (K^+) channel openers. Initially developed as a treatment for hypertension, it was however, discovered to have the interesting side effect of hypertrichosis (excessive hair growth) (Shapiro and Price, 1998; Dawber, 2000), making it unacceptable to patients and it was remarketed as a hair loss treatment. Nevertheless it is unclear how minoxidil functions to stimulate hair growth.

1.6.3 *Alopecia areata*

Alopecia areata is a form of hair loss, characterised by loss of hair in single or multiple localised patches, typically on the scalp, intermittently in the eyebrows, beard, or other hair-bearing areas of the body. There are a range of hair loss patterns resulting from alopecia areata; most commonly a circular patch pattern transpires (Madani and Shapiro, 2000; Papadopoulos *et al.*, 2000). There are two

more extensive forms of alopecia areata, alopecia universalis, a more generalised pattern of total body hair loss, and alopecia totalis, which although less common, can spread to the entire scalp (Hordinsky, 2003). Males and females are affected alike, and it occurs in all ethnic groups (Muller and Winkelmann, 1963; Sharma *et al.*, 1996; Epstein, 2001).

The exact cause of alopecia areata is still unknown, though it is generally believed to be an autoimmune disease (Randall, 2001), but several factors have been recognised in its pathogenesis, e.g., genetic, neurological factors, possible emotional stress and infectious agents (Madani and Shapiro, 2000). A range of treatments have been undertaken for the treatment of alopecia areata, including contact sensitizers, immunomodulators and biologic response modifiers (Hoffmann *et al.*, 1996; Gilhar *et al.*, 1998).

There is no definitive treatment available for alopecia areata as yet (Epstein, 2001), although a series of therapies are available, which include immune enhancers, immune inhibitors, non-specific irritants and minoxidil (Messenger and Simpson, 1997; Ross and Shapiro, 2005). Although these treatments have all had varying success rates, they have also all had negative side effects, and there is no fully satisfactory treatment available for alopecia areata.

The lack of a precise treatment for hair loss is mainly due to insufficient knowledge of normal hair follicles and the mechanism of action of potassium (K^+) channel openers and blockers. Thus this thesis aims to enhance knowledge of this field by investigating further into the roles of potassium channels in hair growth.

1.7   Adenosine triphosphate (ATP) – sensitive potassium channels (K$^+_{ATP}$)

K$^+_{ATP}$ channels are formed by two distinct protein subunits: a sulfonylurea receptor (SUR) and an inwardly rectifying potassium channel subunit (Kir6.x). They were first discovered in cardiac myocytes (Noma, 1983), and subsequently in various other tissues including the pancreatic β-cells (Ashcroft *et al.*, 1984; Cook and Hales, 1984; Rorsman and Trube, 1985), skeletal muscle (Spruce *et al.*, 1985), neurones (Ashford *et al.*, 1988; Bernardi *et al.*, 1988), arterial smooth muscle (Standen *et al.*, 1989), kidney (Wang and Giebisch, 1991) and in the inner mitochondrial membrane (Inoue *et al.*, 1991) and secretory granules (Thevenod *et al.*, 1992). The SUR protein acts as a regulatory subunit, which is the site of interaction for a majority of drugs, whilst Kir6.x subunits form the channel pore, through which ions pass (Nichols, 2006). The expression of both sub-units is necessary to form a functional channel (Inagaki *et al.*, 1995a; Gribble *et al.*, 1997; Yamada *et al.*, 1997).

K$^+_{ATP}$ channels are regulated physiologically by the levels of intracellular nucleotides and pharmacologically by K$^+_{ATP}$ channel openers and blockers such as sulphotransferase (Meisheri *et al.*, 1993). Intracellular nucleotides create polar reactions in K$^+_{ATP}$ channels. Intracellular ATP (ATPi) inhibits the channels, whilst intracellular Mg^{+2} bound adenosine diphosphate (MgADPi) activates the channel (Cook and Hales, 1984; Ashcroft and Rorsman, 1989; Gier *et al.*, 2009; Girard, 2009).

The function of K$^+_{ATP}$ channels is best characterised in the insulin-secreting pancreatic β cells (Cook *et al.*, 1988; Ashcroft and Rorsman, 1989), where they play a key role in insulin secretion. At low plasma glucose levels (2-3mM), in the pancreatic β-cells, the K$^+_{ATP}$ channels are open, therefore allowing K$^+$ to leave the

cell. This action hyperpolarises the voltage-gated calcium (Ca^{2+}) channels, which remain closed, thereby setting the resting membrane potential to approximately -70 mV, and effectively reducing excitability and insulin secretion. In contrast a rise in the plasma glucose level (5-7 mM) increases the intracellular ATP concentration due to the metabolism, closing the K^+_{ATP} channels. This closure depolarises the plasma membrane, leading to the opening of voltage-gated Ca^{2+} channels and the subsequent Ca^{2+} influx results in insulin secretion (Seino, 1999) (Figure 1.6).

Figure 1.6 Illustration of insulin secretion in the plasma membrane of pancreas cells

K^+_{ATP} channel activity modulates insulin secretion in pancreatic beta cells. Glucose-dependent K^+_{ATP} channel closure results in membrane depolarisation and insulin release. Adapted from (Gribble and Reimann, 2003), (constructed by K. Zemaryalai).
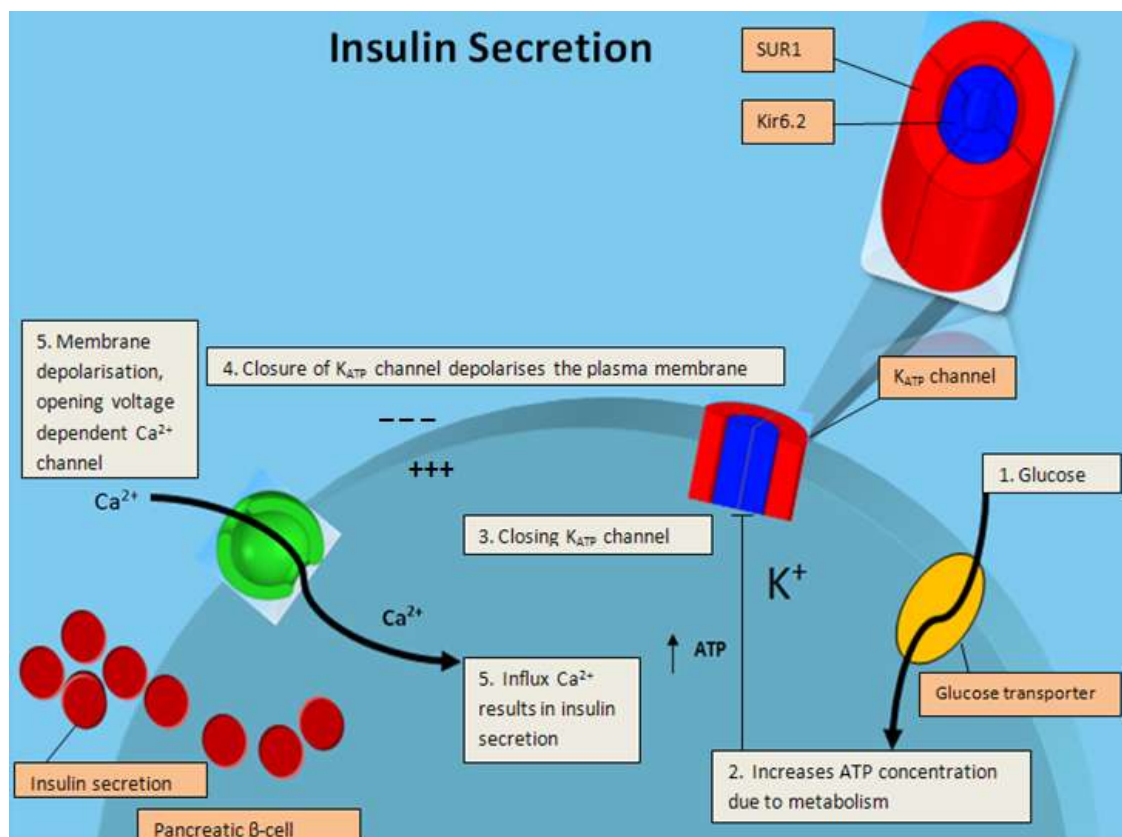
1.7.1 Potassium channel structure

Structurally, K^+_{ATP} channels have been shown to comprise hetero-octameric complexes of four pore-forming (Kir6.x) and four regulatory sulphonylurea receptor (SUR) subunits (Figure 1.7) (Clement *et al.*, 1997; Inagaki *et al.*, 1997).

Figure 1.7 Structure of the K^+_{ATP} channels

K^+_{ATP} channels are composed of an ATP-binding cassette protein family, sulfonylurea receptor **SUR** and an inward rectifying K^+ channel subunit, **Kir6.x**. Note the presence of two intracellular nucleotide binding domains (NBD), consisting of Walker A and B motifs joined by a conserved linker sequence in the SUR protein. Adapted from (Davies *et al.*, 2005; Shorter *et al.*, 2008).
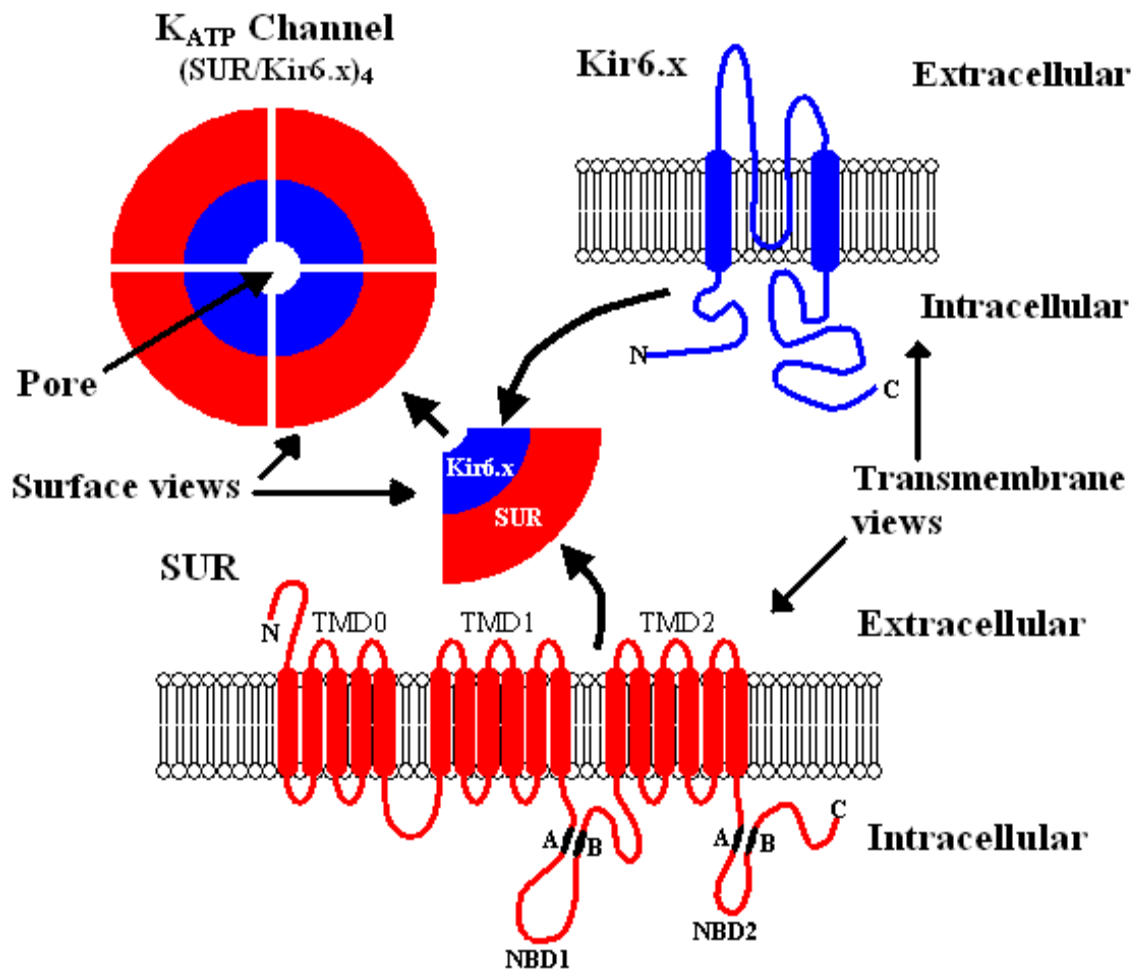
1.7.1.1 SUR proteins

The sulfonylurea receptor (SUR) is an ATP-binding cassette (ABC) protein comprising one, five-helix transmembrane domain (TMD0) and two, six-helix transmembrane domains (TMD1 and TMD2), positioned at the N terminal and is the key regulatory subunit of ATP-sensitive K^+ channels (Inagaki *et al.*, 1995a) as indicated in Figure 1.7. In addition the SUR holds two intracellular loops, nucleotide binding domains 1 and 2 (NBD1 and NBD2); NBD1 connects TMD1 and TMD2, NBD2 follows TMD2 (Nichols, 2006). The NBDs are comprised of two nucleotide binding motifs (Walker A and B concensus motifs) which are involved in channel regulation by ATP and MgADP (Jahangir and Terzic, 2005).

There are three forms of the sulfonylurea receptor (Aguilar-Bryan *et al.*, 1995; Gribble and Reimann, 2003), SUR1 coded by the ABCC8 gene mapped on chromosome 11p15.1 (Inagaki *et al.*, 1995a) which includes a high affinity sulphonylurea receptor (Aguilar-Bryan *et al.*, 1995); SUR2A and SUR2B which are splice variants arising from a single ABCC9 gene mapped to chromosome 12p12.1 (Chutkow *et al.*, 1996) and include a lower-affinity sulphonylurea receptor (Inagaki *et al.*, 1996). The SUR1 gene is made up of 39 exons in its open reading frame and the SUR2 gene of 38 exons, the lower exon number consequent from the removal of exon 18 from the SUR1 gene (Aguilar-Bryan *et al.*, 1998). Alternate splicing at exon 38 in the SUR2 gene, results in SUR2A containing exon 38A and SUR2B; containing exon 38B; these variants vary by 42 amino acids at the C-terminal (Isomoto *et al.*, 1996).

1.7.1.2 Kir6.x proteins

The pore-forming Kir6.x proteins are members of the inwardly rectifying K+ channel family, Kir. Crystallisation of the bacterial K$^+$ channel revealed its structure (Doyle *et al.*, 1998). Two subunits of Kir6.x proteins that have already been identified are Kir6.1 (also known as u-K$_{ATP}$-1) and Kir6.2 (also known as BIR/K$^+_{ATP}$), which have approximately 70% homology with each other, and 40-50% with other Kir channels (Inagaki *et al.*, 1995a). These proteins are responsible for the pore formation in K$^+_{ATP}$ channels, and consist of 2 transmembrane domains, M1 and M2, that confer channel sensitivity to ATP and ADP, and other cell metabolites (Baukrowitz and Fakler, 2000; Schulze *et al.*, 2003). Forming the narrow section of the pore, is an extracellular loop that effectively connects the two domains, and controls ion selectivity (Nichols, 2006). This model is accepted in both eukaryotic and prokaryotic Kir structures (Antcliff *et al.*, 2005; Haider *et al.*, 2005). The human Kir6.1 gene KCNJ8, is composed of 3 exons and is based on the chromosome 12p11.23 (Inagaki *et al.*, 1995b); and the intronless Kir6.2 gene KCNJ11, composed of 1 exon, is situated on the short arm of chromosome 11 at 11p15.1 (Inagaki *et al.*, 1995a).

1.8   Different combinations of K$^+_{ATP}$ channel subunits generates channel diversity

Different combinations of K$^+_{ATP}$ channel subunits (SUR1, SUR2A, or SUR2B and Kir6.1 or Kir6.2) form channels in different tissues with diverse electrophysiological, nucleotide and pharmacological properties (Table 1.1) (Seino and Miki, 2003). Interaction between K$^+_{ATP}$ channel openers and the SUR subunit

enables K^+ ions to exit the cell, instigating hyper-polarisation of the plasma membrane, and as a consequence reduces electrical activity (Ashcroft and Gribble, 2000).

Table 1.1 K^+_{ATP} channel combinations and their tissue distributions

Table modified from Seino and Miki (2003).

Subunit Combination	Location	Reference
SUR1/Kir6.1	Not physiologically relevant	(Babenko *et al.*, 1998a)
SUR1/ Kir6.2	Pancreatic β cells Brain	(Inagaki *et al.*, 1995b) (Sakura *et al.*, 1995) (Babenko *et al.*, 1998a)
SUR2A /Kir6.1	No cellular activity	(Babenko *et al.*, 1998a)
SUR2A /Kir6.2	Cardiac muscle Skeletal muscle	(Inagaki *et al.*, 1996) (Babenko *et al.*, 1998a)
SUR2B/Kir6.1	Vascular smooth muscle	(Yamada *et al.*, 1997)
SUR2B/Kir6.2	Non-vascular smooth muscle	(Isomoto *et al.*, 1996)

K^+_{ATP} channel openers are chemically diverse agents, classified by their ability to directly open ATP sensitive K^+_{ATP} channels (Lawson, 2000). Several of these agents have been identified to cause hair growth as a side effect in human beings, including diazoxide, minoxidil and pinacidil (Koblenzer and Baker, 1968; Goldberg, 1988). The sensitivity of different SUR subunits to K^+_{ATP} channel

openers varies. For example SUR1/Kir6.2 channels expressed in pancreatic β cells are significantly sensitive to diazoxide, to some extent sensitive to pinacidil, and not at all responsive to cromakalin and nicorandil (Trube *et al.*, 1986; Ashcroft and Rorsman, 1989; Ashcroft and Ashcroft, 1990; Seino and Miki, 2003). On the other hand, SUR2A/Kir6.2 channels, expressed in cardiac and skeletal muscles, are sensitive to pinacidil and cromakalin, and only slightly to diazoxide. SUR2A/Kir6.2 channels can be sensitive to diazoxide, when in the presence of MgADP (D'Hahan *et al.*, 1999b), while SUR2B/Kir6.2 channels expressed in non-vascular smooth muscle are sensitive to all the K^+_{ATP} channel openers named above (Inagaki *et al.*, 1995a; Isomoto *et al.*, 1996; Babenko *et al.*, 1998; Gribble *et al.*, 1998; D'Hahan *et al.*, 1999a).

The sensitivity to K^+_{ATP} channel inhibitors is similarly tissue specific. For example SUR1/Kir6.2 channels found in pancreatic β cells are inhibited by lower concentrations of tolbutamide than channels in cardiac and smooth muscle (Ashcroft and Ashcroft, 1990; Faivre and Findlay, 1990; Venkatesh *et al.*, 1991; Allard and Lazdunski, 1993; Zhang and Bolton, 1996; Quayle *et al.*, 1997). All of these varying sensitivities to K^+_{ATP} channel openers and blockers support the model that the K^+_{ATP} channel opener binding site is situated on the SUR subunit (Nichols, 2006).

1.9   Minoxidil stimulates hair growth

Minoxidil is classified as a K^+_{ATP} channel opener, alongside diazoxide, chromakalim, nicorandil and pinacidil (Koblenzer and Baker, 1968; Goldberg, 1988). Different K^+_{ATP} channel openers have varying effects on the prevalence and

severity of hypertrichosis. For example following oral minoxidil treatment 60-80% of adults reported hypertrichosis (Burton and Marshall, 1979; Zins, 1988), whereas, pinacidil treatment caused hypertrichosis in 13% of females and only 2% of males (Goldberg, 1988). During diazoxide treatment most children reported increased hair growth, however only an insignificant 1% of adults reported hypertrichosis (Koblenzer and Baker, 1968; Burton *et al.*, 1975).

The majority of K^+_{ATP} channel openers were initially developed for treatment of hypertension and hypoglycaemia. Minoxidil was one of the first to be introduced into the market, in the early 1970s, in the form of an oral treatment directed at hypertension. It was reported to lower arterial blood pressure, via a relaxation of vascular smooth muscle, most likely through the opening of the vascular K^+_{ATP} channels (Weston and Edwards, 1992), although there was no direct evidence for this (Seino and Miki, 2003).

Patients taking minoxidil reported hypertrichosis, as a common side-effect, in particular on the face, across the upper back and limbs (Limas and Freis, 1973; Mehta *et al.*, 1975; Sica, 2004), additionally, re-growth of hair in male balding was also noted (Zappacosta, 1980). Due to the key role that hair plays in society and social communication, the high frequency of hypertrichosis, was deemed an unacceptable side-effect of systemic minoxidil treatment (Girman *et al.*, 1998; Jansen and van Baalen, 2006). Consequently this encouraged the development of a topical preparation of minoxidil for the treatment of androgenetic alopecia. At its introduction into the market in the United States in 1986, the topical treatment only contained 2% of minoxidil solution. Using this approximately a third of the men with androgenetic alopecia reported an increase in hair density, with no significant difference between 2 and 3% minoxidil (Olsen *et a*l., 1985; Olsen *et al.*,

1987). However in 1993 the solution of minoxidil was increased to 5% (Messenger and Rundegren, 2004). Topical minoxidil prolongs the anagen growth phase and causes premature termination of telogen. Resting hair follicles are induced into the anagen phase and small follicles produce longer, more pigmented hairs with a larger diameter (Messenger and Rundegren, 2004).

In a 48 week study, the 5% and 2% topical minoxidil solutions were compared. The study found the 5% solution to be considerably superior to the 2% solution and the placebo in increasing hair re-growth. Furthermore the 5% caused an earlier increase in hair count (Olsen et al., 2002). A related study, concentrating on female pattern hair loss, also compared 5% and 2% topical minoxidil, rendering similar results to the previous study as the 5% solution produced significantly higher non-vellus hair counts than the 2% minoxidil solution (Lucky et al., 2004). Currently the 5% concentration is licensed for treatment of men in the USA, but only the 2% concentration for women. Six months following discontinuation of topical minoxidil solution hair loss occurs, the gravity of which is equivalent to that of untreated patients. This means that hair growth is not maintainable once minoxidil treatment stops (Olsen and Weiner, 1987; Price et al., 1999).

Despite the popularity of topical minoxidil as a form of treatment for over 25 years, and much research in its field, the mechanism of action by which minoxidil stimulates hair growth remained uncertain. The general accepted view was that it worked via effects on the vasculature to increase blood supply to the follicles (Messenger and Rundegren, 2004).

Recent studies by Shorter et al (2008) have shown that human hair follicles express both the genes and proteins for at least two K^+_{ATP} channels, SUR1/Kir6.2 and SUR2B/Kir6.1. They showed that the expression was variable within the

follicle with the dermal papilla having genes and protein for SUR2B and Kir6.1 and epithelial matrix SUR1 and Kir6.2. There was no detection of SUR2A subunits in human hair follicles. Minoxidil has a specific affinity to K^+_{ATP} channels which contain SUR2A/B subunits, but not those with SUR1. Shorter *et al's* (2008) finding of SUR2B in the dermal papillae suggests that minoxidil affects the human hair follicle via the dermal papillae. This is supported by their observation that minoxidil increased anagen in human hair follicles in organ culture, an effect inhibited by the potassium channel blocker, tolbutamide, and similar to the effects on the growth of deer follicles in organ culture reported by Davies *et al* (2005).

This confirms that minoxidil can act directly on hair follicle K^+_{ATP} channels in human hair follicles and means that its mechanism of action within the follicle merits more investigation to facilitate the development of new treatments to replace the relatively poor effects of minoxidil treatments used currently. Shorter *et al* (2008) also located the genes and proteins SUR1 K^+_{ATP} channels in the hair bulb matrix in human hair follicles. This is particularly interesting since Davies *et al* (2005) found that a selective SUR1 channel opener also stimulated the growth of red deer follicles in organ culture. This suggests that SUR1 K^+_{ATP} channels may also be able to play a role in human hair follicle growth. If true, this opens up the possibility of new therapeutic options with which to treat hair loss. It is important to verify whether SUR1 channels can be actively involved in human hair follicle regulation.

1.10 Aims

Therefore, the overall aim of this thesis was to expand our understanding of K^+_{ATP} channels in hair follicles. The initial specific aim was to confirm the presence of K^+_{ATP} channel subunit genes and proteins in growing (anagen) red deer hair follicles to determine whether this matched that of human hair follicles. This would support the observations by Davies and colleagues (2005) that drugs which selectively open either SUR2 (minoxidil) or SUR1 (NNC55-0118) K^+_{ATP} channels stimulate deer follicle growth in organ culture. This is important for future potential investigations on novel K^+_{ATP} channel opening drugs as the limited availability of human hair follicles prevents their use as a drug testing system involving dose response analysis. Red deer follicles are a well established model in Professor Randall's research group (Thornton *et al.*, 1996; Thornton *et al.*, 2001; Randall *et al.,* 2003; Croft *et al.,* 2003) and, if the genes and protein correspond, they would offer an appropriate model system for examining future K^+_{ATP} channel opening drugs on hair growth.

If the genes and proteins were expressed in the deer follicles, the studies were to be expanded to telogen follicles to compare expression in stages of the hair cycle. Deer follicles are particularly suited to this because of their large size and their seasonal cyclic growth pattern, which facilitates obtaining sufficient telogen follicles.

The second aim was to enhance the understanding of K^+_{ATP} channels in human hair follicles by determining whether human hair follicles would respond to a selective SUR1 K^+_{ATP} channel opening drug in organ culture by increasing growth, as in the study by Davies and colleagues (2005), on deer hair follicles. If so, this would suggest that further investigation into the SUR1 channel mechanism

may offer another route to regulate hair growth and might lead to a further aim to determine whether the two types of drugs given together would give an enhanced effect, indicating separate mechanisms.

The third aim was to investigate the effects of drugs which regulate SUR2 K^+_{ATP} channels on human hair follicle dermal papilla cells in culture since the SUR2B/Kir6.1 had been located in the dermal papilla by Shorter *et al* (2008). This would include assessing their effect on dermal papilla cell growth in culture and the proteins they synthesise, using a proteomic approach. These investigations into K^+_{ATP} channels in the hair follicle hold the potential of enhancing the sophistication of treatments for hair loss.

Chapter 2

ATP-sensitive potassium (K^+_{ATP}) channels in red deer hair follicles

2.1   Introduction

Investigations have offered evidence suggesting that potassium channel regulators influence hair growth via the mechanism of action on K^+_{ATP} channels. Davies *et al* (2005) investigated the effects of minoxidil and other potassium channel modulators on red deer (*Cervus elaphus*) follicles *in vitro*. Minoxidil stimulated hair follicle growth at all concentrations (0.1, 1, 10 and 100 μM), with the highest stimulation occurring at 100 μM. Similarly other potassium channel openers, diazoxide (10 μM) and NNC 55-0118 (0.1, 1, 10 and 100 μM) induced an increase in hair follicle length during culture. The stimulatory effect on hair follicle growth was inhibited with co-incubation of potassium channel blockers, tolbutamide and glibenclamide; this provides support to the hypothesis that K^+_{ATP} channels are expressed in red deer anagen hair follicles.

The recent study in our laboratory by Shorter *et al* (2008) demonstrated that minoxidil (1mM) advanced anagen in human hair follicle organ culture, and tolbutamide (1mM) suppressed this effect. Shorter *et al* (2008) also investigated the gene and protein expression of K^+_{ATP} channels in human hair follicles using reverse transcription-polymerase chain reaction (RT-PCR) and immunohistochemistry techniques. RT-PCR confirmed the expression of K^+_{ATP} channel sub-unit genes SUR1, SUR2B, Kir6.1 and Kir6.2 in anagen human hair follicles; SUR2A was not expressed. Immunohistochemistry further confirmed the protein expression of K^+_{ATP} channels in the hair follicle: SUR1 and Kir6.2 in the hair matrix, and SUR2B and Kir6.1 in the dermal papilla and dermal sheath. These findings hold the potential of advocating the development of better targeted drugs using the particular channel type present, achieving more enhanced stimulation or inhibition of hair growth.

To investigate the regulation of human hair growth, the human hair follicle would be the preferred model. However, sample sizes and ethical approvals can limit experimental design. Red deer hair follicles offer a practical model system for studying hair growth *in vitro* as they are big follicles, readily available in large numbers (Randall *et al.*, 2003). Furthermore, the red deer model has ethical advantages, as it is bred and harvested for food in the United Kingdom and thus skin is readily available. Therefore, to validate the use of the deer follicle as a model for the human follicle, the gene expression of deer must be established as the same as that of human. This would mark deer as a good model system, enabling screening of potential new therapies.

The mammalian hair follicle is subject to transformations throughout its growth cycle (as discussed in Section 1.4). Starting from a resting phase, telogen, to the growth phase, anagen, this is characterised by cell proliferation and keratinocyte differentiation with the production of the hair shaft, then undergoing the transitional regression phase, catagen, and finally leading again to the resting phase. The last phase within the hair growth cycle is exogen, an independent and active shedding phase, during which the original hair is enzymatically released and falls out (Higgins *et al.,* 2009). In order to fully comprehend the role of potassium channels in the hair follicle, it is necessary to investigate the presence of these channels in both the anagen and telogen phases. The recent study by Shorter and colleagues demonstrated the presence of K^+_{ATP} channels in the human anagen hair follicle (Shorter *et al.*, 2008). It is almost impossible to investigate the presence of K^+_{ATP} channels in a human telogen hair follicle, unless methods are employed to induce the telogen phase.

The red deer hair follicle is a well established model (Thomas *et al.*, 1994; Thornton *et al.*, 1996) and is an ideal animal to study hair cycling. The red deer undergoes two complete moults per year (Lincoln and Kay, 1971). The progression of the moult follows from the neck and shoulders, down the back and flanks and ultimately ending at the venter (Ryder, 1977; Whitehead, 1993). For both sexes the first moult takes place in spring, with the hair growing period covering the months of April to June in the Northern Hemisphere. This period of hair growth produces short red hairs tinged with brown (50 mm long), from which the red deer derives its name (Figure 2.1). The second moult takes place over the months of August to September (Northern Hemisphere). A longer anagen period of the follicles in the winter results in the hairs growing to a length of 60mm (Ryder, 1977). The seasonal growth cycles mean follicles in any given area are at the same stage of the hair cycle, making the red deer follicles an ideal model to investigate K^+_{ATP} channels in the telogen phase.

Figure 2.1 A photograph of a mature red deer stag with full grown antlers and mane (arrow) (Davies 2001)

2.2   Aims and experimental design

The overall aim of this chapter was to validate the deer follicle as an ideal model system for investigating the presence of K^+_{ATP} channel subunit genes in varied phases of the hair cycle.

The initial stage of this investigation involved a histological comparison between human and deer hair follicles, followed by the histological comparison of deer hair follicles in varied stages of the hair cycle. To do this human skin samples and red deer skin samples were collected. The deer skin samples were from both seasonal productions of pelage, this presented hair samples at different stages of the hair cycle. These samples were frozen, sectioned and stained.

The first aim was to investigate whether the expression of K^+_{ATP} channel genes in red deer anagen hair follicles were the same as that in human follicles (Shorter *et al.*, 2008), as suggested by the deer pharmacological studies (Davies *et al.*, 2005), using a molecular biological approach: RT-PCR. To do this a total of 60 anagen hair follicles were micro-dissected, and then RNA extracted. After RNA isolation, poly(A)$^+$RNA extraction and treatment with DNase, cDNA was synthesised. The expression of the genes for the sulphonylurea receptor subunits SUR1, SUR2A and SUR2B and the pore forming subunits Kir6.1 and Kir6.2 were all examined. Gene identity was confirmed by size on gel electrophoresis and gene product sequence analysis. The NCBI BLAST programme was used to align the homology of the sequenced deer product against the known human sequence. The second aim was to attempt immunohistochemistry on the frozen anagen deer sections to confirm the presence of the K^+_{ATP} channel subunit proteins within the hair bulb, as was done on human follicles by Shorter *et al* (2008). The final aim was to investigate the gene expression of K^+_{ATP} channel sub-units in telogen stage of the hair cycle.

2.3 Materials and Methods

2.3.1 Histological staining of human and red deer hair follicles

2.3.1.1 Biological material

2.3.1.1.1 Red deer skin

Deer skin samples were gathered, as a waste product, from the neck/mane region (Figure 2.1) of healthy red deer, bred and harvested for sustenance in Yorkshire. The animals used were young male adults, ranging from 12 to 18 months old, for both the anagen and telogen samples. The skin samples were cleaned and the hairs cut off using sterile scissors and dissected into strips immediately after death, and transferred to 50ml falcon tubes, containing transport media RPMI 1640 (RPMI supplemented with: 10% fetal calf serum, 10 units/ml penicillin/streptomycin, 100 ng/ml fungizone (amphotericin B), and 2mM L-glutamate) (Gibco, Paisley, UK), that had been pre-cooled on ice (4°C). The tubes were stored in ice for the duration of transportation, and once at the University the samples were washed in sterile PBS to remove all traces of cell debris and blood. Samples for histology were dissected into 1cm^2 pieces (Figure 2.2), washed thoroughly in sterile phosphate buffered saline (PBS; 137 mM NaCl, 2.7 mM KCl, 10 mM Na_2HPO_4, 1.8 mM KH_2PO_4), and placed individually into 1.5 ml eppendorfs (Sarsted, Numbrecht, Germany) in cryoprotectant Sakura Tissue-Tek O.C.T™ (Raymond A Lamb Ltd, Sussex, UK) at -80°C until further use.

Figure 2.2 Sample of deer skin

A deer neck skin sample was placed in a petri dish, washed in sterile PBS to remove all traces of cell debris and blood and dissected into 1cm² pieces. Photographed on dissecting microscope (Leica MZ8, Leica, Germany) using a Nikon Coolpix4500 (Nikon E4500) digital camera (Bar=2mm).

2.3.1.1.2 Human skin

Human scalp skin samples from non-balding areas (occipital and temporal regions) were obtained from healthy individuals aged between 24-64 years undergoing elective cosmetic facelift surgery. All Ethical Committee approval requirements were met and donors gave fully informed written consent. As described above the human skin samples were collected in RMPI transport medium and dissected into 1cm² pieces (Figure 2.3). The sections were washed thoroughly in sterile PBS and stored in O.C.T™ at -80°C until used.

Figure 2.3 Sample of human skin

A human facelift skin sample was placed in a petri dish, washed in sterile PBS to remove all traces of cell debris and blood and dissected into 1cm^2 pieces. Photographed on light dissecting microscope (Leica MZ8, Leica, Germany) using a Nikon Coolpix4500 (Nikon E4500) digital camera (Bar=1.8mm).
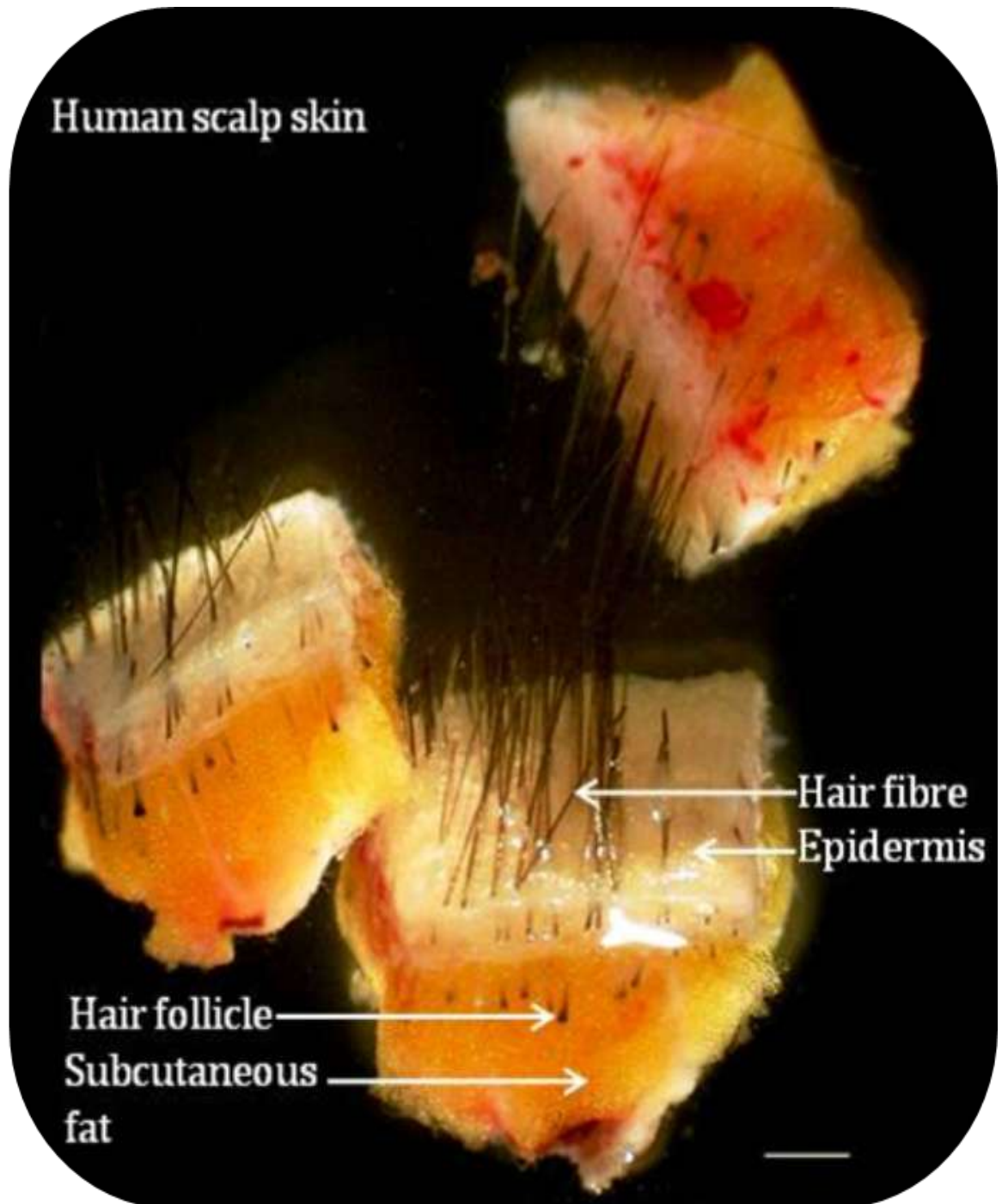
2.3.1.2 Preparation of slides

To assist sections to adhere to twin-frost glass slides (76 x 26 x 1 mm; BDH, Lutterworth, UK) the slides were cleaned and coated in poly-l-lysine (Sigma-Aldrich Ltd, Dorset, UK). The slides were placed individually into a plastic slide carrier, before being immersed in pyroneg (Diversey Lever Ltd, Northampton, UK) and distilled water for 30 minutes. To remove traces of detergent the slides were first rinsed in distilled water then immersed in absolute ethanol (Sigma) for 5 minutes. The slides were allowed to dry in the drying cupboard at 60C, before being immersed in 10% (v/v) poly-l-lysine in distilled water for 10 minutes. Once dry, the slides were stored in the original box and remained at room temperature until required.

2.3.1.3 Preparation of sections

Skin samples were removed from -80°C and placed in a cryostat (Leica CM 1800 Cryostat, Germany) at –27°C. O.C.T™ was applied to the metal holder to form an even disc to freeze solid, ensuring all bubbles were removed. The frozen O.C.T™ disc was then placed into the sample holder of the cryostat and sliced until even. The skin sample was placed onto the O.C.T™ disc and orientated so that longitudinal follicles could be sectioned. The sample was orientated to its side to ensure the blade cut concurrently through the dermis and fat (Figure 2.4). O.C.T™ was applied to the sample until no longer visible, and allowed to freeze solid. 5 μm diameter sections were cut and mounted on to labelled poly-l-lysine coated slides and placed into a labelled slide holder wrapped in foil at -20°C until histological analysis.

Figure 2.4 Cryostat machine with mounted skin sample

The picture of cryostat (Leica CM 1800 Cryostat, Germany) is taken using a Nikon Coolpix4500 (Nikon E4500) digital camera.
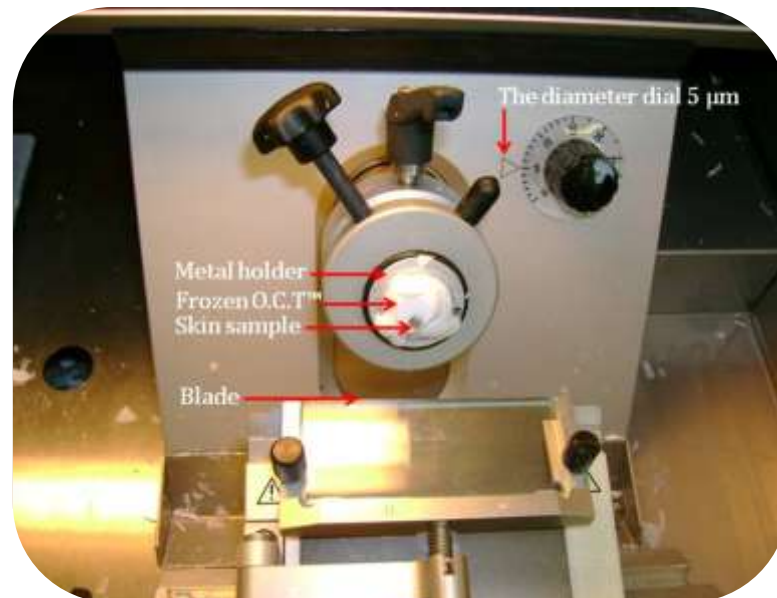
2.3.1.4 Histological investigation using Sacpic staining

Sections of deer and human skin samples were stained with the Sacpic staining technique (Nixon, 1993; Nutbrown and Randall, 1996). This technique employs different dyes applied to stain and distinguish the different components of hair follicles. The frozen slides were removed from -20°C, and allowed to air-dry at room temperature for 30 minutes; gradual defrosting would prevent temperature shock. The sections were then fixed in ice-cold acetone 4°C (Fisher Scientific Loughborough, UK) for 15 minutes and rinsed with distilled water, to rehydrate the slides. The sections were immersed in Celestine blue stain solution for 5 minutes; they were then rinsed in tap water twice before being immersed in Gill's haematoxylin stain solution for a further 5 minutes followed by rinsing in tap water. The sections were blued in Scott's tap water for 2 minutes, before rinsing in

tap water and placed in 2% safranin for 5 minutes at a time. The sections were then dehydrated via 1 minute immersions in: tap water; 70% ethanol; and 95% ethanol. The sections were differentiated in absolute picric acid/ethanol for 5 minutes before rehydration via 1 minute immersions in: 95% ethanol; 70% ethanol; and tap water. The sections were then placed in picro-indigo carmine for 1 minute and rinsed in tap water, before dehydration by immersion in ascending ethanol solutions from 70% ethanol to absolute ethanol, for 5 minutes each. The sections were cleared in histoclear: ethanol (50:50 v/v) and absolute histoclear (National Diagnostics, Hull, UK) for 4 minutes at a time. Coverslips (VWR International, Leicester, UK) were then mounted using histomount (VWR International, Leicester, UK).

2.3.1.5 Histological investigation using haematoxylin and eosin staining

The frozen sections were removed from -20°C, and allowed to air-dry at room temperature for 1 hour. The sections were then fixed in ice-cold acetone 4°C (Fisher Scientific Loughborough, UK) for 10 minutes, and washed with PBS thrice for 3 minutes at a time, to rehydrate. They were placed in haematoxylin (Merk Ltd) for 2-5 minutes depending on how the stain seemed to penetrate the tissue, followed by a rinse in distilled water until all traces of excess haematoxylin was removed. Sections were blued by washing in Scott's tap water for 2 minutes and counter-stained by soaking in 1% w/v eosin (Merck Ltd) for 5 minutes. Excess eosin was removed by rinsing in distilled water; the water was removed by dehydrating sections in ascending alcohol 50%, 70% and 95% ethanol through

immersion for 1 minute in each. Coverslips (VWR International, Leicester, UK) were then mounted using histomount (VWR International, Leicester, UK).

2.3.1.6 Visualising the staining

The stained slides were examined using the Orthodox II light microscope (Leitz, Germany). Images of good sections were captured digitally using a Nikon Coolpix 4500 camera, and transferred to the computer using Nikon View 5 software. The pictures were measured using a stage micrometer (Figure 2.5).

Figure 2.5 Stage micrometer

A picture of a stage micrometer, taken using Orthodox II light microscope (Leitz, Germany), captured digitally using a Nikon Coolpix 4500 camera.
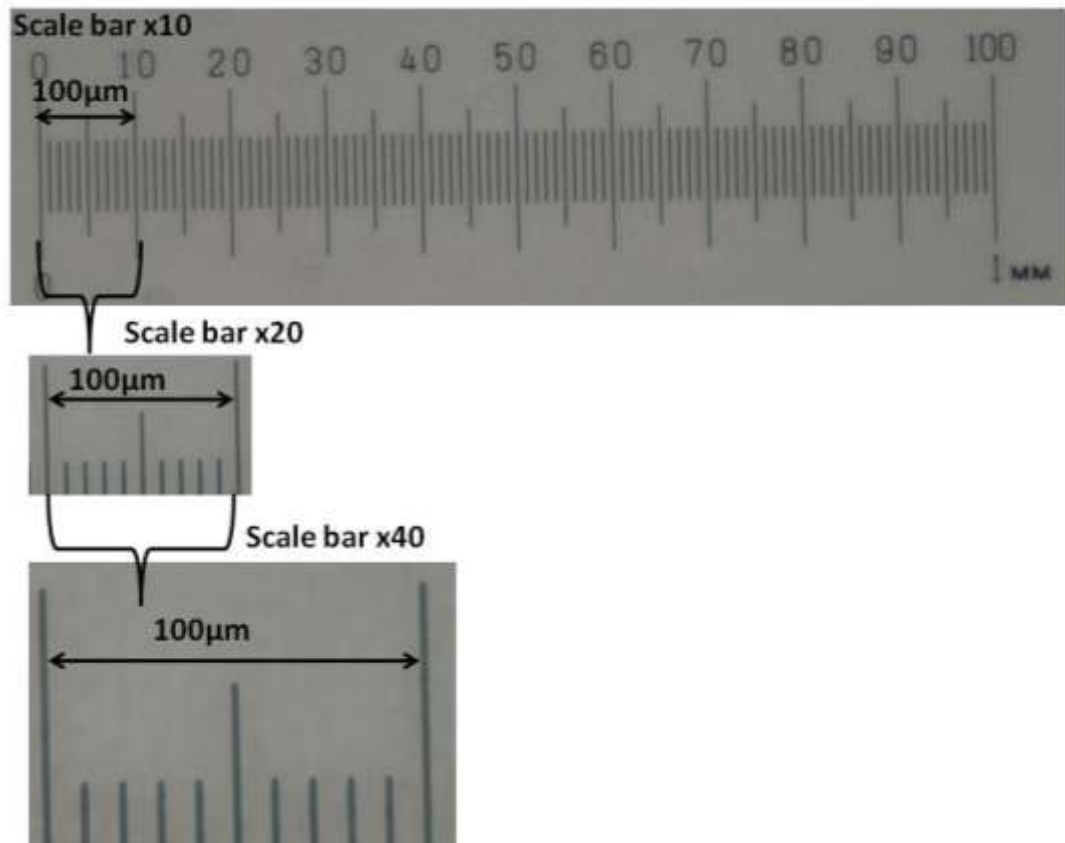
2.3.2 Reverse Transcription - Polymerase Chain Reaction (RT-PCR)

PCR amplifies a specific region of template DNA, which can include genomic, plasmid and phage DNA or RNA converted to complementary DNA (cDNA) (Cha and Thilly, 1995). Investigating mRNA expression reveals the genes expressed in the cell or tissue from which RNA was extracted. The enzyme reverse transcriptase is used alongside oligo (dT) primers, binding to the poly (A) tail of mRNA, synthesising cDNA from mRNA. The cDNA is then applied in the PCR reaction, and the gene of interest is amplified from this cDNA by using specific forward and reverse primers (Kawasaki, 1990).

Specific forward and reverse primers are designed (see table 2.1 for reference) to correspond to the regions bordering the target DNA sequence for PCR amplification. The primers anneal to polar ends of the target DNA sequence spanning the entire target DNA region for amplification. A PCR reaction also requires thermostable Taq DNA polymerase, buffers and a mixture of deoxynucleotide triphosphates (dNTP's) containing the four bases required for synthesis of new DNA strands. DNA amplification is achieved using a thermocycler set at specific temperatures in which the PCR reaction mix is placed. The initial high temperature denatures the DNA template, and if double stranded, separates it. The temperature is then lowered allowing the oligonucleotide primers to anneal to the complementary single-stranded target DNA sequence. However the temperature is subject to the primer used, generally at a few degrees below the average melting temperature of the primers, determined from the base composition of the oligonucleotides. The annealing temperature must be perfectly adjusted both to allow for efficient annealing, therefore not too high, and, to minimise non-specific binding, not too low. At the final stage the Taq DNA

polymerase extends the annealed oligonucleotide primers, at a high temperature, typically at 72-74°C. The PCR cycle produces a new strand DNA if cDNA was used, or two new strands when double stranded DNA was used. This cycle of temperatures is repeated between 25-40 times, with the amplified products from each PCR cycle acting as template for the next cycle, resulting in a significant rise in the number of target DNA sequences (McPherson and Møller, 2000).

If the $MgCl_2$ concentration is too high mismatches in primer hybridisation may occur resulting in undesired amplicons, however, if it is too low a lower yield of amplification occurs. Thus the PCR mix and thermocycling conditions require careful optimisation and are specific to each primer set used (Table 2.1).

Expression of K^+_{ATP} channel subunits in deer hair follicle using RT-PCR

For the purposes of investigating the expression of K^+_{ATP} channel subunits in deer hair follicles, in both the anagen and telogen stages of the hair cycle, the following materials and methods were employed. All work areas were thoroughly cleaned prior to the undertaking of any procedure using 70% ethanol and RNAse Zap solution (Sigma-Aldrich Ltd, Dorset, UK) to prevent contamination, as well as gloves being changed regularly. Only sterilised materials were used throughout the experiment, including plastics and glassware.

2.3.2.1 Tissue collection

The tissues were collected as per the description in section 2.3.1.1, with the exception that the 50ml falcon tubes held 30ml RNA stabilisation solution RNA*later*™, to inhibit RNAses (Sigma). The tubes were stored in ice for the duration of transportation, and once at the University they were placed in to the

fridge (4°C) overnight to allow the RNA*later*™ to penetrate the tissue. The next day these samples were transferred into clean RNA*later*™ and stored at -80 ºC.

2.3.2.2 Microdissections

For this process all containers holding skin samples and dissected hair follicles that were not being worked on were kept on ice throughout. The Leica MZ8 (Leica, Germany) dissecting microscope was used, at x20 magnification for the dissection of whole hair follicles from the skin samples gathered. Initially the skin samples were defrosted in an ice box, at -4°C, transferred to a petri dish (35x10mm) holding RNA*later*™ that had been previously placed in the icebox, to ensure equal temperature to the skin sample. The petri dish containing the skin sample was placed beneath the dissecting microscope and the follicles were dissected from the skin, transferred into another petri dish containing fresh RNA*later*™ and examined at a higher magnification (x50). The freshly isolated follicles were then cleaned of any dermis or fat debris using needles (27G1/2 tuberculin syringe; Sigma) before transfer to a 1.5ml eppendorf containing 1 ml RNA*later*™ placed on ice. A total of 60 hair follicles were collected prior to total RNA isolation. Photographs of the dissection steps are displayed in figure 2.6.

Figure 2.6 Isolation of deer hair follicles by microdissection

The skin sample was cut into small sections to promote conspicuousness of individual hair follicles (a) (Bar=667μm), which were isolated from the skin sample and transferred to a new dish of RNA *later*™ (b) (Bar=291μm). The isolated follicles then required meticulous cleaning, to remove any dermis and subcutaneous fat, with syringe needles (c) (Bar=340μm). The clean isolated hair follicles (d) from the sample were then combined for total RNA isolation (Bar=385μm).
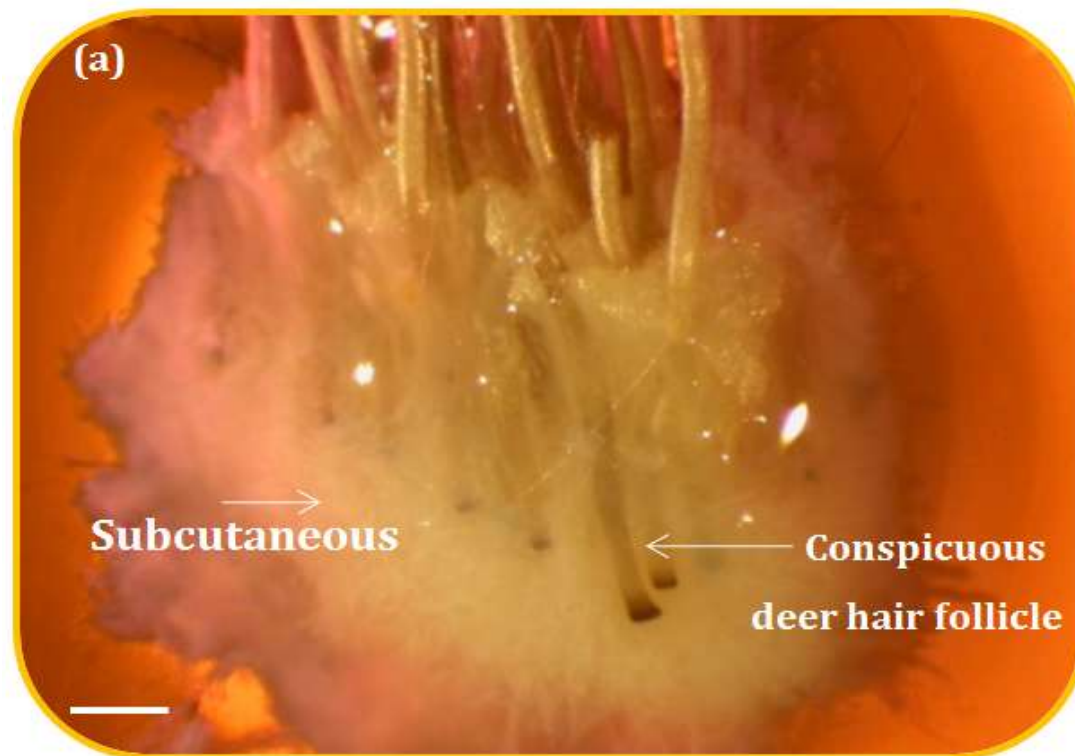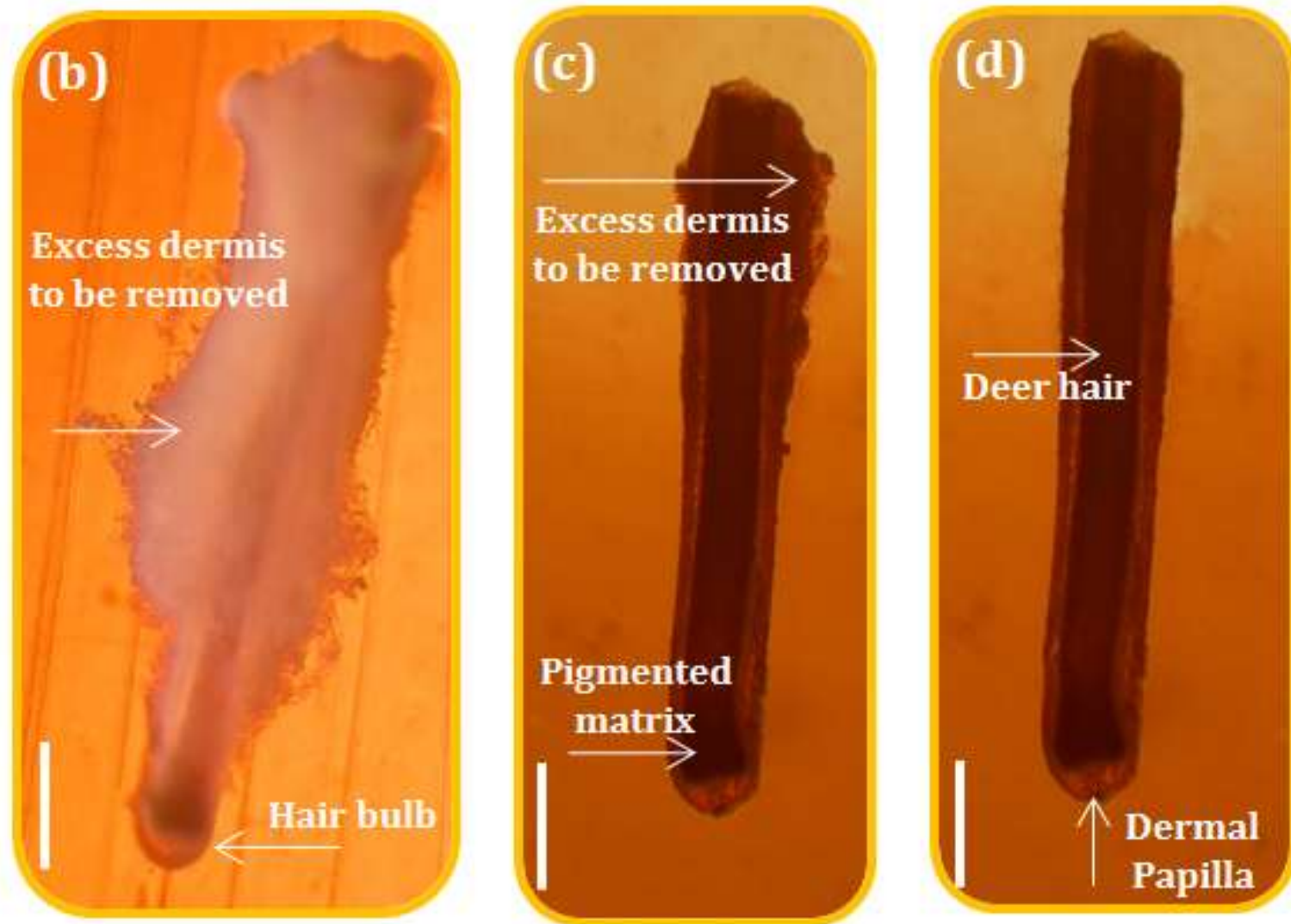
2.3.2.3 RNA isolation, purification and cDNA synthesis

Following dissection of the required number of hair follicles, the process of total RNA isolation was carried out. The total RNA samples were further purified to isolate poly(A)$^+$RNA. DNase treatment of RNA was carried out to remove any contaminating DNA from mRNA, then converted into single stranded cDNA, before PCR amplification.

2.3.2.3.1 Total RNA isolation

Total RNA isolation was carried out in accordance to manufacturer instructions provided with the GenElute Mammalian Total RNA kit (Sigma). The microdissected hair follicles were transferred into a homogeniser with the lysis/2-mercaptoethanol solution. The sample was homogenised until the hair follicles became undetectable and the homogenate was then transferred to a GenElute filtration column. The sample was centrifuged (Eppendorf 5415 R) at 13000x g, for 2 minutes, effectively removing any cellular debris and shearing the DNA. Following centrifugation, the filtration column was discarded, and an equal volume of 70% ethanol (made using 0.05% (v/v) diethyl pyrocarbonate (DEPC); Sigma) treated water was added to the filtered lysate. The sample was mixed thoroughly by vortexing.

The lysate/ethanol mixture 700 µl was then added to the clear binding column and centrifuged at 13000x g, for 15 seconds. The flow through was discarded, and the total RNA would be bound to the binding column. The remaining sample was added to the binding column, and the procedure repeated. The binding column was then transferred to a new collection tube.

The wash solution 1 was added to the binding column 500 μl, and centrifuged for 15 seconds. Once again the column was transferred to a new collection tube. Next 500 μl of wash solution 2 was added and centrifuged for 15 seconds. The flow-through was discarded and the binding column was placed back into the collection tube. A second 500 μl of wash solution 2 was added to column and centrifuged for 2 minutes, removing the ethanol. The column was then transferred to a new collection tube to elute the RNA from the binding column. 50 μl of elution solution was added to the centre of the binding column and centrifuged for a minute. A second 50 μl of elution solution was added to column and centrifuged for a minute. The flow through containing the purified total RNA was collected, and could be used immediately or stored at -80°C until further use.

2.3.2.3.2 Poly (A)[+] RNA isolation

mRNA isolation was carried out in accordance to manufacturer instructions provided with the GenElute mRNA Miniprep kit (Sigma). The total RNA sample was brought up to a volume of 250 μl using RNase-free water, mixed with 250 μl of 2X binding solution and 15 μl of oligo (dT) beads, and vortexed thoroughly. The sample was incubated for 3 minutes at 70°C for RNA denaturing, and then left for 10 minutes at room temperature before centrifuging for 2 minutes at 13000x g to pellet the beads: mRNA complex. At this point the supernatant was removed. The pellet was resuspended in 500 μl of wash solution, transferred to a spin filter/collection tube and centrifuged for 2 minutes at 13000x g. The flow through was discarded and the pellet washed again with a second 500 μl of wash solution. The column was transferred into a fresh collection tube and 50 μl elution solution (preheated to 70°C) was added to the centre of the filter and incubated at 70°C for

5 minutes, followed by centrifugation for 1 minute. This elution procedure was repeated with an additional 50 μl elution solution. The pure mRNA was then either used immediately or stored at -80°C until further use.

2.3.2.3.3 DNase treatment of mRNA samples

Prior to cDNA synthesis by reverse transcription, the mRNA samples were treated with the enzyme dideoxynuclease I (DNase I) to remove any contaminating DNA. A reaction mix was prepared inside a 0.5 ml eppendorf tube (Alpha Laboratories, Ltd, Eastleigh, UK), containing 8μl of mRNA, 1μl DNase I amplification grade and 1μl 10X reaction buffer (Invitrogen Ltd, Paisley, UK). The reaction mix was mixed thoroughly and incubated at room temperature for 15 minutes. 1μl EDTA (25mM; Invitrogen) was added and incubated at 65°C for 10 minutes to inhibit enzyme activity. The DNase treated mRNA could then either be used immediately or stored at -80°C until further use.

2.3.2.3.4 cDNA synthesis by reverse transcription

The Avian Myeloblastosis Virus (AMV) reverse transcription system (Promega, Southampton, UK) was used to convert DNase treated mRNA into cDNA. A reaction mix was prepared, in an 0.5 ml eppendorf tube (Alpha Laboratories), containing 2μl dNTP mix (10mM), 1μl Oligo (dT)$_{15}$ primer (0.5 μg/μl), 2μl 10X reaction buffer, 0.5μl recombinant RNasin® ribonuclease inhibitor (40 units/μl) and 0.75μl AMV reverse transcriptase (high concentration 25 units/μl,). To this mixture a further 3.75μl nuclease free water was added bringing the total volume to 10μl (all provided by Promega). This reaction mix was added to a 0.5 ml eppendorf tube containing 10μl of DNase treated mRNA, and mixed thoroughly.

The eppendorf tubes were then placed in the PCR Sprint thermal cycler (Thermo Hybaid, Ashford, UK) and set to run the reverse transcription programme: incubation for 1 hour at 42°C to allow cDNA synthesis from mRNA by reverse transcription, followed by 5 minutes at 99°C to inhibit the reverse transcriptase and 5 minutes at 4°C. A centrifugation of 5 seconds, ensured that all cDNA was collected at the base of the eppendorf tube. This sample was then aliquoted into 0.5 ml eppendorf tubes (Alpha Laboratories) at 10μl cDNA sample per tube, labelled and stored at -20°C.

2.3.2.4 PCR

A reaction mix was prepared, inside an 0.5 ml eppendorf tube (Alpha), using 3μl of cDNA in a 50 μl reaction volume containing 0.5 μM concentrations of forward and reverse target primers; 200 μM concentrations of each dNTP (Promega, Southampton, UK); 5μl of 10X reaction buffer [200 mM Tris-HCl (pH 8.4), 500 mM KCl; Invitrogen]; 2.5 mM (β-actin, SUR1, and SUR2 reactors) or 1.5 mM (Kir6.1 and Kir6.2) $MgCl_2$ depending upon target primer set (Invitrogen) (For details for each target primer set see table 2.1); and 2.5 U of recombinant Taq DNA polymerase (Invitrogen). Using nuclease free water the volume of the mixture was brought up to 50 μl, and then mixed thoroughly. For every PCR reaction a negative control was prepared, replacing the 3 μl cDNA with 3 μl of nuclease free water. One drop of mineral oil (Sigma) was added on the top of each reaction mixture, to prevent evaporation of reaction components during PCR thermocycling. The PCR products were then placed on ice for immediate analysis by agarose gel electrophoresis or could be stored at -20°C.

Table 2.1 Specific forward (F) and reverse (R) primers for each cDNA target sequence and optimised conditions used in RT-PCR analysis of K$^+_{ATP}$ channel subunits (Shorter *et al.*, 2008)

Name of Primer	Primer Sequence	Optimal concentration of MgCl$_2$	Optimal thermocycling conditions	Expected amplicon size	Accession number from data library
β-actin	F: 5' ATCT GGCACCA CACCTTCTACAAT GAGCT GCG 3' R: 5' CTCATACTCCT GCTTGCTGATCCA CATCTGC 3'	2.5mM	95°C for 15 mins 94°C for 1 min 55°C for 2 mins ⎤ 35 cycles 72°C for 3 mins ⎦ 72°C for 10 mins 4°C ∞	838 bp	NM_001101
SUR1	F: 5' CGATGCCATCATCACAGAA G 3' R: 5' CT GAGCA GCTTCTCT GGCTT 3'	2.5mM	95°C for 15 mins 94°C for 1 min 55°C for 2 mins ⎤ 35 cycles 72°C for 3 mins ⎦ 72°C for 10 mins 4°C ∞	291 bp	AF087138
SUR2A/B	F: 5' GCTGAA GAATATGGTCAAATCTC 3' R: 5' T GGAGT GTCATATTCTAAAATA 3'	2.5mM	95°C for 5 mins 96°C for 15 secs ⎤ 55°C for 30 secs ⎬ 35 cycles 72°C for 78 secs ⎦ 72°C for 11 mins 4°C ∞	SUR2A = 451 bp SUR2B = 312 bp	NM_005691
Kir6.1	F: 5' CATCTTTACCAT GTCCTTCC 3' R: 5' GT GAGCCT GAGCT GTTTTCA 3'	1.5mM	95°C for 5 mins 95°C for 20 secs ⎤ 52°C for 45 secs ⎬ 35 cycles 72°C for 1 min ⎦ 72°C for 10 mins 4°C ∞	336 bp	NM_004982
Kir6.2	F: 5' GCTTT GT GTCCAAGAAAGG 3' R: 5' CCAAAGCCAATA GTCACTTG 3'	1.5mM	95°C for 5 mins 95°C for 20 secs ⎤ 52°C for 45 secs ⎬ 35 cycles 72°C for 1 min ⎦ 72°C for 10 mins 4°C ∞	301 bp	D50582

2.3.2.4.1 Agarose gel electrophoresis of PCR products

RT-PCR products were analysed using a 1.5% (w/v) agarose gel. 1.5 g of agarose (Invitrogen) was added to 100 ml of 1 X tris-acetate-EDTA (TAE, 0.04 M Tris Acetate, 0.001 M EDTA) buffer. Using a 950 W microwave (Proline Microchef ST44), the agarose was dissolved by sporadic swirling of the mixture until the boiling point (∽ 135 sec). The dissolved agarose was allowed to cool to around 50-55°C before adding 25μl of ethidium bromide (1 mg/ml; Sigma). The gel was immediately poured into plastic gel trays that had gel combs inserted to form wells. This gel was left for approximately 40 minutes to set and form wells before the gel combs were gently removed. The prepared agarose gel was placed into the electrophoresis tank containing 1X TAE buffer with 0.5 μg/ml ethidium bromide. To assist loading and monitor the progression of the product through the gel throughout electrophoresis, 15 μl of each PCR product was mixed with 5 μl of blue/orange 6X loading dye (Promega). The mixture and the negative controls were loaded into the wells, and their positions recorded. In order to estimate the product size 10 μl of standard DNA fragments was mixed with 4 μl of loading dye, and then loaded onto the gel to provide a DNA ladder (The ladder consisted of eleven fragments that ranged in size from 100–1,500bp in 100bp increments; Promega). The tank was set to run at 100 volts for approximately 35 minutes. Using the Uvitec gel documentation system (UVItec Limited, Cambridge, UK) the PCR products were visualised at 312nm wavelength and the image captured and stored on a computer.

2.3.2.4.2 Sequencing of PCR products

To verify and confirm the PCR products, they were sent to a commercial company for sequencing. The PCR products were prepared as described in section 2.3.2.4 except that only small, thin walled PCR tubes were used (VWR International Ltd, Poole, UK) and a hot lid was applied in the thermocycler instead of adding mineral oil, as it may interfere with the sequencing. The PCR products were separated on a low-melting point agarose gel (Invitrogen), to permit the use of a lower temperature for dissolving the gel, at the purification stage of the PCR products, preventing the possibility of DNA degradation. The commercial sequencing service requires approximately 50 ng/μl of DNA therefore 30 μl of weaker PCR products were loaded onto the gel allowing for sufficient product for sequencing. Using the MinElute Gel Extraction kit (Qiagen, Crawley, UK), these products were first purified in accordance with the instruction set by the manufacturer. The target DNA fragment was cut out from the gel using a scalpel blade, and transferred into a pre-weighed 1.5 ml eppendorf tube. The tube was re-weighed to obtain the gel weight. Buffer QC was then added in the proportion of 3 volumes of buffer to 1 of gel (300 μl of Buffer QC to 100 mg of gel). This was incubated for 10 minutes at 50°C, with vortexing every 3 minutes during this incubation, to dissolve the gel slice. One volume of isopropanol (Sigma) was added after the gel was fully dissolved, and mixed by inversion. The mixture was added to a MinElute column and centrifuged (13000 x g) for 1 minute to bind the DNA to the column. After the flow-through from the column was discarded, 500 μl of Buffer QC was added and the column was centrifuged (13000 x g) for 1 minute. The flow-through was discarded and the column returned to the collection tube. The column was washed with 750 μl of buffer PE with incubation for 5 minutes at

room temperature before being centrifuged for 1 minute. Once again the flow-through was discarded, while the tube was centrifuged (13000 x g) for another minute to remove residual ethanol from buffer PE. The MinElute column was placed into a fresh 1.5 ml eppendorf tube, for elution of DNA by incubation at room temperature for 1 minute with 10 µl of buffer EB. Followed by a minute of centrifugation (13000 x g) to elute DNA from the column. The purified PCR product was sent with 20 µl of forward and reverse primers (10 µM) for sequencing at Geneblitz (Sunderland, UK).

The NCBI BLAST programme (http://www.ncbi.nlm.nih.gov/blast/bl2seq/wblast2.cgi) was used to compare the homology of the sequenced PCR products with the previously identified sequences of the human genes. The chromatogram of the sequencing data was produced using the Chromas Lite software (version 2.0) available from http://www.technelysium.com.au/. Any non-matching nucleotides between the sequenced and known data were analysed using the chromatogram. Each base is allocated a different colour, in the chromatogram, and the sequence is determined by the highest peak. However, if more than one peak is of a similar height, without significant distance, then the base is recorded as 'n' in the sequence. Thus 'n' does not indicate an incorrect base.

2.3.3 Immunohistochemistry

Immunohistochemistry was attempted to investigate protein expression to confirm the presence of K^+_{ATP} channel subunits in deer hair follicles. Slides were coated with poly-l-lysine (as described in section 2.3.1.2) and 5μm cryosections of deer hair follicle were mounted upon them (as described in section 2.3.1.3). The sections underwent 1 hour of air drying at room temperature, followed by 10 minutes fixation in ice-cold acetone and 10 minutes of rehydration in PBS. Endogenous peroxide activity was blocked by 30 minutes of incubation in 3% hydrogen peroxide in methanol and a subsequent rinse in PBS. Incubation with normal mouse serum (5%) (Sigma-Aldridge Ltd) in PBS for 20 minutes blocked potential non-specific binding (Serum must be from the host of the secondary antibody) (Ramos-Vara 2005). Sections were incubated with the primary polyclonal goat antibody SUR1 1:5 (sc-5789), SUR2A 1:5 (sc-32461), SUR2B 1:5 (sc-5793), Kir6.1 1:5 (sc-11225), and Kir6.2 1:5 (sc-11228) (Santa Cruz Biotechnology, Santa Cruz, CA, USA) in a moist chamber to prevent sections from dehydrating at 4°C for 18 hours. Antibodies were diluted in 1.5% normal mouse serum in PBS. Unbound primary antibody was removed from the slides with two rinses in PBS for 20 minutes, prior to incubation with a mouse monoclonal anti-goat biotin-conjugated secondary antibody (Sigma-Aldrich Ltd) diluted 1:20 with 5% normal mouse serum in PBS for 30 minutes. The sections were washed twice in PBS before ExtraAvidin horseradish peroxidise (Sigma-Aldridge Ltd) was applied diluted 1:20 with PBS for 30 min. The sections were washed twice in PBS. Peroxide substrate, 3-amino-9-ethylcarba-zole (AEC; Vector Laboratories Ltd., Peterborough, UK) visualised antibody binding. Chromogen formation was monitored under the light microscope and when sufficient colour had developed

the reaction was halted by placing the slides in distilled water. The sections were counterstained in Mayer's hematoxylin, blued in Scott's tap water and finally rinsed in tap water before being mounted with Aquamount (VWR International, Leicester, UK). The resultant staining was inspected and visualised using a Nikon Eclipse 80i light microscope with a Nikon ACT-2U photo-graphic system. Each time the procedure was conducted negative controls were also performed to determine potential non-specific binding. These were performed by replacing the primary antibody with PBS; the secondary antibody; both primary and secondary antibodies. The negative controls are described below:

Experimental: Primary antibody + secondary antibody + Chromogen system

Negative control: PBS + secondary antibody + Chromogen system

Negative control: Primary antibody + PBS + Chromogen system

Negative control: PBS + PBS + Chromogen system

2.4 Results

2.4.1 Histological investigation of human and red deer hair follicles

2.4.1.1 A comparison of human and red deer anagen hair follicles

Cryosections and horizontal cross-sections were prepared from human and deer skin and stained with Sacpic (as described in section 2.3.1.4). The histological staining of human scalp hair and red deer neck hair follicles indicated that the overall structure of the follicles were similar. The general structure in the anagen follicles showed a thin epidermis with longitudinal hair follicles. The human follicle extended down into the subcutaneous fat layer (Figure 2.7b), whilst the deer follicle extended into the thick dermal layer (Figure 2.8b). The structure of hair follicle components were highlighted by the Sacpic stain. The connective/dermal sheath encapsulated the entire follicle separating it from the dermis. In the hair bulb, the dermal papilla was surrounded by the hair matrix and the hair fibre was surrounded by the inner and outer root sheaths. Overall, the red deer hair follicles were visibly larger than human scalp hair follicles, with an obvious medulla present within the deer hair. A midway cross section of the deer hair follicle noticeably exhibits the medulla and other minute components of the hair follicle (Figure 2.9).

Figure 2.7 Histology of human scalp skin

(a) The intact skin sample displays a longitudinal hair follicle (**HF**), extending into the subcutaneous far layer (**SF**), with a thin epidermis (**E**) and dermis (**D**) (Scale bar = 500μm), and at higher magnification of an isolated hair follicle (**HF**) the connective/dermal sheath (**DS**)**,** pigmented and non-pigmented matrix (**M**) in the hair bulb are clear. Large sebaceous gland (**SG**) can be seen on the left of the upper follicle and the dark pigmented hair is visible from the upper bulb upwards (Scale bar = 220μm).

(b) The Sacpic staining further emphasises the histology of the intact skin sample. At the higher magnification the staining visibly highlights the longitudinal hair follicle's components, with its attachment to the sebaceous gland (**SG**). Also visible are some of the components of the hair follicle, including the hair fibre (**HF**), the outer root sheath (**ORS**), the inner root sheath (**IRS**), and the connective/dermal sheath (**CTS/DS**) (Scale bar = 220μm). The lower right image of H&E staining of the hair follicle shows the structure of an anagen hair bulb. The dermal papilla (**DP**) is connected to the dermal sheath (**DS**) at its base and surrounded by the matrix (**M**). The hair bulb is deep within the skin located in the subcutaneous fat (**SF**) (Scale bar = 75μm).

(a)

(b)

E

D

SF

HF→

D

HF→

SF

SG

DS→

HF

M

220μm

220μm

D

SG

DS→

ORS→

IRS→

HF→

M→

SF

DS

HF

IRS

ORS

DP

75μm

Figure 2.8 Histology of red deer skin showing follicles in anagen

Side-views of deer skin showing hair follicles in anagen (**a**) (Bar=531µm) and cryosections of deer skin stained with the histological stain, Sacpic with hair follicles in anagen (**b**) (Bar=316µm).

General structure of anagen follicles (**b**) showing a thin epidermis (E) with longitudinal hair follicles extending into the thick dermal layer (D). The structure of hair follicle components are highlighted by the Sacpic stain including the red inner root sheath (IRS), the outer root sheath (ORS), hair medulla (HM), sebaceous gland (SG), dermal papilla (DP) and hair matrix (MA). The connective tissue sheath encapsulates the entire follicle separating it from the dermis. (**c**) A cross section through an anagen hair follicle located mid way up the follicle. The Sacpic staining clearly highlights the connective/dermal tissue sheath (CTS/DS), the outer root sheath (ORS), the red inner root sheath (IRS), the cortex (C) of the hair and medulla (M), (Bar= 17µm).
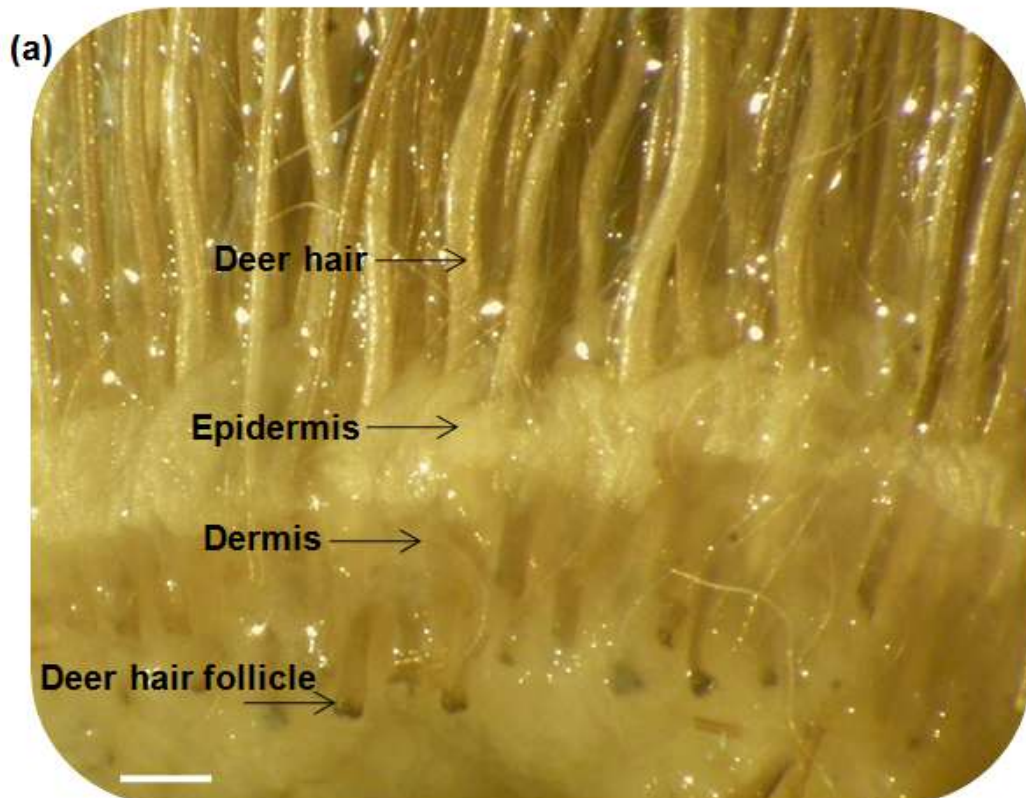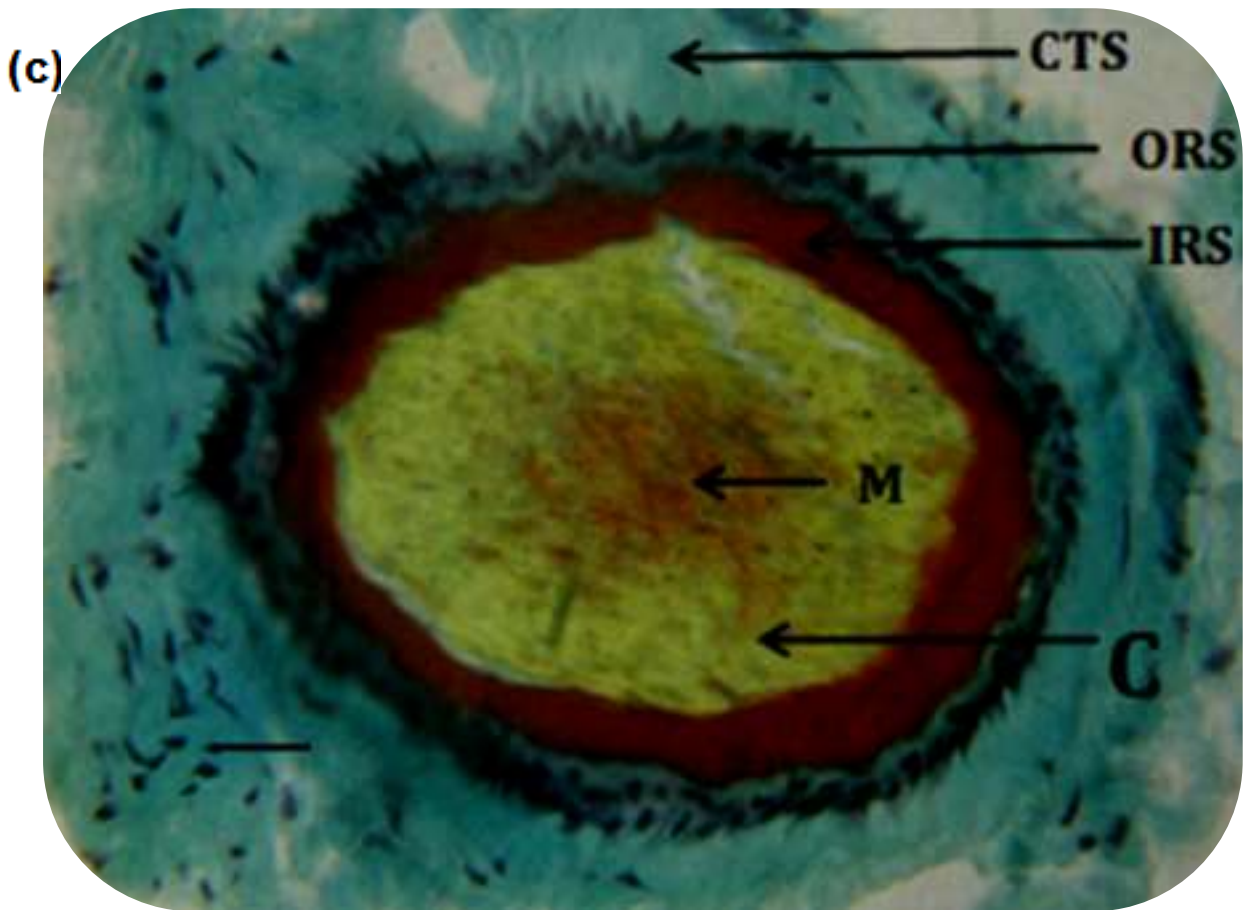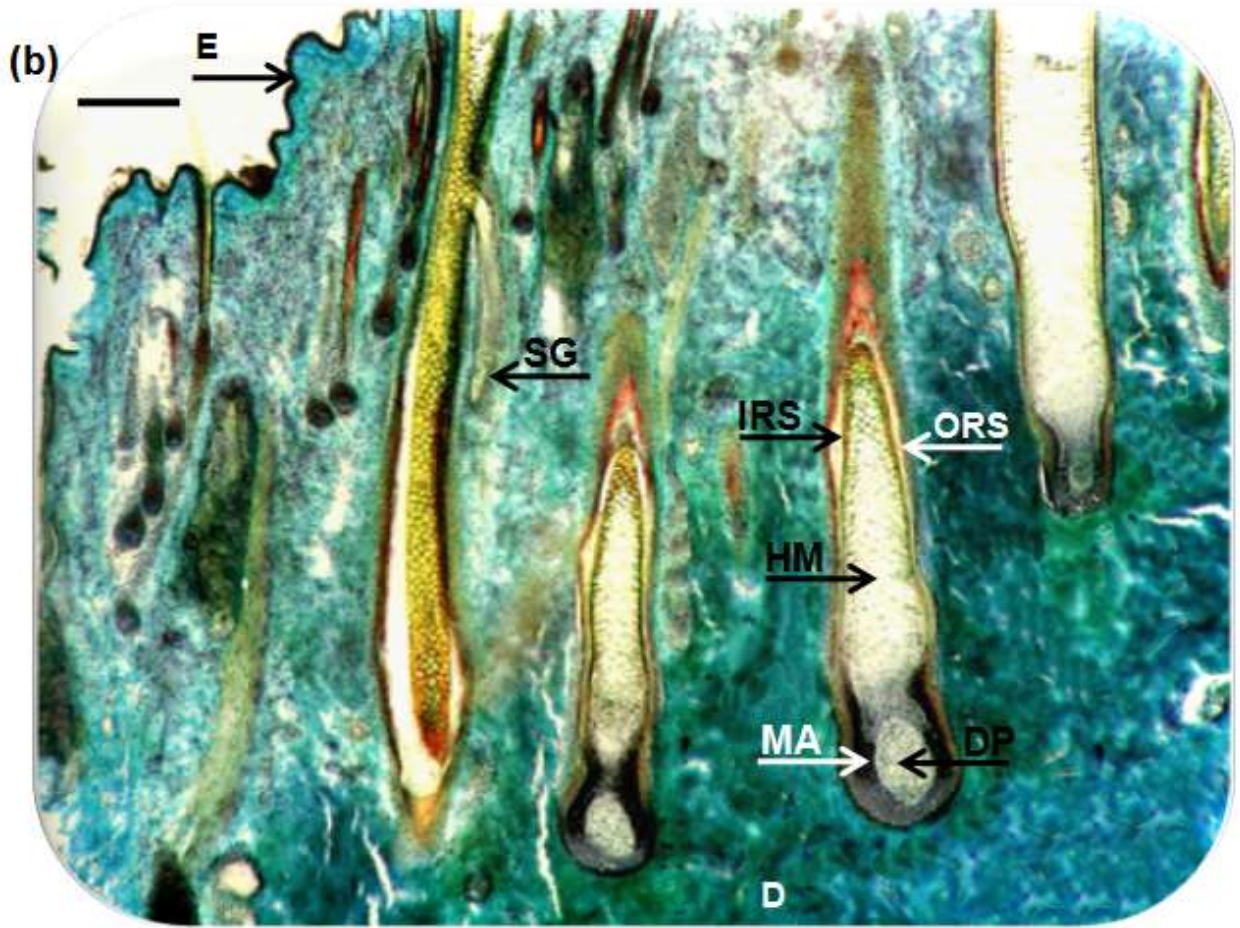
Figure 2.9 Histology of red deer skin showing follicles in telogen

Side-views of deer skin showing hair follicles in telogen (a) (Bar=318.6µm) and cryosections of deer skin stained with the histological stain, Sacpic with hair follicles in telogen (b) (Bar=207µm).

(b) In telogen follicles, the inner root sheath stained bright red, the fully keratinised parts of the hair stained yellow and at higher magnification (c) the fully keratinised hair fibre base surrounded by and interdigitated with inner root sheath (IRS-red) is clear (Bar=30µm).

(b) Epidermis, keratinised hair fibre, Interdigitated base, Dermis

(c) Keratinised hair fibre, Inner root sheath, Outer root sheath, Connective/dermal sheath
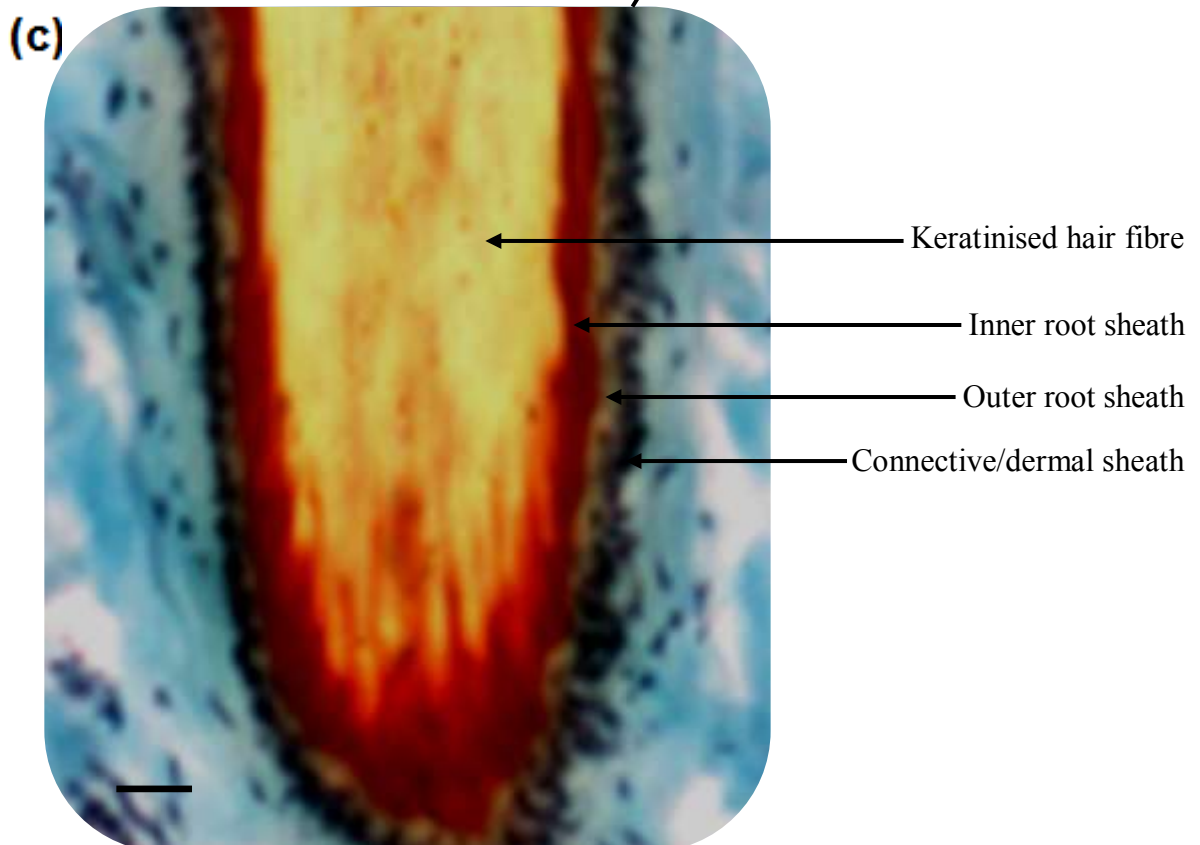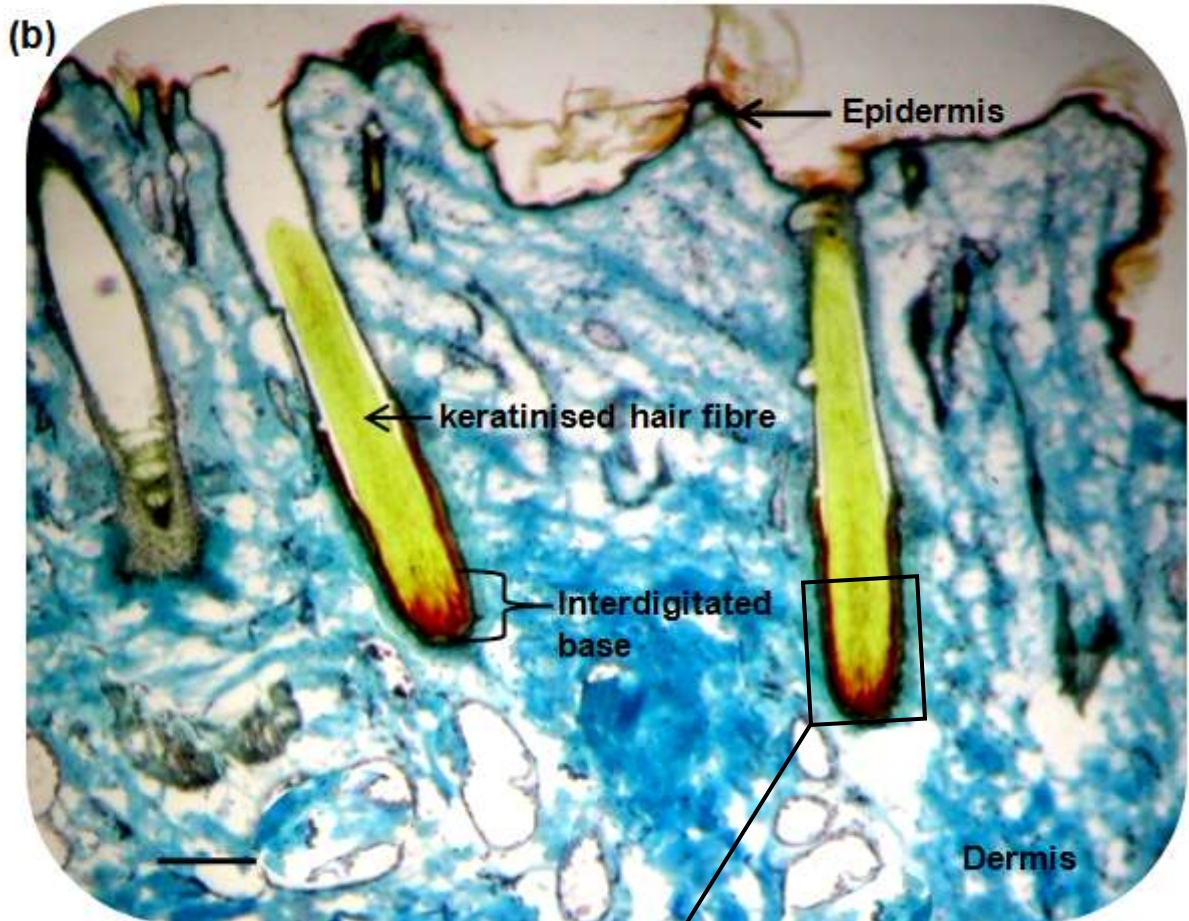
2.4.1.2 A comparison of red deer hair follicles at different stages of the hair follicle cycle

Deer hair follicles were cryosectioned at different stages of the hair follicle cycle. Sacpic staining was used to enable a histological comparison of the follicle structures. The general structure of catagen follicles revealed the shrinking of the hair follicle and the regression of the lower follicle (Figure 2.10 c & d). The staining clearly showed the deterioration of the dermal papilla and the formation of the club hair. Similar to the anagen phase (Figure 2.10 a & b), the connective/dermal tissue sheath surrounded the entire follicle separating it from the dermis. This was also true for telogen hair follicles (Figure 2.10 e & f). Figure 2.10f notably visualised the club-shaped proximal end of the telogen hair, which was surrounded by a thick epithelial sac, and the fully keratinised hair fibre interdigitated with inner root sheath (Figure 2.10 e & f). The medulla is lost in fully keratinised hair fibre and this has led to the hair fibre outside of the follicle splitting (Figure 2.10e).

The dissected early mid anagen hair follicle with removing telogen hair (Figure 2.10g) and the above Sacpic staining were used to reconstruct the classical hair growth cycle (see Figure 1.2) with higher definition.

Figure 2.10 Deer hair follicles in different growth cycle stages

Stained hair follicle in anagen (a) (Bar=443μm), (b) (Bar=49μm); stained catagen hair follicle showing the regressing lower follicle (c) (Bar=59μm), (d) (Bar=30μm). Stained telogen hair follicle showing the fully keratinised hair fibre base interdigitated with inner root sheath (e) (Bar=151μm), (f) (Bar=21μm); (g) showing dissected hair follicle in mid anagen showing original and new hair follicle (Bar=159μm).
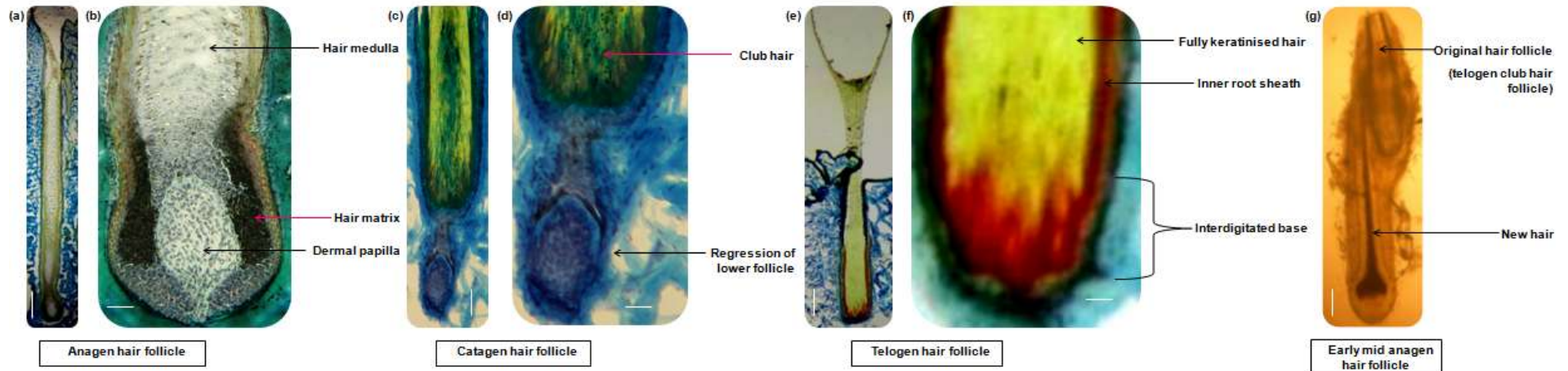
2.4.2 RT-PCR analysis of K$^+_{ATP}$ channel sub-units in anagen red deer hair follicles

To investigate anagen red deer hair follicles, five different red deer stags were used to gather the neck/mane skin samples. Individual hair follicles were microdissected & pooled separately for each individual deer for poly (A) RNA extraction, cDNA preparation and identification of 5 K$^+_{ATP}$ channel subunit genes (as described in section 2.3.2.2).   Gene identity was confirmed by size on gel electrophoresis and gene product sequence analysis. The NCBI BLAST programme was used to align the homology of the sequenced deer product against the known human sequence.

Prior to investigating the expression of K$^+_{ATP}$ channel sub-units, RT-PCR was performed using the primer pair specific to the cytoskeletal protein β-actin. The detection of this housekeeping gene would indicate that the isolated RNA is of sufficient quality for RT-PCR to be performed effectively (Croft, 2002; Davies, 2001). PCR products from all hair follicle samples corresponded to the anticipated size of β-actin (Figure 2.11).

In the negative control, in which the template cDNA was excluded from the reaction mix, no PCR products were present, indicating that the amplification of the cDNA synthesised from the mRNA samples produced the PCR products. Furthermore, it also demonstrated that no DNA contamination occurred in the reaction mix.

To ascertain the identity of the β-actin PCR product sequence analysis was used (as described in section 2.3.2.4.2).   Through the use of the NCBI BLAST programme the homology of the sequenced PCR product was compared to the

known expected human sequence. The β-actin PCR product of the deer hair follicle, exhibited 94% homology to the known human sequence (accession number: NM_001101) (Figure 2.12). This indicates the product is from the β-actin gene. The successful amplification of β-actin on all cDNA samples verified that the cDNA samples were of adequate quality for further RT-PCR analysis to be performed, investigating the expression of K^+_{ATP} channel sub-units.

Figure 2.11 PCR detection of β-actin in anagen red deer hair follicles

The quality of the cDNA samples for anagen (A) follicles were investigated by PCR using specific primers for β-actin (see table 2.1); 5μl of cDNA was used for each reaction mix. The PCR products were separated by 1.5% agarose gel electrophoresis and visualised with ethidium bromide staining. M- DNA ladder (The DNA ladder ranges from 100–1,500bp; in 100bp increments, 10μl of DNA ladder was loaded); Lanes A1-A5 show expression of β-actin in anagen follicles from 5 deer stags (30 μl of PCR product/lane); N-negative control: cDNA was omitted from the PCR reaction. The expected amplicon size for β-actin is 838 bp.

Figure 2.12   Sequencing results for β-actin RT-PCR product, following amplification from deer hair follicle cDNA, compared to known human sequence

To ascertain the identity of the PCR product the expected amplicon size band (838 base pairs) was cut out from the gel, purified and sequenced. The NCBI BLAST programme was used to align the homology of the sequenced deer product (black; sbjct) against the known human β-actin sequence (blue; query). The bases that match in the two sequences are shown by a vertical line. The β-actin PCR product of the deer hair follicle exhibited 94% homology to the known human sequence (accession number: NM_001101).

```
Query  247  GAGGGGTATGCCCTCCCCCATGCCATCCTGCGTCTGGACCTGGCTGGCCGGGACCTGACT  306
            ||||||||  ||||||||||| |||||||||||||||||||||||||||||||||||||||
Sbjct  556  GAGGGGTACGCCCTCCCCCACGCCATCCTGCGTCTGGACCTGGCTGGCCGGGACCTGACA  498

Query  307  GACTACCTCATGAAGATCCTCACCGAGCGCGGCTACAGCTTCACCACCACGGCCGAGCGG  366
            ||||||||||||||||||||||||  || || || ||||||||| |||||||| |||||||
Sbjct  497  GACTACCTCATGAAGATCCTCACGGAACGGGGTTACAGCTTTACCACCACAGCCGAGCGG  438

Query  367  GAAATCGTGCGTGACATTAAGGAGAAGCTGTGCTACGTCGCCCTGGACTTCGAGCAAGAG  426
            |||||  ||||||||||| |||||||||||||||||||||||||||||||||||| |||  |||
Sbjct  437  GAAATTGTGCGTGACATCAAGGAGAAGCTGTGCTACGTCGCCCTGGACTTCGAGCAGGAG  379

Query  427  ATGGCCACGGCTGCTTCCAGCTCCTCCCTGGAGAAGAGCTACGAGCTGCCTGACGGCCAG  486
            ||||||||| |||||| |||    ||||||| |||||||||||| ||||||||||| || |||
Sbjct  378  ATGGCCACTGCTGCATCCTCCTCCTCCTTGGAGAAGAGCTATGAGCTGCCTGATGGTCAG  320

Query  487  GTCATCACCATTGGCAATGAGCGGTTCCGCTGCCCTGAGGCACTCTTCCAGCCTTCCTTC  546
            || |||||||||||||||||||||||||| || || |||||||||||||||||||||||||
Sbjct  319  GTGATCACCATTGGCAATGAGCGGTTCCGGTGTCCCGAGGCACTCTTCCAGCCTTCCTTC  260

Query  547  CTGGGCATGGAGTCCTGTGGCATCCACGAAACTACCTTCAACTCCATCATGAAGTGTGAC  606
            ||||| |||||||||||||||||||||||||| ||| ||||||||||||||||||||||||
Sbjct  259  CTGGGTATGGAGTCCTGTGGCATCCACGAAACCACCTTCAACTCCATCATGAAGTGTGAC  200

Query  607  GTGGACATCCGCAAAGACCTGTACGCCAACACAGTGCTGTCTGGCGGCACCACCATGTAC  666
            |||||||||||||||||||||||| |||||||||| |||||||||||| || |||||||||
Sbjct  199  GTGGACATCCGCAAAGACCTGTATGCCAACACGGTGCTGTCTGGTGGGACCACCATGTAC  140

Query  667  CCTGGCATTGCCGACAGGATGCAGAAGGAGATCACTGCCCTGGCACCCAGCACAATGAAG  726
            ||||||||  ||||||||||||||||| |||||||||||||||||| ||||||||||||||
Sbjct  139  CCTGGCATCGCCGACAGGATGCAGAAAGAGATCACTGCCCTGGCTCCCAGCACAATGAAG  80

Query  727  ATCAAGATCATTGCTCCTCCTGAGCGCAAGTACTCCGTGTGGATCGGCGGCTCCATCCTG  786
            |||||||||||||||||||||||||||||||||||| |||||||||||||||||||||||||
Sbjct  79   ATCAAGATCATTGCTCCTCCTGAGCGCAAGTACTCGGTGTGGATCGGCGGCTCCATCCTG  20

Query  787  GCCTCGCTGTCCACCTTCC  805
            |||||  |||||||||||||
Sbjct  19   GCCTCCCTGTCCACCTTCC  1
```

-82-

The expression of regulatory sulphonylurea sub-units of K^+_{ATP} channels in red deer anagen hair follicles was investigated, using specific primers for SUR1, SUR2A and SUR2B. A single pair of primers was used to investigate the expression of the SUR2 genes, as SUR2A and 2B are different splice variants of the SUR2 gene (Isomoto *et al.*, 1996). All cDNA samples from anagen hair follicles produced PCR products of the expected size 291 bp for the SUR1 gene (Figure 2.13) and 312 bp for SUR2B gene (Figure 2.15).

The gene expression for SUR2A was not detected in anagen follicles (Figure 2.15). However, deer skeletal muscle cDNA used as a positive control for the SUR2A gene did produce an appropriately sized band at 451 bp (Figure 2.15) validating the method used. The negative control (N) for all PCR products, where the template cDNA was excluded from the reaction mix, was clear of any bands, indicating the PCR products are a direct result of cDNA amplification, and demonstrating an absence of contamination. The identity of SUR1 and SUR2B gene products was confirmed via sequencing. The SUR1 PCR product of deer hair follicle cDNA exhibited 95% homology to the known human sequence (accession number: AF087138) (Figure 2.14), while the SUR2B PCR product correlated with 91% homology with the known human sequence (accession number: AF087138) (Figure 2.16).

These results indicate that red deer hair follicles express the genes for at least two forms of sulphonylurea subunits of K^+_{ATP} channels in anagen hair follicles.

Figure 2.13 PCR detection of SUR1 in red deer anagen hair follicles

The PCR products were separated by 1.5% agarose gel electrophoresis and visualised with ethidium bromide staining. M- DNA ladder (The DNA ladder ranges from 100–1,500bp; in 100bp increments, 10µl of DNA ladder was loaded); Lanes A1-A5 show expression of SUR1 in anagen follicles from 5 deer stags (30 µl of PCR product/lane); N-negative control: cDNA was omitted from the PCR reaction, B- blank. The expected amplicon size for SUR1 is 291bp.

Figure 2.14 Sequencing results for SUR1 RT-PCR product, following amplification from deer hair follicle cDNA, compared to known human sequence

To ascertain the identity of the PCR product the expected amplicon size band (291 base pairs) was cut out from the gel, purified and sequenced. The NCBI BLAST programme was used to align the homology of the sequenced deer product (black; sbjct) against the known human SUR1 sequence (blue; query). The bases that match in the two sequences are shown by a vertical line. The SUR1 PCR product of the deer hair follicle exhibited 95% homology to the known human sequence (accession number: AF087138).

```
Query  1    CGATGCCATCATCACAGAAGGCGGGGAGAATTTCAGCCAGGGACAGAGGCAGCTGTTCTG  60
            |||||||||||||||||||||||||||||| |||||||||||| ||||||||||||||||
Sbjct  242  CGATGCCATCATCACAGAAGGCGGGGAGAACTTCAGCCAGGGCCAGAGGCAGCTGTTCTG  183

Query  61   CCTGGCCCGGGCCTTCGTGAGGAAGACCAGCATCTTCATCATGGACGAGGCCACGGCTTC  120
            ||||||||| |||||||||||||||||||| |||||||||||||||| ||||| ||||||
Sbjct  182  CCTGGCCCGAGCCTTCGTGAGGAAGACCAGTATCTTCATCATGGACGAAGCCACAGCTTC  123

Query  121  CATTGACATGGCCACGGAAAACATCCTCCAAAAGGTGGTGATGACAGCCTTCGCAGACCG  180
            ||| |||||||||||||||||||||||||| || |||||||||| |||||||||||||||
Sbjct  122  CATCGACATGGCCACGGAAAACATCCTCCAGAAAGTGGTGATGACGGCCTTCGCAGACCG  63

Query  181  CACTGTGGTCACCATCGCGCATCGAGTGCACACCATCCTGAGTGCAGACCTGGTGA  236
            ||| |||||||||||||||| || ||||||||||||||||||||||||||||||||
Sbjct  62   CACCGTGGTCACCATCGCGCACCGCGTGCACACCATCCTGAGTGCAGACCTGGTGA  7
```

Figure 2.15 PCR detection of SUR2A/B in red deer anagen hair follicles

The PCR products were separated by 1.5% agarose gel electrophoresis and visualised with ethidium bromide staining. M- DNA ladder (The DNA ladder ranges from 100–1,500bp; in 100bp increments, 10μl of DNA ladder was loaded); Lanes A1-A5 show expression of SUR2A/B in anagen follicles from 5 deer stags (30 μl of PCR product/lane); N-negative control: cDNA was omitted from the PCR reaction, SM- deer skeletal muscle. The expected amplicon size for SUR2A is 451bp and 312bp for SUR2B.
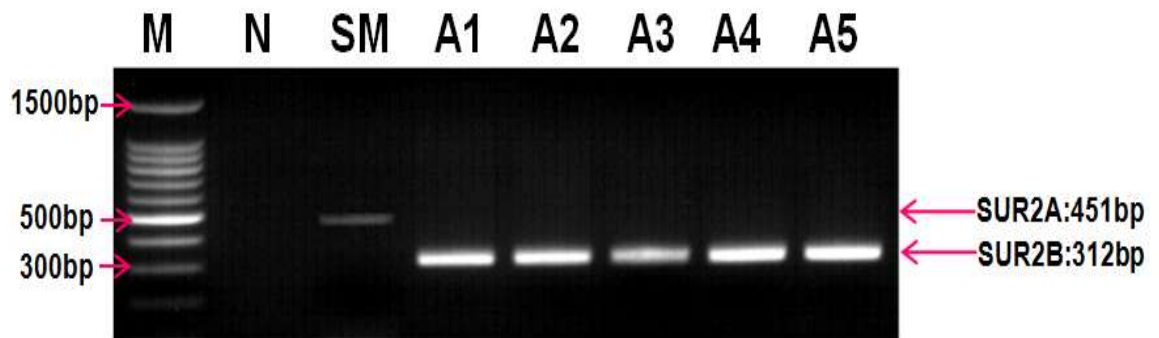
Figure 2.16 Sequencing results for SUR2A/B RT-PCR product, following amplification from deer hair follicle cDNA, compared to known human sequence

To ascertain the identity of the PCR product the expected amplicon size band (312 base pairs) was cut out from the gel, purified and sequenced. The NCBI BLAST programme was used to align the homology of the sequenced deer product (black; sbjct) against the known human SUR2A/B sequence (blue; query). The bases that match in the two sequences are shown by a vertical line. The SUR2A/B PCR product of the deer hair follicle exhibited 91% homology to the known human sequence (accession number: NM_005691).

```
Query   8    AATATGGTCAAATCTCTACCTGGAGGTCTAGATGCGGTTGTCACTGAAGGTGGGGAGAAT   67
             |||||||||||||||||||||| |||||||||||||| ||||||||||||||||||||||
Sbjct   280  AATATGGTCAAATCTCTACCAGGAGGTCTAGATGCAGTTGTCACTGAAGGTGGGGAGAAT   221

Query   68   TTTAGCGTTGGACAGAGACAGCTATTTTGCCTTGCCAGGGCCTTTGTCCGCAAAAGCAGC   127
             |||||||||||||||||||||||| || ||||||||||||||||||||||||||||||||
Sbjct   220  TTTAGCGTTGGACAGAGACAGCTGTTCTGCCTTGCCAGGGCCTTTGTCCGCAAAAGCAGT   161

Query   128  ATTCTTATTATGGATGAGGCAACAGCTTCCATTGACATGGCCACAGAGAATATTTTGCAA   187
             ||||| || ||||||||| ||||| ||||||||| |||||||||| || || ||||||||
Sbjct   160  ATTCTCATCATGGATGAAGCAACGGCTTCCATCGACATGGCCACGGAAAACATTTTGCAG   101

Query   188  AAAGTAGTAATGACAGCCTTTGCAGACCGGACCGTGGTGACAATAGCTCATCGAGTACAC   247
             ||||| || ||||||||| ||||||||| || ||||| || |||||||||||||| |||
Sbjct   100  AAAGTGGTCATGACAGCTTTTGCAGATCGCACCGTTGTTACAATAGCTCATCGGGTTCAC   41

Query   248  ACTATTCTGACGGCAGACCTGGTTATTGTGA   278
             ||||||||||||||||||| ||||||||||
Sbjct   40   ACTATTCTGACGGCAGACCTAGTTATTGTGA   10
```

K^+_{ATP} channels only function in the presence of both a pore forming sub-unit (Kir6.x) and a regulatory sulphonylurea sub-unit (SUR) (Inagaki *et al.*, 1996; Yamada *et al.*, 1997). Thus the gene expression of the pore forming sub-units Kir6.1 and Kir6.2 were also investigated. The PCR products of anagen red deer whole hair follicle revealed the expression of Kir6.1 (Figure 2.17), exhibiting 91% homology (Figure 2.18) with the known human sequence (accession number: NM_004982). The expression of Kir6.2 gene was also identified in the anagen follicle (Figure 2.19), with a correlating homology of 94% with the known human sequence (accession number: D50582) (Figure 2.20).

Figure 2.17 PCR detection of Kir6.1 in red deer anagen hair follicles

The PCR products were separated by 1.5% agarose gel electrophoresis and visualised with ethidium bromide staining. M- DNA ladder (The DNA ladder ranges from 100–1,500bp; in 100bp increments, 10μl of DNA ladder was loaded); Lanes A1-A5 show expression of Kir6.1 in anagen follicles from 5 deer stags (30 μl of PCR product/lane); N-negative control: cDNA was omitted from the PCR reaction, B- blank. The expected amplicon size for Kir6.1 is 336bp.
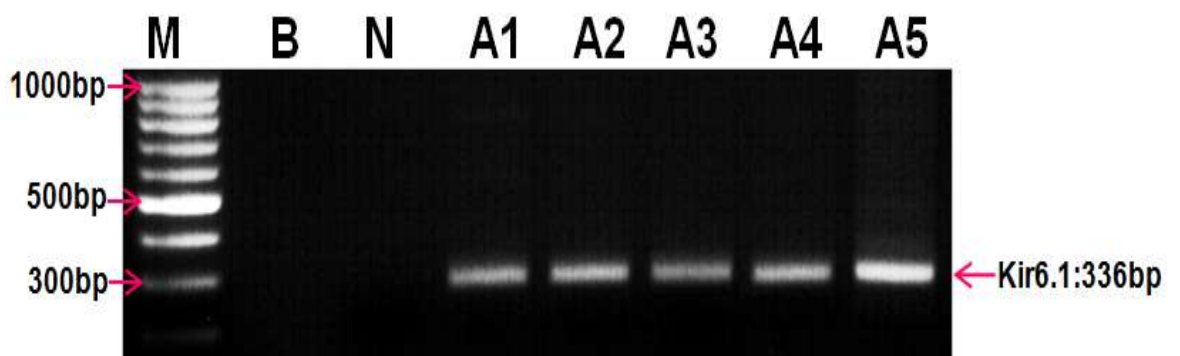
Figure 2.18   Sequencing results for Kir6.1 RT-PCR product, following amplification from deer hair follicle cDNA, compared to known human sequence

To ascertain the identity of the PCR product the expected amplicon size band (336 base pairs) was cut out from the gel, purified and sequenced. The NCBI BLAST programme was used to align the homology of the sequenced deer product (black; sbjct) against the known human Kir6.1 sequence (blue; query). The bases that match in the two sequences are shown by a vertical line. The Kir6.1 PCR product of the deer hair follicle exhibited 91% homology to the known human sequence (accession number: NM_004982).

```
Query  33   TGCTCTTCGCTATCATGTGGTGGCTGGTGGCCTTTGCCCATGGGGACATCTATGCTTACA  92
            ||||||||||   |||||||||||||||||||||||||||| ||||||||||||||||||
Sbjct  1    TGCTCTTCGCC-TCATGTGGTGGCTGGTGGCCTTTGCCCACGGGGACATCTATGCTTACA  59

Query  93   TGGAGAAAAGTGGAATGGAGAAAAGTGGTTTGGAGTCCACTGTGTGTGTGACTAATGTCA  152
            |||||||||| || ||||||||||||||| |||||| |||| |||||||||||| ||||
Sbjct  60   TGGAGAAAAGCGGGATGGAGAAAAGTGGCTTGGAGGCCACCGTGTGTGTGACTAACGTCA  119

Query  153  GGTCTTTCACTTCTGCTTTTCTCTTCTCCATTGAAGTTCAAGTTACCATTGGGTTTGGAG  212
            |||||||||| ||||| || |||||||||||||||||||||||| || ||||| |||||||
Sbjct  120  GGTCTTTCACCTCTGCCTTCCTCTTCTCCATTGAAGTTCAAGTGACAATTGGATTTGGAG  179

Query  213  GGAGGATGATGACAGAGGAATGCCCTTTGGCCATCACGGTTTTGATTCTCCAGAATATTG  272
            |||| ||||||||| |||||||||||| |||| ||||| ||  ||||||| ||||| ||||
Sbjct  180  GGAGAATGATGACTGAGGAATGCCCTCTGGCTATCACAGTCCTGATTCTACAGAACATTG  239

Query  273  TGGGTTTGATCATCAATGCAGTCATGTTAGGCTGCATTTTCATGAAAACAGCTCAGGCTC  332
            |||||||||||||||||||| |||||||| |||||||||||||||||||||||||||||||
Sbjct  240  TGGGTTTGATCATCAATGCGGTCATGTTGGGCTGCATTTTCATGAAAACAGCTCAGGCTC  299

Query  333  ACA  335
            |||
Sbjct  300  ACA  302
```

Figure 2.19 PCR detection of Kir6.2 in red deer anagen hair follicles

The PCR products were separated by 1.5% agarose gel electrophoresis and visualised with ethidium bromide staining. M- DNA ladder (The DNA ladder ranges from 100–1,500bp; in 100bp increments, 10μl of DNA ladder was loaded); Lanes A1-A5 show expression of Kir6.2 in anagen follicles from 5 deer stags (30 μl of PCR product/lane); N-negative control: cDNA was omitted from the PCR reaction. The expected amplicon size for Kir6.2 is 301bp.
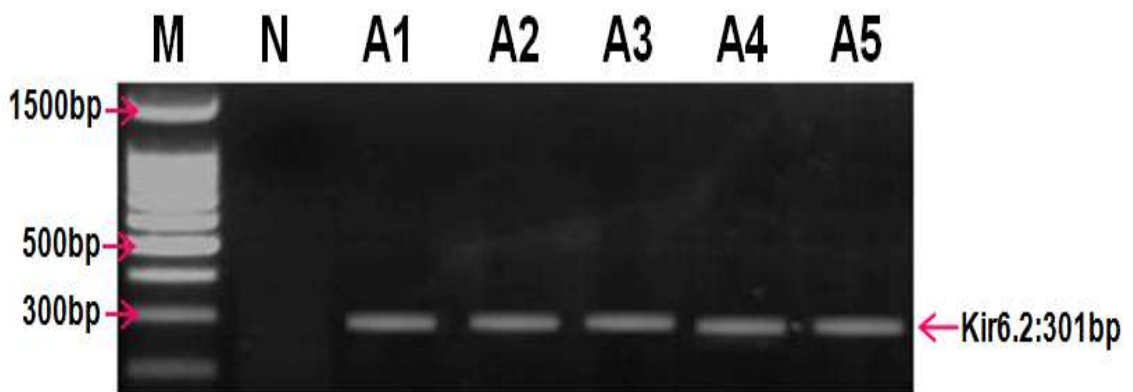
Figure 2.20   Sequencing results for Kir6.2 RT-PCR product, following amplification from deer hair follicle cDNA, compared to known human sequence

To ascertain the identity of the PCR product the expected amplicon size band (301 base pairs) was cut out from the gel, purified and sequenced. The NCBI BLAST programme was used to align the homology of the sequenced deer product (black; sbjct) against the known human Kir6.2 sequence (blue; query). The bases that match in the two sequences are shown by a vertical line. The Kir6.2 PCR product of the deer hair follicle exhibited 94% homology to the known human sequence (accession number: D50582).

```
Query  34   CCCACAAGAACATCCGGGAGCAGGGCCGCTTCCTGCAGGACGTGTTCACCACGCTGGTGG  93
            |||||||||||||||||||||| ||||||||||||||| ||||||||||   |||   |||||
Sbjct  1    CCCACAAGAACATCCGGGAGCNGGGCCGCTTCCTGCNGGACGTGTTCANNACGNNGGTGG  60

Query  94   ACCTCAAGTGGCCACACACATTGCTCATCTTCACCATGTCCTTCCTGTGCAGCTGGCTGC  153
            |||||||||||||||||||||| |||||||||||||||||||||||||||||||||||||||
Sbjct  61   ACCTCAAGTGGCCACACACATTGNTCATCTTCACCATGTCCTTCCTGTGCAGCTGGCTGC  120

Query  154  TCTTCGCCATGGCCTGGTGGCTCATCGCCTTCGCCCACGGTGACCTGGCCCCCAGCGAGG  213
            || |||||||||||||||||||| |||||||||||||||||||||||||||||||||||||||
Sbjct  121  TCNTCGCCATGGCCTGGTGGCTCNTCGCCTTCGCCCACGGTGACCTGGCCCCCAGCGAGG  180

Query  214  GCACTGCTGAGCCCTGTGTCACCAGCATCCACTCCTTCTCGTCTGCCTTCCTTT  267
            |||||||||||||||||||||| ||||||||||||| ||||||||| ||||
Sbjct  181  GCACTGCTGAGCCCTGTGTCACCNGCATCCACTCCTTCNCGTCTGCCTTNCTTT  234
```

-92-

2.4.3 Immunohistochemical localisation of K$^+_{ATP}$ channel subunits in anagen red deer hair follicle bulbs

To confirm protein expression and to localise K$^+_{ATP}$ channel subunits in red deer hair bulb, 5 μm cryosections of five different red deer stags were used. When frozen sections of red deer skin were stained with polyclonal antibodies for the various K$^+_{ATP}$ channel subunits, no staining was seen in any of the negative control sections (Figures 2.21a to 2.21e). Staining with SUR2B and Kir6.1 antibodies was seen in the dermal papilla and connective tissue/dermal sheath (Figures 2.21h & 2.21i respectively). There was no staining in lower matrix or developing hair but some in the upper bulb in the developing inner root sheath. In contrast, there was no staining in the dermal papilla or dermal sheath with the antibodies for SUR1 and Kir6.2 (Figures 2.21f & 2.21j respectively). The antibody for Kir6.2 appeared to stain the upper matrix (Figure 2.21j), but this was closely associated with the black pigment and the staining took a brown hue rather than red. The dermal papilla and dermal sheath showed no expression of Kir6.2. The dermal papilla and dermal sheath also showed no staining when the SUR1 antibody was used (Figure 2.21f). There was a suggestion of some redness in the upper matrix giving a reddish colour but this was not convincing. This leads to difficulty in determining the expression of SUR1 and Kir6.2. This could be as a result of species cross reactivity. In addition pre-adsorbed antibodies were not used as a control, as the antigen was not available. SUR2A did not stain any area of the hair bulb (Figure 2.21g).

Figure 2.21 Immunolocalisation of K⁺$_{ATP}$ channel subunits in the anagen red deer hair follicle bulb

Immunohistochemical analysis of deer cryosections localised same K⁺$_{ATP}$ channel subunits; SUR2B and Kir6.1 were expressed in the dermal papilla and dermal sheath (h & i). No staining occurred in the hair bulb with the antibody to SUR2A (g) similar to the negative controls when the primary antibody was omitted (a-e). No staining was evident in the dermal sheath or papilla with the antibodies to SUR1 and Kir6.2 (f & j), but the upper matrix appeared to have some red staining associated with pigmented regions. Normal dark pigment (melanin) is visible in the hair bulb. CTS/DS- connective tissue/dermal sheath; RS- developing root sheaths; HM- hair matrix and DP- dermal papilla (Bar=50μm).
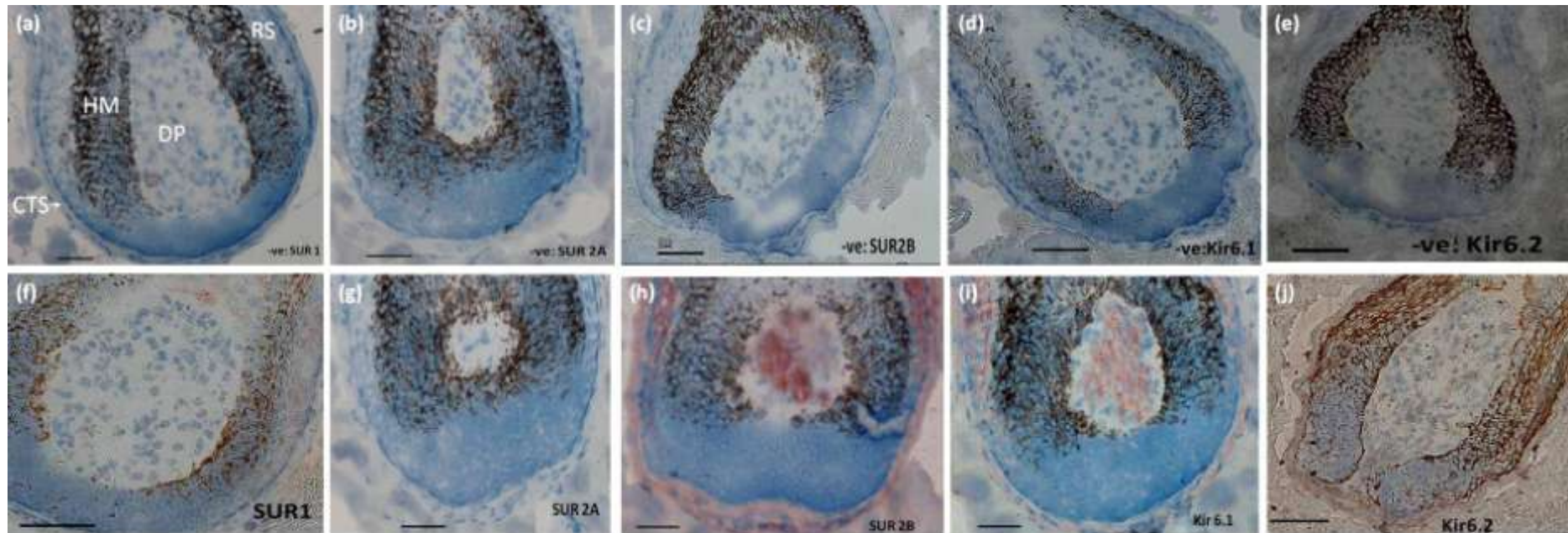
2.4.4 RT-PCR analysis of K$^+_{ATP}$ channel sub-units in telogen red deer hair follicles

      To investigate K$^+_{ATP}$ channel sub-units in telogen red deer hair follicles the same procedures were followed as detailed in section 2.4.2, for anagen red deer hair follicles. PCR products from all telogen hair follicle samples corresponded to the anticipated size of the β-actin, confirming that the isolated RNA was of sufficient quality for RT-PCR to be performed effectively (Figure 2.22). The cDNA from anagen follicles were used in parallel to the telogen follicles as a positive control. Telogen hair follicles did not express any of the regulatory sulphonylurea sub-units of K$^+_{ATP}$ channels: SUR1 (Figure 2.23), SUR2A/B (Figure 2.24). Similarly, the PCR products of telogen red deer hair follicles rendered no expression of the pore forming sub-unit Kir6.1 (Figure 2.25) or Kir6.2 (Figure 2.26).

Figure 2.22 PCR detection of β-actin in telogen red deer hair follicles

The quality of the cDNA samples for telogen (T) follicles were investigated by PCR using specific primers for β-actin (see table 2.1); 5µl of cDNA was used for each reaction mix.   The PCR products were separated by 1.5% agarose gel electrophoresis and visualised with ethidium bromide staining. M- DNA ladder (The DNA ladder ranges from 100–1,500bp; in 100bp increments, 10µl of DNA ladder was loaded); Lanes T1-T5 show expression of β-actin in telogen follicles from 5 deer stags (30 µl of PCR product/lane); A- anagen sample, was used parallel with telogen samples as positive control; N-negative control: cDNA was omitted from the PCR reaction. The expected amplicon size for β-actin is 838 bp.
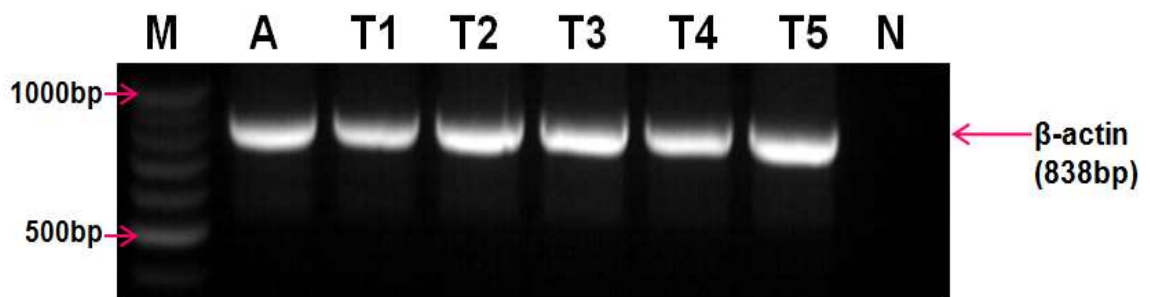
Figure 2.23 PCR detection of SUR1 in red deer telogen hair follicles

The PCR products were separated by 1.5% agarose gel electrophoresis and visualised with ethidium bromide staining. M- DNA ladder (The DNA ladder ranges from 100–1,500bp; in 100bp increments, 10μl of DNA ladder was loaded); Lanes T1-T5 show expression of SUR1 in telogen follicles from 5 deer stags (30 μl of PCR product/lane); A- anagen sample, was used parallel with telogen samples as positive control; N-negative control: cDNA was omitted from the PCR reaction; PDs- Primer dimers. The expected amplicon size for SUR1 is 291bp.
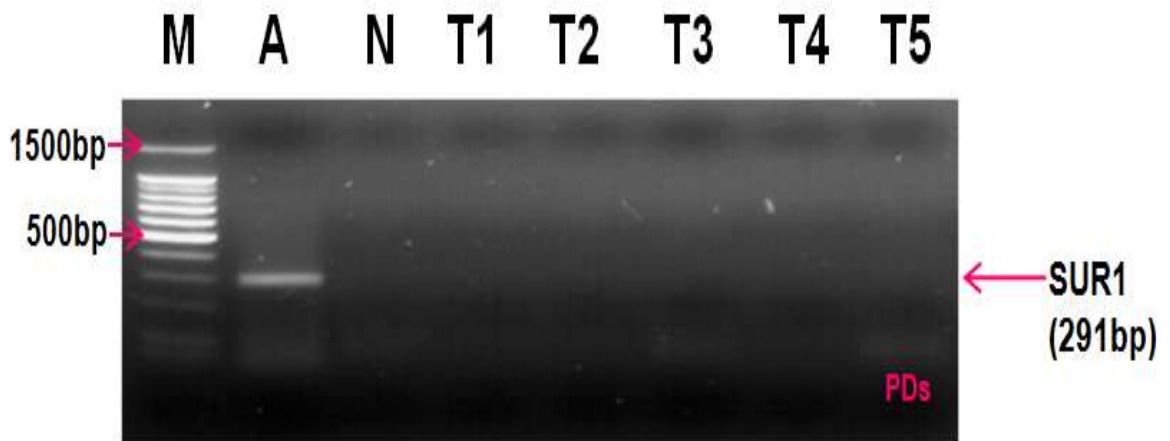
Figure 2.24 PCR detection of SUR2A/B in red deer telogen hair follicles

The PCR products were separated by 1.5% agarose gel electrophoresis and visualised with ethidium bromide staining. M- DNA ladder (The DNA ladder ranges from 100–1,500bp; in 100bp increments, 10µl of DNA ladder was loaded); Lanes T1-T5 show expression of SUR2A/B in telogen follicles from 5 deer stags (30 µl of PCR product/lane); A- anagen sample, was used parallel with telogen samples as positive control; N-negative control: cDNA was omitted from the PCR reaction; PDs- Primer dimers. The expected amplicon size for SUR2A is 451bp and 312bp for SUR2B.

Figure 2.25 PCR detection of Kir6.1 in red deer telogen hair follicles

The PCR products were separated by 1.5% agarose gel electrophoresis and visualised with ethidium bromide staining. M- DNA ladder (The DNA ladder ranges from 100–1,500bp; in 100bp increments, 10μl of DNA ladder was loaded); Lanes T1-T5 show expression of Kir6.1 in telogen follicles from 5 deer stags (30 μl of PCR product/lane); A- anagen sample, was used parallel with telogen samples as positive control; N-negative control: cDNA was omitted from the PCR reaction; PDs- Primer dimers. The expected amplicon size for Kir6.1 is 336bp.
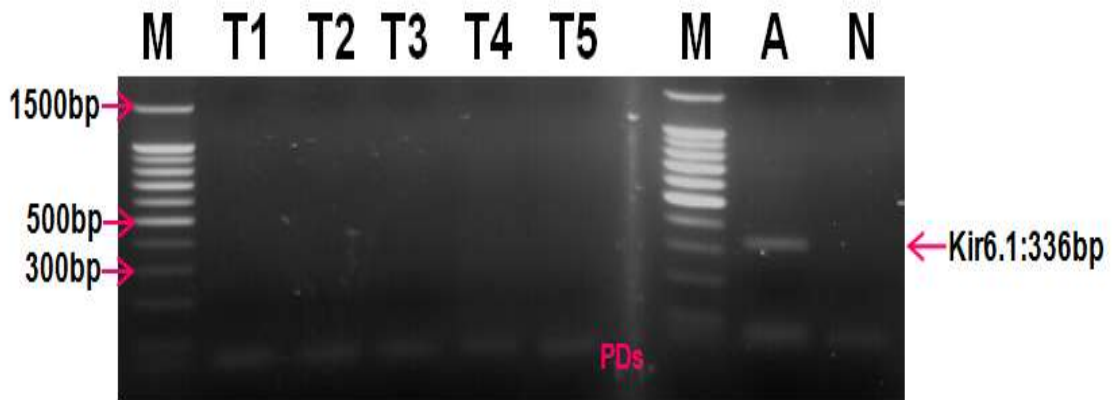
Figure 2.26 PCR detection of Kir6.2 in red deer telogen hair follicles

The PCR products were separated by 1.5% agarose gel electrophoresis and visualised with ethidium bromide staining. M- DNA ladder (The DNA ladder ranges from 100–1,500bp; in 100bp increments, 10µl of DNA ladder was loaded); Lanes T1-T5 show expression of Kir6.2 in telogen follicles from 5 deer stags (30 µl of PCR product/lane); A- anagen sample, was used parallel with telogen samples as positive control; N-negative control: cDNA was omitted from the PCR reaction; PDs- Primer dimers. The expected amplicon size for Kir6.2 is 301bp.
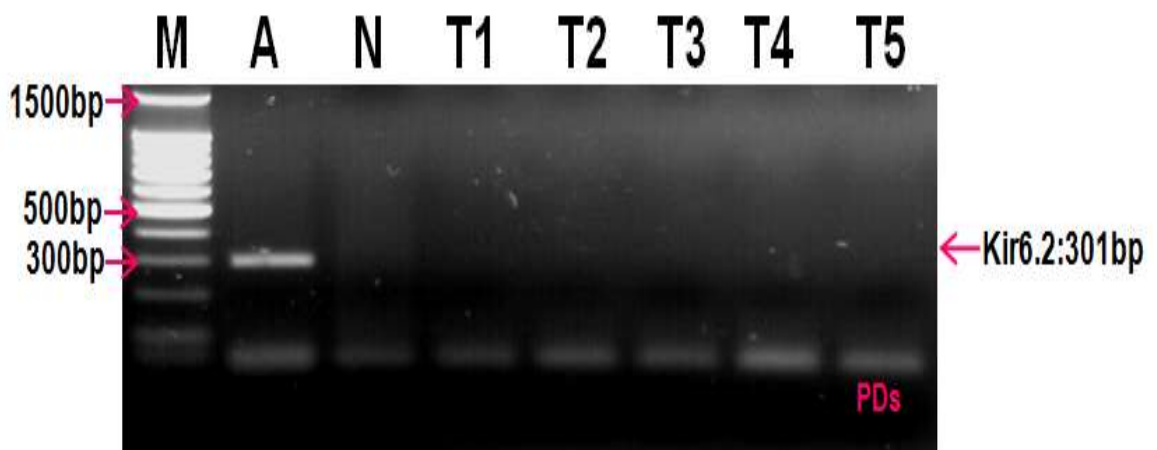
2.5 Discussion

The main aim of this study was to confirm the pharmacological responses of red deer (*Cervus elaphus*) follicles in organ culture reported by Davies *et al* (2005), which suggested the presence of K^+_{ATP} channels in deer hair follicles, by investigating the gene expression of K^+_{ATP} channel sub-units using RT-PCR in anagen red deer whole hair follicles. This would improve its practicality as a hair growth model system. The second aim was to determine whether the gene expression of K^+_{ATP} channel sub-units occurred in the telogen stage of the hair cycle. Red deer hair follicles were selected for this study because deer hair growth is synchronous, which meant that in any given area the hair follicles would be at the same hair cycle stage. This allowed for a sufficient amount of hair follicles, approximately 60, to be pooled for RNA isolation from the same deer.

At the initial stage of the investigation a histological comparison was drawn between human and red deer hair follicles. The deer hair follicles were then further investigated at the different stages of the hair cycle. To do this human skin samples and red deer anagen and telogen skin samples were frozen, sectioned and stained using Sacpic staining, which provides an excellent visualisation of the hair follicle structure (Nixon 1993; Nutbrown and Randall 1996). The large size of deer hair follicles allowed for ease in tissue sectioning, serving better in sample orientation within the cryostat. Human scalp hair follicles are smaller and less densely packed, compared to deer hair follicles, proving both more difficult to section and also reducing room for error because of the diminished sample size.

The Sacpic staining technique employed was more complex but offered a superior result in comparison to the other staining methods attempted, such as haematoxylin and eosin histochemical staining. The staining provided clear

visualisation of the hair follicle structure, highlighting the various layers of the hair follicle. The histological staining of the human scalp skin exhibited the hair follicle extending down into subcutaneous fat layer (Figure 2.7) and the staining results of the red deer skin showed hair follicles extending deep into the dermis (Figure 2.8). Though the human hair follicle was smaller in structure than that of the deer, rendering the medulla visible in the deer hair follicle, the structure was on the whole similar, thereby reinforcing the deer hair follicle as a good model system for the research.

Following histological staining, the gene expression of all components of potassium channel sub-units in isolated red deer anagen hair follicles was investigated. Detection of cytoskeletal protein β-actin (Figure 2.11) confirmed that the isolated RNA from each red deer sample was of sufficient quality for RT-PCR to be performed effectively (Croft, 2002; Davies, 2001). Negative controls without the template cDNA in all RT-PCR investigations yielded no PCR products, indicating that the amplification of the cDNA synthesised from the mRNA samples produced the PCR products. Furthermore, it also demonstrated that no DNA contamination occurred in the reaction mix.

The expression of both types of sub-units, the sulphonylurea sub-unit (SUR) and the pore-forming (Kir6.x), are necessary to form a functional K^+_{ATP} channel (Gribble *et al.*, 1997; Inagaki *et al.*, 1995a; Yamada *et al.*, 1997). Red deer hair follicles expressed SUR1 (Figure 2.13) and SUR2B (Figure 2.15) regulatory units and both pore forming units Kir6.1 (Figure 2.17) and Kir6.2 (Figure 2.19) in anagen follicles. The identity of these PCR products were confirmed by sequencing with over 91% homology with the human genes (Figures 2.14, 2.16, 2.18 and 2.20). Therefore red deer hair follicles expressed the genes for both components of K^+_{ATP}

channels in the anagen phase of the hair cycle. The gene expression for SUR2A was not detected, although it was seen in the positive control of deer skeletal muscle (Figure 2.15).

The immunohistochemical localisation K^+_{ATP} subunits in deer hair bulb, confirmed the presence of SUR2B and Kir6.1 proteins, which are expressed in the dermal papilla and connective tissue/dermal sheath (Figures 2.21h & 2.21i respectively) similar to the human (Shorter *et al.*, 2008), therefore it is most probable that SUR2B forms a K^+_{ATP} channel with Kir6.1; and SUR1 can form a K^+_{ATP} channel with Kir6.2, thereby suggesting the existence of a possible two K^+_{ATP} channels, in deer hair follicles. Furthermore such K^+_{ATP} channel combinations have been indicated in different tissues, such as SUR1/Kir6.2 K^+_{ATP} channel in the pancreatic β cells and brain (Inagaki *et al.*, 1995b; Sakura *et al.*, 1995; Babenko *et al.*, 1998a), supporting the suggestion that SUR1/Kir6.2 are likely to combine to form a K^+_{ATP} channel. SUR2B/Kir6.1 have been identified in vascular smooth muscle and SUR2B/Kir6.2B in non-vascular smooth muscle (Babenko *et al.*, 1998; Inagaki *et al.*, 1995b; Isomoto *et al.*, 1996; Yamada *et al.*, 1997). Further investigation may be required to indisputably establish that the staining exhibited in the dermal papilla is not vascular smooth muscle cells. This can be done by culturing dermal papilla cells and performing immunocytochemistry.

These findings are similar to a recent study in human anagen hair follicles, which also indicated the detection of SUR1, SUR2B, Kir6.1 and Kir6.2 subunits (Shorter *et al.*, 2008). They also correspond strongly with pharmacological observations in red deer hair follicles, where it was found that both minoxidil and the selective SUR1 channel opener, NNC 55-0118 (Novo Nordisk), stimulate hair follicle growth *in vitro* (Davies *et al.*, 2005), indicating the presence of both SUR1

and SUR2 types of channel, both playing a role in hair growth. The detection of SUR2B corresponds with minoxidil's affinity for SUR2B channels (Schwanstecher *et al*., 1998). Taken together these results confirm the existence of at least two types of K^+_{ATP} channels with SUR1 and SUR2B sulphonylurea receptors in deer hair follicles in the anagen phase. This is analogous with the findings of both SUR1 and SUR2B K^+_{ATP} channels in pig urethra (Yunoki *et al*., 2003). SUR1/Kir6.1 channels have been suggested not to be physiologically relevant (Babenko *et al*., 1998). An advantage to the fact that SUR2A was not detected in the anagen hair follicle, suggests that the K^+_{ATP} channels found in the cardiac tissue, formed by SUR2A/Kir6.2, are not expressed in the hair follicle, therefore allowing for the development of treatments for heart conditions, with the employment of the SUR2A sulphonylurea receptor, that would eliminate the undesirable side effect of hair growth.

Investigations into K^+_{ATP} channel sub-units in telogen red deer hair follicles detected no expression of any of the regulatory sulphonylurea sub-units: SUR1 (Figure 2.23), SUR2A/B (Figure 2.24). Similarly, the PCR products of telogen red deer hair follicles rendered no expression of the pore forming sub-unit Kir6.1 (Figure 2.25) or Kir6.2 (Figure 2.26).

To conclude, there is a strong correlation in the RT-PCR and immunohistochemical staining analysis of K^+_{ATP} channel sub-units in deer anagen hair follicles with those found in human hair follicles. Both express the genes SUR1, SUR2B, Kir6.1 and Kir6.2. Thereby exhibiting that both of the essential components, the sulphonylurea receptor and the pore forming sub-unit (Kir6.x) are expressed, enabling a functional channel to be present at the anagen phase of the hair cycle. This strengthens the use of deer hair follicles as a model system for

understanding hair follicle biology or screening new hair growth treatments. Furthermore, the absence of gene expression in telogen follicles supports the importance of K^+_{ATP} channels in the normal anagen processes.

Several investigations have reported that minoxidil may modulate the hair cycle. Price and Menefee's (1996) clinical observations suggested that topical minoxidil induced anagen. Minoxidil has also been reported to prolong the duration of the anagen phase (Messenger and Rundegren, 2004). An increase in the anagen/telogen follicle ratios in the scalp of balding men, after 12 months of minoxidil treatment was reported using histological staining (Abell, 1988). The application of topical minoxidil (2%) did not prevent alopecia as a result of chemotherapy (Granai *et al.*, 1991), but it did reduce the severity and duration of chemotherapy-induced alopecia (Duvic *et al.*, 1996; Wang *et al.*, 2006), suggesting that minoxidil promotes renewed anagen in resting follicles. Shorter *et al*'s (2008) investigations showed that minoxidil prolonged anagen in human hair follicle organ culture.

Several of these studies suggest that minoxidil advances anagen, suggesting an active K^+_{ATP} channel sub-unit in telogen, presumably by acting on telogen follicles. The absence of K^+_{ATP} channels in the red deer telogen hair follicles here indicate that they are possibly expressed at the end of the telogen phase, when exogen takes place.

The detection of SUR1 subunit gene expression in the deer anagen hair follicle is of key interest, as SUR1 receptors are unaffected by minoxidil and Davies *et al* (2005) showed that the selective SUR1 K^+_{ATP} channel opening drug NNC 55-0118 stimulated deer follicle growth in organ culture. This raises the prospect of novel pharmaceutical developments that stimulate hair growth via the SUR1 K^+_{ATP}

channels or combined treatment with minoxidil acting via SUR2B channels that enhance treatments for hair growth.

The red deer hair follicles model therefore appears to offer a useful, practical model for testing new molecules for treatment of hair growth disorders. This system should aid the development of better therapies for hair disorders.

Chapter 3

The role of SUR1 containing ATP-sensitive potassium channels in human hair growth

3.1   Introduction

With the introduction of hair follicle organ culture, researchers were offered an *in vitro* assay for the investigation of hair follicles (Philpott *et al.*, 1989). Previous research employed full-depth skin organ culture; this process involved the culture of both embryonic and post-embryonic skin plugs containing hair follicles (Tammi and Maibach, 1987). Due to the nature of the model associated skin cells surrounding the hair follicles were also made available thus proving excellent in resembling *in vivo* conditions. However, using skin plugs also presented some limitations; biochemical or morphological analysis of individual hair follicles was not possible, furthermore, analysis of hair growth was further complicated due to epithelial outgrowths from the skin plugs (Kollar, 1966; Frater and Whitmore 1973; Tammi and Maibach 1987). The development of organ culture of individual hair follicles overcame these limitations (Buhl *et al.*, 1989; Philpott *et al.*, 1989; Kondo *et al.*, 1990; Philpott *et al.*, 1990).

Research by Philpott *et al* (1990) established the most successful method of isolated hair follicle culture. Micro-dissected human hair follicles were incubated in William's E medium containing 1% fetal calf serum, supplemented with L-glutamine, insulin, hydrocortisone, transferrin and antibiotics. The hair follicles showed an increase in length at a rate of 0.3mm/day when grown in the presence of insulin at 10ng/ml, closely similar to the *in vivo* growth rate of 0.32 - 0.35 mm/day of hairs at the vertex of the scalp (Myers and Hamilton, 1951). Furthermore the growth of the hair follicle was attributed to an increase in the length of the keratinised hair shaft, and not as a result of degeneration during culture. Since then this model system has been used to investigate several factors that influence hair growth e.g IGF-1 (Randall *et al.*, 2003; Randall, 2008).

3.1.1 Effect of minoxidil on hair follicles *in vitro*

A series of investigations have looked into the effects of minoxidil on single whole hair follicles in organ culture. However, the research has rendered inconsistent results, which at times conflict. Table 3.1 is a summary of relevant literature on the effects of minoxidil on whole hair follicles *in vitro.* There are several possibilities as to how such disparities could have arisen. Different studies have concentrated on different species for their research, thus growth rates and cycle lengths *in vivo* would naturally be dissimilar. Furthermore, the concentrations at which minoxidil has been applied varies widely. Culture conditions utilised are a further cause of extensive variation between results, the choice of medium type, incubation conditions and supplements are also variable. Thus, with such variations between the studies documented in this field, it is difficult to realistically make direct comparisons between them and to draw any firm conclusion on the effect of minoxidil on the hair follicle *in vitro.*

Minoxidil and other potassium channel openers like diazoxide and a novel diazoxide analog, NNC 55-0118, induced a dose-responsive stimulation of hair follicle growth in organ culture of red deer hair follicles (Davies *et al.*, 2005). Of particular interest was the finding that co-incubation with potassium channel blockers, tolbutamide and glibenclamide, inhibited the inductiveness of 10μM minoxidil, diazoxide and NNC 55-0118, on deer hair follicle growth. This strongly supported the role of the potassium channel openers was actually via K^+_{ATP} channels within

Table 3.1 Hair follicle organ culture studies using minoxidil

Summary of relevant literature on the effects of minoxidil on whole hair follicles *in vitro.*

Species	Culture period	Minoxidil Conc.	Effect	Culture conditions	Reference
Mouse	72 hours	0.5 mM	Significantly stimulated hair follicle growth	DMEM medium supplemented With: 20% FCS 12.5 µg/ml gentamicin	**Buhl *et al.*, 1989**
Human • Facelift skin • donor ages between: 35-55 yrs	72 hours 5 days	 0.95 µM 48 µM 0.95 mM 0.95 µM 48 µM 0.95 mM	• Measured every 24 hrs No effect on hair follicle growth No effect on hair follicle growth Inhibition of hair follicle growth Stimulation of hair follicle growth No effect on hair follicle growth Inhibition of hair follicle growth	William's E Medium supplemented with: 1% FCS, 10 ng/ml hydrocortisone, 10 ng/ml insulin, 2 mM L-glutamine, 2.5 µg/ml transferrin, 2.5 µg/ml amphotericin B, 50 U/ml / 50 µg/ml penicillin/streptomycin.	Philpott *et al.*, 1990
Mouse	3 days	5 mM	No effect on hair length (days 0-3) Inhibitory effect after day 3.	DMEM medium supplemented With: 20% FCS	**Waldon *et al.*, 1993**
Human • Only 3 patients	10 days	0.01 mM 0.1 mM 1 mM	No effect on hair follicle length Stimulation of hair follicle growth Stimulation of hair follicle growth • greatest elongation occurred at 1 mM	Williams E medium supplemented with : 10 µg/ml insulin, 10 ng/ml hydrocortisone, 100 µg/ml streptomycin, 100 U/ml penicillin 2 mM L-glutamine,	**Han *et al.*, 2004**

Human • 36 donors, • mean 40 years	12 days	1 μM 100 μM 1 μM 100 μM	• Measured every 3 days Cultured in the presence of insulin: No effect on hair follicle growth No effect on hair follicle growth – catagen promoting effect towards end of culture period Cultured in the absence of insulin: Inhibition of hair follicle growth Inhibition of hair follicle growth	Williams E medium supplemented with: • 10 μg/ml ciprofloxacin, • 10 μg/ml insulin, • 10 ng/ml hydrocortisone, • 2 mM L-glutamine, • 2.5 μg/ml amphotericin B	**Magerl _et al._, 2004**
Red deer	8 days	0.1 μM 1 μM 10 μM 100 μM 10 μM	• Measured every 24 hrs Stimulation of hair follicle growth Stimulation of hair follicle growth Stimulation of hair follicle growth Stimulation of hair follicle growth – greatest elongation occurred at 100 μM When incubated in combination with 1 mM tolbutamide or 10 μM glibenclamide, stimulatory effects of minoxidil were inhibited.	Williams E medium supplemented with: • 100 U/ml penicillin, • 2 mM L-glutamine, • 2.5 μg/ml amphotericin B, • 5 mM glucose.	**Davies _et al._, 2005**
Human • 2 donors • 25 year old males	6 days	10 μM	Stimulates hair follicle growth only in those follicles which showed the fastest growth rate _in vivo_.	Phenol red free William's E medium supplemented with: • 0.01% DMSO vehicle, • 10 μg/ml insulin, • 10 μM ciprofloxacin, • 10 ng/ml hydrocortisone, • 100 U/ml penicillin • 2 mM L-glutamine,	**Kwon _et al._, 2006**

Human • Scalp skin, from nonbalding areas • 1 women & 12 men • Aged between 21 and 40 year	9 days	1mM 10µM 1mM	Anagen follicles were assessed daily for changes in morphology. Cultured in the presence of insulin: Minoxidil alone had no effect, but combined with Tolbutamide (1mM), it abolished the inhibitory effects of Tolbutamide. Cultured in the absence of insulin: Minoxidil increased the number of follicles maintaining anagen; this effect was greatest at 1mM.	Williams E medium supplemented with: • 10 µg/ml insulin, • 10 µg/ml phenol red • 10 ng/ml hydrocortisone, • 10 U/ml penicillin • 2 mM L-glutamine,	**Shorter *et al.*, 2008**

the cultured follicles. In addition, when incubated with only tolbutamide, hair follicles grew at a slower rate in comparison to follicles incubated with the vehicle control suggesting that K^+_{ATP} channels may be actually at least partially open in normal culture medium (Davies *et al.*, 2005). In a study by Shorter *et al* (2008) on the effects of minoxidil (1mM) and tolbutamide (1mM), on the morphology of human hair follicles in the presence of insulin. Minoxidil alone was found to have no effect, however when combined with tolbutamide (1mM), it hindered the inhibitory effects of tolbutamide. Whereas, in the absence of insulin, minoxidil (10µM, 1mM) increased the number of follicles maintaining anagen in a dose-responsive manner; tolbutamide (1mM) blocked this stimulation (Shorter *et al.*, 2008). This suggested that stimulation of K^+_{ATP} channels was also able to increase hair follicle growth in human follicles, an observation supported by the detection of the genes and proteins of one type of K^+_{ATP} channel that would be able to respond to minoxidil, SUR2B/Kir6.1.

On the whole when considering the results of all these studies, there is an indication that several potassium channel openers can alter hair follicle growth *in vitro.* As all investigations were conducted *in vitro,* no vascular interaction could have taken place, thereby reinforcing the premise that potassium channel openers have a direct effect on the follicle, presumably via potassium channels in the hair follicle.

In deer follicles, NNC 55-0118, a drug which would only open SUR1 containing channels, had also stimulated hair follicle growth (Davies *et al.*, 2005). Since both human (Shorter *et al.*, 2008) and deer (see Chapter 2) follicles express the genes for such SUR1 channels, it seems likely that SUR1 channel openers may also stimulate hair growth in human follicles. This is an important area to clarify

because if SUR1 channels are related to hair growth this could offer a novel route for new hair promoting therapies.

3.2 Aims and experimental design

3.2.1 Aims

The aim of this chapter was to see whether SUR1 K^+_{ATP} channels were involved in human hair growth using the organ culture model. Ideally this would be carried out using selective SUR1 K^+_{ATP} channel opening and closing drugs. Initially these proved difficult to source and comparative experiments were carried out using tolbutamide at concentrations which would inhibit SUR1 channels with high affinity, 1μM, (Zunkler *et al.*, 1988) and both SUR1 and SUR2 channels, i.e 1mM.

Later, a further selective SUR1/Kir6.2 channel opener, a novel diazoxide analog 3-isopropylamino-7-methoxy-4H-1,2,4-benzothiadiazine 1,1-dioxide (NNC-55-9216) (Dabrowski *et al.*, 2002), was donated by Dr John Hansen of Novo Nordisk, Denmark as a personal favour to Professor V A Randall. The effects of this drug on hair follicle growth were investigated in the presence, and absence, of 1μm tolbutamide to determine whether direct regulation of SUR1 channels would alter hair growth. Then, to determine whether the effect of the SUR2B channel stimulation by minoxidil could be enhanced by the SUR1 acting NNC-55-9316, both drugs were supplied together.

3.2.2 Experimental design

This human hair follicle organ culture study followed closely the culture conditions described by Philpott *et al* (1996), with the exception of the use of streptomycin in the medium, as it has been shown to inhibit the opening of K^+ channels by minoxidil (Sanders *et al.*, 1996). Minoxidil's action on 3T3 fibroblasts *in vitro* was unaffected by penicillin and therefore penicillin was included (Sanders *et al.*, 1996). Serum was not added to the culture medium, as research has shown it to have an inhibitory effect on hair growth *in vitro* (Philpott *et al.*, 1991).

Human hair follicles were incubated in organ culture with 1 mM of minoxidil, as this concentration of minoxidil has been shown to increase human hair follicle growth (Han *et al.*, 2004) and maintain them in anagen in organ culture (Shorter *et al.*, 2008). Though, typically a 2-5% topical concentration of minoxidil is applied to the scalp clinically (Olsen *et al.*, 2002), only 1.7% of it is absorbed, apparently equating to 1 mM (Han *et al.*, 2004; Magerl *et al.*, 2004). A study by Davies and colleagues (2005), in red deer hair follicles *in vitro,* showed that tolbutamide at the dose of 1mM counteracted the stimulatory effects of several potassium channel openers. This concentration was selected as it has been shown to inhibit native (Trube *et al.*, 1986; Ashcroft *et al.*, 1989) and recombinant (Gribble *et al.*, 1997a) K^+_{ATP} channels. It also prevented human follicles responding to minoxidil (Shorter *et al.*, 2008) and is able to inhibit SUR2 channels with low affinity binding (Hambrock *et al.*, 2001). As previous studies have shown that low concentrations of tolbutamide selectively inhibit the SUR1/Kir6.2 channel (Zunkler *et al.*, 1988), 1μM of tolbutamide was chosen to investigate the mechanism of action of the novel diazoxide analog, NNC55-9216. NNC55-9216 was used at 100μM as described in a previous functional study of the SUR1/Kir6.2

channel where this concentration appeared to produce a near maximal response in the activation of the above channel (Dabrowski *et al.*, 2002).

Skin samples were collected from 20 donors (aged 24-64) for this study. The changes in follicular length were measured daily to investigate the effects of the potassium channel modulators on the hair follicles. Follicles were, in parallel, monitored for changes in morphology throughout culture, as changes in hair follicle cycle stage are significant to hair growth *in vivo.* A minimum of 10 follicles were cultured from each patient for each investigation.

3.3 Materials and Methods

3.3.1 Investigation into the effects of potassium channel modulators on human hair follicles in organ culture.

3.3.1.1 Samples

Human skin samples were collected from non-balding occipital scalp. The donors were healthy males undergoing elective cosmetic hair transplantation surgery. All Ethical Committee approval requirements were met and donors gave fully informed, written consent. Samples were obtained from 20 donors aged between 24-64 years (albeit only two individuals were aged above 60). Samples were collected as whole skin specimens or as individual follicles into 50 ml falcon tubes containing 30 ml transport medium: William's E Medium (containing 10μg/ml phenol red) (Sigma-Aldrich Ltd, Dorset, UK) supplemented with 100 ng/ml hydrocortisone (Sigma-Aldrich Ltd), 2 mM L-glutamine (Gibco, Paisley, UK) and 10 units/ml penicillin (Sigma-Aldrich Ltd). Each tube was identified by labelling with the patient's age, gender and date. This information was noted again in an information sheet accompanying the tube with further particulars of the donor, such as date of sample collection and sample site. The samples were then transported to the University of Bradford on ice, and stored at 4°C. Micro-dissection of the hair follicles was performed within 24 hours of removal.

3.3.1.2 Isolation of human hair follicles

Using the Leica MZ8 dissecting microscope anagen hair follicles were micro-dissected from skin samples. Plastic ware was rinsed in PBS thrice prior to use and all equipment sterilised by autoclaving. Each sample was placed into a

petri dish of PBS at 4^0C (Figure 2.4). The skin was cut at the level of the dermal-subcutaneous fat interface with a scalpel blade (Figure 3.1a). Undamaged anagen hair follicles were removed from the subcutaneous fat with great delicacy using fine forceps (110mm length, 0.05mm width, 0.01mm thick, straight); great finesse was necessary to ensure the follicles remained intact, as undamaged follicles are essential for successful culture (Philpott *et al.*, 1990). The isolated follicles were then placed into another dish of sterile PBS at 4^0C (Figure 3.1b). The dissected follicles were further cleansed of any attached dermis or subcutaneous fat using 27½ gauge sterile syringe needles (Figure 3.1c).

Each isolated human anagen hair follicle was then gently transferred to an individual well of a 24-well plate (Corning Inc.) containing 1 ml of William's E medium supplemented as described in section 3.3.1.1 above. At least 10 hair follicles were cultured for each condition. Follicles were maintained free-floating at 37°C in an atmosphere of 5% CO_2 and 95% air in a humidified incubator over a period of nine days. Fresh medium was introduced at three day intervals, with particular care being taken to leave follicles undamaged.

Figure 3.1 Isolation of human scalp hair follicles by micro-dissection

Individual anagen hair follicles were micro-dissected to investigate the effects of potassium channel modulators on human hair follicles *in vitro.* The stages were photographed under an inverted dissecting microscope (Leica MZ8, Leica, Germany) using a Nikon Coolpix4500 (Nikon E4500) digital camera.

(**a**) Whole human skin samples were placed in a petri dish and cut at the junction of subcutaneous fat. Scale bar = 500μm (**b**) the exposed follicles were then dissected. Scale bar = 300μm before (**c**) further dissection of any debris. Scale bar = 300μm
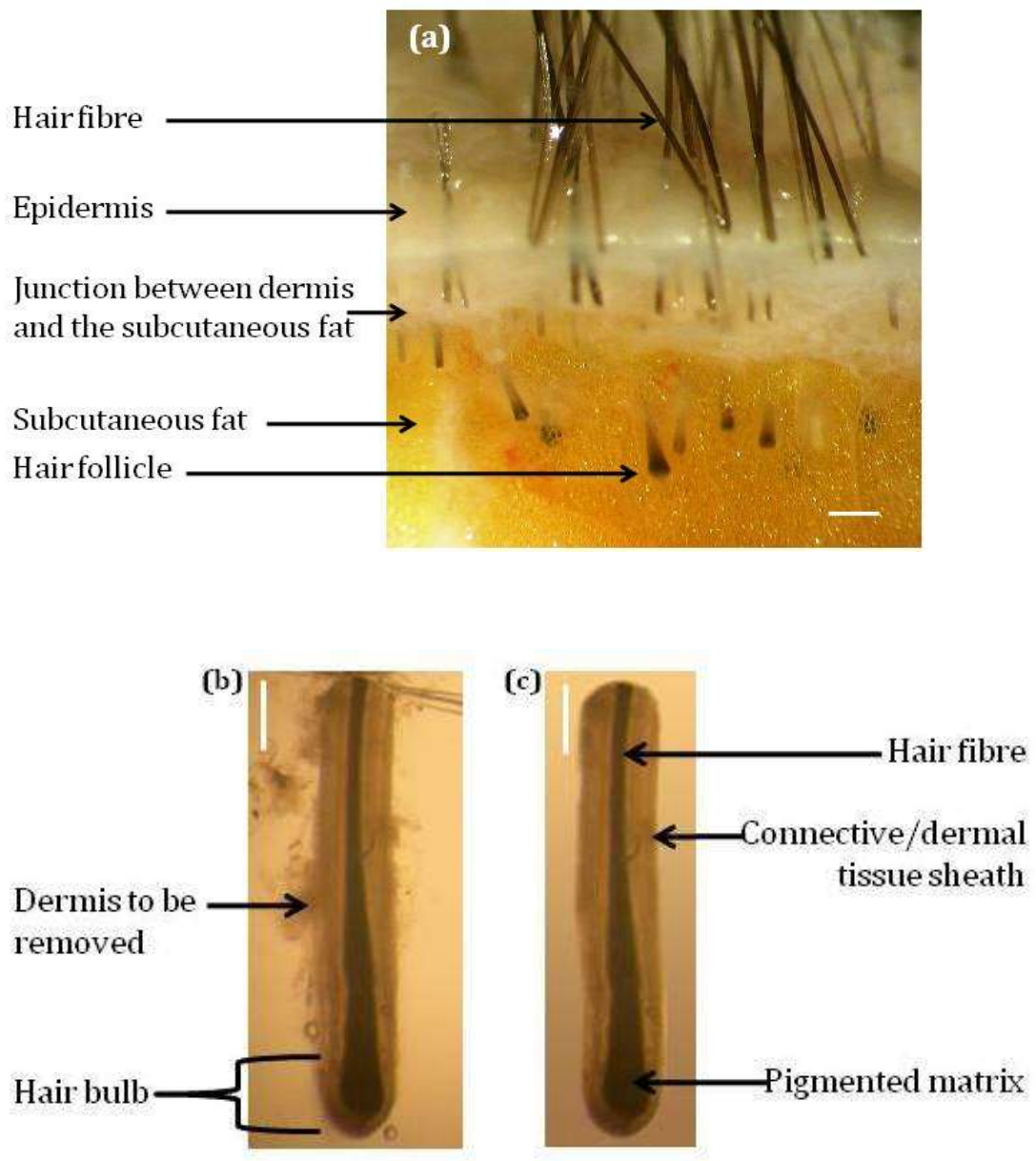
3.3.1.3 Hair growth culture conditions

William's E medium (containing 10μg/ml phenol red) (sigma) supplemented with, 2mM L-glutamine (Gilbco), 10units/ml penicillin (Sigma) and 100ng/ml hydrocortisone (Sigma), was prepared. This culture medium was further supplemented depending on which experiment was being conducted, with one of the following: minoxidil (1 mM; dissolved into a stock solution of William's E medium; Sigma), tolbutamide (1mM or 1μM; dissolved into a stock solution of dimethyl sulfoxide (DMSO); Sigma), both minoxidil (1 mM) and tolbutamide (1mM or 1μM), NNC 55-9216 (100μM; dissolved into a stock solution of DMSO), both tolbutamide (1μM) and NNC 55-9216 (100μM), both minoxidil (1mM) and NNC 55-9216 (100μM), minoxidil (1mM) and NNC 55-9216 (100μM) and tolbutamide (1μM). Stock solutions of minoxidil, NNC 55-9216 and tolbutamide were dissolved using a sonicating water bath (Dawe Instruments Ltd., Middlesex, UK). Control medium was prepared without supplements, but the vehicle (0.001% DMSO) was added to each medium. Depending on which experiment was being conducted insulin (10 μg/ml; Sigma) was included as a supplement. All culture media were sterile-filtered (0.2μm; Sarstedt, Nu¨mbrecht, Germany) before use.

3.3.1.4 Measurement of hair follicles in culture

Hair follicles were examined for increase in follicle length and morphology of the hair bulb, at 24 hour intervals using a Leitz Labovert inverted microscope fitted with an eyepiece graticule. Measurements were made at x50 magnification (eyepiece x12.5 & objective x4) and converted to mm by comparison with a stage micrometer. To ensure that variations between hair follicles were accounted for, the initial length of hair follicle was deducted from the measurements obtained at

every point of examination. Therefore, the results reflected the increase in hair follicle length over time. Follicles that showed no sign of growth by the third day in culture were classed as non-viable samples and thus excluded from further study. Measurements of follicle elongation and the state of follicle morphology were recorded daily over a period of nine days. A Nikon Coolpix 4500 digital camera was also used to photograph the follicles daily.

3.3.1.5 Statistical analysis

Prior to calculating the group mean, the mean growth of follicles per person in each group was ascertained. The elongation of hair follicles in each individual treatment group was expressed as the mean increase in length (mm) ± SEM of the number of individuals used. The Kolmogorov-Smirnov test was used to analyse data for normal distribution. The General Linear Model for Repeated Measures by a two-factor, within-subjects ANOVA using the SPSS statistical analysis program (SPSS Inc., Chicago, Illinois), was used to determine the effect of the different treatments on hair length and percentage of follicles in anagen with time in culture and the total increase in hair follicle length during the experiment.

3.3.2 Histological investigation of individually cultured human hair follicles

Hair follicles were cultured for a period of nine days, and assessed daily for any changes in morphology. To visualize these changes follicles were taken out from the culture media, placed individually into 1.5 ml eppendorfs (Sarsted, Numbrecht, Germany) containing the cryoprotectant Sakura Tissue-Tek O.C.T™ (Raymond A Lamb Ltd, Sussex, UK) and stored at -80°C until further use.

Slides were prepared as described in section 2.3.1.2, individual follicles were sectioned following the same method as was applied to skin samples in section 2.3.1.3. Histological investigation of hair follicle structure was carried out using Sacpic staining as described in section 2.3.1.4 and staining visualised as described in section 2.3.1.6.

3.4 Results

3.4.1 The effect of insulin in the medium in organ culture on the response of human hair follicles to potassium channel regulators

Micro-dissected anagen scalp hair follicles were maintained in organ culture, and observed daily in the presence and absence of insulin, over a period of nine days. Hair follicles in media containing insulin generally increased in length and most maintained anagen. The increase in hair follicle length was a result of the growth of hair fibre, and the inner and outer root sheaths. The connective/dermal tissue sheath remained at the constant length of day 0 throughout the culture period (Figure 3.2a & 3.2c). When follicles displayed catagen-like changes in the hair bulb region, pigmentation ceased, the hair moved upwards and the matrix became detached from the dermal papilla (Figure 3.2c, 3.2d & 3.2e). Hair follicles that had not grown by day 2 were rejected from the calculations. The hair follicles were monitored daily for both the follicles remaining in anagen and daily increase in growth. However, the results were plotted for the percentage of follicles remaining in anagen and the overall increase in hair follicle length over 9 days, as so many follicles entered telogen in some conditions that the rate of growth by day 9 would be due to relatively few follicles, rendering it meaningless. Therefore the rate of growth was discarded for analysis.

After three days in culture the number of follicles remaining in anagen, in the absence of insulin, declined to about 17%, whilst in the presence of insulin 86% were still growing. By day 5 all follicles in the insulin-free media entered catagen. However, a significant (p<0.001) number of follicles in the presence of insulin remained in anagen (Figure 3.3a). Overall, the increase in hair follicular

123

length in the absence of insulin was only 0.3 mm, whilst in the presence of insulin there was a significant growth of 1.9 mm over 9 days ($p<0.001$) (Figure 3.3b). The overall increase in hair follicular length was calculated by taking the mean average of the overall growth of all follicles over the 9 day culture period, i.e. the increase in length of each follicle on day 9 or on the last day that the follicle was in anagen, were taken and the average total growth in length of follicles, during the culture period, was calculated to deduce the overall increase in length.

Figure 3.2 Sequential photomicrographs of human hair follicles cultured in the presence or absence of insulin in organ culture

Isolated anagen follicles were grown in William's E medium containing 10 μg/ml phenol red, supplemented with 100 ng/ml hydrocortisone, 2 mM L-glutamine, 10 units/ml penicillin, 0.001% DMSO and with, and without, 10 μg/ml insulin.

Photomicrographs taken under an inverted microscope, at 24 hour intervals, exhibit the changes in an individual scalp hair follicle cultured for 9 days in the presence and absence of insulin.

(a) An anagen hair follicle cultured in presence of 10μg/ml of insulin. The sequential photomicrographs show the synthesis of new hair fibre (HF), but no growth of the connective tissue sheath/dermal sheath (CTS/DS). Hair follicles increased in length regularly at a rate of 0.2mm/day. At the end of the culture period the follicle was sectioned and stained with Sacpic stain to examine the morphological state of the individual hair follicle during the culture period (last photomicrograph). Scale bar = 0.3 mm

(b) Enlarged photomicrographs of the hair follicle bulb (HB) (pictured in **a**), showing anagen morphology throughout the 9 days in culture.

(c) A hair follicle cultured in the absence of insulin showed a much smaller increase in the length than those in insulin containing medium (see **a**), at a rate of 0.12mm/day. The photomicrographs only extend up to day 5, as the hair follicle had entered a catagen-like state, showing catagen-like changes in its hair bulb morphology. The follicle was sectioned and stained with Sacpic stain to examine the morphological state of the hair bulb (far right photomicrograph). The hair had moved up and left the dermal papilla at the bottom of the hair bulb. Scale bar = 0.3mm.

(d) Enlarged photomicrographs of the hair follicle bulb (pictured in **c**), showing changes in hair bulb morphology during the 5 days in culture.

(e) Enlarged photomicrographs of the anagen (Day 0) and catagen-like (Day 5) hair follicle bulbs sectioned and stained with Sacpic stain, clearly exhibit the changes in morphology of the hair bulb when entering the catagen-like state.

125

(a)

0.3mm

(+ Insulin)

1.9 mm

HF

CTS

HB

DP

HF

CTS

Day 0 Day 1 Day 2 Day 3 Day 4 Day 5 Day 6 Day 7 Day 8 Day 9

126

(b)

(c)

0.3mm

(- Insulin)

HF
ORS
CTS

Catagen-like hair bulb

Day 0   Day 1   Day 2   Day 3   Day 4   Day 5

(d)

(e)
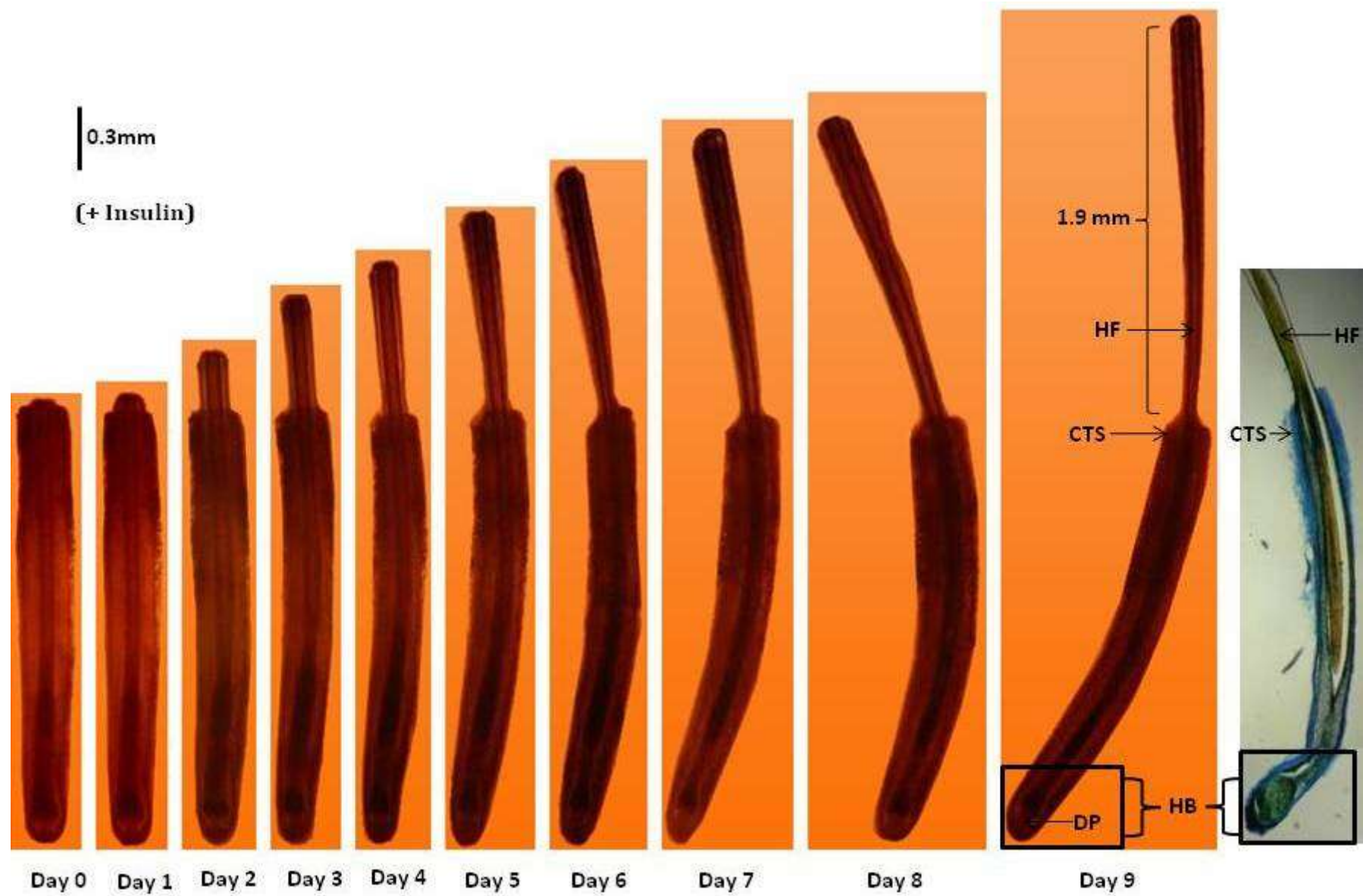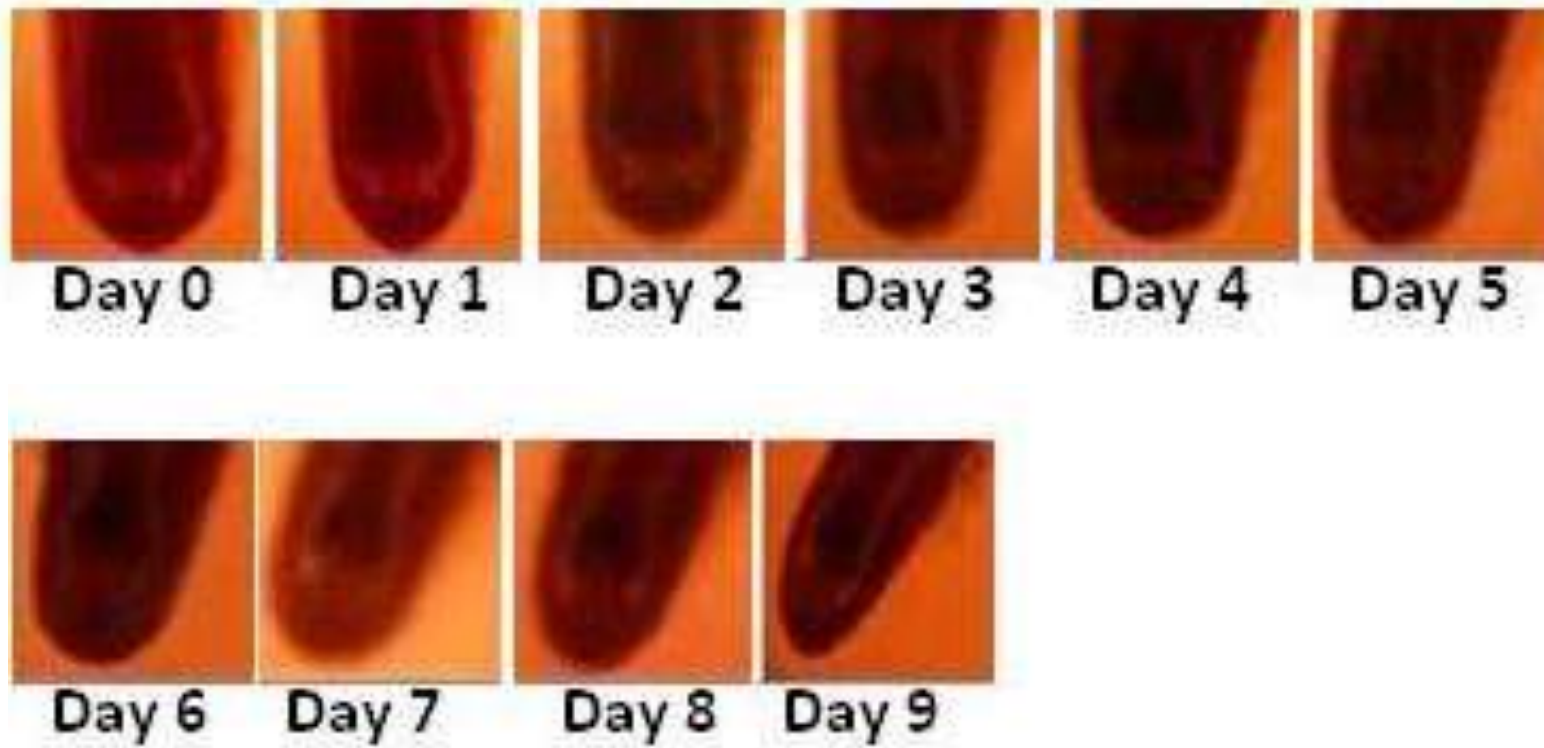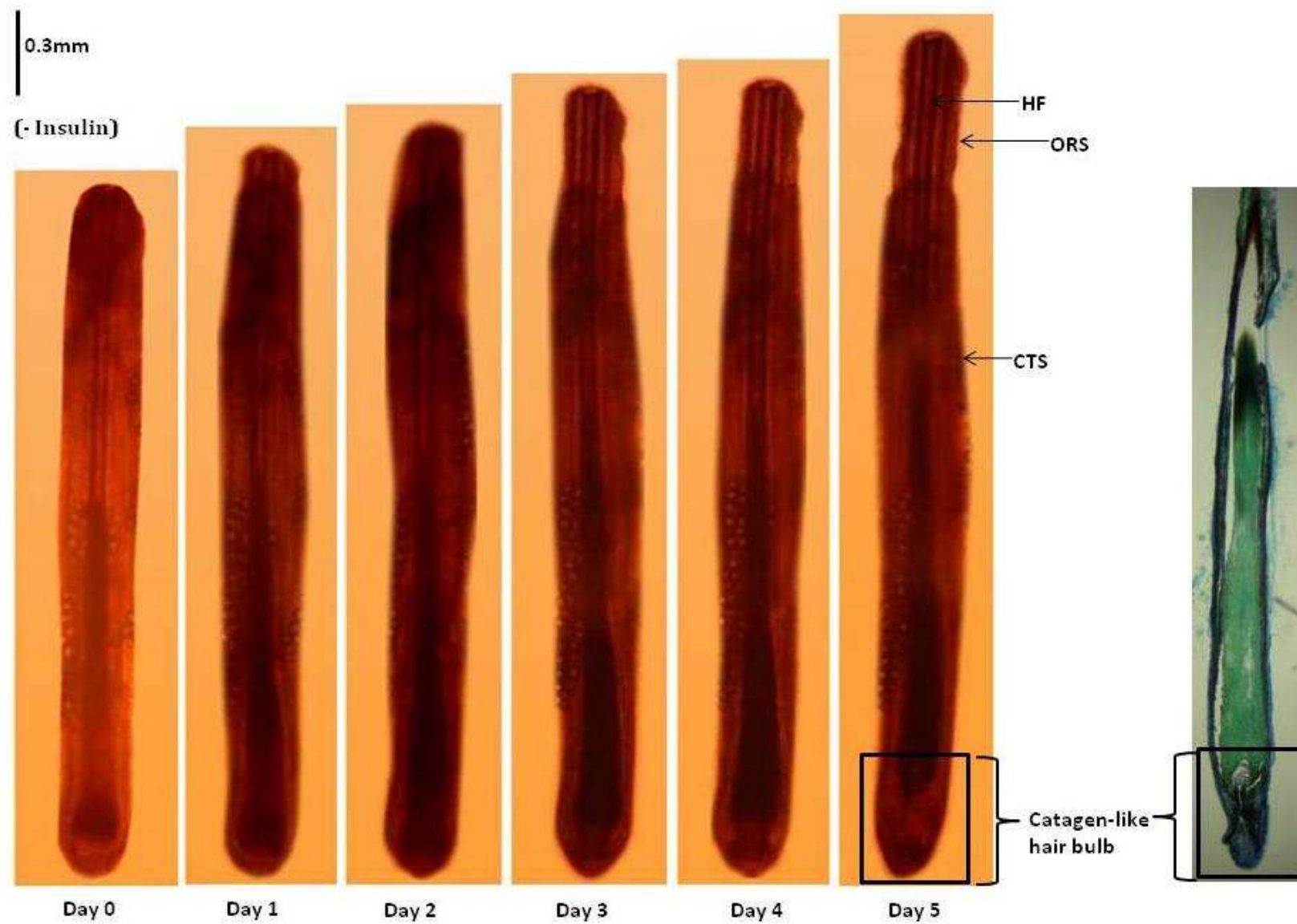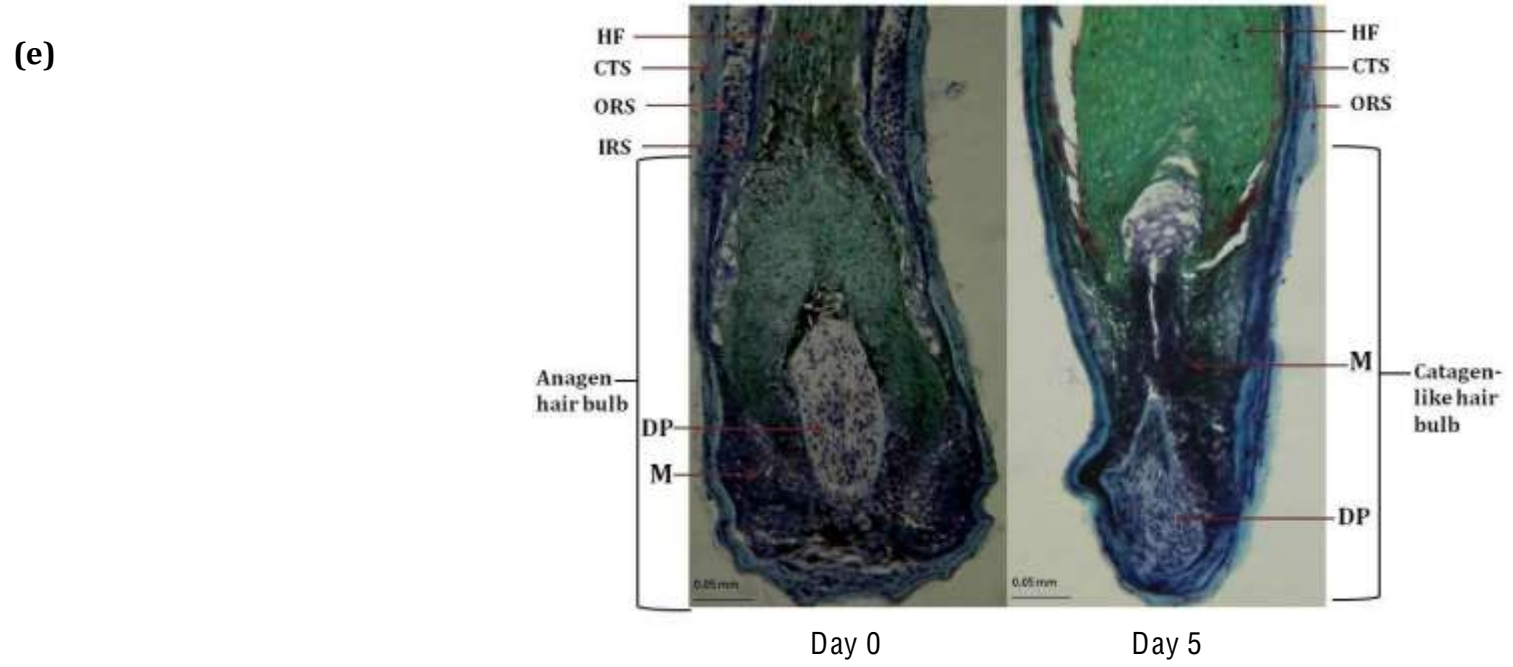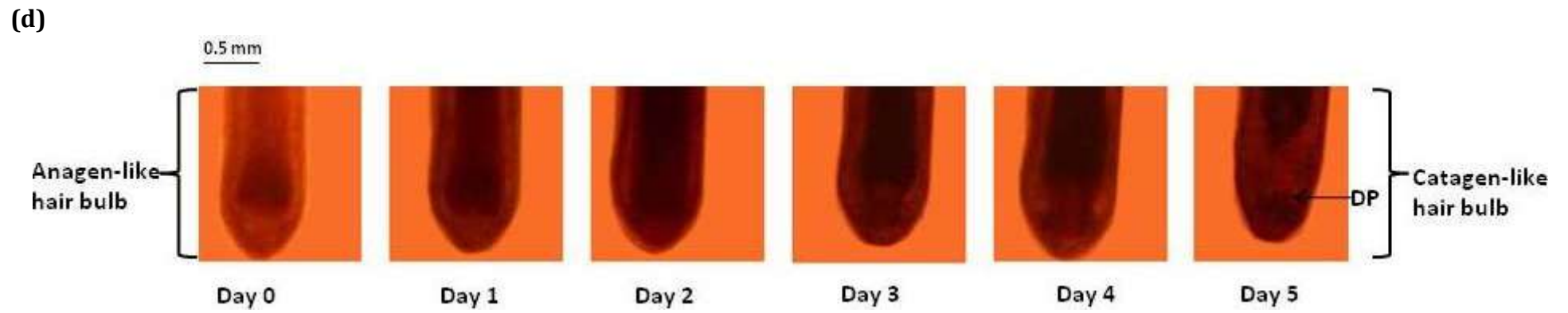
Figure 3.3 Human hair follicle growth in organ culture

The percentage of follicles remaining in anagen over the length of the culture period was calculated from day 0. In the presence of insulin the follicles remaining in anagen gradually decreased throughout the culture period. Follicles in the absence of insulin rapidly entered catagen after day two in culture, and the number of follicles remaining in anagen was significantly lower ($p < 0.001$***) **(a)**. Increase in hair follicle length was measured consecutively over the 9 day culture period using an inverted microscope fitted with an eyepiece graticule, in follicles which remained in anagen. The overall increase in hair follicle length over the experiment was calculated from the maximum increase in length in anagen or the length on day 9 if the follicle was still growing, at the end of the culture period. In the presence of insulin the average final hair follicle length significantly increased ($p < 0.001$***) **(b)**. Mean values ± S.E.M of 5 people are plotted; a minimum of 10 hair follicles were isolated per person for each condition. Statistical analysis was performed using a two-factor within-subjects ANOVA using SPSS after confirming normal distribution.

(a) Percentage of follicles remaining in anagen
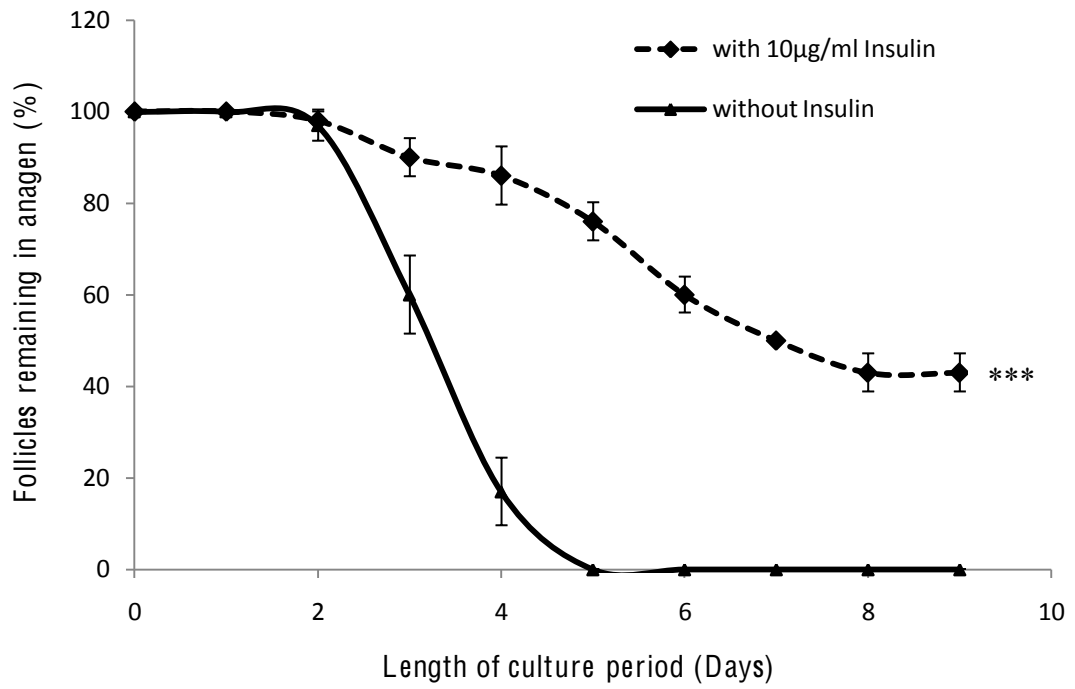
(b) The overall increase in hair follicle length over 9 days
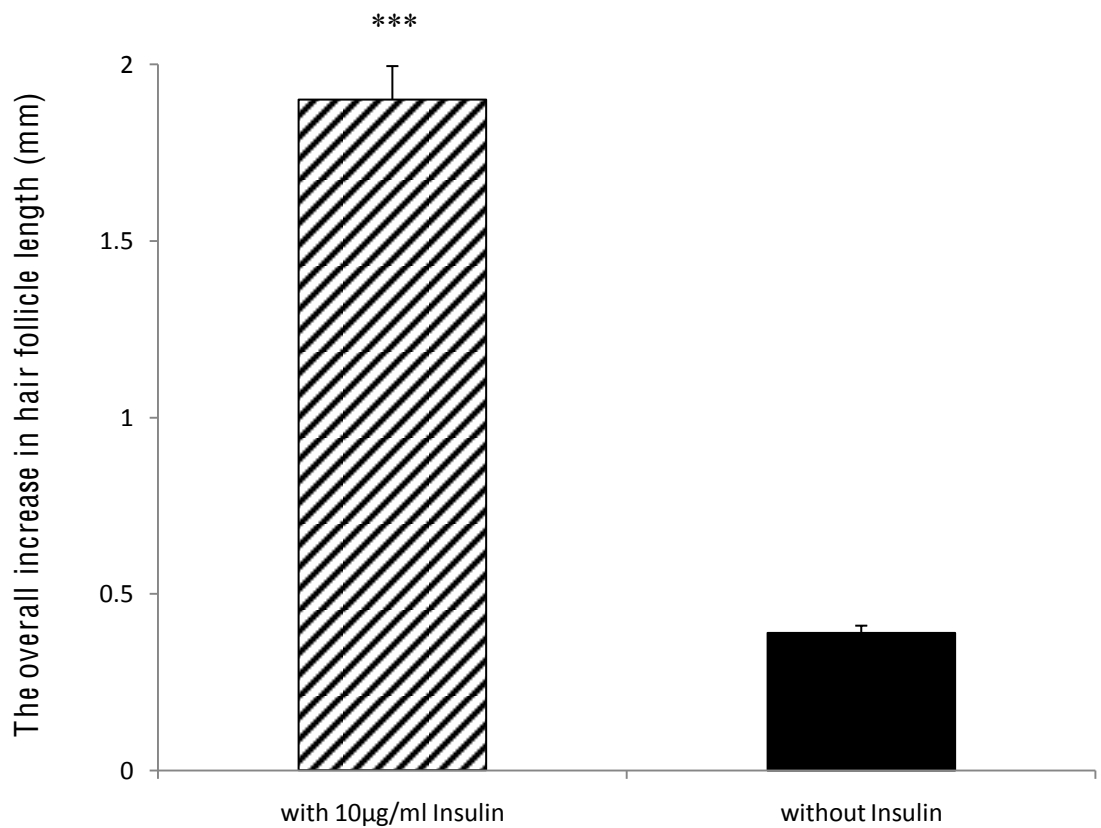
3.4.2 The effect of potassium channel regulators on human hair follicles in organ culture

3.4.2.1 Response of human hair follicles incubated with minoxidil in the presence and absence of insulin in organ culture

Isolated human hair follicles were cultured in the presence, and absence, of insulin with minoxidil. The addition of 1mM of minoxidil to the culture medium, in the presence of insulin, had no affect on the percentage of follicles remaining in anagen ($p=0.525$) (Figure 3.4a), however it significantly decreased the overall increase in hair follicle length over the 9 day culture period, in comparison to the control ($p=0.016$) due to inhibition of the daily growth rate (Figure 3.5a). Whereas, in the absence of insulin, minoxidil significantly stimulated the percentage of follicles remaining in anagen ($p<0.001$) (Figure 3.4b) and the overall hair follicle growth ($p<0.001$) (Figure 3.5b). When expressed as a percentage of the control hair follicle growth over the 9 days, minoxidil showed a significant ($p<0.05$) inhibition of hair follicle growth in the presence of insulin and significant ($p<0.001$) stimulation in the absence of insulin (Figure 3.6).

Figure 3.4 The effect of minoxidil in the presence and absence of insulin on the percentage of follicles remaining in anagen in organ culture

Minoxidil had no notable effect on the proportion of follicles remaining in anagen in the presence of 10μg/m insulin (p=0.525) **(a)**, but in the absence of insulin, minoxidil had significantly stimulated the proportion of follicles remaining in anagen (p<0.001***) **(b)**. The percentage of follicles remaining in anagen over the length of the culture period was calculated from day 0. Mean values ± S.E.M of 5 people are plotted; a minimum of 10 hair follicles were isolated per person, n=50. Statistical analysis was performed using a two-factor within-subjects ANOVA using SPSS, after confirming normal distribution.

(a) With insulin
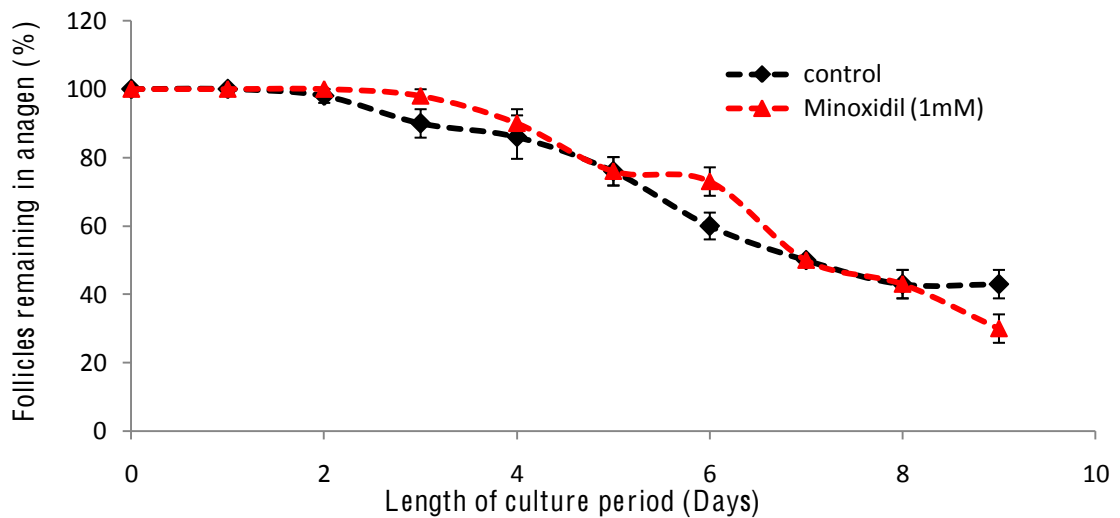
(b) Without insulin
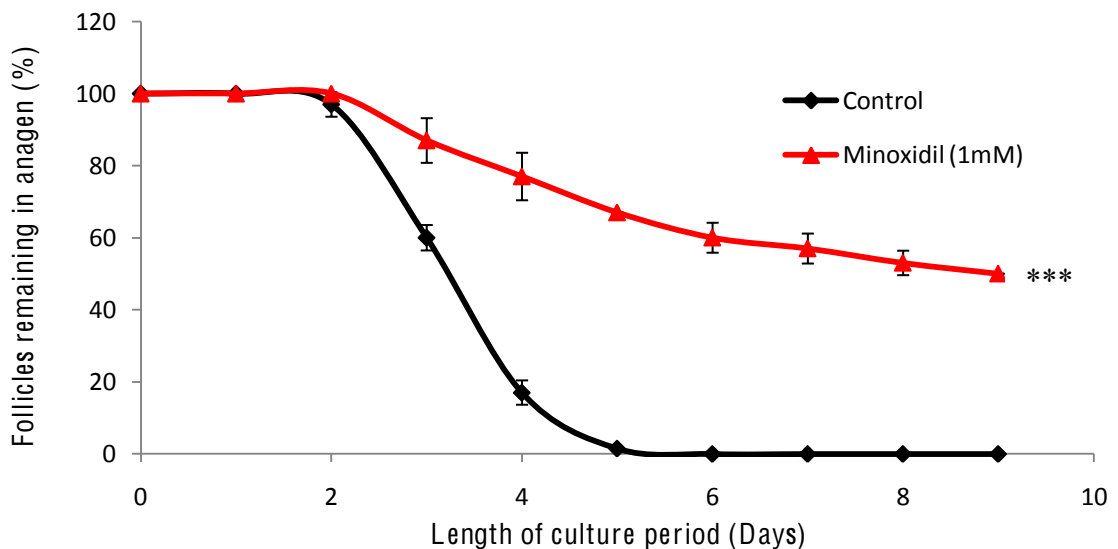
Figure 3.5 The effect of minoxidil on hair follicle growth in the presence and absence of insulin in organ culture

In the presence of insulin minoxidil significantly decreased follicle length (p=0.016*) **(a)**, but in the absence of insulin, minoxidil significantly increased follicle length (p<0.001***) **(b)**. Mean values ± S.E.M of 5 people are plotted; a minimum of 10 hair follicles were isolated per person. Statistical analysis was performed using t-test.

(a) With insulin
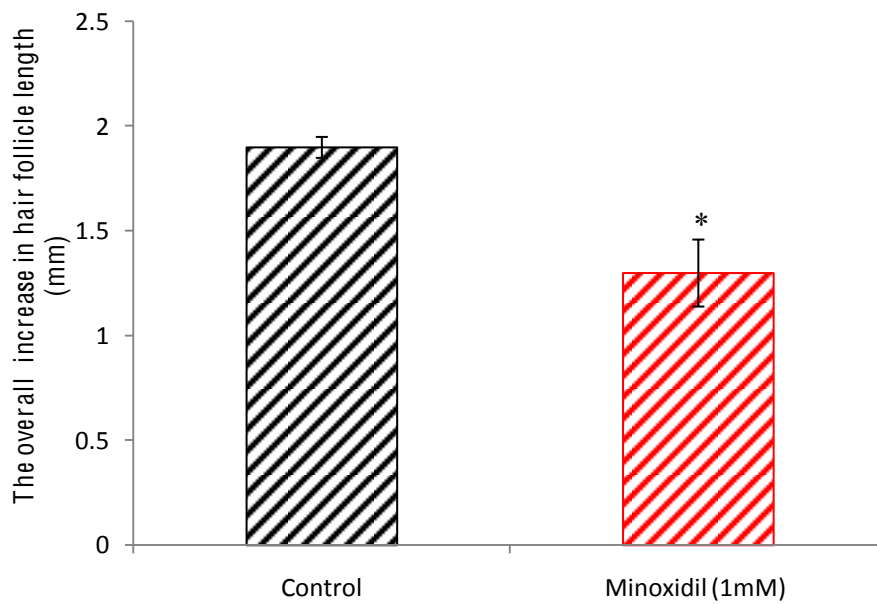
(b) Without insulin
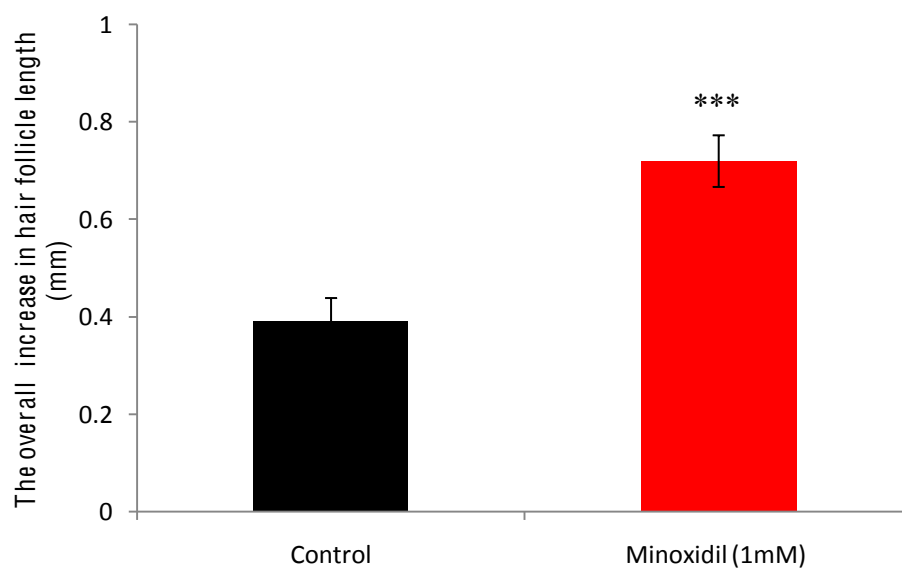
Figure 3.6 Alterations of hair follicle growth in the presence of minoxidil expressed as a percentage of the control

In the presence of insulin hair growth decreased significantly ($p<0.05^*$), whereas in the absence of insulin hair length significantly increased ($p<0.001^{***}$). Mean values ± S.E.M of 5 people are plotted; a minimum of 10 hair follicles were isolated per person. Statistical analysis was performed using a two-factor within-subjects ANOVA using SPSS after confirming normal distribution.

Percentage of control growth over 9 days
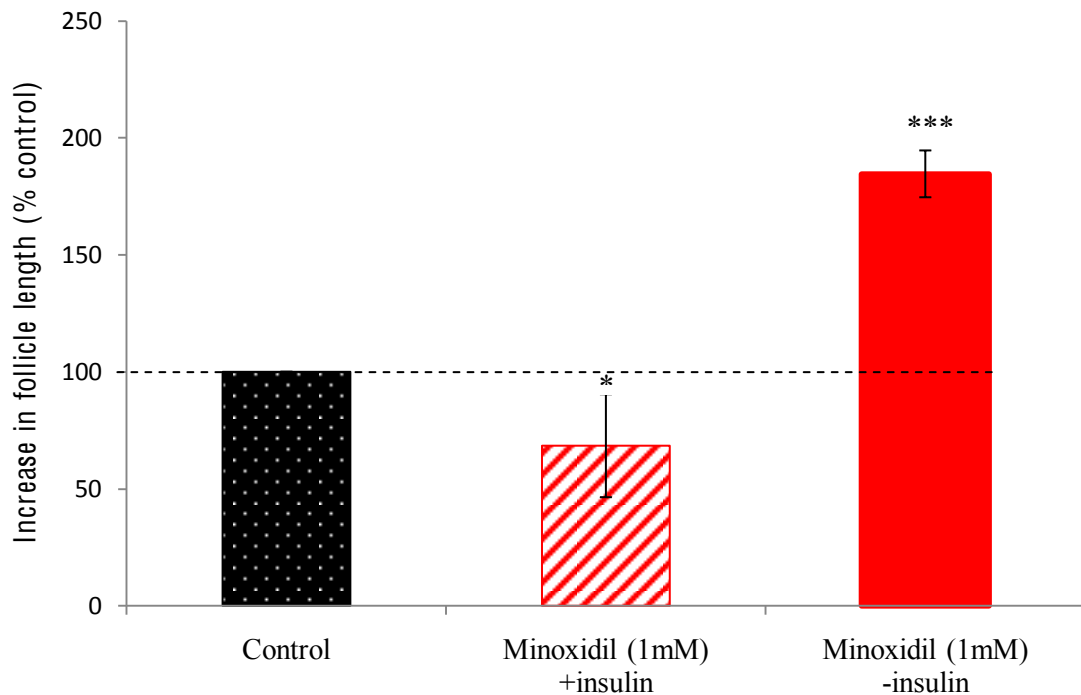
3.4.2.2 Response of human hair follicles incubated with tolbutamide in the presence and absence of insulin in organ culture

Isolated human hair follicles were cultured in the presence and absence of insulin with the potassium channel closer tolbutamide (1µM & 1mM). Tolbutamide in the presence of insulin, reduced the percentage of follicles in anagen significantly at both 1µM (p=0.004) and 1mM (p<0.001) (Figure 3.7a). Similarly this inhibiting affect was seen in the overall hair follicle growth at 1µM (p=0.01) and 1mM (p<0.001) (Figure 3.8a).

In the absence of insulin, the percentage of follicles remaining in anagen appeared higher but was insignificant compared to the control at both concentrations, 1µM (p=0.063) and 1mM (p=0.064) (Figure 3.7b). The same effect occurred in the overall hair follicle growth at 1µM (p=0.055) and 1mM (p=0.613) (Figure 3.8b).

When recalculated as a percentage of hair follicle growth in control medium, over the 9 days, the effects of insulin were very clear. There was a significant decrease in hair follicle growth in the presence of insulin, at both concentrations of tolbutamide, while in the absence of insulin, there was no significant change in hair follicle length (Figure 3.9).

Figure 3.7 Tolbutamide inhibited the percentage of follicles remaining in anagen in organ culture in the presence and absence of insulin

Both the high (1mM) and low (1µM) concentrations of tolbutamide reduced the percentage of follicles remaining in anagen **(a)**. In the absence of insulin **(b)**, neither concentration of tolbutamide maintained follicles in anagen significantly longer than the control. The percentage of follicles remaining in anagen over the length of the culture period was calculated from day 0. Mean values ± S.E.M of 5 people are plotted; a minimum of 10 hair follicles were isolated per person. Statistical analysis was performed using a two-factor within-subjects ANOVA using SPSS, after confirming normal distribution.

Statistics:

(a) Percentage of follicles remaining in anagen in the presence of insulin

Concentration	p-value (ANOVA)
Tolbutamide (1µM)	0.004 **
Tolbutamide (1mM)	<0.001***

(b) Percentage of follicles remaining in anagen in the absence of insulin

Concentration	p-value (ANOVA)
Tolbutamide (1µM)	P=0.063 (NS)
Tolbutamide (1mM)	P=0.064 (NS)

(a) With insulin
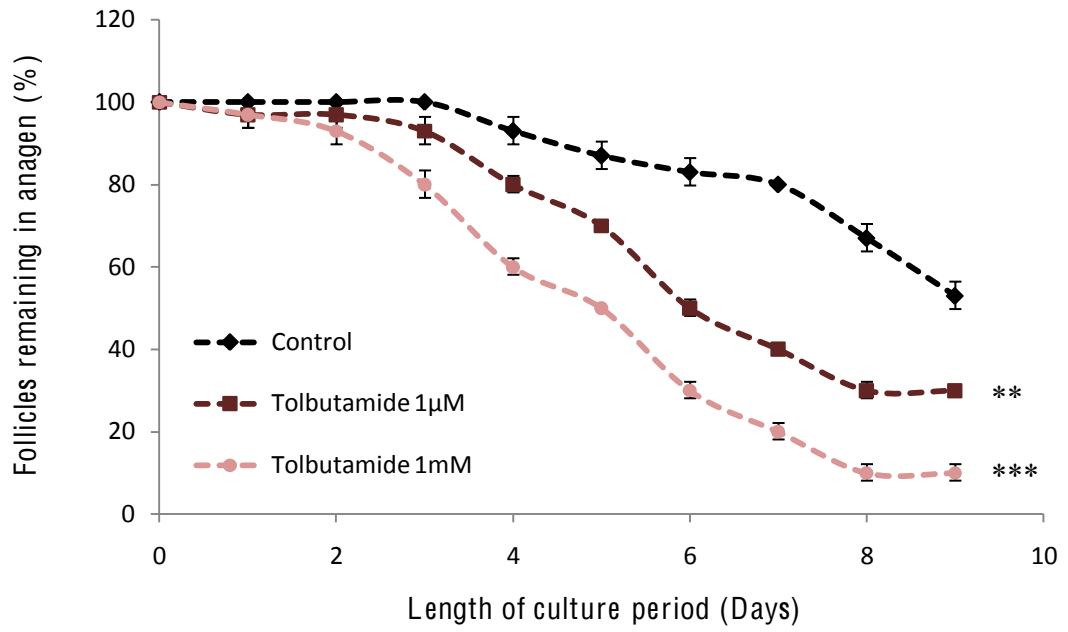
(b) Without insulin
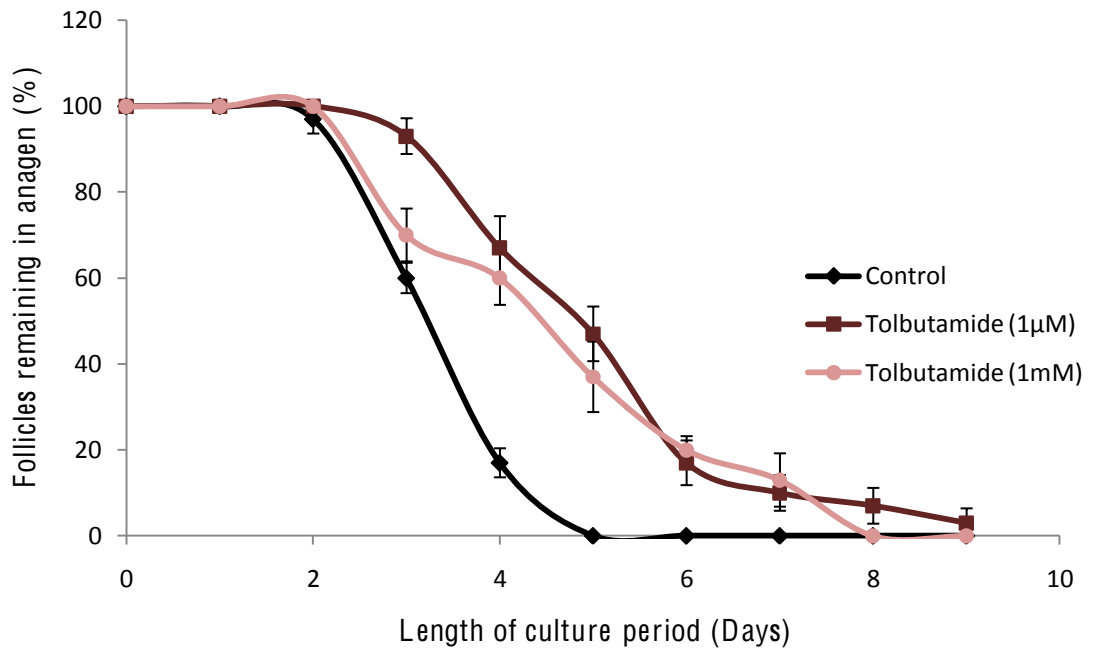
Figure 3.8 The effect of tolbutamide on hair growth in the presence and absence of insulin in organ culture

Increase in hair follicle growth was measured each day for each follicle that remained in anagen over the 9 day culture period using an inverted microscope, fitted with an eyepiece graticule. Tolbutamide was excluded from the vehicle control. In the presence of insulin **(a),** both the high (1mM) and low (1μM) concentrations of tolbutamide significantly decreased follicle length. In the absence of insulin **(b)**, neither concentrations of tolbutamide significantly altered the hair growth length. Mean values ± S.E.M of 5 people are plotted; a minimum of 10 hair follicles were isolated per person. Statistical analysis was performed using a two-factor within-subjects ANOVA using SPSS, after confirming normal distribution.

Statistics:

(a) The overall increase in hair follicle length over 9 days in the presence of 10μg/ml of insulin

Concentration	p-value (ANOVA)
Tolbutamide (1μM)	0.01 **
Tolbutamide (1mM)	0.001***

(b) The overall increase in hair follicle length over 9 days in the absence of insulin

Concentration	p-value (ANOVA)
Tolbutamide (1μM)	P=0.055 (NS)
Tolbutamide (1mM)	P=0.061 (NS)

(a) Overall increase in hair follicle length over 9 days in the presence of 10μg/ml of insulin
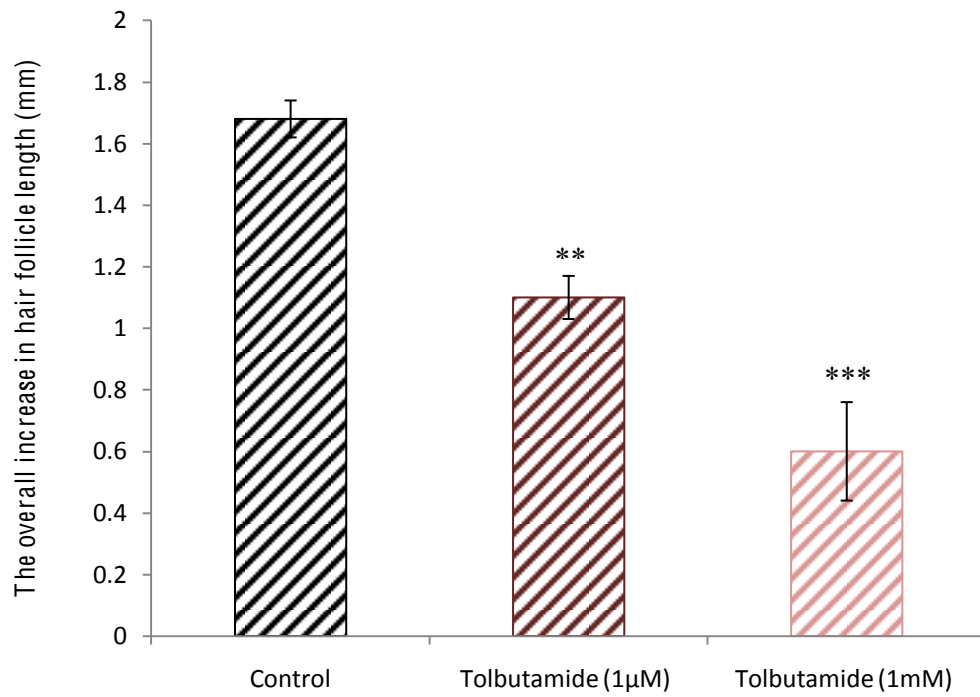
(b) Overall increase in hair follicle length over 9 days in the absence of insulin
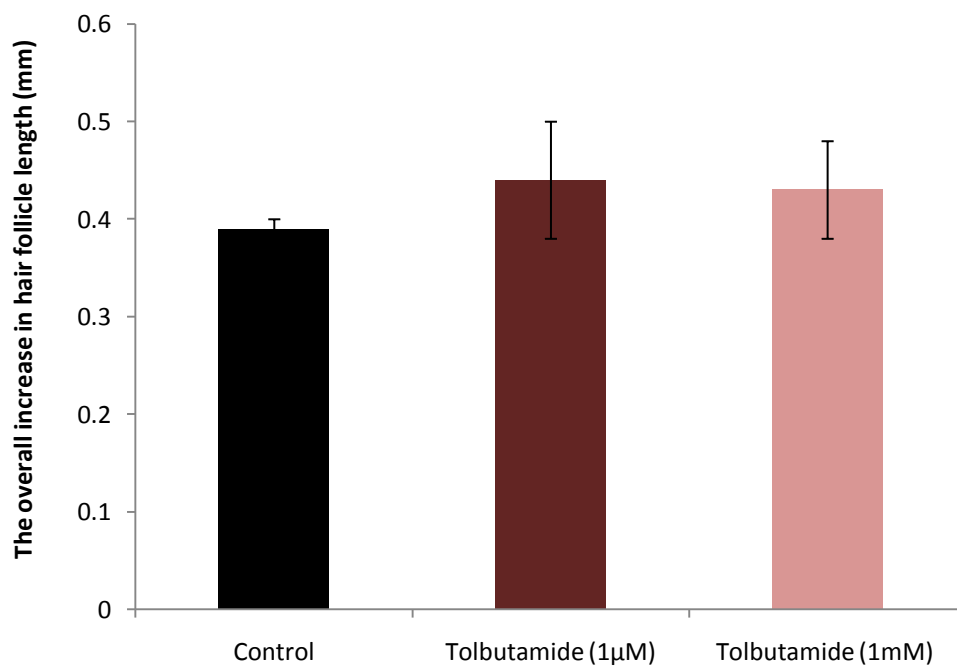
Figure 3.9 The effect of tolbutamide on the increase in hair follicle length expressed as a percentage of their control values

The increase in hair follicle length over the 9 day culture period was calculated as a percentage of the samples over the control values to enable comparison between $\pm$ insulin conditions. In the presence of insulin hair growth decreased significantly, but not in its absence. Mean values $\pm$ S.E.M of 5 people are plotted; a minimum of 10 hair follicles were isolated per person. Statistical analysis was performed using a two-factor within-subjects ANOVA using SPSS, after confirming normal distribution.

Percentage of control growth over 9 days
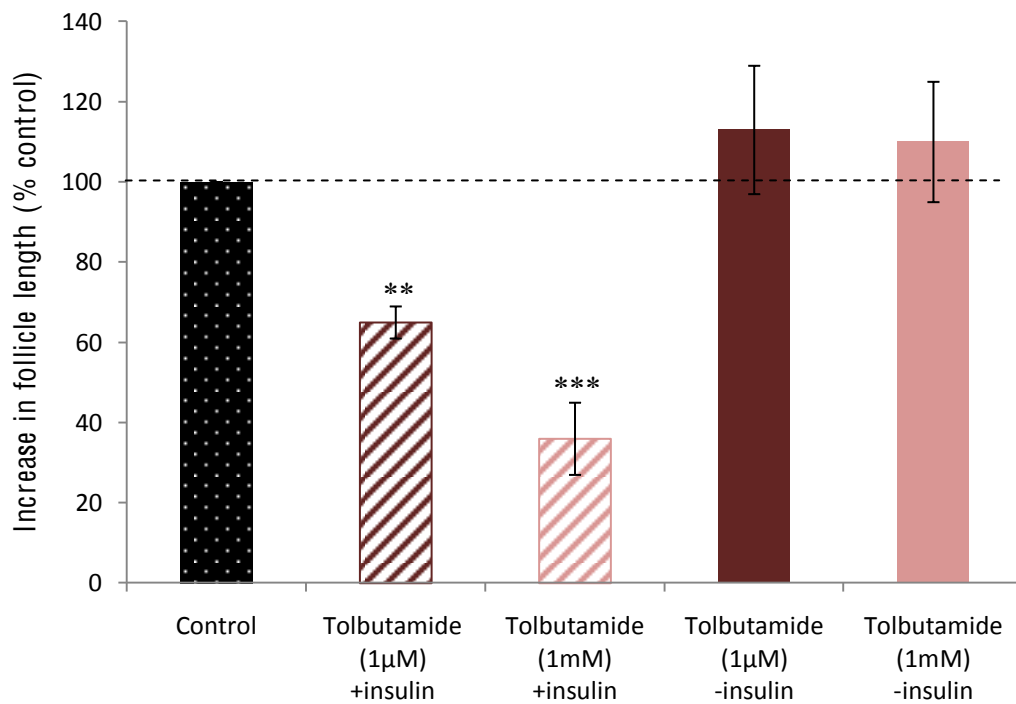
3.4.2.3 Response of human hair follicles to K^+_{ATP} channel regulators, minoxidil and tolbutamide in organ culture

Since the presence of insulin in the medium had altered the results significantly, all further experiments were carried out in its absence. Minoxidil notably increased the number of follicles maintained in anagen when insulin was omitted from the medium ($p<0.001$) (Figure 3.10). This effect was inhibited greatly by the addition of potassium channel blocker tolbutamide at 1mM ($p=0.0043$). Therefore there was no longer any increase compared to the control ($p=0.063$). Tolbutamide at 1mM had no effect alone (Figure 3.10a). When the lower concentration of 1μM tolbutamide was used it had less effect, still significantly ($p=0.018$) (Figure 3.10b), inhibiting the minoxidil effect, but not blocking it completely, remaining just significantly higher than the control ($p=0.049$). Minoxidil also significantly increased the overall hair follicle length over 9 days ($p<0.001$) (Figure 3.11). This effect was extensively inhibited by both concentrations of tolbutamide (1 mM ($p=0.0036$) and 1 μM ($p=0.019$)) (Figure 3.11a and Figure 3.11b respectively), but again the 1μM concentration had less effect remaining significantly higher than the control ($p=0.055$) (Figure 3.11b). This effect was better highlighted when expressed as a percentage of hair follicle growth against the control (Figure 3.12).

Figure 3.10   Percentage of follicles remaining in anagen incubated with minoxidil and channel blocker tolbutamide in organ culture

Isolated anagen follicles were cultured in William's E medium containing 10 µg/ml phenol red, supplemented with 100 ng/ml hydrocortisone, 2 mM L-glutamine, 10 units/ml penicillin and 0.001% DMSO, in the absence of insulin.

The stimulatory effect of minoxidil on the percentage of follicles remaining in anagen was significantly inhibited with the high concentration of tolbutamide (1mM) **(a)**. The low concentration tolbutamide (1µM) **(b)** had also affected the percentage of follicles remaining in anagen, however it did not block the channel completely.

Mean values ± S.E.M of 5 people are plotted; a minimum of 10 hair follicles were isolated per person. Statistical analysis was performed using a two-factor within-subjects ANOVA using SPSS, after confirming normal distribution.   Data are expressed as original values.

Statistics:

(a) Percentage of follicles remaining in anagen, with a high concentration of tolbutamide (1mM)

Condition	Control
Minoxidil (1mM)	p=0.001***
Minoxidil (1mM) & Tolbutamide (1mM)	p=0.063 (NS)
Tolbutamide (1mM)	p=0.064 (NS)

Condition	Minoxidil (1mM)	Tolbutamide (1mM)
Minoxidil (1mM) & Tolbutamide (1mM)	p=0.0043**	p=0.9978 (NS)

(b) Percentage of follicles remaining in anagen, with a low concentration of tolbutamide (1µM)

Condition	Control
Minoxidil (1mM)	p=0.001***
Minoxidil (1mM) & Tolbutamide (1µM)	p=0.003**
Tolbutamide (1µM)	p=0.063 (NS)

Condition	Minoxidil (1mM)	Tolbutamide (1µM)
Minoxidil (1mM) & Tolbutamide (1µM)	p=0.018*	p=0.8154 (NS)
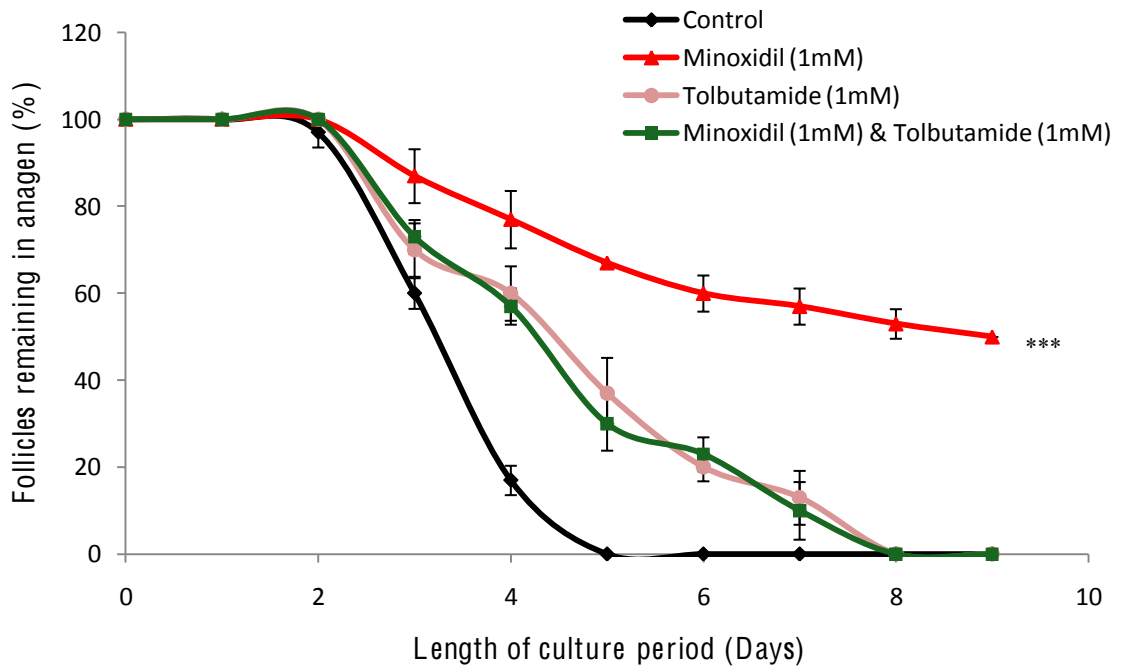
(a) 1mM Tolbutamide

(b) 1μM Tolbutamide

Figure 3.11 The effect of minoxidil and channel blocker tolbutamide on hair growth in organ culture

Increase in hair follicle length with high concentration of tolbutamide (1mM) **(a)** was significantly inhibited in comparison to the control. Increase in hair follicle length with low concentration of tolbutamide (1µM) **(b)** was also significantly inhibited in comparison to the control.

Increase in hair follicle growth was measured each day for each follicle remaining in anagen over the 9 day culture period. Mean values ± S.E.M of 5 people are plotted; a minimum of 10 hair follicles were isolated per person. Statistical analysis was performed using a two-factor within-subjects ANOVA using SPSS, after confirming normal distribution. Data are expressed as original values.

Statistics:

(a) The overall increase in hair follicle length over 9 days, with 1mM Tolbutamide

Condition	Control
Minoxidil (1mM)	P<0.001***
Minoxidil (1mM) & Tolbutamide (1mM)	P=0.556 (NS)
Tolbutamide (1mM)	P=0.061 (NS)

Condition	Minoxidil (1mM)	Tolbutamide (1mM)
Minoxidil (1mM) & Tolbutamide (1mM)	P=0.0036**	P=0.5286 (NS)

(b) The overall increase in hair follicle length over 9 days, with 1µM Tolbutamide

Condition	Control
Minoxidil (1mM)	p<0.001***
Minoxidil (1mM) & Tolbutamide (1µM)	p=0.049*
Tolbutamide (1µM)	p=0.055 (NS)

Condition	Minoxidil (1mM)	Tolbutamide (1µM)
Minoxidil (1mM) & Tolbutamide (1µM)	P=0.019*	P=0.9852 (NS)

(a) 1mM Tolbutamide

(b) 1μM Tolbutamide

Figure 3.12 The effects of minoxidil and different concentrations of K^+_{ATP} channel blocker tolbutamide on hair follicle growth, expressed as a percentage of the control in organ culture

The increase in hair follicle length over the 9 day culture period was calculated as a percentage of the samples over the control values to enable comparison between different conditions. Minoxidil significantly increased hair follicle length; this effect was inhibited by both concentrations of tolbutamide. Mean values ± S.E.M of 5 people are plotted; a minimum of 10 hair follicles were isolated per person. Statistical analysis was performed using a two-factor within-subjects ANOVA using SPSS, after confirming normal distribution.

Statistics:

Condition	Control
Minoxidil (1mM)	p<0.001***
Minoxidil (1mM) & Tolbutamide (1µM)	p<0.05*
Minoxidil (1mM) & Tolbutamide (1mM)	p=0.7 (NS)
Tolbutamide (1µM)	p=0.6 (NS)
Tolbutamide (1mM)	p=0.6 (NS)

Percentage of control hair follicle growth over 9 days

147
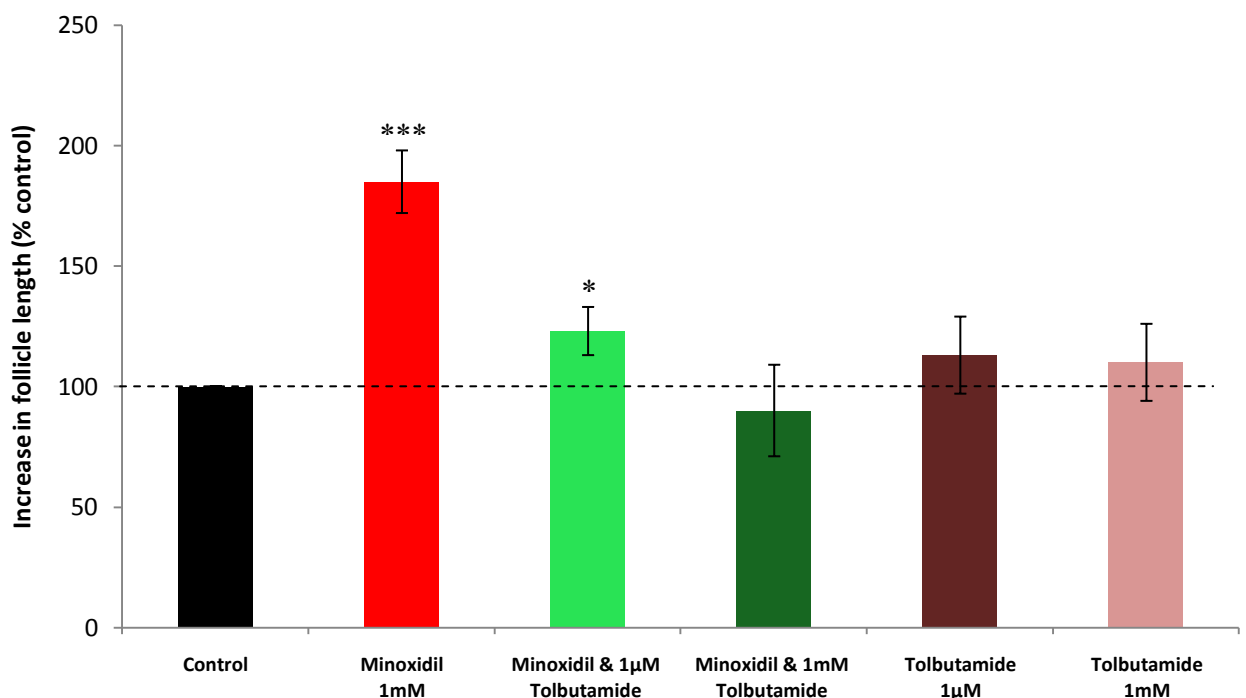
3.4.2.4 Human hair follicles respond to a selective SUR1 K^+_{ATP} channel opener, NNC 55-9216 and combined treatment with minoxidil in organ culture

Minoxidil opens SUR2 K^+_{ATP} channels but not those with SUR1 sulphonylurea subunits. To assess whether SUR1 channels regulate human hair growth the effect of the selective SUR1 channel opener NNC 55-9216 was assessed in organ culture. NNC 55-9216 at 100μM effectively maintained follicles in anagen in insulin-free medium (p=0.003) (Figure 3.13a). This effect was significantly inhibited by the addition of channel blocker tolbutamide at the lower concentration of 1μM (p=0.008). The same pattern was evident in the overall increase in hair follicle length over 9 days with NNC 55-9216 causing a significant increase of about 72 % (p=0.002) (Figure 3.13b). This effect was significantly inhibited by the addition of 1μM tolbutamide (p<0.001).

Since minoxidil and NNC 55-9216 are able to open different K^+_{ATP} channels, their effects when given together were examined. The combined treatment of minoxidil and NNC 55-9216 had the greatest effect on the follicles remaining in anagen causing a very significant increase (p<0.001) (Figure 3.14a). The effect of the combined treatment was significantly higher than that with NNC 55-9216 alone (p<0.001), but only slightly and insignificantly higher than minoxidil (Figure 3.14b). However, the combined treatment produced an overall increase in hair follicle length over 9 days which was significantly higher than either minoxidil (p<0.001) or NNC 55-9216 (p=0.002) alone. The overall growth over 9 days in control medium of 0.3 ± 0.05mm was increased by 0.8 ± 0.04mm while minoxidil caused an increase of 0.4 ± 0.043 mm and NNC55-9216 by 0.37 ± 0.03mm. This difference appears to be additive (Figure 3.14b).

The addition of 1 μM tolbutamide to the combined K^+_{ATP} channel openers reduced the percentage of follicles remaining in anagen but in comparison to the control, the percentage of follicles remaining in anagen were still significantly higher ($p=0.01$) (Figure 3.15a). However, the addition of 1 μM tolbutamide significantly reduced the overall increase in hair follicle length to control values ($p<0.001$) (Figure 3.15b).

The overall effects of NNC 55-9216 and the combined treatment with minoxidil and the channel blocker tolbutamide, on hair follicle length, is better demonstrated when the overall hair follicle growth is expressed as a percentage of that of each experiment's control values (Figure 3.16).

Figure 3.13 The selective SUR1 K$^+_{ATP}$ channel opener NNC 55-9216 stimulated hair follicle growth in organ culture

Isolated anagen follicles were cultured in insulin-free control medium, as described in Figure 3.10, in the presence of either: vehicle alone, 100 µM NNC 55-9216, 1 µM tolbutamide, or both 100 µM NNC 55-9216 and 1µM tolbutamide. Mean values ± S.E.M of 5 people are plotted; a minimum of 10 hair follicles were isolated per person per condition. Statistical analysis was performed using a two-factor within-subjects ANOVA using SPSS, after confirming normal distribution. **(a)** The percentage of follicles remaining in anagen was significantly stimulated by NNC 55-9216; this affect was inhibited with the channel blocker tolbutamide at 1 µm. **(b)** The increase in hair follicle length over 9 days was significantly stimulated with NNC 55-9216; this effect was inhibited with the channel blocker tolbutamide at 1µm.

Statistics:

(a) Percentage of follicles remaining in anagen

Condition	Control
NNC55-9216 (100µM)	p=0.003**
NNC55-9216 (100µM) & Tolbutamide (1µM)	p=0.056 (NS)
Tolbutamide (1µM)	p=0.063 (NS)

Condition	NNC55-9216 (100µM)	Tolbutamide (1µM)
NNC55-9216 (100µM) & Tolbutamide (1µM)	p=0.008**	p=0.984 (NS)

(b) The overall increase in hair follicle length over 9 days

Condition	Control
NNC55-9216 (100µM)	p=0.002**
NNC55-9216 (100µM) & Tolbutamide (1µM)	p=0.032*
Tolbutamide (1µM)	p=0.055 (NS)

Condition	NNC55-9216 (100µM)	Tolbutamide (1µM)
NNC55-9216 (100µM) & Tolbutamide (1µM)	p<0.001***	p=0.039*

(a) Percentage of follicles remaining in anagen

(b) The overall increase in hair follicle length over 9 days

151
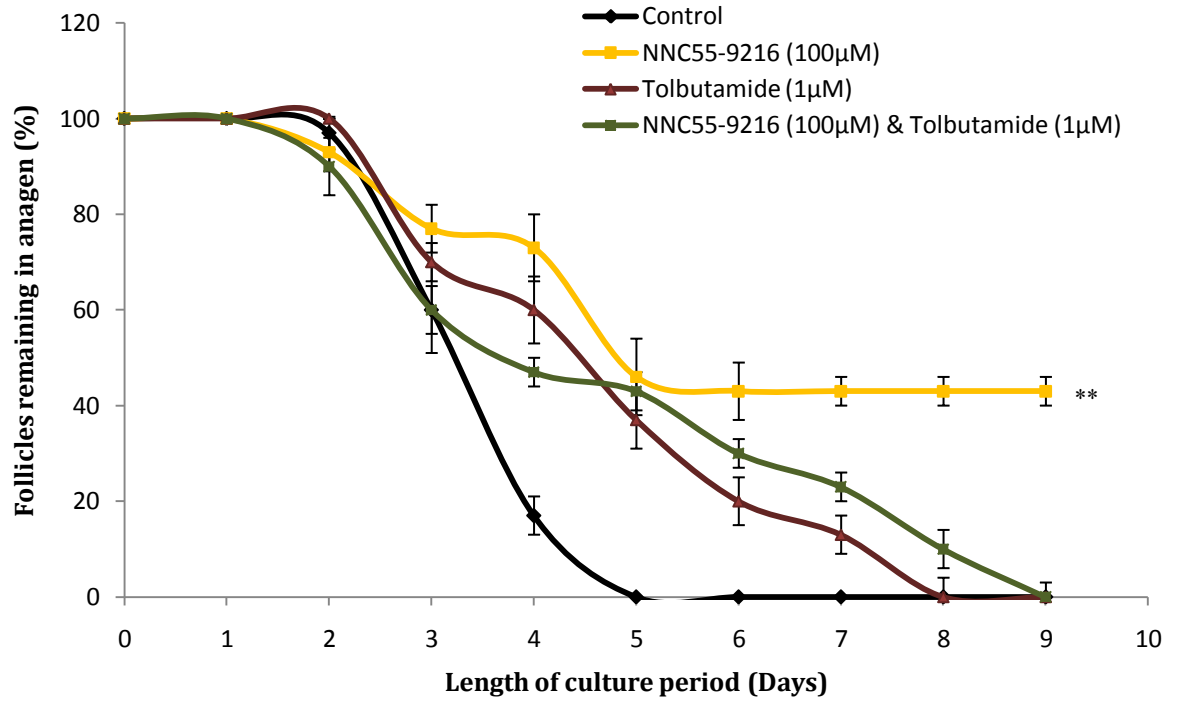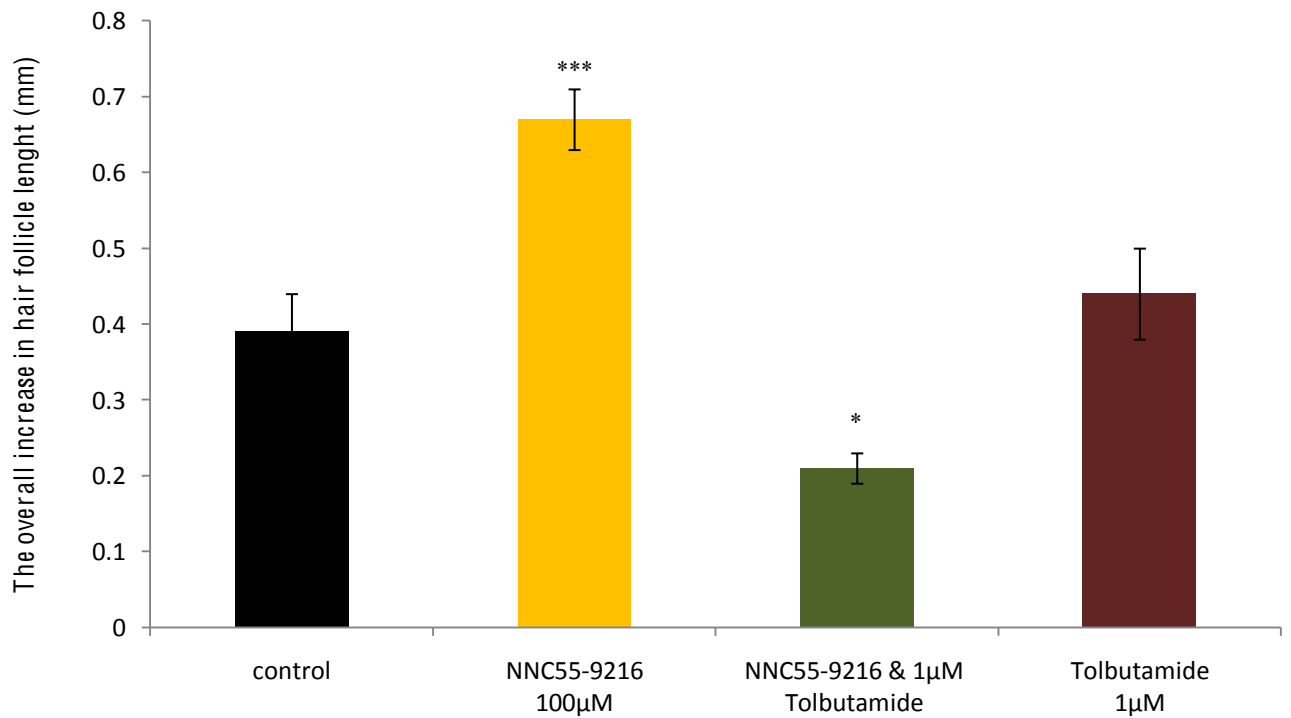
Figure 3.14 Response of human hair follicles incubated with both the SUR2 channel opener, minoxidil, and the SUR1 opener NNC 55-9216 in organ culture

Isolated anagen follicles were cultured in insulin-free control medium, as described in Figure 3.10, in the presence of either: vehicle alone, 100 μM NNC 55-9216, 1 mM minoxidil, or both 100 μM NNC 55-9216 and 1mM minoxidil. Mean values ± S.E.M of 5 people are plotted; a minimum of 10 hair follicles were isolated per person. Statistical analysis was performed using a two-factor within-subjects ANOVA using SPSS, after confirming normal distribution. The combined treatment with minoxidil and NNC 55-9216 stimulated hair growth causing a significantly higher percentage of follicles in anagen than NNC 55-9216 alone **(a)**. Hair follicle length was also significantly increased to higher levels than with either opener individually **(b)**.

Statistics:

(a) Percentage of follicles remaining in anagen

	Control	NNC55-9216 (100μM)	Minoxidil (1mM) & NNC55-9216 (100μM)
Minoxidil (1mM)	p<0.001***	p=0.049*	p=0.099 (NS)
NNC55-9216 (100μM)	p=0.003**	-------	p=0.03*
Minoxidil (1mM) & NNC55-9216(100μM)	p<0.001***	p=0.03*	--------

(b) The overall increase in hair follicle length over 9 days

	Control	NNC55-9216 (100μM)	Minoxidil (1mM) & NNC55-9216 (100μM)
Minoxidil (1mM)	P<0.001***	P=0.264 (NS)	P=0.006**
NNC55-9216 (100μM)	P=0.002**	-------	P=0.001***
Minoxidil (1mM) & NNC55-9216(100μM)	P<0.001***	P=0.001***	--------

(a) Percentage of follicles remaining in anagen
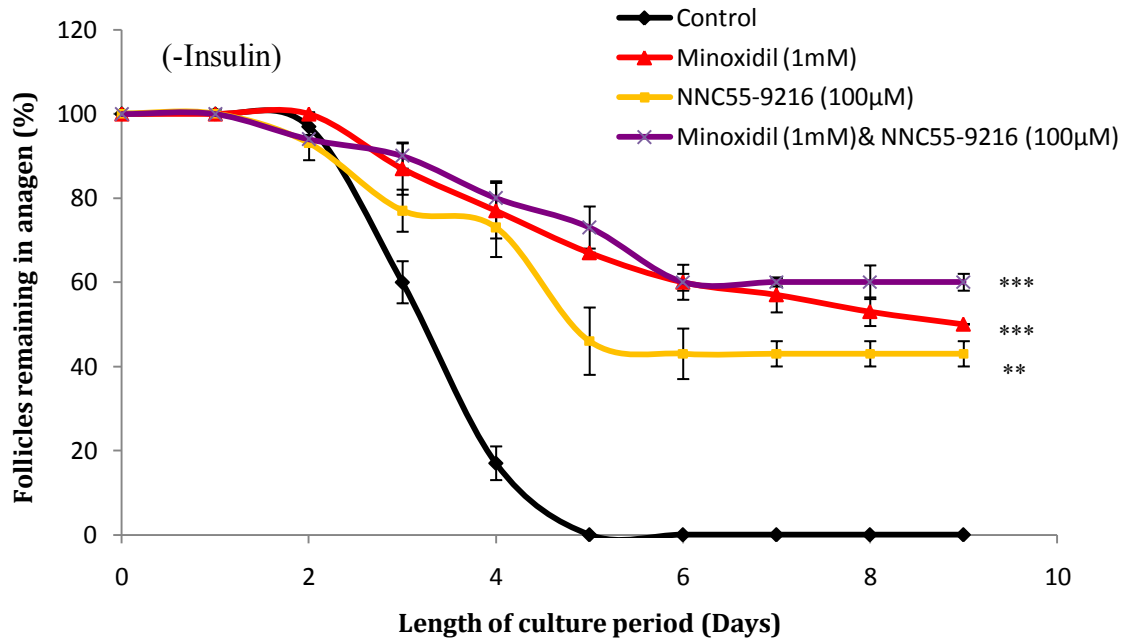
(b) The overall increase in hair follicle length over 9 days
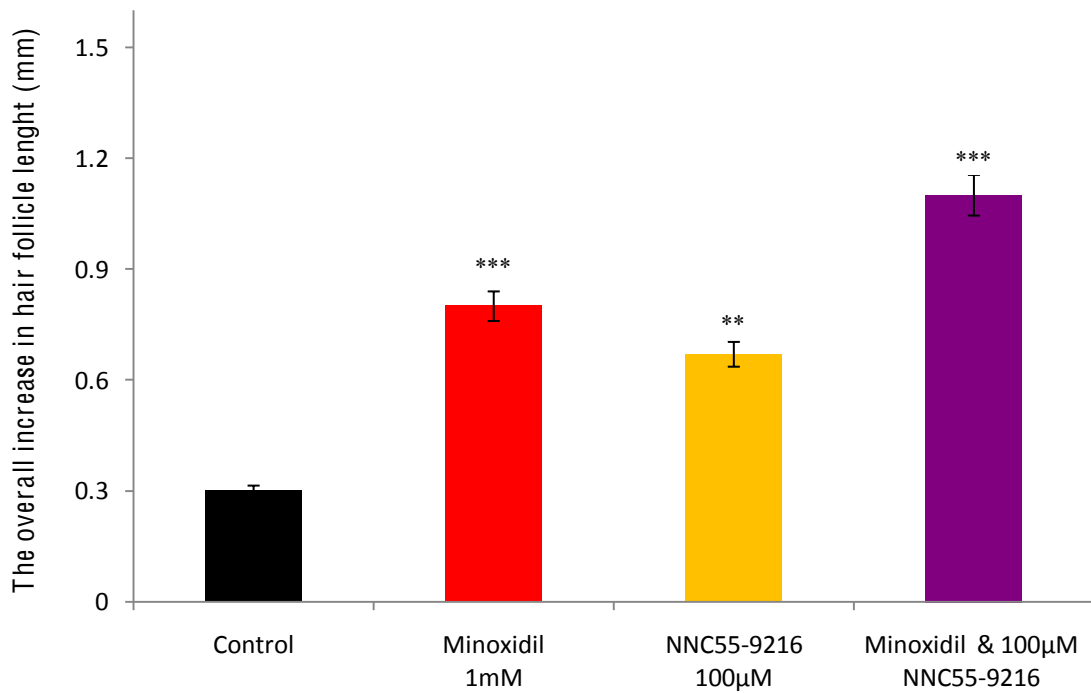
Figure 3.15 The effect of tolbutamide on the combined treatment of NNC 55-9216 and minoxidil, on hair follicle growth in organ culture

Isolated anagen follicles were cultured in insulin-free control medium, as described in Figure 3.10. Mean values ± S.E.M of 5 people are plotted; a minimum of 10 hair follicles were isolated per person. Statistical analysis was performed using a two-factor within-subjects ANOVA using SPSS, after confirming normal distribution. The combined effect of minoxidil and NNC 55-9216 on the percentage of follicles remaining in anagen was significantly inhibited by tolbutamide **(a)**. Similarly the effect of combined minoxidil and NNC 55-9216 on overall increase in hair follicle length was significantly inhibited by tolbutamide **(b)**.

Statistics:

(a) Percentage of follicles remaining in anagen

	Control	Minoxidil (1mM) & NNC55-9216(100μM) & Tolbutamide (1μM)	Tolbutamide (1μM)
Minoxidil (1mM) & NNC55-9216(100μM)	p<0.001***	p=0.002**	p=0.02**
Minoxidil (1mM) & NNC55-9216(100μM) & Tolbutamide (1μM)	p=0.01*	-------	0.613 (NS)
Tolbutamide (1μM)	p=0.063(NS)	0.613 (NS)	--------

(b) The overall increase in hair follicle length over 9 days

	Control	Minoxidil (1mM) & NNC55-9216(100μM) & Tolbutamide (1μM)	Tolbutamide (1μM)
Minoxidil (1mM) & NNC55-9216(100μM)	p<0.001***	p<0.001***	p<0.001***
Minoxidil (1mM) & NNC55-9216(100μM) & Tolbutamide (1μM)	p=0.15 (NS)	-------	p=0.227 (NS)
Tolbutamide (1μM)	p=0.055(NS)	p=0.227 (NS)	--------

(a) Percentage of follicles remaining in anagen
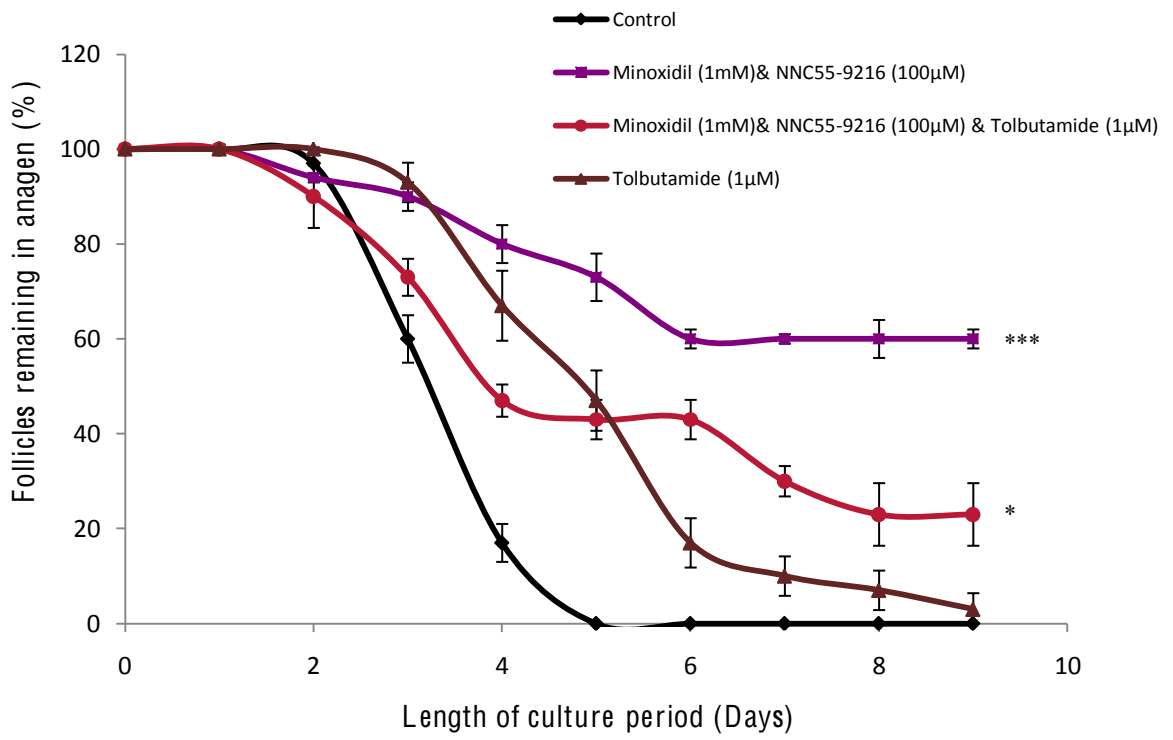
(b) The overall increase in hair follicle length over 9 days
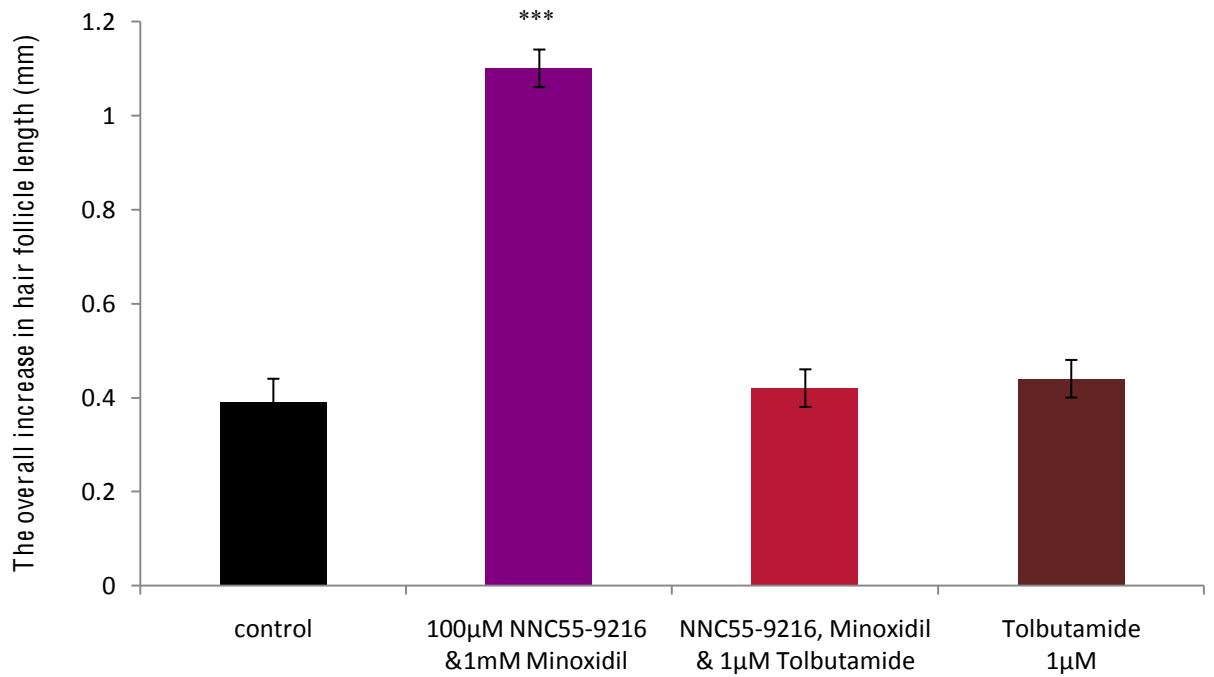
Figure 3.16 Percentage of hair follicle growth with channel blocker tolbutamide on the combined treatment of NNC 55-9216 and minoxidil against the control in organ culture

The increase in hair follicle length over the 9 day culture period was calculated as a percentage of the samples over the control values to enable comparison between conditions. The hair follicle growth decreased significantly, with addition of tolbutamide. Mean values ± S.E.M of 5 people are plotted; a minimum of 10 hair follicles were isolated per person. Statistical analysis was performed using a two-factor within-subjects ANOVA using SPSS, after confirming normal distribution.

Percentage of control hair follicle growth over 9 days
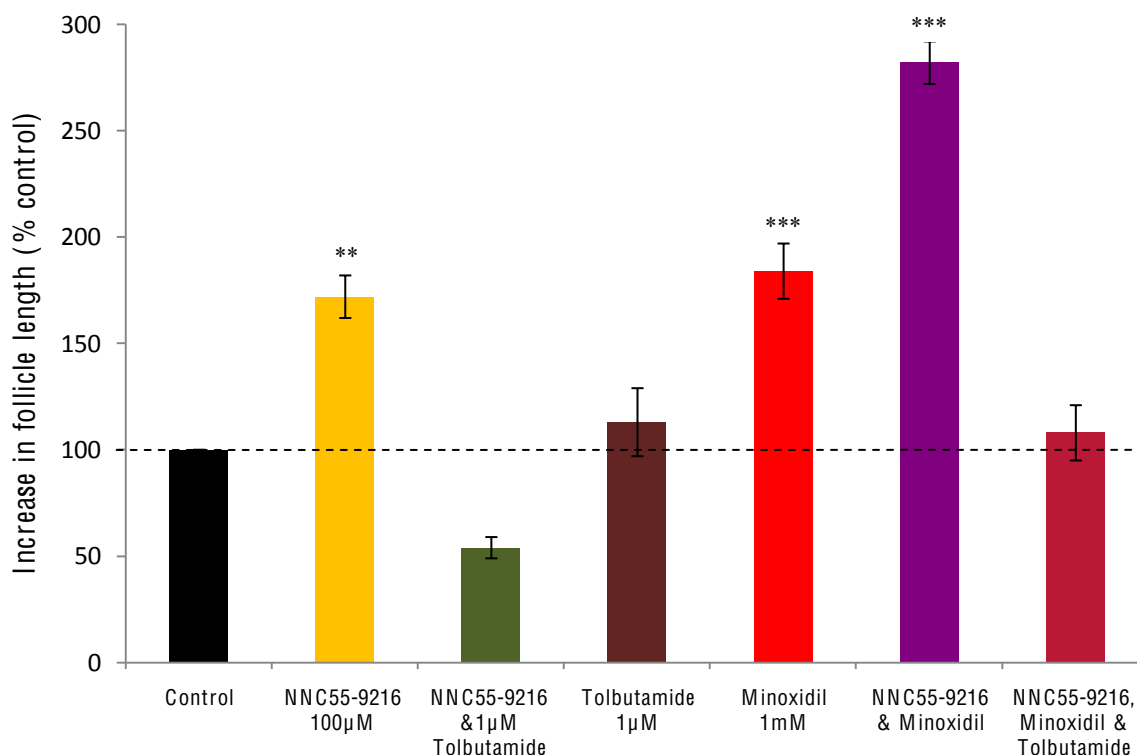
3.5 Discussion

The organ culture system for human hair follicles pioneered by Philpott *et al* (1989) routinely includes supplements such as insulin in the medium to increase hair follicle growth (Philpott *et al.*, 1989; Philpott *et al.*, 1990; Randall *et al.*, 2003). Since the overall aim of this chapter was to determine whether the opening of SUR1 K^+_{ATP} channels would enable the stimulation of human hair growth in organ culture, a culture system where follicles are already heavily stimulated to achieve good growth is not ideal. Insulin has a range of effects on cells, dependant on the cell type, though on the whole it acts as a stimulant in the uptake of glucose, by promoting the translocation of glucose transporter 4 (GLUT-4) proteins from an intracellular membrane pool to the plasma membrane, and facilitates the incorporation of glucose into storage molecules as glycogen (Cushman and Wardzala, 1980; Suzuki and Kono, 1980; Chiang *et al.*, 2003; Leney and Tavare, 2009). The initial investigations of this study examined the effect of 10 μg/ml insulin in the medium, on the growth of human scalp anagen hair follicles. Hair follicles were examined for alteration in length and changes in morphology, particularly in the hair follicle bulb, at 24 hour intervals for 9 days. All investigations took place in serum-free medium as serum inhibits hair follicle growth in organ culture (Philpott *et al.*, 1996) and in the absence of streptomycin which can interfere with minoxidil's actions (Sanders *et al.*, 1996).

In follicles which maintained an anagen morphology the production of a hair fibre and associated inner root sheath induced gradual hair follicle growth during organ culture, while the connective tissue sheath underwent no change and remained at the same level throughout the culture period (Figure 3.2). This is in agreement with previous reports on human hair follicle culture (Philpott *et al.*, 1990;

Shorter *et al.,* 2008). Hair follicle rate of growth in the presence of insulin was 0.20±0.02 (mean ± SEM) mm/day (Figure 3.2a) over 9 days, similar to that observed by Han *et al* (2004) who reported a growth of approximately 0.25 mm/day over 10 days, using the same concentration of insulin (10μg/ml). The experimental conditions were the same, except for the inclusion of streptomycin within their medium. A slightly higher growth rate was noted by Philpott *et al* (1996) (approx. 0.27 mm/day over 9 days in 10μg/ml of insulin), in serum-free medium supplemented with streptomycin. This is closer to the *in vivo* human growth rate of 0.32-0.35 mm/day of male scalp hair (Myers and Hamilton, 1951). Omitting insulin from the medium had a dramatic effect on hair follicle growth. At the end of the culture period, the total increase in hair follicle length in insulin-free medium was only 0.30±0.049mm, in contrast to the 1.90±0.046mm in the presence of insulin (p<0.001; Figure 3.3b).

During the culture period the hair bulb of some follicles displayed catagen-like morphological changes, where the hair fibre retracted up the follicle, leaving behind a cluster of dermal papilla cells (Figure 3.2e). The number of follicles that remained in the anagen growth phase was calculated for each day of the culture period. In the presence of insulin, the proportion of follicles in the anagen phase declined slowly and steadily, whereas follicles in the absence of insulin rapidly began entering catagen. On the third day only 60% of follicles remained in anagen in the absence of insulin, unlike 90% of follicles in the presence of insulin (Figure 3.3a). No follicles remained in anagen by day 5 in the insulin-free medium; in the presence of insulin this was about 80% and 43% of follicles remained in anagen at day 9. Past research has indicated that to maintain anagen in human hair follicles in organ culture beyond 4 days the presence of insulin is essential (Westgate *et al.,* 1993) and follicles that are cultured in insulin-free medium rapidly enter a

catagen-like state (Philpott *et al.*, 1994). Shorter *et al's* findings in 2008 similarly indicated that hair follicles in insulin-free medium rapidly entered a catagen-like state, and by day 9 no follicles remained in anagen, whilst in the presence of insulin about 65% of follicles remained in anagen.

The effect of the potassium channel opener, minoxidil, was investigated on human hair follicles in organ culture in both the presence, and absence, of insulin (Figures 3.4 and 3.5). The concentrations at which minoxidil was used in this study were selected with regard to investigations by both Shorter *et al* (2008) and Han *et al* (2004). Shorter *et al* (2008) reported that 1 mM of minoxidil stimulated anagen in insulin-free medium, whilst Han *et al* (2004) described that, during 10 days in serum-free culture in the presence of 10μg/ml of insulin, 100 μM and 1 mM minoxidil significantly increased hair follicle length, though 10 μM did not. Han *et al* (2004) claimed that the 1 mM concentration of minoxidil resembled that *in vivo* from topical applications of 3-5% minoxidil on human hair follicles*.* Therefore, 1mM was selected for this study. The percentage of follicles remaining in anagen was unaffected by 1 mM minoxidil in the presence of insulin (p=0.525; Figure 3.4a); however, in the absence of insulin minoxidil significantly increased the percentage of follicles maintained in anagen with over 50% of follicles still growing at day 9 (p<0.001; Figure 3.4b). A similar prolongation of anagen by 1 mM minoxidil was reported in scalp follicles cultured in serum-free medium by Shorter *et al* (2008). These effects concur with observations of minoxidil's effects *in vivo* where anagen is often prolonged (Messenger and Rundegren, 2004). The presence of insulin also altered the amount of hair follicle growth in response to minoxidil.

With insulin, minoxidil had an inhibitory effect on the average overall increase in the length of the hair follicle reducing it from 1.90 $\pm$ 0.046mm to 1.30 $\pm$

0.16mm (p=0.016; Figure 3.5a), whilst in its absence overall hair follicle length significantly increased from 0.30±0.049 mm to 0.72±0.053mm (p<0.001; Figure 3.5b).

Due to the diverse range of culture conditions used in investigations into minoxidil's effect on hair growth, it is difficult to make direct comparisons between studies. An earlier report by Philpott *et al* (1990) indicated that human hair follicle growth in organ culture was unaffected by minoxidil at 0.95 μM and 48 μM or inhibited by 0.95 mM in the presence of 10 ng/ml insulin, 50 μg/ml streptomycin and 1% fetal calf serum during 72 hours of culture; there was also no effect on DNA or protein synthesis. However, after 5 days of culture in the presence of 10 ng/ml insulin, 50 μg/ml streptomycin and 1% fetal calf serum, 0.95 μM minoxidil had a stimulatory effect, whilst the effects of 48 μM and 0.95 mM minoxidil remained the same. The report also indicated that serum had an inhibitory effect on hair follicle growth following 4 days in culture and there was no significant difference between hair follicles maintained in 1 % and 20 % serum. The group reasoned that the 0.95 μM minoxidil seemed to have counteracted the inhibitory effect of the serum, resulting in hair growth, rather than minoxidil having a stimulatory effect on hair growth alone. The omission of serum from the medium by Philpott *et al* (1991) resulted in steady hair follicle growth for up to 10 days in culture, thereby suggesting that serum is not essential for hair follicle growth *in vitro* and leading to the current standard culture conditions.

In order to overcome the interference of streptomycin with K⁺ channels Magerl *et al* (2004) substituted streptomycin with another antibiotic, ciprofloxacin. They showed that human hair follicle elongation after 12 days in culture using ciprofloxacin (10 μg/ml) was unaffected by 1 μM and 100 μM

minoxidil in the presence of 10 µg/ml insulin, but inhibited in its absence. In contrast Han *et al* (2004) reported a dose responsive stimulatory effect on hair follicle growth with 100 µM and 1 mM minoxidil during 10 days culture in the presence of 10 µg/ml insulin and 100 µg/ml streptomycin; however 10 µM minoxidil had no effect. It is noteworthy to highlight that Han's group only used 3 young male subjects aged between 20-35 but only 30 hair follicles were used, with 10 follicles per subject/per condition. In this study 50 hair follicles from 5 male subjects aged between 24-57 years, were used; however contrasting results were observed as 1 mM minoxidil in the presence of insulin had an inhibitory effect on hair follicle growth and no affect on the percentage of follicles remaining in anagen (Figures 3.5a and 3.4a). Philpott *et al* (1990), as discussed previously, also reported that 0.95 mM minoxidil had an inhibitory effect on hair follicle growth in the presence of 10 ng/ml insulin, 50 µg/ml streptomycin and 1% serum. Magerl *et al's* (2004) study which employed similar culture conditions to this thesis, reported that 1 and 100 µM minoxidil had no effect on hair follicle growth. However, the above studies have tended to involve follicles from older subjects. Shorter *et al's* (2008) research also used young male subjects, aged between 21-40, similar to Han *et al* (2004), but with the larger sample size of 11 donors and reported that 1mM minoxidil had no effect in maintaining follicles in anagen in insulin containing medium. This eliminates the prospect that the stimulatory effect of 1 mM minoxidil reported by Han *et al* (2004) was influenced by the use of younger subjects. Thus, Han *et al's* stimulatory effect on human hair follicle growth in the presence of insulin has not been confirmed by any other researchers.

Follicles from other species have also been used to investigate the effect of minoxidil *in vitro*. Buhl *et al* (1989) carried out a series of initial experiments on

minoxidil action using neonatal mouse vibrissae follicles, in medium containing 20% serum and 12.5 µg/ml gentamicin (antibiotic). Minoxidil at 1 mM maintained follicular morphology over 48 hours culture, while in the absence of minoxidil follicular morphology rapidly altered. In a subsequent study the K^+_{ATP} channel blockers, tolbutamide 0.5 mM and glyburide (0.5, 5 and 50 µM), failed to prevent the stimulatory effect of 1mM minoxidil (Buhl *et al.*, 1993) suggesting this was not K^+ channel mediated effect. Red deer (*Cervus elaphus*) follicles have also been used as a model system. The first deer hair follicle organ culture studies omitted serum, insulin and hydrocortisone as they were designed to investigate the effect of androgens (Thomas *et al.*, 1994; Thornton *et al.*, 1996; Randall *et al.*, 2003) and therefore no other hormones were included. Davies *et al* (2005) continued using these conditions to investigate potassium channel regulators on deer hair follicles, though additionally excluding streptomycin due to its reported interference with minoxidil's action (Sanders *et al.*, 1996). Davies *et al* (2005) found that the minoxidil was stimulatory during 8 days in culture. Minoxidil (0.1, 1, 10 and 100 µM) stimulated deer hair follicle growth in a dose responsive manner. Increased hair follicle growth was also observed with other potassium channel openers in culture, diazoxide (10 µM) and NNC 55-0118 (0.1, 1, 10 and 100 µM). The stimulatory effect of hair follicle growth was inhibited with the K^+_{ATP} channel blockers tolbutamide and glibenclamide.

In the comparison carried out in this study, in the presence of insulin minoxidil had no effect, whereas, in the absence of insulin it had a significant stimulatory effect (Figure 3.4). Overall, it is clear that insulin in the medium affects follicular responses to minoxidil. Insulin advances the movement of potassium ions into the cell and sodium out of the cell via the activation of $Na^+ K^+$ ATPases in

the plasma membrane (Irwin and Rippe, 2008). These alterations may result in the opening of K^+_{ATP} channels, as inhibition of $Na^+ K^+$ ATPases by ouabain has been shown to completely close K^+_{ATP} channels (Ding *et al.*, 1996), i.e. the same as the probable main action of minoxidil. Alternatively, as insulin acts as a stimulant of glucose uptake into cells and storage (Cushman and Wardzala, 1980; Suzuki and Kono, 1980; Leney and Tavare, 2009), follicles may have achieved maximum growth already.

The effect of the potassium channel blocker, tolbutamide, on human scalp hair follicle growth in organ culture was also investigated in the presence, and absence, of insulin. Tolbutamide, has been described as instigating hair loss in human beings (Litt, 2007) and was patented for use as a hair removal agent in 2007 (US patent 7160921, issued on 9.2.07). This leads to the prospect of research focused on a different aspect of hair growth, other than concentrating on the stimulatory effects of K^+_{ATP} channel openers for hair loss disorders, as current research has done (Ross and Shapiro, 2005), by looking into the inhibition of excessive hair growth. In the presence of insulin, tolbutamide induced catagen-like morphological changes in the hair bulb in both lower (1 μM) and high (1 mM) concentrations. The hair fibre retracted upwards in the follicle, detaching from a rounded cluster of dermal papilla cells left behind. In the presence of insulin, tolbutamide at 1 μM reduced the percentage of follicles in anagen to about $30\pm1\%$ by day 9 (p=0.004), and at 1 mM to about $10\pm2\%$ (p<0.001) (Figure 3.7a). The overall hair follicle growth exhibited a similar inhibitory affect; this fell from 1.68 ± 0.06mm in control medium to 1.10 ± 0.07mm (p=0.01) in 1μM tolbutamide and to 0.6 ± 0.16mm in 1 mM (p<0.001) over 9 days (Figure 3.8a). In the absence of insulin, the percentage of follicles remaining in anagen appeared higher than the

control but this was not significant, tolbutamide (1 μM) $3\pm2.4\%$ (p=0.063) follicles remained in anagen, while at 1 mM 0% (p=0.064) (Figure 3.7b). The same effect occurred in the overall hair follicle growth. In 1 μM tolbutamide the follicles had grown by 0.44 ± 0.06mm (p=0.055) after 9 days and in 1 mM tolbutamide 0.43 ± 0.05mm after 9 days (p=0.061) (Figure 3.8b) compared to the control follicles 0.39 ± 0.01mm. These results concur with the investigation by Shorter *et al* (2008) which showed tolbutamide (1 mM) shortened anagen in cultured human hair follicles significantly in the presence of insulin during 9 days in culture, while in the absence of insulin tolbutamide had no effect. Similarly Davies *et al's* (2005) study in insulin-free medium reported that tolbutamide (1 mM) inhibited deer hair follicle growth in culture. Whereas Buhl *et al* (1993) observed that 0.5 mM tolbutamide had no effect on mouse vibrissae follicles, in medium containing 20 % serum. The different effects of tolbutamide in the presence, and absence, of insulin support the concept that the K^+_{ATP} channels may be open in the presence of insulin as discussed earlier. Tolbutamide's inhibiting effect on hair growth in insulin containing medium is presumably due to the closing of the channels, whilst in the insulin-free medium, tolbutamide had no real effect, presumably as the channels were closed. Our understanding of the effect of insulin on hair follicle growth *in vitro* is currently rather inadequate and further research is required.

To indicate whether minoxidil and tolbutamide were acting via K^+_{ATP} channels they were used in combination. All further investigations omitted insulin in the medium, because of its significant effect in organ culture on hair follicles. William's E medium was used containing 10 μg/ml phenol red, 2 mM L-glutamine, 10units/ml penicillin, 0.001% DMSO. The medium was also supplemented with

100ng/ml hydrocortisone as it has been reported to enhance the morphology of hair follicles, though it does not affect the rate of growth (Westgate *et al.*, 1993).

The stimulatory effect of 1mM minoxidil on the number of follicles remaining in anagen was significantly inhibited when co-incubated with 1mM of tolbutamide reducing from about 50 ± 0 % to 0 % after 9 days culture (p= 0.0043; Figure 3.10a). Though the lower concentration of tolbutamide (1μM) also had some effect on the percentage of follicles in anagen reducing it to about $20\pm4\%$ (p=0.018; Figure 3.10b), it did not block the minoxidil effect entirely. Similarly, the minoxidil-stimulated increase in mean overall hair follicle length to 0.80 ± 0.043mm was greatly inhibited by tolbutamide at both concentrations; at 1 mM it was reduced to 0.50 ± 0.06mm (p=0.004; Figure 3.11a), while at 1 μM it reduced growth to 0.55 ± 0.072mm (p=0.019; Figure 3.11b). This corresponds to Shorter *et al's* (2008) investigation that showed 1 mM minoxidil in insulin and streptomycin-free medium significantly increased the number of follicles remaining in anagen, an effect blocked by 1 mM tolbutamide. Similarly Davies *et al's* (2005) study on deer hair follicles cultured in serum-and streptomycin-free conditions showed that minoxidil (0.1, 1, 10 and 100 μM) stimulated hair follicle growth in a dose responsive manner and that 1 mM tolbutamide significantly inhibited the stimulatory effects of 10 μM minoxidil.

The susceptibility of human hair follicles in organ culture to stimulation by the potassium channel opener, minoxidil, and the inhibition of this effect by the potassium channel closer, tolbutamide, strongly supports the hypothesis that the mechanism of action of minoxidil in promoting hair growth is via K^+_{ATP} channels.

Minoxidil opens SUR2B K^+_{ATP} channels, but not those with SUR1 sulphonylurea subunits (Schwanstecher *et al.*, 1998) and tolbutamide selectively

inhibits SUR1 K^+_{ATP} channels at a low concentration up to 100 nM and SUR2B K^+_{ATP} channels at a high concentration from 10μM (Babenko *et al.*, 1998; Ashcroft and Gribble, 2000; Fujita and Kurachi, 2000; Reimann *et al.*, 2001; Gribble and Reimann, 2003; Seino and Miki, 2003).

To determine more fully whether SUR1 channels can be involved in regulating human hair follicle growth, the selective SUR1 channel opener, NNC 55-9216, was investigated in organ culture using insulin-free medium. NNC 55-9216 (100 μM) effectively promoted follicles to remain in anagen with 43±3% at day 9 compared to 0% in the control medium (p=0.003; Figure 3.13a). The mean overall increase in hair follicle length also showed a significant increase from 0.30±0.05mm to 0.67±0.03mm over the 9 day culture period (p=0.002; Figure 3.13b). This corresponds with Davies *et al's* (2005) findings where another selective SUR1 channel opener, NNC 55-0118, effectively stimulated growth in deer hair follicles in organ culture, an effect which was inhibited by 1 mM tolbutamide. In the human follicles the lower concentration of tolbutamide, 1 μM, successfully hindered the stimulatory effect of NNC 55-9216 on percentage anagen (p=0.008; Figure 3.13a) and reduced the overall increase in hair follicle length to 0.21 ± 0.03mm (p<0.001; Figure 3.13b) supporting the concept that NNC 55-9216 is acting via a SUR1 K^+_{ATP} channel. Interestingly, the combination of NNC 55-9216 and 1 μM tolbutamide reduced the overall growth to less than two thirds of that of the control (p=0.032), indicating a very strong inhibition of hair growth rate as anagen was insignificantly prolonged compared to the control (p=0.06).

The response of human hair follicles to the SUR1 channel opener in culture fits well with Shorter *et al's* (2008) detection of SUR1 gene expression in human hair follicles, suggesting a possible role for SUR1 K^+_{ATP} channels in human hair

follicles. It also agrees with the detection of SUR1 gene expression in deer follicles reported in Chapter 2 and the pharmacological effects on deer follicle growth reported previously by Davies *et al* (2005). Unfortunately, this suggests that the development of novel drugs for pancreatic disorders, which act via selective stimulation of the SUR1 K^+_{ATP} channels, is also likely to facilitate hair growth as a side effect, like the broad acting diazoxide. When diazoxide is used for hyperinsulinemia in babies it generally causes such pronounced general hypertrichosis that the parents often feel their child is becoming like a monkey and request a pancreatectomy (Stanley, 2002). It had been hoped that as the hair growth promoting potassium channel openers in the clinic, minoxidil and diazoxide, were either a SUR2B channel opener (the former) or a broad spectrum SUR1 and SUR2 opener (the latter) that a selective SUR1 channel opening drug would improve pancreatic symptoms without promoting hair growth. However, the stimulation of hair follicle growth in organ culture does suggest a novel field of pharmaceuticals that act via SUR1 K^+_{ATP} channels with the objective of stimulating hair growth. In addition, this raises the possibility that if incorporated with the currently used minoxidil hair loss treatment, which acts via the SUR2B channel, novel therapies could prove to be far superior to current treatments. As SUR1 channels are expressed in the matrix of the hair follicle bulb and SUR2B channels in the dermal sheath and dermal papilla cells (Shorter *et al.,* 2008), such treatment holds the possibility of effectively acting on different parts of the hair bulb.

With the above suggestion for novel pharmaceuticals in mind, the effects of combined minoxidil and NNC 55-9216 were examined. Minoxidil (1mM) significantly stimulated the percentage of follicles remaining in anagen to about $50\pm0\%$ compared to 0% in the control medium (p<0.001), whilst 100 µM NNC 55-

9216 prolonged anagen to about $43\pm3\%$ (p=0.003) and the combined treatment had the greatest effect on the follicles with about $60\pm2\%$ remaining in anagen (p<0.001; Figure 3.14a). This increase was significantly higher by about $17\pm1\%$ than that achieved with NNC 55-9216 alone (p=0.03), whilst it was insignificantly higher than minoxidil (p=0.099) (Figure 3.14a). Similarly, the overall increase in hair follicle growth over 9 days in culture was significantly stimulated by 1mM minoxidil to 0.80 ± 0.043mm compared to the control 0.30 ± 0.05mm (p<0.001); whereas in 100 μM NNC 55-9216 the follicles grew 0.67 ± 0.03mm (p=0.002) and the combined treatment had the most effect, promoting growth of 1.10 ± 0.04 mm (p<0.001) (Figure 3.14b). The combined effect was significantly higher compared to that produced by NNC 55-9216 (p=0.001) and minoxidil alone (p=0.006) (Figure 3.14b).

This increase with the two drugs combined appears to be additive rather than synergistic and does suggests that they are not necessarily acting on the same point, i.e that there are two routes involving SUR2B and SUR1 K^+_{ATP} channels that can regulate hair growth. The stimulatory effect of the combined treatment on the number of follicles remaining in anagen was reduced with 1 μM tolbutamide from about $60\pm2\%$ to about $23\pm3.4\%$ after 9 days culture, but in comparison to the control, the percentage of follicles remaining in anagen were still significantly raised (p=0.01) (Figure 3.15a). However, the overall increase in hair follicle length was significantly inhibited with the addition of 1 μM tolbutamide from 1.10 ± 0.04mm to 0.42 ± 0.04mm (p<0.001) over 9 days (Figure 3.15b). This inhibition strongly supports the idea that SUR1 channel opener, NNC 55-9216, is stimulating human hair follicles via K^+_{ATP} channels.

We have not yet realised the full functioning and potential of K^+_{ATP} channels in any tissue and have limited knowledge of the elaborate mechanism involved in nucleotide binding or channel regulation (Ashcroft, 2006; Nichols, 2006). We also do not know what the mechanisms are in the hair follicle beyond altering the opening of K^+_{ATP} channels. Presumably, this involves the alteration of potential differences across cell membranes in dermal papilla cells and possibly matrix keratinocytes. When the channels are prompted to open by either of the channel opening drugs, K^+ ions will move out of the cells or organelles. Presumably, this will cause the opening of voltage-gated channels allowing other positively charged ions such as Ca^{++} to move into the cells. Ca^{++} are commonly involved in cell signalling and frequently induce secretion of stored proteins from secretory vesicles by exocytosis (Berridge *et al.*, 2003; Clapham, 2007). If this occurred in dermal papilla cells, this could stimulate paracrine signalling via growth factors, which could target other cells such as matrix keratinocytes or melanocytes or even autocrine regulation of dermal papilla cells. Such communication is believed to occur between dermal papilla and other cells in hair follicle development, growth and hormonal regulation (Jahoda and Reynolds, 1996; Richardson *et al.,* 2005; Hamada and Randall, 2006; Randall, 2007; Waters *et al.*, 2007). The closing of K^+_{ATP} channels by tolbutamide can also affect the balance of ions, which could result in a similar disruption to ion movement as described above. This could be the cause of changes in hair follicle morphology.

Further research will increase our understanding of hair follicle biology and hopefully enhance our ability to structure therapies so that they can either promote or inhibit hair growth more effectively in accordance with clinical need.

Chapter 4

Proteomics and potassium channels

4.1 Introduction

The effect of potassium channel modulators on human and deer hair follicle growth in organ culture (see Chapter 3), and the absence of the K^+_{ATP} channel subunit gene expression in telogen follicles, though present in anagen follicles, as demonstrated in the deer model (Chapter 2), signify the importance of K^+_{ATP} channels within hair follicles. They suggest that hair follicle K^+_{ATP} channels are implicated in the clinical observation of increased hair growth with treatment by potassium channel openers such as minoxidil and diazoxide (Olsen *et al.*, 1987; Olsen *et al.*, 1990). At present, the specific mechanisms by which K^+_{ATP} channel openers modulate hair growth remain unclear. Schwanstecher *et al* (1998) reported minoxidil to have specific affinity to the SUR2B subunit, and Shorter *et al* (2008) indentified SUR2B in the dermal papilla of human hair follicles. This raises the intriguing prospect of the dermal papilla providing the target through which at least some K^+_{ATP} channel openers function.

The dermal papilla is known to play a major role in mesenchymal-epithelial interactions in the hair follicle and to regulate many aspects of hair follicle activity including determining the type and size of hair produced (Reynolds and Jahoda, 1991; Jahoda and Reynolds, 1996; Richardson *et al.,* 2005; Waters *et al*., 2007). It is also believed to be the focus of androgen alteration of hair follicle size by changing the production of paracrine factors such as soluble growth factors or extracellular matrix proteins when androgens bind to receptors in dermal papilla cells (Randall *et al.*, 1991; Randall, 2008). Therefore, a possible mechanism is the binding of minoxidil to SUR2B containing K^+_{ATP} channels in the dermal papilla which would be the signal for the alteration of factors that could act on cells of the

hair follicle such as the keratinocytes. This makes the dermal papilla an essential subject for further investigation.

In 1981, Jahoda & Oliver successfully cultured cells from isolated rat vibrissa dermal papilla. The dermal papilla cells retain at least some of their inductive characteristics for a short time in culture and can induce hair growth when implanted into follicles which otherwise would not grow hair (Jahoda *et al.*, 1984).   Retaining androgen-sensitivity differences of their parent follicles in culture (Randall *et al.*, 1991; Randall, 2008) also marks dermal papilla cells as a useful model with which to investigate the action of hair follicle regulatory factors. Furthermore, in cultured human dermal papilla cells, minoxidil stimulated the vascular endothelial growth factor (VEGF) (Lachgar *et al.*, 1998). Minoxidil was also found to increase the production of prostaglandin E_2 in cultured rat vibrissae dermal papilla cells (Lachgar *et al.*, 1996a). Interestingly, Sanders *et al* (1996) found that minoxidil was initially inhibiting the NIH 3T3 fibroblast cell proliferation, however omitting streptomycin from the medium, reversed that effect.

Proteins are essential in cell behaviour and determine their phenotypes, therefore the study of proteins altered by potassium channel regulators using proteomic methods should grant us a greater comprehension of the mechanisms of minoxidil action.   The term proteomics refers to the characterisation of the complete set of proteins encoded by the genome of a given organism (Wilkins *et al.*, 1996).

The genomes of organisms include the nucleotide sequence and within that: structural genes, regulatory sequences and non-coding DNA segments, in the chromosomes of an organism. The study of genomes (genomics) was established

by Fredrick Sanger with his success in sequencing the complete genomes of a virus and mitochondrion (Fiddes *et al.*, 1977). His group pioneered techniques of sequencing, genome mapping, data storage, and bioinformatics analyses. It received incredible media attention in 2001, with sequencing of the human genome (Venter *et al.*, 2001). Though research in the field of genomics has contributed abundantly to medical research, the study of genes alone is not sufficient to understand how cells, tissues and the body functions. Synthesised proteins are the main components of the physiological and metabolic pathways of cells and their structure. Thus, analysis of proteins affected by minoxidil should contribute greatly to our understanding of the processes and pathways involved.

Coined as an analogy to genomics by Marc Wilkins in 1994, proteomics has the capacity to merge analytical techniques with complex bioinformatics to allow for further biological investigation. Earlier protein research used the Edman degradation sequencing (Edman, 1949) and two-dimensional polyacrylamide gel electrophoresis (2D-PAGE) (O'Farrell, 1975). Breakthrough development of mass spectrometry technologies, which has led to characterisation of proteins, not only propelled mass spectrometry as a prominent force in the field of proteomics but also established proteomics as a leading research field. Mass spectrometry is incredibly proficient at identifying peptides. Prevalently in proteomics research, the complex mixture of proteins is digested into peptides prior to mass spectrometry analysis (Rappsilber and Mann, 2002). This digestion step is undertaken for two primary reasons: the peptides are rendered more soluble in solution than as a whole protein, and though mass spectrometry measures mass with high precision, it does not merit confident identification of a protein *de novo* ascertained exclusively on its molecular weight. Thus, the peptide enables the

identification of the protein it originates from, by proxy. Typically, peptide fragments formed by digestion by an enzyme, such as trypsin, produce a mass spectrum; this is referred to as a "peptide map" or a "peptide fingerprint" (Blackstock and Weir, 1999). Identification of a protein can then be achieved by the comparison of the collected masses to *in silico* (computer simulated) peptide maps, obtained from either a protein or genomic database.

Data mapping is most preferable for the purposes of identifying a single protein within a simple mixture; furthermore access to data is realised with ease. However, this process does not offer conclusive identification for complex mixtures (e.g. cell lysates), as the peptide masses recorded in the mass spectrum will arise from scores of different species. Nevertheless, the available instrumentation allows for a greater depth of information to be obtained from peptide masses observed in mass spectrometry. Rather than depend upon the accurate mass of a specific peptide, collision induced dissociation (CID) can be employed to isolate and fragment individual peptide ions (Martin *et al.*, 1987). Following this, the masses of the fragment ions are recorded and are drawn upon to acquire partial or complete sequence information. This process, typically referred to as tandem mass spectrometry (MS/MS), does not completely reduce the peptides into their constituent amino acids; rather, what is achieved is a collection of fragments containing diverse lengths of the peptide (Nesvizhskii and Aebersold, 2004). The 'sequence ladders' that are then obtained from this information lead to the deduction of primary sequence information of the peptide. The following step involves the use of software programmes that are capable of comparing the experimental data to *in silico* MS/MS mass spectra calculated from

the protein sequences in the database to analyse the collected raw data (Chamrad *et al.*, 2004).

Originally research in proteomics strived to identify all the components of a proteome and generate a complete protein database or biological map. In order for comparisons to be made between different experimental states the proteins must be studied quantitatively. Quantitative proteomics has several formats (Bantscheff *et al.*, 2007), however, stable isotope labelling by amino acids in cell culture (SILAC) is both a simple and powerful approach. SILAC efficiently reveals how inhibitors or perturbations affect the dynamic properties, as well as cellular distribution of proteins. Mass spectrometry analysis then determines and quantitates the relative ratios of each isotopic form of every peptide; thereby measuring any increase, decrease or consistency in the level of each protein in the complex following use of treatment.

4.2   Aims and experimental design

The overall aim of this chapter was to clarify further the modes of action of minoxidil in human hair follicle dermal papilla cells. Initially, the aim was to see if minoxidil would affect dermal papilla cell proliferation, and, if so, whether this could be inhibited by the opposing effects of the potassium channel blocker, tolbutamide. The second aim was to investigate the mechanisms of action of minoxidil by determining which proteins had been altered via a mass spectrometry-based, quantitative proteomics approach.

To investigate the effect of minoxidil in cell proliferation in cultured dermal papilla cells, cells were established from non-balding scalp hair follicles of five

individuals between the ages of 42-60. The cells were incubated in medium RPMI 1640 (supplemented with: 10% fetal calf serum, 100 units/ml penicillin G, 100 ng/ml amphotericin B and 2 mM L-glutamate), containing 0.001% of DMSO. The latter was added as the tolbutamide had to be dissolved in DMSO, and the media for all conditions were similarly supplemented in order to maintain consistency. Streptomycin was reported to inhibit the stimulatory effect of minoxidil (50 μM) on dermal fibroblast cell proliferation; therefore it was excluded from the culture conditions of this investigation (Sanders *et al.*, 1996).

The concentration of minoxidil selected for this study was 100 μM, which is within the range of concentrations used in previous investigations that had reported stimulation with minoxidil in dermal papilla cell proliferation e.g. 500 μM by Kurata *et al* (1996) and 1 μM by Han *et al* (2004). Tolbutamide was used at 1 mM to assess whether the channel blocker inhibited any effect of minoxidil.

To study the effect on cell proliferation several methods were employed, initially the Trypan-Blue exclusion technique was employed to identify viable cells to perform manual viable cell counting, using a haemocytometer. To validate the results further, the protein in cell extracts was quantified using a protein assay. Finally an MTT cell proliferation assay was also performed similar to a study by Han *et al* (2004). However, they seeded cells at 1.5×10^4 cells per well in 96-well plates for 5 days in the presence of minoxidil, while in this investigation the cells were seeded at 5×10^3 cells per well in 96-well plates and when they reached 80% confluence the treatments were added for 48 hours. The 48 hours of exposure was decided upon in light of the study by Lachgar *et al* (1998) in which dermal papilla cells incubated for 48 hours with various concentrations of minoxidil showed that

minoxidil stimulated VEGF expression (vascular endothelial growth factor) (Lachgar *et al.*, 1998).

To investigate the effect of minoxidil on protein profiles, dermal papilla cells from four individuals were used, the cells were seeded at 20% confluence in duplicate in SILAC (Stable Isotopic Labelling of Amino acids in Cell culture) medium, in either a 'light' (i.e. unlabelled arginine and lysine amino acids) or 'heavy' (i.e. ^{13}C labelled arginine and lysine amino acids) form of the amino acid supplemented with 10% of dialysed fetal calf serum. For cell labelling to be completed, the cells were grown to 80% confluence, which was approximately five population doublings, in the appropriate 'light' and 'heavy' media. Dialysed fetal calf serum was then omitted from the 'light' and 'heavy' media. The cells in the 'heavy' media were then treated with 100μM minoxidil for 48 hours. The cells in the 'light' media were used as the vehicle control. The proteins were then extracted from both sets of media and combined. After reduction and alkylation, the combined proteins were separated by SDS PAGE and peptides were generated, separated and analysed by mass spectrometry. Subsequently, the proteins were identified through database search, enabling quantitative differences of minoxidil at the protein level to be determined.

4.3 Materials and Methods

4.3.1 Investigation into the effects of potassium channel modulators on human hair follicle derived dermal papilla cells *in vitro*

4.3.1.1 Hair follicle dermal papilla isolation

The skin specimens were obtained as described in section 3.3.1.1, with the exception of the transport media. The medium used for this procedure consisted of RPMI 1640 (RPMI supplemented with: 10% fetal calf serum, 10 units/ml penicillin/streptomycin, 100 ng/ml fungizone and 2mM L-glutamate) (Gibco, Paisley, UK). Anagen hair follicles were dissected from the skin as described in section 3.3.1.2 (Figure 3.1), with the exception that the entire procedure was carried out inside the transport medium.

Once the anagen follicles were isolated the hair fibre and the connective tissue sheath (dermal sheath) were gently disengaged, using sterile needles (271/2G tuberculin syringe). This left the dermal papilla (DP) intact within the dermal sheath (DS)/connective tissue sheath (CTS) (Figure 4.1b). The connective tissue sheath was then cut above the bulb, with the dermal papilla remaining intact in the bulb (Figure 4.1d). An incision was made along the bulb allowing for the dermal papilla to be exposed (Figure 4.1e) and subsequently detached from the connective tissue sheath (Figure 4.1f). The isolated dermal papilla (Figure 4.1g) was then placed into tissue culture dishes (35mm), which had been pre-coated with fetal calf serum (FCS) creating a sticky surface that would assist adhesion of the DP to the surface. This was achieved by overnight incubation of the dishes with 1 ml of FCS at 37°C. With the tip of a 271/2G needle the papilla was fixed onto the 35mm dish, containing 2 ml RPMI growth medium (RPMI growth medium comprising: FCS 20%, 10 units/ml penicillin/streptomycin, 2.5 ng/ml fungizone

(amphotericin B) and 2mM L-glutamate) (Gibco, Paisley, UK), at an average of four dermal papillae per dish. Inside the petri dish the DPs were 'scored' thereby fixing them further as well as breaking the capsule, this aided better cell explantation (Figure 4.1h). The dishes were left undisturbed for a week. Once cell multiplication was evident (Figure 4.2), the medium was changed every two days. Cells were incubated in a Heraeus incubator in a humid atmosphere of 5% CO_2, 95% air at 37°C.

Figure 4.1 Isolation of hair follicle dermal papilla by micro-dissection

(a) The anagen hair follicle was micro-dissected from scalp skin, as described in Figure 2.3, Scale Bar = 190 μm. **(b)** The connective tissue sheath and dermal papilla, were isolated **(c)** by the separation of the epithelial components of the follicle, Scale Bar = 200 μm **(d)** The connective tissue sheath containing the intact dermal papilla was cut above the bulb level, with great dexterity, Scale Bar = 200 μm. An incision along the side of the bulb was made **(e)** and the remaining connective tissue sheath was carefully peeled away, leaving the DP exposed. **(f)** The connection between the DP and remnants of the sheath were then completely severed and any excess connective tissue sheath removed, **(g)** leaving a completely isolated DP, Scale Bar = 22.4 μm. **(h)** The isolated dermal papilla was then transferred into a tissue culture dish and scored to break the capsule and aid better adhesion, Scale Bar = 133 μm. Photographed on dissecting microscope (Leica MZ8, Leica, Germany) using a Nikon Coolpix4500 (Nikon E4500) digital camera.

(d)

Connective tissue sheath

Dermal papilla

Hair bulb 400µm

(e)

Dermal papilla

112µm

Connective tissue sheath

(f)

Dermal papilla

Excess connective tissue sheath to be removed

Connective tissue sheath

(g) Dermal papilla

(h)

Scratches on dish coating made during transfer of dermal papilla and breaking of capsule
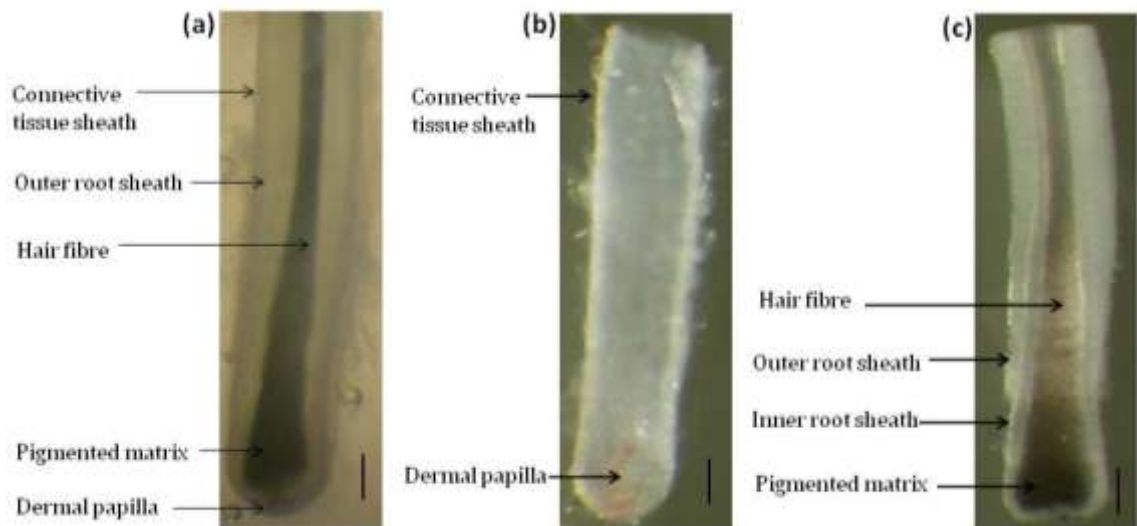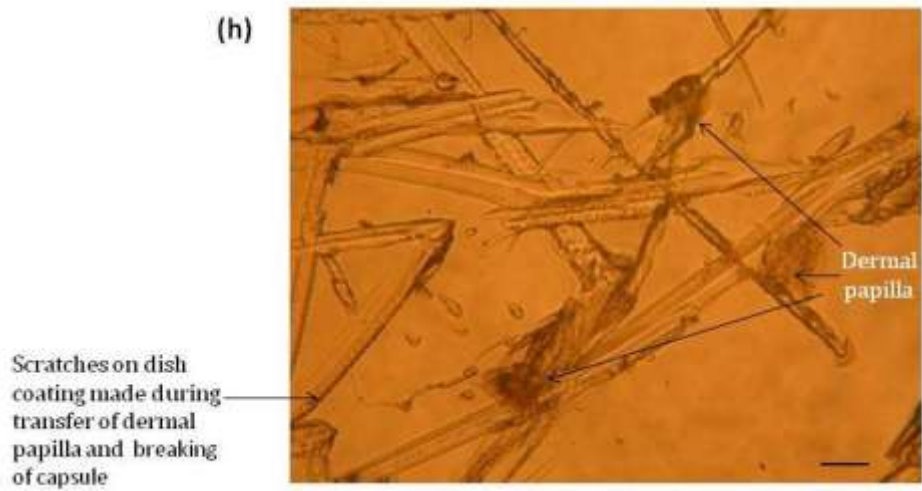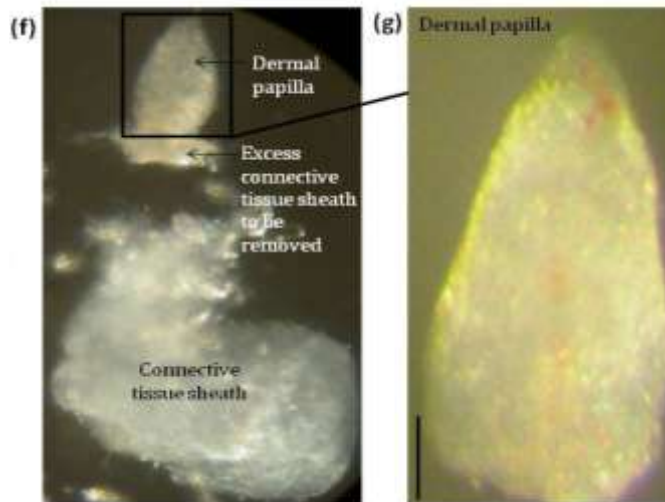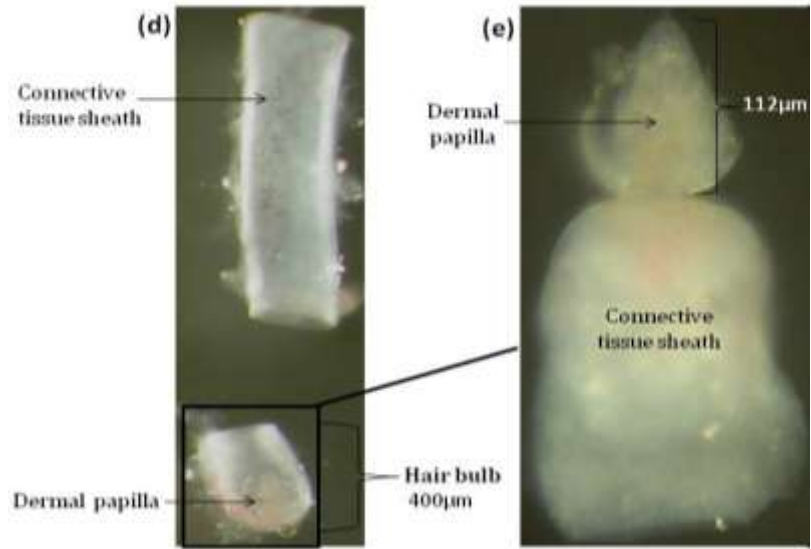
Dermal papilla

Figure 4.2 Dermal papilla primary cultures

Early dermal papilla fibroblast explantation outgrowth began to appear within two weeks after the incubation of the primary culture, Scale Bar = 50 μm.
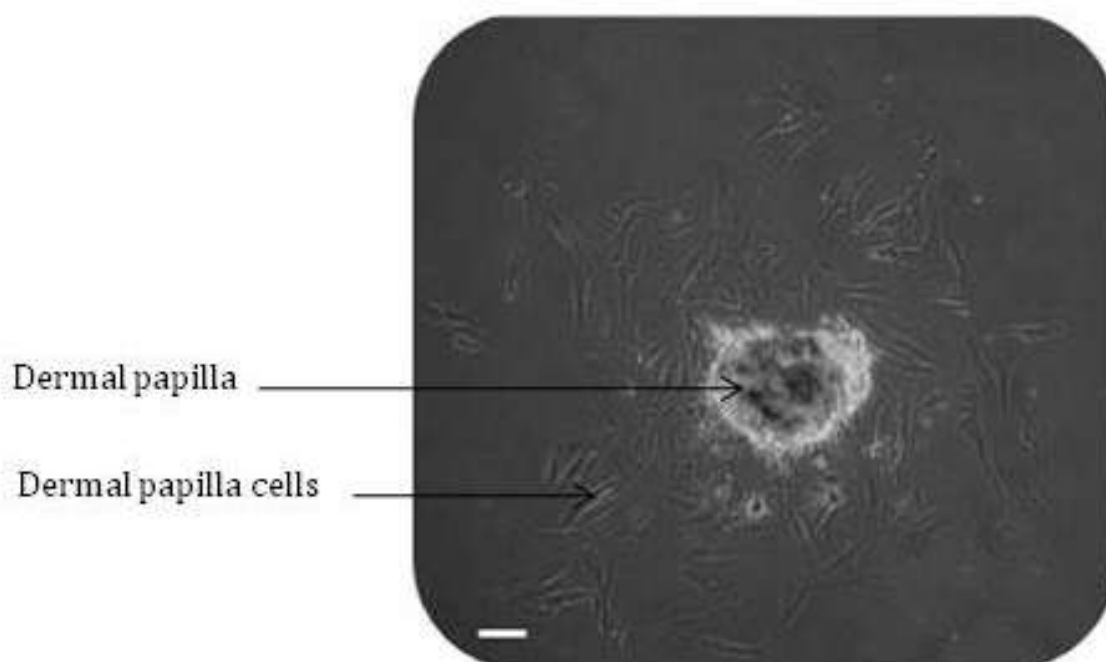
4.3.1.2 Maintenance of cell cultures

Rectangular canted-neck plastic cell culture flasks were used to culture cells; these were sealed with vented caps (Corning Life Sciences, UK). Three sizes of flask, with surface areas 25 cm², 75 cm² and 225 cm², were used depending on the number of cells. DP cell cultures had the medium changed every 2 days. Medium consisted of RPMI 1640 with 10% FCS, 10 units/ml penicillin/streptomycin (Gibco, UK), 25 ng/ml fungizone (amphotericin B), 2mM L-glutamate (Biowest, UK) and 0.001% dimethyl sulfoxide (DMSO) (Sigma).

4.3.1.3 Passaging of cell cultures

When cell cultures reached around 80% confluence, passaging was performed. The medium was removed from the flasks, and the cells were washed thrice in a suitable volume of sterile PBS, to ensure the removal of any trace serum that could possibly inactivate the trypsin/EDTA. A suitable volume of trypsin/EDTA (500 µl in 25 cm^2, 1ml in 75 cm^2 and 3ml in 225 cm^2 flasks) was then added to the cell culture flask and placed in an incubator at 37°C with 5% CO_2 and 95% O_2 until the cells had detached, typically after a minute. Following this the flask was positioned under an inverted microscope (Olympus, CKX41, Olympus Optical Co Ltd, UK) and lightly tapped until all cells had detached from the surface of the flask. To inactivate the trypsin/EDTA, growth medium (containing serum) was added to the cell culture flask. The cells were transferred to a larger flask (1:3) and placed back in the incubator for about 24 hours, allowing the cells to attach to the surface of the culture flask.

4.3.1.4 Freezing and thawing of cell cultures

Confluent cells that needed to be frozen down for storage and later use, were trypsinised (as described in section 4.3.1.3) and spun down in a centrifuge (Sanyo Harrier 15/80) at 1200 rpm (290 g) for about 5 minutes. The supernatant was then carefully removed to avoid disruption of the cell pellets, which were resuspended in cell freezing solution consisting of 90% FCS and 10% dimethyl sulphoxide (DMSO, Sigma, UK), which acts as a cryoprotectant. Approximately 1 x 10^6 cells were aliquoted into 1 ml cryovials (Nunc, UK) from the cell suspension, and placed in an isopropanol bath, at -80°C, overnight before being transferred to liquid nitrogen for long-term storage.

183

Thawing of the cells required the removal of the cryovials from the liquid nitrogen, and their placement into a water bath at 37.5°C. Near the completion of the thawing the contents of the cryovial were added to a T75 culture flask, with 10 ml growth medium. For cells to attach to the surface of the flask, the flask was placed in the incubator for 24 hours. The medium was changed every 2 days.

4.3.1.5 Cell counting using the haemocytometer method

The Trypan-Blue technique was employed to perform manual viable cell counting by observation in triplicate. Trypan-Blue technique is most commonly used to distinguish viable from nonviable cells. Viable cells prevent uptake of the dye, whereas nonviable cells absorb the dye and become blue.

Cells were detached from the culture flasks as described in section 4.3.1.3. The cell suspension was then transferred to a 25 ml universal tube and mixed meticulously for equal cell distribution. The cell suspension (100 μl) was added to a 1.5 ml eppendorf tube containing 100μl of 0.4% Trypan-Blue in PBS; this solution was pipetted repetitively to ensure the cells were equally distributed. Then 10 μl of Trypan Blue stained cell suspension was transferred into each of the two chambers of a coverslipped Improved Neubauer Counting Chamber (Gallencamp, UK), with care not to overfill the chamber (Figure 4.3a).

The viable (unstained) cells in each of the four large corner squares and the centre square (Figure 4.3c) (viewed under x20 magnification) (Olympus, CKX41, Olympus Optical Co Ltd, UK) were counted with an average number being calculated. The cell numbers were counted three times, and to obtain the total yield of cells, the average value calculated was multiplied by 10^4 (volume factor for chamber) giving the total number of cells per ml of cell suspension and multiplied

by the dilution factor (x2) and total medium used to resuspend the cells after trypsinisation. The average cell count was calculated with ± standard error of the mean (SEM) based on the triplicate counts.

Figure 4.3 The principle of haemocytometer

Diagrams highlighting the principle of haemocytometry. Number of cells per ml calculated= Average cell count in each of the four large corner squares and the centre square (c) x 10^4 x dilution factor (The cell suspension was mixed in 1:1 ratio with Trypan blue, therefore dilution factor is 2) (Adapted and modified from Experimental Biosciences).
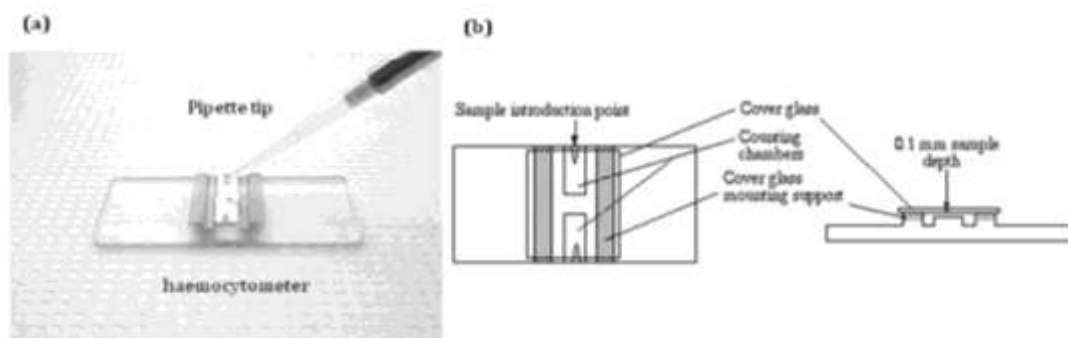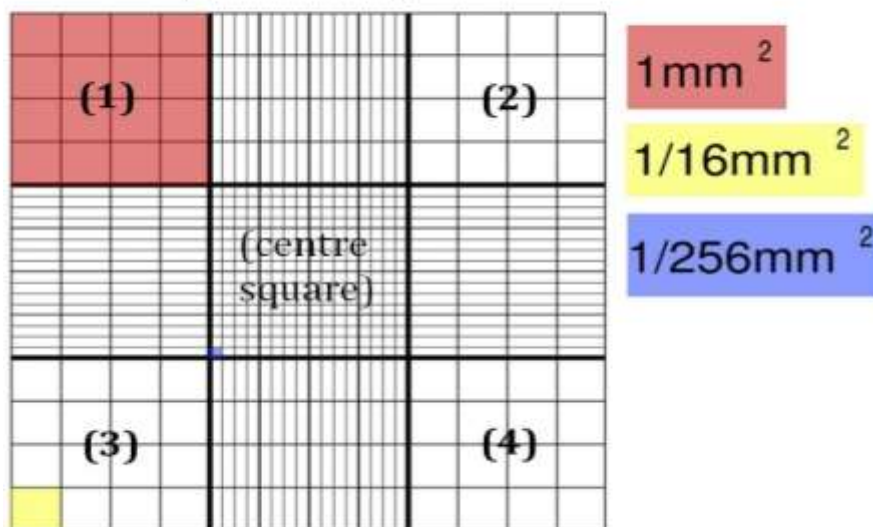
4.3.1.6 Cell seeding for growth curve construction

Dermal papilla cells from five individuals between the ages of 42-60 were used to assess the effect of potassium channel regulators on growth of dermal papilla cells in culture. The growth media used consisted of RPMI 1640 supplemented with 10units/ml penicillin G (sigma), 10% FCS, 25 ng/ml fungizone (amphotericin B), 2mM L-glutamate, and 0.001% DMSO (Biowest, UK). The cells were cultured in the presence of either: vehicle control as above, minoxidil (100 μM); tolbutamide (1 mM); or a combination of both minoxidil (100 μM) and tolbutamide (1 mM).

The cells were counted as described in Section 4.3.1.5, and the volume of cell suspension containing 1×10^4 cells was determined and seeded into 12-well plates. The final volume in each well was brought up to 1 ml using growth medium. Overall, 21 wells were seeded for each condition, from each sample to perform 7 counts in triplicate over a period of 15 days. The cell counting was performed on days 3, 5, 7, 9, 11, 13 and 15.

The medium was changed every two days throughout the experiment. Cells were incubated in a Heraeus incubator in a humid atmosphere of 5% CO_2, 95% air at 37ºC. Using Microsoft Excel (Microsoft Corporation, Ca., USA) the growth curves were plotted with 'Time' at the x-axis and 'Cell number' at the y-axis. The data was analysed with the ANOVA test using SPSS statistical analysis program (SPSS Inc., Chicago, Illinois). All cells used for proliferation were from the fourth passage.

4.3.1.7 Protein extraction of dermal papilla cells at completion of cell counting study

Cell suspensions in all conditions were retained at the completion of the cell counting study, at day 15. Across the five samples the same conditions were pooled together and protein was extracted from these cells to perform a protein assay. A comparison could then be drawn between the cell counting and resultant protein values.

Each cell suspension was transferred to a 1.5 ml eppendorf tube. This was centrifuged at 1,200 rpm (290 g) (Sanyo Harrier 15/80) for the duration of 7 minutes. When this process ended the supernatant was disposed of and the pellet was resuspended in 100μl of sample buffer (Glycerol (BDH Lab Supplies) 2.5 ml; ethylenedaiminetetraacetic acid (EDTA) (Sigma) 0.185 g; sodium dodecyl sulphate (SDS) (Sigma) 1.5 g; Tris (Sigma) 0.19 g; 25 ml distilled water). This was then transferred to a 0.5 ml eppendorf tube with protease inhibitor cocktail (1:20) (Sigma). Using a 1 ml syringe, the cell suspension was triturated several times to ensure the protease inhibitor cocktail was thoroughly dispersed. The sample was put on to ice for three hours, at which point the cell suspension was vortexed at 30 minute intervals for 10 seconds at a time. After three hours the cell extract was centrifuged for three minutes, at 13,000 rpm (13,000 g) and the resultant supernatant, which contained the solubilised protein, was transferred to a clean eppendorf and frozen at -80^0C, until further use.

4.3.1.8 Quantification of protein in cell extracts (Bradford Assay)

Protein standard (see Appendix 1) or test protein sample (5 μl) was added to the appropriate well on a 96 well-plate in triplicate. Reagents A' (25 μl) and B

(200 μl) (see Appendix 1) was added to every well. The plate was shaken for 20 minutes, using a plate shaker; it was then placed into a plate reader (Dynex MRX) that measured each sample absorbance at 750 nm. The calibration curve and the noted absorbance of the protein samples were used to ascertain the protein concentration of cell extract samples.

4.3.1.9 MTT, (3-(4, 5-dimethylthiazol-2-yl)-2,5-diphenyltetrazolium bromide) cell proliferation assay.

The MTT assay is a quantitative colorimetric technique used to determine cell proliferation or cell survival. When cells are exposed to the dye, live mitochondria cleave MTT (tetrazolium salt) turning the dye from pale yellow salt to a dark formazon product. Dead cells are unable to cleave the MTT therefore less of the blue colour signifies less living cells. The absorbance of the solution is measured with a plate reader at a wavelength of 570 nm. The absorbance value is directly proportional to the number of living cells (Mossman, 1983).

The cells were counted as described in Section 4.3.1.5, and the volume of cell suspension containing 5×10^3 cells was determined. 96-well flat-bottomed tissue culture plates were used to seed the cells at the above density and the final volume in each well was brought up to 0.1 ml using growth medium. The experiment was performed three times with 12 wells seeded from each sample for every condition. The culture conditions and media used were the same as stated in Section 4.3.1.5. After 15 days in culture the MTT assay was performed, and 0.01 ml of MTT (5mg/ml) was added to all wells. The plates were then incubated in a humidified atmosphere of 37^0C, for 4 hours. During this time formazan crystal was able to form at the base of the wells. Following incubation the spent media was

removed along with the suspension of cultured cells. To ensure that minimal or no lighting disturbed the next processes, 200 μl of DMSO was added to each well, thoroughly mixed to dissolve the dark blue crystals and the plates were covered with foil and left undistributed for 15 minutes at room temperature. This allowed for the formazon to precipitate and for air bubbles to dissolve. The plates were then read using a plate analyser with a test wavelength of 570 nm. The results were charted and the percentage viability was calculated.

$$\% \text{ Viability} = \frac{\text{Mean Absorbance of Sample}}{\text{Mean Absorbance of Control}} \times 100$$

The data was analysed using the ANOVA test using SPSS statistical analysis program (SPSS Inc., Chicago, Illinois). All cells used for the MTT assay were from the fourth passage.

4.3.1.10 Statistical analysis and interpretation methodology

Statistical analysis was performed using the SPSS Version 16 software package. Statistical significance for these tests was set to a probability value of $P<0.05*$ ($P< 0.01**$, $P<0.001***$) statistical significance. The software runs tests to check whether the data is parametric (normally distributed) or non-parametric (not normally distributed); i.e. the histogram plot; probability-probability (P-P) plot; and the Kolmogorov-Smirnov test. If two sets of these tests are normal then it can be assumed that the data is parametric, at which point Analysis of Variance (ANOVA) can be applied. However, if two of these tests are not normally distributed then the non-parametric Kruskal-Wallis test is applied. The processes that these tests run on are clarified below:

Histogram plot:

The histogram plots the values of observations on the horizontal axis, and the frequency with which each value occurs in the data set on the vertical axis. Its advantage is that it not only clearly shows the largest and smallest categories but gives an immediate impression of the distribution of the data. In fact, a histogram is a representation of a frequency distribution (Field and Hole, 2003).

Probability-Probability (P-P) plot:

The P-P plot is used to see whether a given set of data follows some specified distribution. It should be approximately linear if the specified distribution is the correct model (Field, 2009).

Kolmogorov-Smirnov test (K-S test):

The K-S test is one of several referred to as non-parametric tests. It is used to compare the scores in the sample to a normally distributed set of scores with the same mean and standard deviation (SD). If the test is non-significant ($p>0.05$) then the distribution of the sample is not significantly different from a normal distribution (i.e. it is probably normal). If, however, the test is significant ($p<0.05$) then the distribution in question is significantly different from a normal distribution (i.e. it is non-normal).

The decision rule is:

If Sig. ≤ 0.05, then the sample is almost certainly not normal.

If Sig. ≥ 0.05, then the sample is reasonable to assume normality.

4.3.2 Investigating the mechanisms of action of minoxidil via a mass spectrometry (MS)-based quantitative proteomics approach

Figure 4.4 exhibits the mass spectrometry quantitative proteomics approach, using SILAC (Stable Isotopic Labelling of Amino acids in Cell culture), in its entirety. The processes involved have been visually simplified. The following section discusses each step in detail.

4.3.2.1 Cell preparation

Dermal papilla cells were established from four individuals for this experiment and were seeded at 5 x 10^4 cells in duplicate in T25 (surface area 25cm^2) rectangular canted-neck flasks. One set of the cells was cultured in 'heavy' SILAC media (DMEM-containing carbon-13 labelled arginine and lysine amino acids (R6K6)), and the other set was cultured in 'light' SILAC media (DMEM-containing unlabelled arginine and lysine amino acids (R0K0)) (Dundee Cell Products Ltd, Dundee), both media were supplemented with 10% of dialysed fetal calf serum so that unlabelled lysine and arginine had been excluded. Cell cultures had their media changed every 3 days. When the cells had grown to 80% confluence the cells were washed five times with PBS, the new media placed into the flask did not contain serum. The cells in the 'heavy' media were treated with 100μM minoxidil for 48 hours. Cells in 'light' media were maintained as the vehicle control. At the completion of the 48 hour period, the media was carefully removed from the flasks and immediately replaced by 1.5 ml of PBS. The cells were gently scraped from the base of the flasks into the PBS, using a cell scraper. The flasks were gently agitated to ensure that the cell suspension was thoroughly mixed and the cells were rapidly placed into a 1.5 ml eppendorf tube. This was centrifuged at

Figure 4.4 Quantitative proteomics approach, using SILAC

Cells were cultured in SILAC medium containing a 'light' or 'heavy' form of the amino acids. The cells in the 'heavy' media were then treated with 100μM minoxidil; the cells in the 'light' media were used as vehicle control. The proteins were then extracted from both sets of media and combined. After reduction and alkylation, the combined proteins were then separated by one dimensional SDS-polyacrylamide gel electrophoresis (1D SDS-PAGE), peptides were generated, separated and analysed by mass spectrometry, using the liquid chromatography - tandem mass spectrometry method (LC-MS/MS). Metabolic integration of the amino acids into the proteins leads to a mass shift of the corresponding peptides, and the mass spectrometer detects shift in the mass. When both samples are combined, the ratio of peak intensities in the mass spectrum reflects the relative (rel) protein abundance vs. m/z (mass-to-charge ratio). In this example, the labelled protein has the same abundance in both samples (ratio=1) (Ratio= R0K0/R6K6), if the ratio is <1 it means stimulation with treatment, and if ratio is >1 it means inhibition with treatment. (Adapted and modified from Max-Delbruck-Centre, Berlin-Buch).
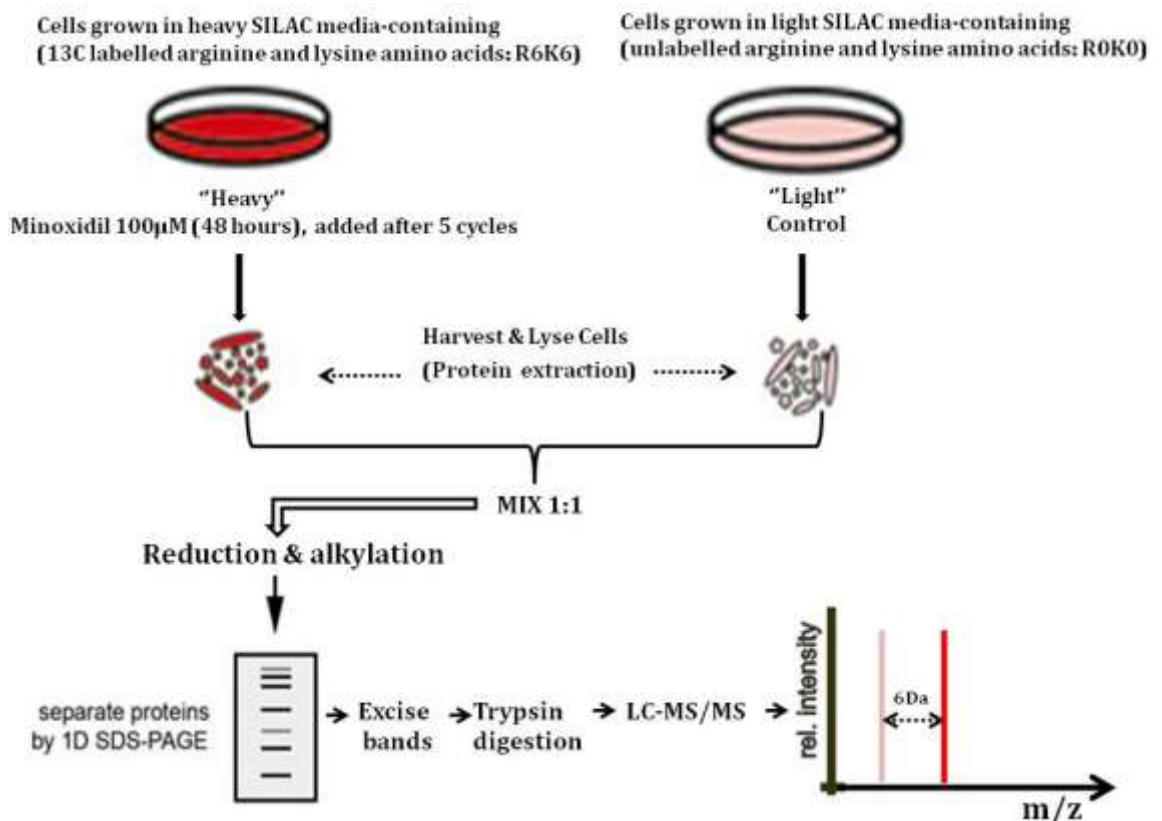
1,200 rpm (290 g) (Sanyo Harrier 15/80) for 7 minutes. The supernatant was disposed of and all pellets were stored at -80ºC, until protein extraction could be performed.

4.3.2.2 Protein extraction and quantification

The pellets were removed from -80ºC and placed on ice for protein extraction to be performed. The pellets were dissolved in 50µl of sample buffer (Glycerol (BDH Lab Supplies) 2.5 ml; ethylenedaiminetetraacetic acid (EDTA) (Sigma) 0.185 g; sodium dodecyl sulphate (SDS) (Sigma) 1.5 g; Tris (Sigma) 0.19 g; 25 ml distilled water) added with protease inhibitor cocktail (1:20) (Sigma) and protein extraction was carried out as described in Section 4.3.1.7. Protein quantification was carried out as described in Section 4.3.1.8, using the Bradford Assay.

4.3.2.3 Reduction and alkylation

Reduction and alkylation was a necessary procedure to unfold the proteins for gel electrophoresis and separate them according to their molecular weight. Protein was pooled together from 4 samples of both the 'light' (40µg) and 'heavy' (40µg) conditions (see Figure 4.4) and reduced (cysteines) by adding 10µl of 50mM dithiothreitol (DTT) for 20 minutes at 60°C. Once reduced, the proteins were alkylated using 10µl of 100mM iodoacetamide (IAA) for 20 minutes at room temperature in the dark. The solution was then lyophilised (dried) (EZ-2 personal evaporator, GENEVAC); this procedure allowed for the protein sample (Total: 320 µg) to be stored in a stable form, at -80°C, by removing all volatile components from the solution.

4.3.2.4 Protein separation using one-dimensional sodium dodecyl sulphate-polyacrylamide gel electrophoresis (SDS-PAGE) of proteins

The lower separating/running gel was prepared using the materials listed in (see Appendix 2), and was subsequently poured into a gel cassette (Invitrogen) 1 mm above the first division line (see Figure 4.5). Iso-butanol (1 ml) was added on top of the acrylamide running gel to overlay the lower separating gel to prevent drying and oxidation of the gel surface. The lower separating gel polymerised after about 60 minutes at room temperature. The upper stacking gel was prepared, whilst the

Figure 4.5 An illustration of an apparatus used for SDS-PAGE

(Adapted and modified from the School of Chemistry and Biochemistry, Georgia Institute of Technology, with permission of author)
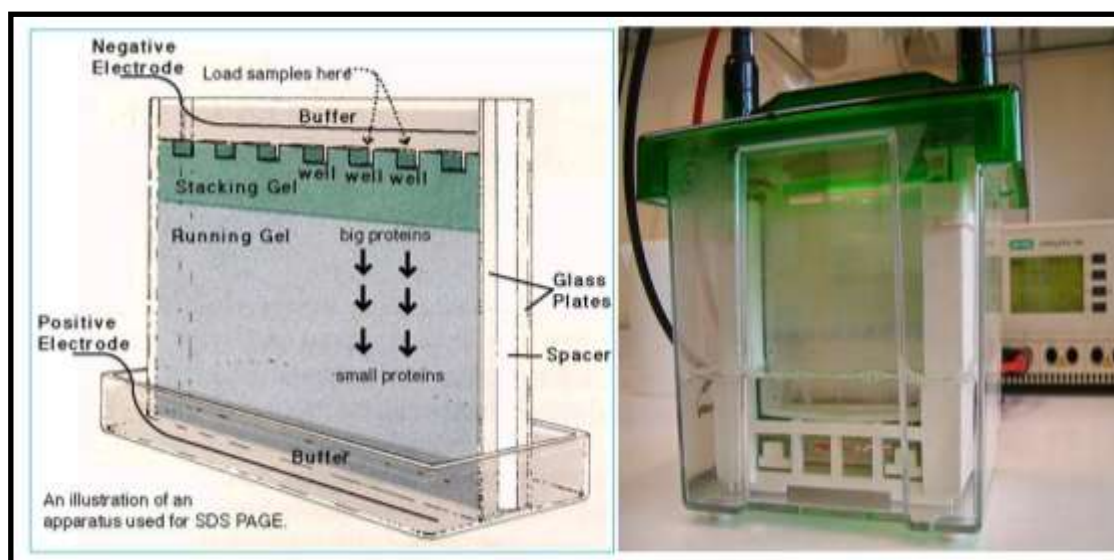
gel was polymerising, with the list of materials in Appendix 2. After 60 minutes the iso-butanol was discarded and the top of the acrylamide was then rinsed with water and the upper stacking gel was added to the cassette. The comb was then

placed into the gel whilst the gel was setting; this was done with care to avoid air bubbles forming in the gel. This was then left undisturbed for about 30 minutes to polymerise.

While the upper stacking gel was polymerising, the protein extract (see 4.3.2.3) was readied for electrophoresis. For this process 85 µl sample loading dye (outlined in Appendix 2) was added to re-dissolve the protein sample (320 µg), and was subsequently boiled for 3 minutes at 80ºC. The sample was then centrifuged for 1 minute, at 12,000 rpm (Sanyo Harrier 15/80). Following this, the electrophoresis chamber was assembled and filled midway with electrophoresis buffer (See Appendix 2). Once the gel cassette was added to the chamber, the protein samples were loaded into the correct well on the gel, c. 40 µg of protein was loaded per lane. Next the electrophoresis chamber was sealed and run at 80 V for 20 minutes, followed by a further 70 minutes run at 150V. The gels were then stained with Coomassie Blue (R-250) for 2 hours on a shaker, and then destained with HPLC grade water overnight.

4.3.2.5 Peptide generation using in-gel digestion of Coomassie Blue stained proteins using trypsin

Mass spectrometry's ability to provide highly accurate molecular weight information is at the core of its utility for protein and peptide analysis. On the whole, the sensitivity for protein analysis is lower than that for peptides, as protein size is larger. Proteins hit the detector with lower velocity than peptides resulting in less secondary electron emission. Furthermore, peptides are ionized more readily than intact proteins. Thus, it is preferable to digest proteins into peptides using specific proteases for mass spectrometry to be conducted. The most

commonly employed enzyme for this process is trypsin. Trypsin hydrolyzes proteins, predominantly cleaving peptide chains at the C-terminus side of the amino acids lysine and arginine, except if either is followed by proline. Therefore, trypsin was used for the digestion of proteins into peptides.

After destaining the gels were photographed (Figure 4.6a). To minimise the chances of human error each protein band was marked out on the resultant image, this would also ensure that the entire sample was taken into consideration (Figure 4.6b). As shown in the figure 4.6b, the separated proteins in the SDS gel were divided into 20 bands. Using this image as a guide the coomassie-stained bands were then excised from the gel into 1-2 mm sizes, to make the bands more susceptible to trypsin digestion using the method of Shevchenko *et al* (1996). The bands in all four lanes were excised similarly, and equivalent bands were pooled together (Figure 4.6c).

Figure 4.6 Illustration of excising bands procedure from SDS gel for in-gel digestion

(a) A photograph of gels after electrophoresis, prepared for bands to be cut. **(b)** The illustration of marked gel bands, the bands were cut from all the gels for in-gel digestion. **(c)** The photograph of the gel after the bands were excised. Images were taken by the author.
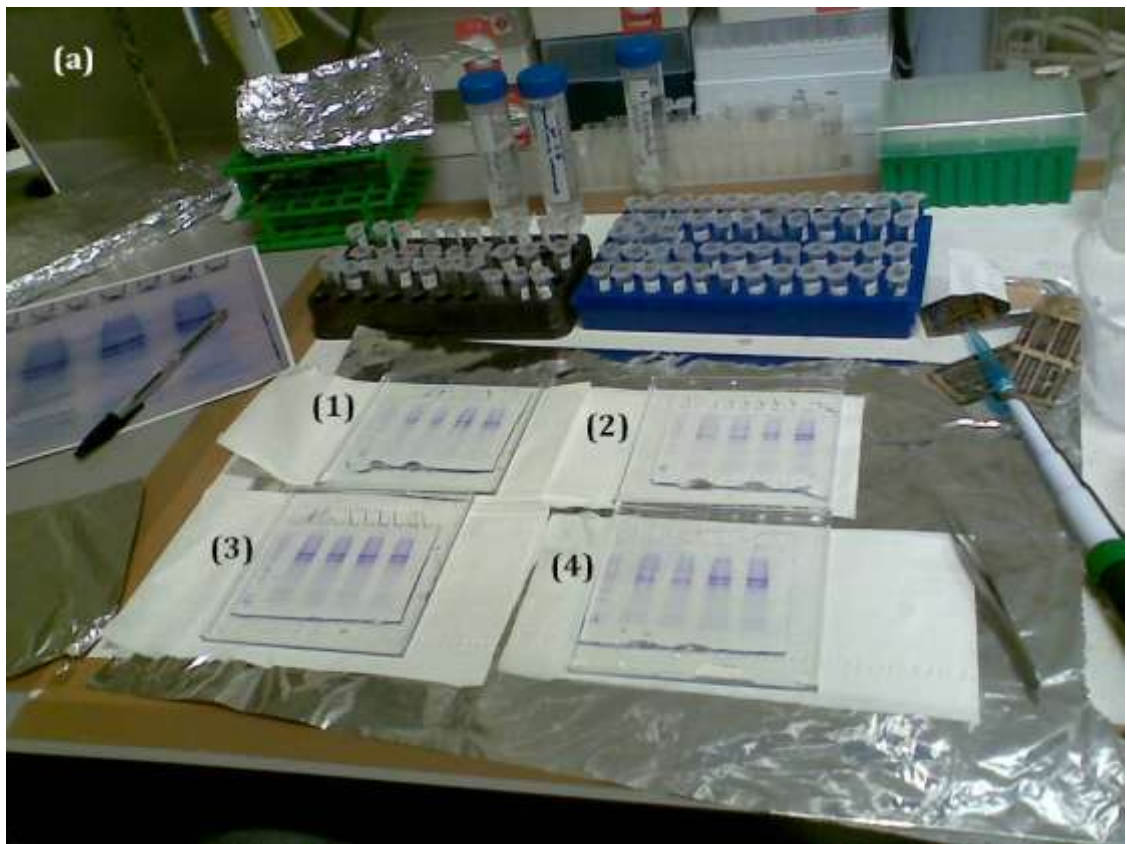
(b) Coomassie Blue stained 1D SDS gel
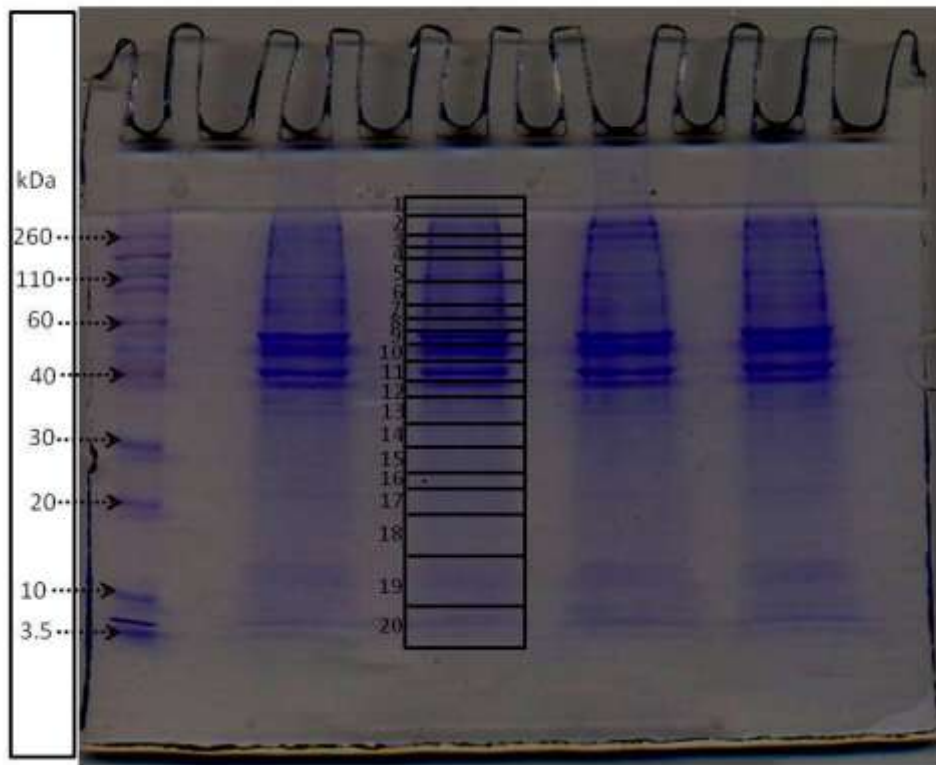
Acetonitrile (100 μl; 10%) in HPLC water (Fisher Scientific) was added to the gel pieces and left for 15 minutes. This was a dehydration step and during this time the gel pieces shrank, becoming opaque. The supernatant was then removed, ammonium bicarbonate (20 μl; 25mM) (Fluka) was added to the gel pieces and left for a further 15 minutes to ensure rehydration. These steps were repeated twice and the gel pieces were dehydrated for 15 minutes whilst acetonitrile (100 μl; 10%) was added. The supernatant was removed and a further 50 μl acetonitrile was added, this was then left for 15 minutes. All liquid was decanted, and the gel pieces were allowed to dry in a tube at room temperature, for approximately 30 minutes. The dry gel pieces were then resuspended in 10ng/μl trypsin in 25 mM ammonium bicarbonate. Depending on the size of the gel pieces either 10 μl (for small gel pieces) or 20 μl (for larger gel pieces) was used. For the next 24 hours the gel was digested at 28°C. Upon completion of digestion, most of the buffer had evaporated and was affixed to the lid; the samples were then spun down in a centrifuge (Sanyo Harrier 15/80) at 1200 rpm (290 g) for about 5 minutes.

4.3.2.5.1 Peptide extraction from gel slices

For each in-gel digest, the incubation liquid was decanted from around the gel to a new 0.5 ml eppendorf tube and 50 μl of 100% acetonitrile was added to the gel slice. This was then vortexed and left for 15 minutes at room temperature before centrifugation at 1200 rpm (Sanyo Harrier 15/80). The supernatant was transferred to the tube containing the incubation liquid and 5 μl of 25 mM ammonium bicarbonate was added to the gel and left for 10 minutes at room temperature. After this process had been repeated, 50 μl of 100% acetonitrile was added to the gel slice, vortexed and left for 15 minutes at room temperature. This

was again centrifuged and transferred to the 0.5 ml eppendorf tube. The extracts from all 20 samples were lyophilised separately and this alongside the residual gel was stored at -80°C.

4.3.2.6 Mass spectrometry using Matrix-Assisted Laser Desorption Ionization-(MALDI)

Matrix assisted laser desorption ionization mass spectrometry (MALDI MS) (Karas *et al.*, 1987) is one of the main techniques used in proteomics. The diagram below outlines the main components of the MALDI MS process.
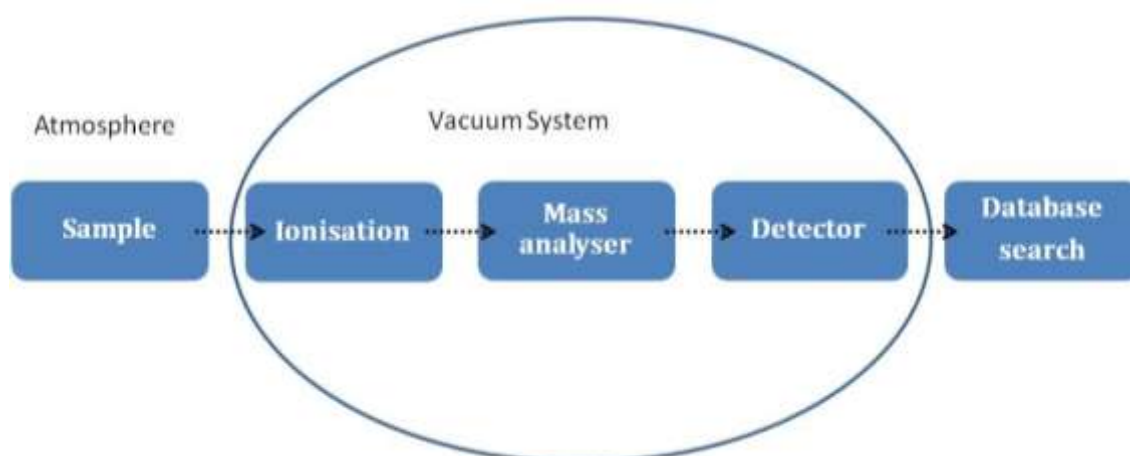
In this process the analyte is mixed with an organic compound, acting as a matrix, which has the same wavelength of absorption as that of the MS laser. When mixed with analyte, this results in the formation of a crystalline layer on the target plate (Gobom *et al.*, 2001). The most commonly used matrix solution is α-cyano-4-hydroxycinnamic acid (CHCA). The matrix has an important role in protecting biomolecules from being destroyed by the beam of the direct laser. The

matrix also facilitates absorption of the laser energy, heating of the matrix/analyte crystals and allowing vaporisation and ionisation to occur.

A pulse of laser energy is fired at the dried analyte/matrix mixture in a vacuum, creating a plume of ions (Figure 4.7). By applying a voltage of 25 kV to an extraction lens in the source, the ions are accelerated into a field-free flight tube, which separates the ions on the basis of mass-to-charge. An MS spectrum is generated by measuring the time it takes for ions of different mass-to-charge to reach the detector at the end of the flight tube.

Figure 4.7 Analyte ionization

The cartoon of laser beam is adapted and modified from the National High Magnetic Field Laboratory (http://www.magnet.fsu.edu/education/tutorials/tools/ionization_maldi.html), with permission of author.
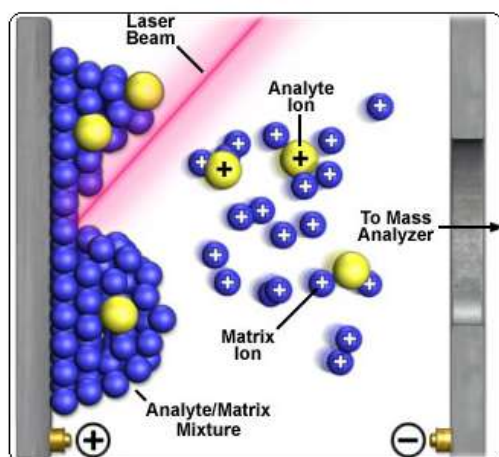
True to its name tandem mass spectrometry (MS/MS) involves two stages of mass analysis. The first stage involves separation of the parent ions in MS mode as described above. An ion gate is then employed to allow only the parent ion of interest to continue along the flight path and all the others are deflected. In the

second stage the selected parent ion is fragmented by collision-activated (CAD) or collision-induced decomposition (CID) in the second part of the flight tube. The parent ions are fragmented along their peptide backbone, this results in the production of signature daughter or product ions, with masses that correspond to the amino acid from which they originate (Roepstorff and Fohlman, 1984).

Depending on the type of trypsin-digested sample, protein identification can be achieved using MS data (parent ions only) also known as peptide mass fingerprinting (PMF), or MS/MS data (parent and fragment ions) also known as peptide fragment fingerprinting (PFF) to search a database of all known proteins (for example, Swissprot) using a search engine such as Mascot (http://www.matrixscience.com/).

4.3.2.6.1 Preparation of analyte and matrix on target plate

As the samples are complex heterogeneous mixtures following trypsin digestion, peptide separation was achieved using nano-High Performance Liquid Chromatography (nano-HPLC) and fraction collection system on to a MALDI target prior to analysis by mass spectrometry.

The following materials were prepared for the nano-HPLC system:
(a) Matrix

α-Cyano-4-hydroxycinnamic acid (CHCA) was used as the matrix of choice. A stock solution was prepared by solubilising CHCA in 1ml of 30% (v/v) acetonitrile (CH_3CN) (Fisher) with 0.1% (v/v) TFA (Trifluoroacetic acid, CF_3CO_2H, Fluka). CHCA is solubilised through vortexing for 2 minutes and sonicated for 30 minutes to generate a saturated solution.

(b) Working solution preparation

From the stock solution a working solution was prepared. CHCA stock solution (120μl) was added to 1.056 ml of ethanol:acetone (2:1 ratio), followed by the addition of 12 μl of 100 mM ammonium phosphate $(NH_4)_3PO_4$ and 12μl 10% trifluoroacetic acid (TFA), with vortexing between each added component and placed in the ProteineerFC fraction collector (Bruker Daltonic GmbH).

(c) Preparing a sample

The lyophilised in-gel digested peptides were re-dissolved in 6.5 μl of 10% acetonitrile (CH_3CN) (Fisher), vortexed for 30 seconds, and then centrifuged for 1 minute. The sample was transferred with care to a HPLC vial using a pipette with a gel-loading tip to avoid formation of any bubbles; the sample was then positioned into the nano-HPLC system (Figure 4.8a).

The Procedure for nano-HPLC separated peptides:

The prepared sample was placed into the auto sampler in the nano-HPLC system (Figure 4.8b). The autosampler needle injects the sample onto a column where peptide separation takes place; this is done using an LC Packing UltiMate 3000 capillary high-performance liquid chromatography system (Dionex, Camberley, Surrey, UK).

A sample loop injected the sample into the LC system onto a pre-column (C_{18}, 100Å PepMap, 300μm inner diameter x 5mm length, 5μm particle size) (LC Packings, Sunnyvale, CA). The sample was then washed at a flow rate of 300nl/min, for 3.5 minutes with carrier solvent (carrier solvent, 0.05% TFA). The sample was switched onto another column (C_{18}, 100 Å PepMap, 75μm inner diameter x 15cm length, 3μm particle size) (LC Packings), equilibrated with 2% CHCN with 0.05% TFA.

Peptides were eluted from the column, passing through the UV detector, which produces UV profile at 215 nm (detects peptide bonds) and 280 nm (detects aromatic amino acids) and then on to the fraction collector.

The LC-MALDI fraction collector (Proteineer fc (fraction collector), Bruker Daltonik Bremen, Germany) (Figure 4.8c) enables automatic liquid handling for MALDI preparation of a sample. The fraction collector gathers samples separated on nano-HPLC and deposits discrete fractions of the eluted peptides on MALDI targets (MTP 800/384 AnchorChip™) (Bruker Daltonics, Bremen, Germany). Each fraction comprised of 75nl of sample, collected every 15 second, co-eluted with 1.2µl CHCA working solution (Figure 4.8e). A total of 384 fractions were collected for each band. In total 20 plates were prepared for MALDI analysis for the 20 1D gel bands treated with trypsin.

Figure 4.8 A guide to the MALDI target preparation process using the nano-HPLC system

(a) An overall view of the system with each instrument identified. **(b)** displays the position in which the samples must be placed in the nano-HPLC system. **(c & d)** show the position of the capillary on the MALDI target, **(e)** which deposits the sample into the plate (75nl of sample co-eluted with 1.2µl CHCA working solution). Images (a), (b) and (c) were taken by the author at Institute of Cancer Therapeutics, University of Bradford. Image (c) adapted from Bruker manual, and (e) adapted from Shimadzu Biotech.
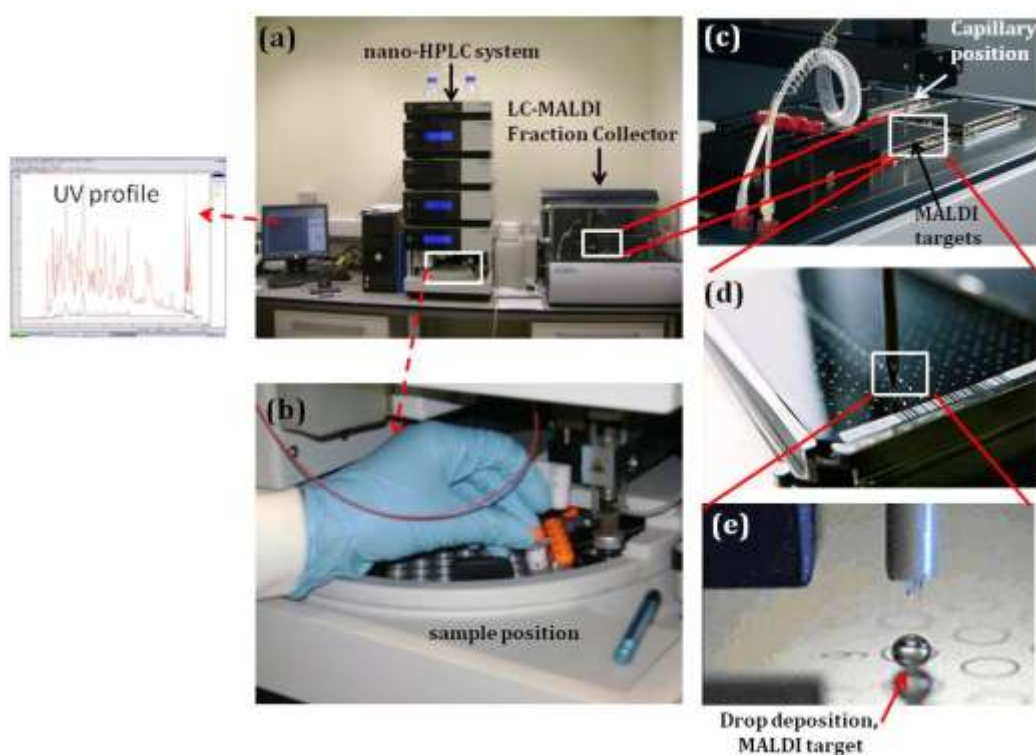
4.3.2.6.2 MALDI mass spectrometry

Mass spectrometric analysis was carried out using a MALDI-TOF/TOF UltraFlex II instrument (Bruker Daltonics, Bremen, Germany) (Figure 4.9); this was done using reflector positive ion mode. Peptides were screened using fully automated analysis, firing 400 laser shots per fraction (mass range of 700-4000Da). A non-redundant peptide list was compiled from spectra of the 384 fractions and data-dependent MS/MS of each peptide was generated using 1500 laser shots to acquire each spectrum.

4.3.2.6.3 Data interpretation

The use of SILAC (see Section 4.3.2) allowed for quantitative information to be obtained from the mass spectrometry (MS) spectra. Peptides that occurred in the mixture were identified as pairs (SILE pairs). The intensity ratio of the two peaks (Light/Heavy) of the pair was a measure of any differentiation in peptide abundance within the mixture.

Figure 4.9 Significant components in the matrix-assisted laser desorption Ionisation mass spectrometry machinery

Images were taken by the author at Institute of Cancer Therapeutics, University of Bradford. The cartoon of laser beam is adapted and modified from the National High Magnetic Field Laboratory, with permission of author.
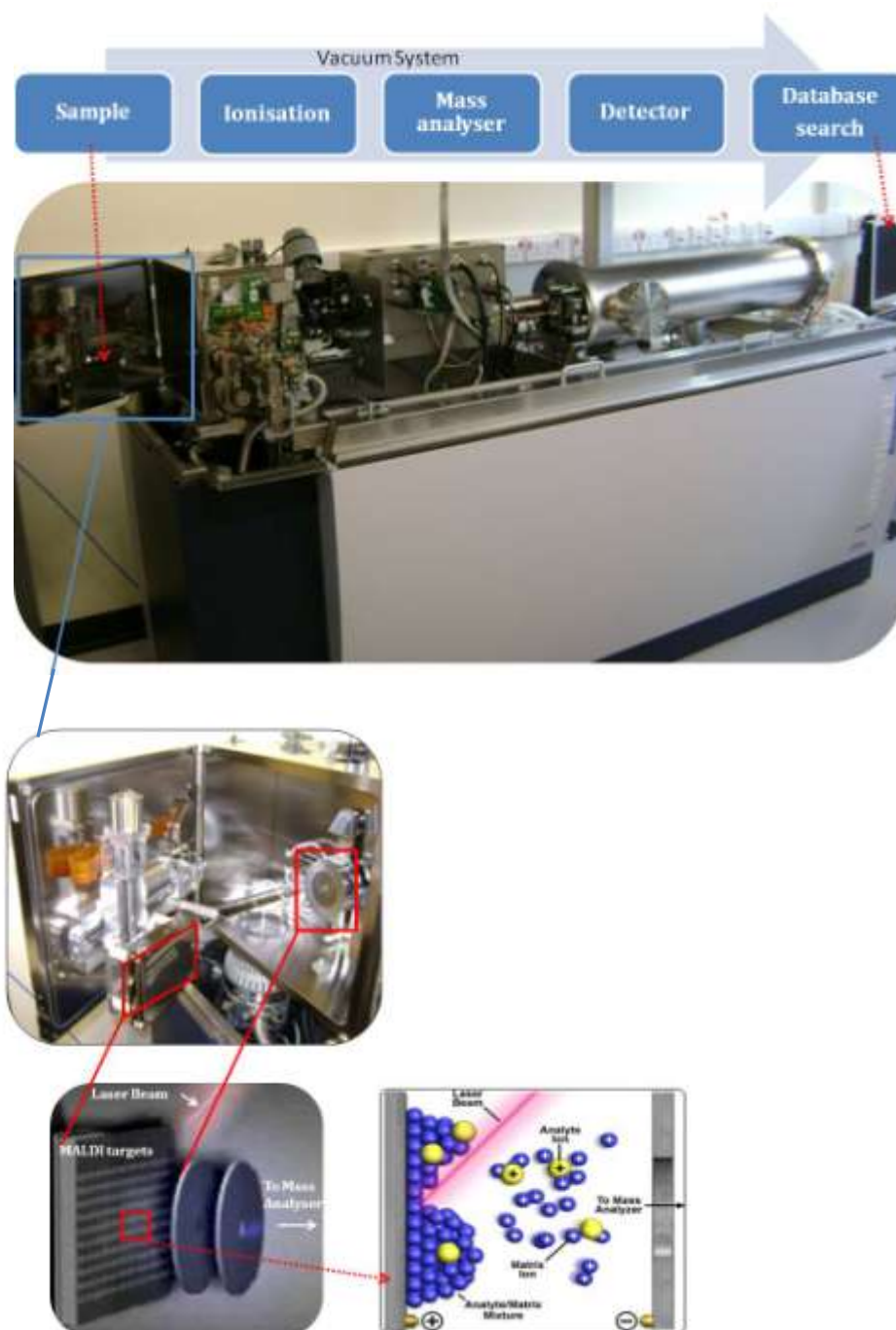
4.3 Results

4.3.1 Investigation into the effects of minoxidil and tolbutamide on human scalp hair follicle derived dermal papilla cells *in vitro*

Cultured dermal papilla cells from 5 individuals aged 42-60 were used to investigate the effects of minoxidil, tolbutamide, and the combined effect of minoxidil and tolbutamide on cell proliferation by counting cells using the haemocytometer method**,** protein quantification, and MTT assay. The dermal papilla cells in culture gradually increased in number, exhibited a lean kite-like multipolar shape and formed small clumps (Figure 4.10); when confluent they formed packed, parallel arrays.

To construct the growth curve, dermal papilla cells were used from five individuals, and cell counting was performed in triplicate on these cells for each condition, over a period of 15 days. The average cell count was used for all conditions to construct the growth curve. Cells grown under all conditions exhibited a similar pattern of growth. They grew rapidly from day 3 to 7 before slowing and plateauing from day 11. The maximum rate of cell doubling time for all conditions during the experimental phase was 48 hours (Figure 4.11).

When cell proliferation between conditions were statistically compared during the experimental phase, there was no significant overall difference in comparison to the control (Figure 4.11) with either 100µM minoxidil (P=0.495), 1mM tolbutamide (P=0.318) or when they were combined (P=0.270). Treatment with 100µM minoxidil and 1mM tolbutamide appeared to inhibit any further proliferation after day 11; this effect was greatest when minoxidil and tolbutamide were combined (Figure 4.11). Statistical analysis comparing the total cell proliferation at the end of the culture period revealed that 1mM tolbutamide significantly inhibited cell proliferation (P=0.05*), however minoxidil had no effect (P=0.21) and did not alter the tolbutamide effect significantly when given in combination (Figure 4.12).

Figure 4.10 Phase contrast images of dermal papilla cells in culture

Dermal papilla (DP) cells were cultured for 15 days for the purposes of constructing a cell proliferation growth curve. These phase contrast images of the DP cells, taken at x100 magnification on days 2 (a) scale bar = 25µm, 5 (b) scale bar = 25µm and day 15 (c) scale bar = 25µm, show the morphology of cells during the period of culture.

The DP cells in culture increased in number exhibited a lean kite-like multipolar shape and formed small clumps; when confluent they formed packed, parallel arrays. (d) The magnified image, displays the lean kite-like multipolar shape of the cells, scale bar = 50µm.
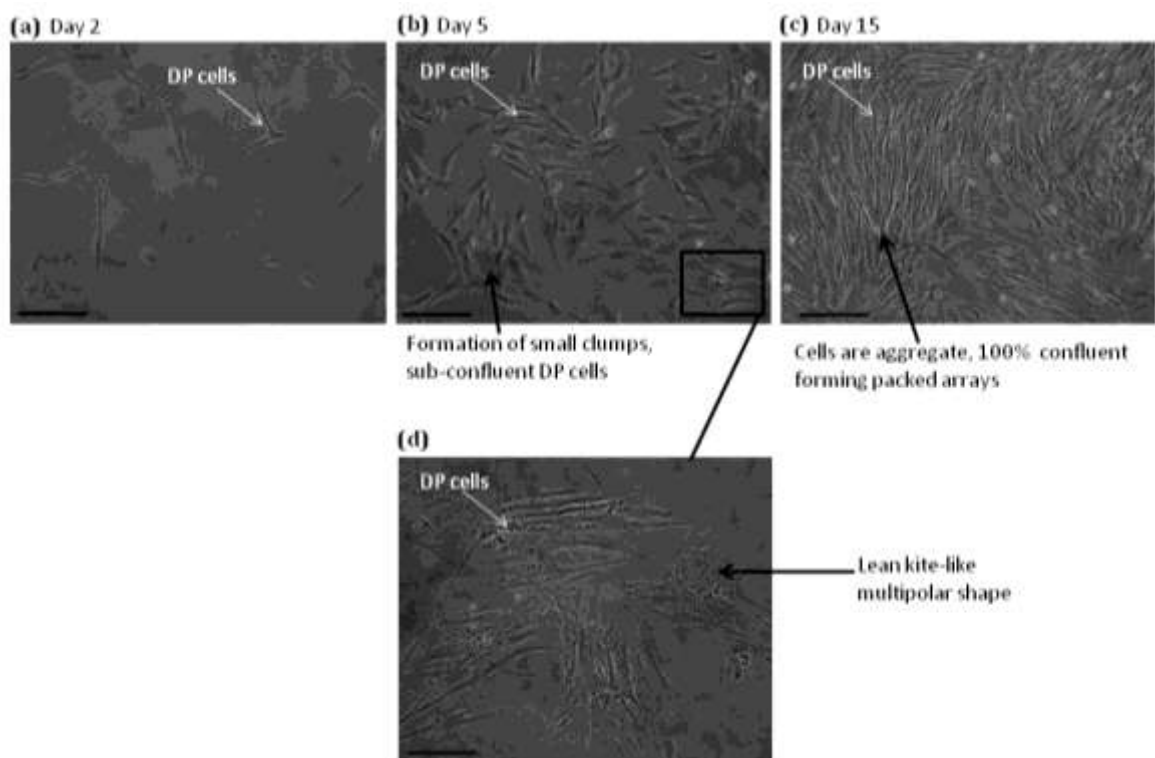
Figure 4.11 Minoxidil and tolbutamide did not alter the growth kinetics of human dermal papilla cells

The cells were cultured for 15 days in the four conditions outlined. The cells grown in all conditions exhibited a similar pattern of growth. The cells grew rapidly from day 3 to 7 before slowing and plateauing from day 11. There was no significant difference in comparison to the control, with 100μM minoxidil (p=0.495), 1mM tolbutamide (p=0.318) or when they were combined (p= 0.270). Values are the mean $\pm$ SEM of 5 samples; each condition was calculated in triplicate at each time point. Statistical analysis was performed using a two-factor within-subjects ANOVA using SPSS after confirming normal distribution.
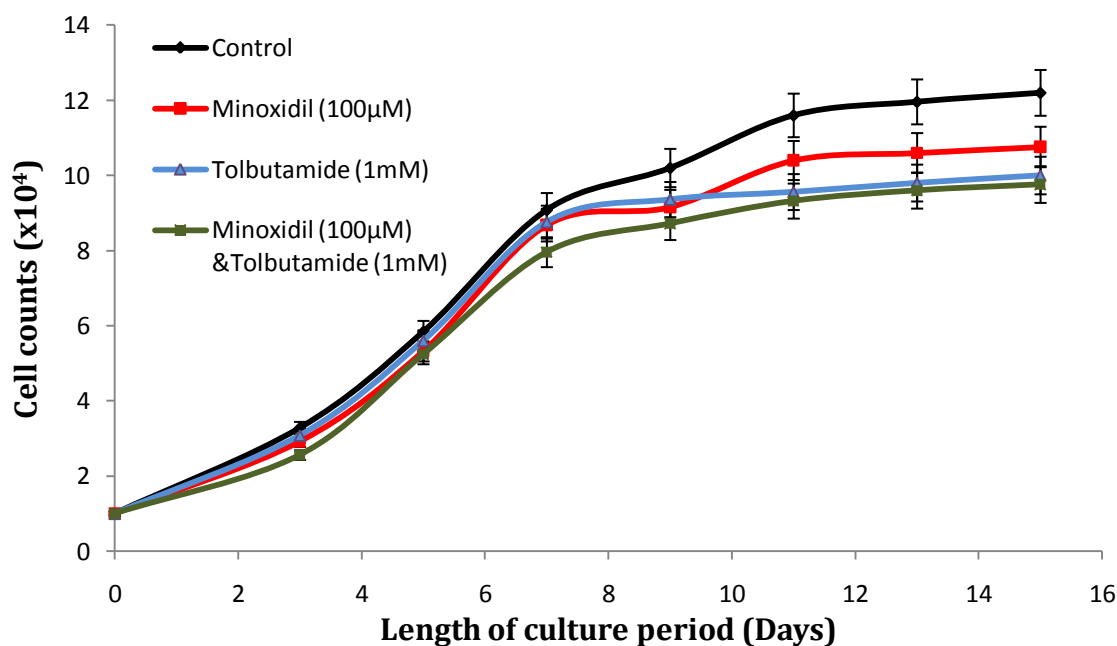
Figure 4.12 Proliferation of human dermal papilla cells at day 15 in culture determined by haemocytometer

(a) The cell count at day 15 in culture expressed as a percentage of the control. Values are the mean ± SEM, n=5 with triplicate count for each sample.
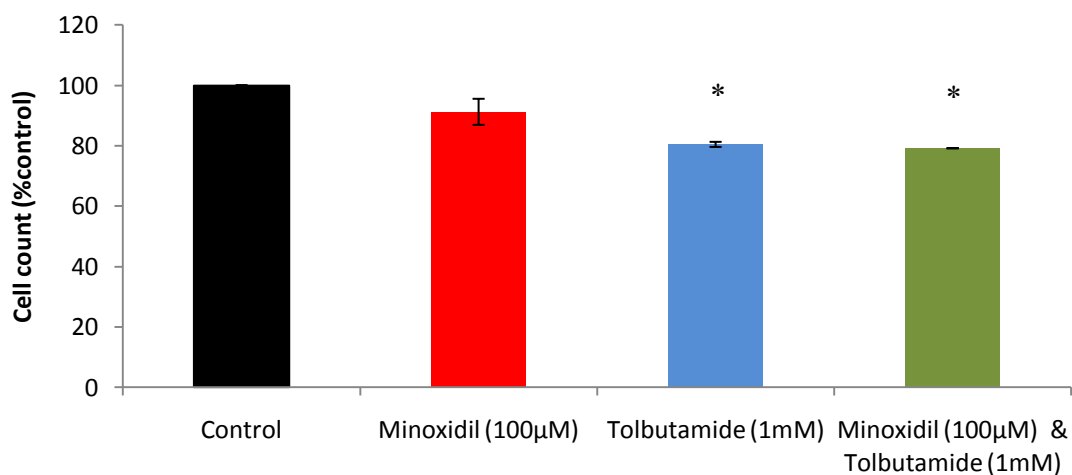
(b) Statistical differences in cell proliferation at day 15, the values represent the mean ± SEM from triplicate assays of 5 samples.

Condition	Cell count on Day 15 ± SEM	P–value (ANOVA)
Control	123,180 (± 1,180)	-
Minoxidil (100µM)	112,454 (± 4,854)	0.21 NS
Tolbutamide (1mM)	99,167 (± 834)	0.05*
Minoxidil (100µM) & Tolbutamide (1mM)	97,582 (± 118)	0.03*

The total cellular protein content from the cells on day 15, followed the same pattern, with no effect of minoxidil (p=0.15), but significant inhibition by tolbutamide (p=0.01**) and combined minoxidil and tolbutamide (p=0.05*) (Figure 4.13). The difference between the application of minoxidil alone and that of the combined treatment of minoxidil and tolbutamide was significant (p=0.03*).

The cells for the viability assay (MTT) were incubated with the same concentration of potassium channel regulators as described above for 48 hours. All five samples were cultured in triplicate for each condition and the assay was repeated thrice i.e. 9 measurements per sample per condition. The average cell viability was calculated in comparison to the control (Figure 4.14). The results showed that 48 hour treatment with 100μM minoxidil had no effect on cell viability (p=0.487), whereas tolbutamide and the combined treatment of minoxidil and tolbutamide caused significant inhibition after 48 hours in culture (p=0.037*). The combined treatment of minoxidil and tolbutamide was significant against minoxidil alone (p=0.04*).

Therefore, the assessment of potassium channel regulators effect on dermal papilla cell growth by all three methods gave the same results, with slight, but significant inhibition with 1mM tolbutamide, but no effect of 100μM minoxidil.

Figure 4.13   Total cellular protein content of dermal papilla cells from 5 individuals following treatment of minoxidil and tolbutamide

Cells were seeded at 1×10^4 and cultured for 15 days in the stated conditions. At day 15 the proteins were extracted from cells in all treatments. Values are the mean $\pm$ SEM, n=5.
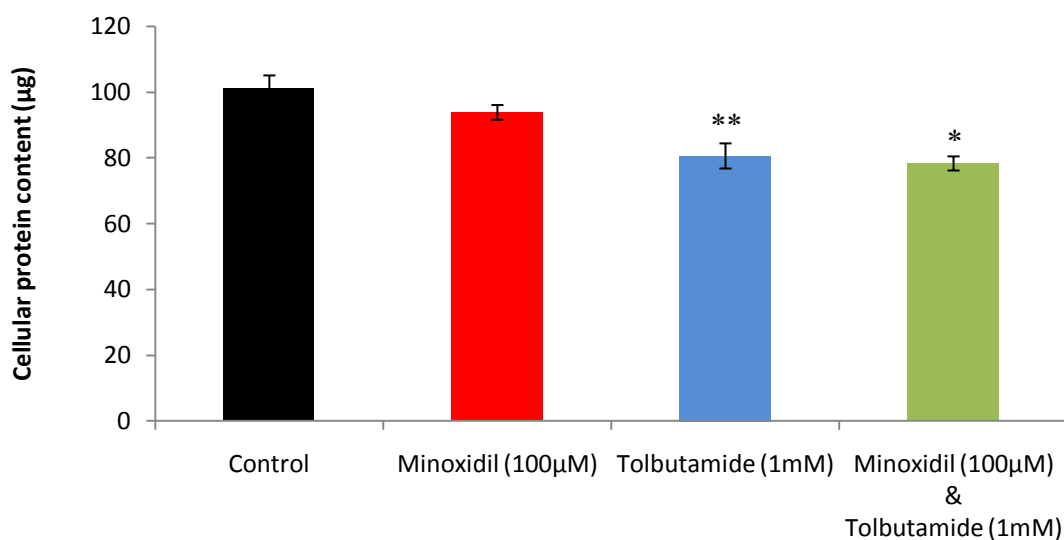
(b) Statistical differences in total cellular protein content from 5 cell lines at day 15; the values represent the mean $\pm$ SEM from triplicate assays (n=5).

Condition	Cellular protein content (µg) $\pm$ SEM	P–value (ANOVA)	
Control	101 ($\pm$ 4)	-	
Minoxidil (100µM)	93.75 ($\pm$ 2.25)	0.15 NS	
Tolbutamide (1mM)	80.52 ($\pm$ 3.82)	0.01**	P=0.03*
Minoxidil (100µM) &Tolbutamide (1mM)	78.25 ($\pm$ 2.15)	0.05*	

Figure 4.14 Proliferation of human dermal papilla cells determined by MTT

(a) Cell proliferation was determined by MTT assay. Cells were incubated for 48 hours with minoxidil; tolbutamide; a combination of minoxidil and tolbutamide; and a vehicle control. The results are expressed as percentages in comparison to the control; values are based on the mean from five samples in 9 replicates $\pm$ SEM.
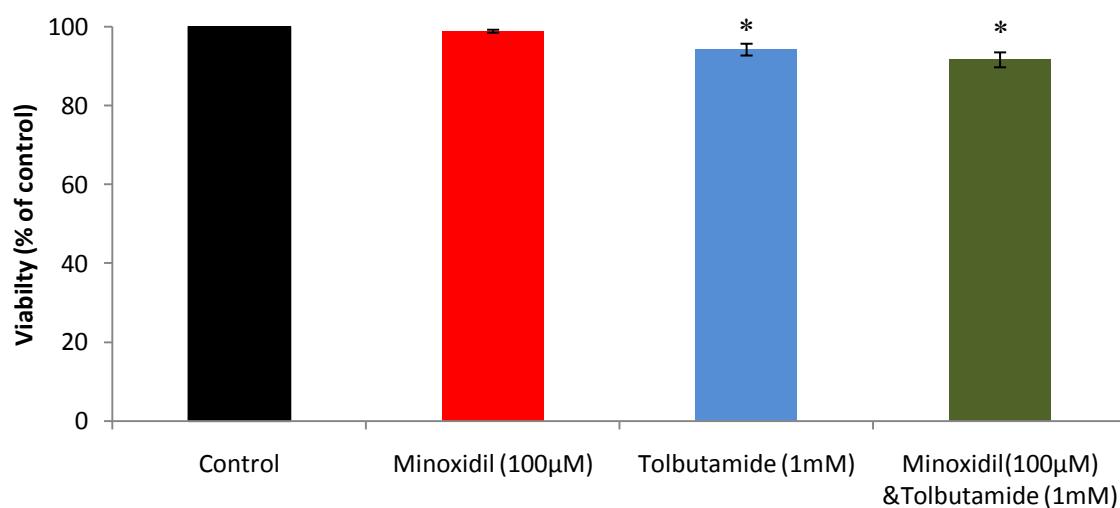
(b) Statistical differences in percentage of the cell viability, in comparison to the control at day 15; the values represent the mean $\pm$ SEM from triplicate assays, (n=5).

Condition	Viability (%) $\pm$ SEM	P–value (ANOVA)	
Minoxidil (100µM)	98.97 ($\pm$ 0.374)	0.487 NS	
Tolbutamide (1mM)	94.29 ($\pm$ 1.496)	0.037*	P=0.04*
Minoxidil (100µM) &Tolbutamide (1mM)	91.69 ($\pm$ 1.891)	0.037*	

4.3.2 Proteomics Results

The effect of minoxidil on protein profiles in cultured dermal papilla cells were investigated by culturing cells in SILAC (Stable Isotopic Labelling of Amino acids in Cell culture) medium. Dermal papilla cells used for this experiment were from four women aged between 42-60 years. The cells from each individual were cultured in duplicate, one set of the cells was cultured in a 'light' (i.e. unlabelled arginine and lysine amino acids) and the other set was cultured in a 'heavy' (i.e. ^{13}C labelled arginine and lysine amino acids) form of the amino acid (for more information see section 4.3.2.1).

Following labelling, the cells in the 'heavy' media were treated with 100μM minoxidil for 48 hours. The cells in the 'light' media were used as the vehicle control. The proteins were then extracted from all the samples, quantified and combined together to increase biological validity of the data (Figure 4.4; for more information see section 4.3.2.3).

These were then separated by SDS PAGE and trypsin-digested for peptide generation (section 4.3.2.5). The resulting peptides were separated by reverse phase chromatography on a nanoHPLC (Figure 4.8; section 4.3.2.6.1). Peptides were analysed by MALDI MS/MS analysis and were identified through a database search, using Mascot search engine (http://www.matrixscience.com/) (Figure 4.9; section 4.3.2.6). The use of SILAC allowed for quantitative information to be obtained from the mass spectrometry spectra. Peptides that occurred in the mixture were identified as pairs (SILE pairs). The intensity ratio of the two peaks (light/heavy; i.e. control/minoxidil) of the pair was a measure of any differentiation in peptide abundance within the mixture (Figure 4.4). This enabled the determination of quantitative differences due to minoxidil at the protein level

(i.e. if proteins had up-regulated, down-regulated or remained unaltered when treated with minoxidil), if the labelled protein had the same abundance in both the control and the minoxidil treated cells the ratio was =1 (Ratio= control/+minoxidil), if the ratio was <1 it was indicative of a stimulation with the treatment, and if the ratio was >1 it indicates an inhibition with treatment.

The Mascot search engine (http://www.matrixscience.com/) identified 941 proteins in the cultured dermal papilla cells. These were then separated into networks with regard to their functions within the cell, using the IPA Software (www.ingenuity.com). Protein–protein interactions (PPIs) are a regulating factor in many fundamental cellular processes. Therefore, it is essential to identify all potential interacting partners in order to establish an understanding of the functions of a protein in its cellular context. This will also allow for a more comprehensive visualisation of the functional and dynamic properties of the cell.

By nature the breadth of the full functioning of the identified proteins are too vast to be investigated in this report. Thus, this study narrowed its focus to proteins implicated in cellular assembly, maintenance and protein trafficking functions (**CAMPTF**), due to their central role in cell survival. The software generated a visual representation of all the proteins involved in the selected network using the database information, including associated proteins that may not have been expressed by the cultured dermal papilla cells (Figure 4.15). This offers an advanced representation of the results; Image 4.15a and 4.15b are the same network, however 4.15b is a generated image of the proteins in a subcellular layout.

Figure 4.15 Networks of proteins associated in cellular assembly, maintenance and protein trafficking in cultured dermal papilla cells

Image **(a)** displays proteins associated in the networks and the effect of minoxidil in the protein profile. Proteins in green are up-regulated by minoxidil, and proteins in red are down-regulated. The intensity of the colour is an indicator of the degree of up-regulation or down-regulation. Those in grey represent identified proteins that underwent no change and those marked in white are suggested as possible linking proteins, but not identified. Image **(b)** is the same network but proteins in normal subcellular layout at the forefront. Molecules for which currently no information on subcellular localisation is present are also displayed as an unknown category.

217
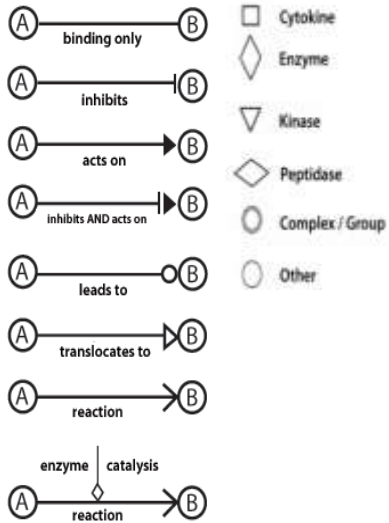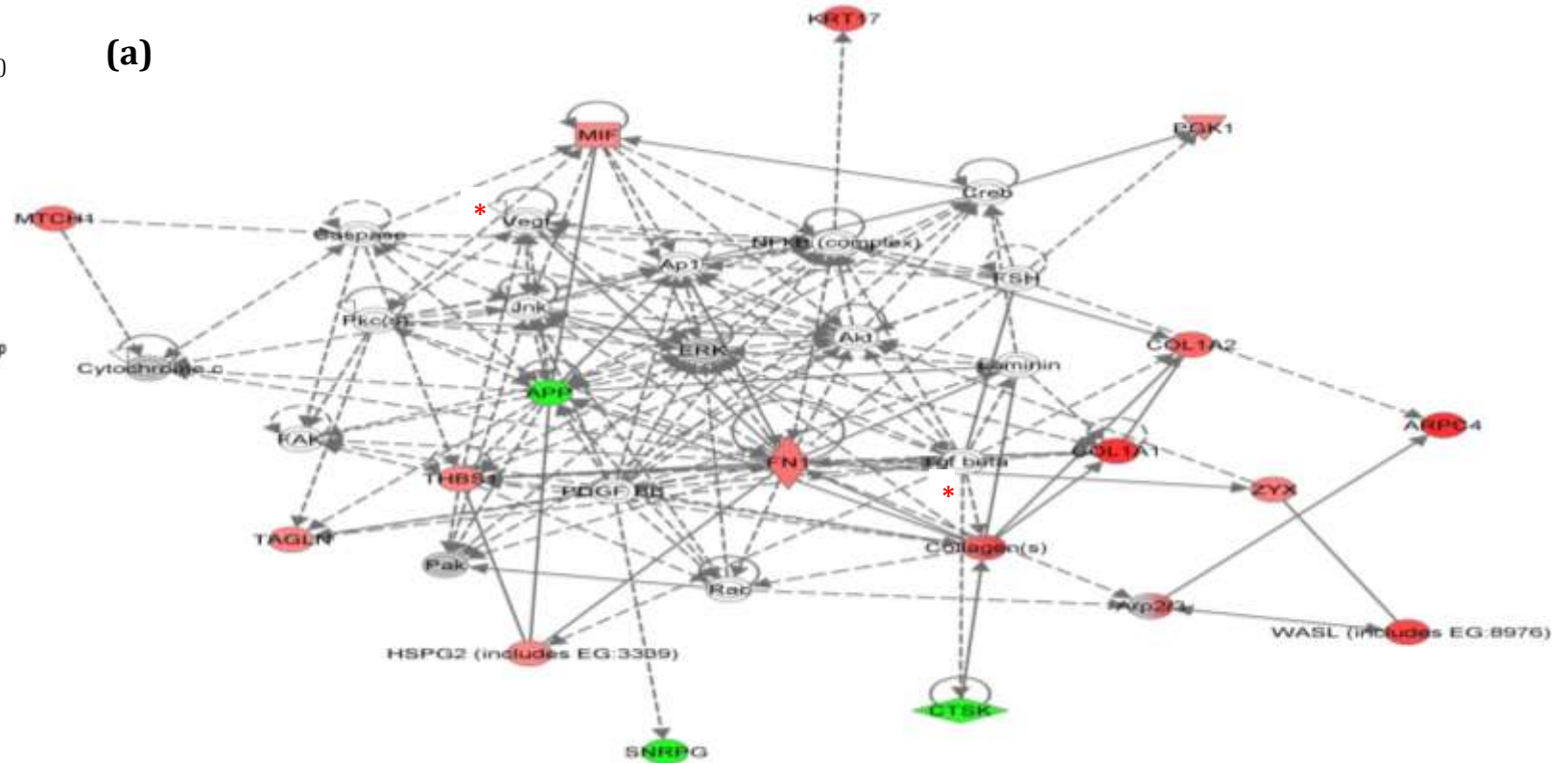
(b)
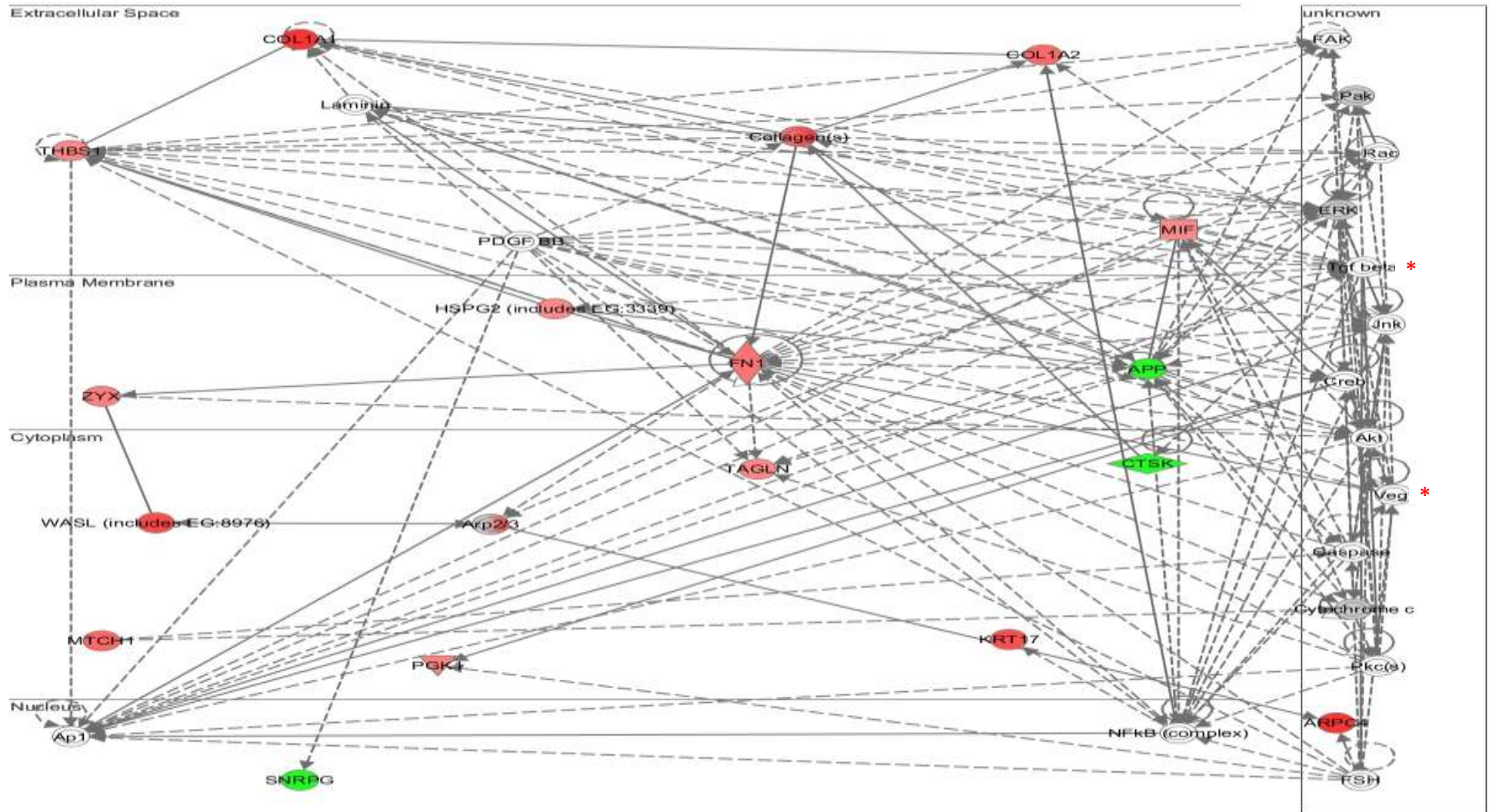
To analyse statistical significance in the alteration of protein levels the Ingenuity pathway analysis (IPA) Software (www.ingenuity.com) was used; the threshold value was set at P≤0.05. This revealed that from the 941 proteins only 8 of the proteins were significantly up-regulated by minoxidil (Table 4.1), and only a further 9 were down-regulated (Table 4.2).

Some proteins that were up-regulated were of particular interest: Cathepsin K precursor (CTSK) which has high specificity for kinins has been associated with prostaglandin production; DNAj homolog subfamily C member 3 (DNAJC3) down-regulates apoptosis. Down-regulated proteins of particular interest from Table 4.2 include Mitochondrial carrier homolog 1 (MTCH1) and Fibronectin 1 (FN1) both of which have been associated with inducing apoptosis.

Since this study focused on the (CAMPTF) network, attention was given to proteins altered in that network. Within the network 15 proteins had been down-regulated with 5 reaching statistical significance (P<0.05); while only 3 proteins were significantly up-regulated (P<0.05) (Figure 4.15).

The proteins involved in the cellular assembly network which were significantly up-regulated by minoxidil were: Amyloid beta (A4) precursor (APP) (p=0.005), Small nuclear ribonucleo protein G (SNRPG) (p=0.004) and Cathepsin K precursor (CTSK) (p=0.007). The APP protein is normally located in the plasma membrane, the SNRPG protein is located in the nucleus, and CTSK located in the cytoplasm.

The five proteins significantly down-regulated by minoxidil were: Actin related protein 2/3 complex subunit 4 (ARPC4) (p=0.0004), Collagen, type I, alpha 1 (CO1A1) (p=0.005), Mitochondrial carrier homolog 1 (MTCH1)

(p=0.007) located within the cytoplasm, Collagen alpha-2(I) chain (CO1A2) (p=0.007) and Fibronectin (FN1) (p=0.01) located in the plasma membrane. Interestingly this pathway implicated several proteins which have been reported to be produced by cultured dermal papilla cells, but were not identified in this experiment including vascular endothelial growth factor (VEGF) (Lachgar *et al.*, 1996c; Hibberts, 1996a; Merrick, 1999) and transforming growth factor-β1 (TGF-β1) (Heine *et al.*, 1987; Inui *et al.*, 2002; 2003) (Figure 4.15).

Table 4.1 Up-regulated proteins identified in cultured dermal papilla cells treated with 100µM minoxidil

Protein	Increase by minoxidil (Ratio)	Role in cell growth (Source: Ingenuity Knowledge Base and The Human Gene Compendium: www.genecards.org)
Gamma-glutamyl hydrolase precursor (GGH)	x 5.0 (0.20)	Crucial enzyme in the metabolism of folic acid
Amyloid beta A4 protein precursor (APP)	x 3.2 (0.31)	Limited information available about its function, could bind to other proteins on the surface of cells or could possibly assist in attachment of cells to one another
Cathepsin K precursor (CTSK)	x 2.9 (0.34)	Protease that is defined by high specificity for kinins, (small peptides that act on phospholipase and increase arachidonic acid release and thus prostaglandin (PGE$_2$) production)
Small nuclear ribonucleo protein G (SNRPG)	x 2.8 (0.36)	Has been shown to interact with DDX20 (DEAD); associated in cellular processes involving stimulation of RNA secondary structure (translation initiation, nuclear and mitochondrial splicing, and ribosome and spliceosome assembly)
Thyroid hormone receptor-associated protein 3 (THRAP3)	x 2.6 (0.38)	Nuclear receptor with association in transcriptional co-activation of RNA polymerase II, which is an enzyme found in eukaryotic cells. It catalyses the transcription of DNA to synthesize precursors of mRNA.
DNAJ homolog subfamily C member 3 (DNAJC3)	x 2.5 (0.40)	Inhibits the apoptosis influencing protein kinase resource (PKR), i.e. down-regulates apoptosis
Heme oxygenase 1 (HMOX1)	x 2.2 (0.46)	Acts as a protective protein against oxidative stress
Aldose reductase (AKR1B1)	x 2.2 (0.46)	Stress inducible protein, that stimulates glucose metabolism

Table 4.2 Down-regulated proteins identified in cultured dermal papilla cells treated with 100µM minoxidil

Protein	Decreased by minoxidil (Ratio)	Role in cell (Source: Ingenuity Knowledge Base and The Human Gene Compendium: www.genecards.org)
Actin Related Protein 2/3 Complex subunit 4 (ARPC4)	x 0.23 (4.38)	Stimulates actin polymerisation
Heterogeneous Nuclear Ribonucleoprotein U-like 1 (HNRNPUL1)	x 0.36 (2.77)	Represses basic transcription
Collagen, type I, alpha 1 (CO1A1)	x 0.37 (2.69)	Functions as a mechanical support for structural organisation
Wiskott-Aldrich syndrome-like (WASL)	x 0.37 (2.40)	Stimulates actin polymerisation via stimulation of the actin-nucleating activity of the Arp2/3 complex subunit 4
Collagen, type XII, alpha 1 (COCA1)	x 0.43 (2.30)	An anchoring fibril between the external epithelia and the underlying stroma
Mitochondrial carrier homolog 1 (MTCH1)	x 0.50 (2.00)	Induces apoptosis when over-expressed
Procollagen-lysine 1, 2-oxoglutarate 5-dioxygenase 1 (PLOD1)	x 0.50 (1.99)	Provides instructions for making an enzyme called lysyl hydroxylase 1 (this is key to the stability of the intermolecular collagen cross-links)
Collagen alpha-2(I) chain (CO1A2)	x 0.51 (1.97)	Functions as a mechanical support for structural organisation
Fibronectin 1 (FN1)	x 0.54 (1.84)	Induces apoptosis

4.5 Discussion

The dermal papilla plays a significant role in mesenchymal-epithelial interactions within the hair follicle and in the regulation of hair follicle activity (Reynolds and Jahoda, 1991; Jahoda and Reynolds, 1996; Rendl *et al.,* 2005; Richardson *et al.,* 2005; Waters *et al.*, 2007). The presence of SUR2B in the human follicular dermal papilla (Shorter 2008) and minoxidil's specific affinity to SUR2B (Schwanstecher *et al.*, 1998) flagged the dermal papilla cell as a possible site through which at least some K_{ATP} channel modulators function, thereby making dermal papilla cells a significant model to investigate the effects of minoxidil. This study investigated the effect of 100μM minoxidil on cell proliferation. This concentration was selected based on previous studies (Kurata *et al.*, 1996; Sanders *et al.,* 1996; Han *et al.*, 2004). Normal scalp dermal papilla cells were cultured in the presence of minoxidil over a period of 15 days and to construct a growth curve cell counting was performed in triplicate dishes at 48-hour intervals. Minoxidil at 100μM had a slight, but insignificant, inhibitory effect on cell proliferation over the 15 days in culture (p=0.495; Figure 4.11), though the pattern of growth was unchanged. This result mirrored that of Katsuoka *et al* (1987) who looked at the effect of an increasing concentration of minoxidil (10 to 160 μM) on dermal papilla and connective tissue sheath cells cultured from human occipital scalp. This group detected no alteration in growth over a 14 day culture period. The effect of the potassium channel blocker tolbutamide (1mM), and the combined treatment of minoxidil and tolbutamide was also investigated; both inhibited cell proliferation insignificantly (p=0.318; p=0.270) (Figure 4.11). Statistical analysis comparing cell proliferation on day 15 revealed that tolbutamide inhibited cell

proliferation significantly (p=0.05*), but that minoxidil had no effect (p=0.21). Combined minoxidil and tolbutamide cell numbers were similar to those with tolbutamide and significantly lower than control (Figure 4.12).

Protein quantification revealed that the total cellular protein content from the cells on day 15 followed the same pattern, with minoxidil having no effect (p=0.15), but significant inhibition exhibited by tolbutamide (p=0.01**) and combined minoxidil and tolbutamide (p=0.05*) (Figure 4.13). However, in this instance the difference between the application of minoxidil alone and that of the combined treatment of minoxidil and tolbutamide was significant (p=0.03*). Since Han *et al* (2004) reported that minoxidil stimulated the proliferation of cultured human dermal papilla cells using a MTT (3-(4, 5-dimethylthiazol-2-yl)-2,5-diphenyltetrazolium bromide) assay, at varying concentrations (0.01, 0.1, 1 µM) in a dose-responsive manner, a MTT assay was also carried out on cultured dermal papilla cells, treated with minoxidil, tolbutamide, or the combined effect of minoxidil and tolbutamide, for 48 hours. The results showed that 100µM minoxidil had no effect on cell viability (p=0.487; Figure 4.14), in contrast to the significant inhibitory effect that tolbutamide (p=0.037*) and the combined treatment had (p=0.037*). Similar to the difference between the total cellular protein content, the difference between the application of minoxidil alone and that of the combined treatment of minoxidil and tolbutamide was also significantly different for the cell viability assay (p=0.04*). Han *et al* (2004) also reported that minoxidil exerted an inhibitory affect on cell growth, but at the highest concentration of 2mM. Interestingly, Sanders *et al* (1996) reported minoxidil at 50µM to have a stimulatory effect on dermal fibroblast cell proliferation. Additionally, another

investigation revealed that minoxidil stimulated ^{3}H-thymidine uptake in dermal papilla (500 μM) and outer root sheath cells (100 μM) cultured from stump-tailed macaque scalp hair follicles (Kurata *et al.*, 1996) although minoxidil had no effect on cells that were non-follicular. The diverse range of culture conditions and concentrations used across this area of research make it difficult to ascertain the exact effect of minoxidil on dermal papilla cell proliferation (Katsuoka *et al.*, 1987; Lachgar *et al.,* 1996a; Kurata *et al.*, 1996; Sanders *et al.,* 1996; Lachgar *et al.*, 1998; Han *et al.*, 2004). This may not be a particularly biologically relevant *in vitro* assay parameter since dermal papilla cells are not seen to divide very often in adult follicles (Pierard and Brassinne, 1975). Therefore, it is more appropriate to investigate the mechanism of action of minoxidil with an alternative, more comprehensive method which assesses the actual proteins altered by minoxidil.

The study of proteins elucidates cell behaviour and identifies the particular phenotypes of a cell. Using proteomics to analyse dermal papilla cell proteins has the potential of revealing the mechanisms of action of minoxidil on cells via the alteration of protein levels. Quantitative analysis of the proteins allows comparisons to be drawn between different experimental states. From the several formats available (Bantscheff *et al.*, 2007) stable isotope labelling by amino acids in cell culture (SILAC) was chosen for its simplicity and strength in efficiency. The effect of external agents such as minoxidil on a protein's concentration can be clearly demonstrated with SILAC. To increase biological validity four individual scalp dermal papilla cells were derived from four women aged between 42 and 60 were used for this experiment. Each line was cultured in duplicate and the first set was placed in 'light' medium, i.e. medium

containing unlabelled arginine and lysine amino acids, and the second set in 'heavy' medium, i.e. that containing ^{13}C-labelled arginine and lysine amino acids. Five cell cycles were necessary to allow for complete labelling of the cells with SILAC. The cells in the 'heavy' media were treated with 100µM minoxidil for 48 hours and those in the 'light' media were used as vehicle control. Following the extraction of protein from the cells, quantification and peptide generation, mass spectrometry analysis was carried out on cell protein extracts combined from all 4 samples of dermal papilla cells. This determined and quantitated the relative ratios of each isotopic form of every peptide, which was analysed to measure any increase, decrease or consistency in the level of each protein after treatment. The intensity ratio of the two peaks from the 'light' and 'heavy' pair (control *vs.* minoxidil) was a measure of any differentiation in peptide abundance within the mixture (Figure 4.4). This highlighted the quantitative differences introduced with the application of minoxidil at a protein level. The Mascot search engine identified 941 proteins in the cultured dermal papilla cells (http://www.matrixscience.com/).

Using IPA Software (www.ingenuity.com) all 941 proteins were separated into networks depending on their functions. As mentioned previously, the extent of all the functions of the 941 proteins identified is too widespread to be followed in one investigation, thus this report narrowed its concentration to cellular assembly, maintenance and protein trafficking functions (CAMPTF), as these are essential for cell survival. The visual representation of the proteins within that network also revealed proteins that may not have been identified in the cultured dermal papilla cells, but have possible associations with that network (Figure 4.14), including vascular

endothelial growth factor (VEGF) which has been shown to have been secreted and expressed in cultured human dermal papilla cells (Lachgar *et al.*, 1996c; Hibberts, 1996a; Merrick, 1999).

Interestingly minoxidil stimulated VEGF mRNA expression in cultured dermal papilla cells (Lachgar *et al.,* 1998). The visual representation of the proteins in Figure 4.14 also revealed transforming growth factor-β1 (TGF-β1) as a possible associated protein (Figure 4.15). Minoxidil has been reported to have an inhibitory effect on TGF-β1 induced apoptosis (Otomo, 2002). This growth factor also inhibits human hair follicle growth *in vitro* (Philpot, 2000) and has been suggested as a factor associated with androgenetic alopecia. Hamada and Randall (2006) reported that cultured balding dermal papilla cells produced inhibitory autocrine factors and TGF-β1 has been found to be stimulated by androgens in balding dermal papilla cells (Heine *et al.*, 1987; Inui *et al.*, 2002; 2003; Hamada and Randall, 2006).

To our knowledge, the only other research conducted using proteomics in human dermal papilla cells was by Rushan and colleagues (2007), who looked at the aggregative behaviour of dermal papilla cells by comparing proteins in the cells before and after aggregation. They identified the following 5 proteins: Annexin A2 isoform 1, Heat shock 70kDa protein, Mitochondrial ribosomal protein, Transgelin and Transgelin 2 which were all over expressed in the dermal papilla cells following aggregation. All 5 proteins were amongst the identified proteins in this investigation but their levels were unchanged by minoxidil.

The Ingenuity pathway analysis (IPA) Software (www.ingenuity.com) analysis of the statistical significance in alteration of protein levels, with the set

threshold of P≤0.05, revealed that from the 941 proteins only 8 of the proteins were significantly up-regulated by minoxidil (Table 4.1), and a only a further 9 were down-regulated (Table 4.2). Such a finding is not entirely unpredictable, as there was no change in cell proliferation with minoxidil (Figure 4.11), the cells were confluent and as there are so many processes that all cells need to perform simply for their existence.

In the CAMPTF network 15 proteins had been down-regulated, though only 5 were significantly inhibited by minoxidil under the statistical analysis, and 3 proteins had been up-regulated, all significantly, by minoxidil (P≤0.05). The proteins that were significantly up-regulated by minoxidil in the CAMPTF network were Amyloid beta (A4) precursor (APP) (p=0.005), Small nuclear ribonucleo protein G (SNRPG) (p=0.004) and Cathepsin K precursor (CTSK) (p=0.007) (Figure 4.15a). The APP protein is located in the plasma membrane: its functions have not been fully ascertained, however it may bind to other proteins on the surface of the cell or be a facilitator in the attachment of cells to one another (Soba *et al.*, 2005; Zheng and Koo, 2006). Recent investigations on rat brains have shown evidence that a soluble APP has growth-promoting properties and may have a crucial role in the formation of nerve cells (Sayer *et al.*, 2008). SNRPG protein is located in the nucleus of the cell, and has been shown to interact with DDX20 (DEAD), which is associated with several cellular processes involving stimulation of RNA secondary translation initiation, nuclear and mitochondrial splicing, and ribosome and spliceosome assembly (Godbout and Squire, 1993; Charroux *et al.*, 1999; Solem *et al.*, 2006). DEAD protein is implicated in cellular growth and division (The Human Gene Compendium: www.genecards.org). Thus both these minoxidil-stimulated proteins are

believed to increase cell activity/growth, although their roles in dermal papilla cells are currently unknown; this type of effect would be consistent with the generally increased growth of hair follicles with minoxidil treatment *in vivo*. Although minoxidil had no effect on dermal papilla cell proliferation in the experimentation of this thesis, further investigations are required to ascertain the role of other factors in culture conditions, as the conditions in the medium for the cell proliferation and proteomic study differed. Hence, future investigations must look at the effect and interaction of such other factors, e.g. serum, insulin, antibiotics and the time lapse during which cells were exposed to minoxidil.

CTSK is located in the cytoplasm and is a protease, which is defined by its high specificity for kinins. Kinins are small peptides that act on phospholipase and increase arachidonic acid release and thereby the production of prostaglandins. CTSK was up-regulated by minoxidil, this is worthy of note as the prostaglandin analogue (Latanoprost) used in the treatment of glaucoma has been reported to induce hair growth (Johnstone and Albert, 2002) and it has been suggested from studies of the activation of cytoprotective prostaglandin synthase-1 in dermal papilla cells that minoxidil can increase prostaglandin synthesis (Michelet *et al.*, 1997). Recently, prostaglandin F_2 analogues used to treat glaucoma (Arranz-Marquez and Teus, 2008), have been shown to stimulate eyelash growth (Wester *et al.*, 2010) and isolated hair follicle growth in organ culture (Khidhir and Randall – personal communication).

Outside the CAMPTF network, the following proteins also exhibited significant up-regulation out of the 941 (Table 4.1) with $P<0.05$: Gamma-glutamyl hydrolase precursor (GGH), Thyroid hormone receptor-associated

protein 3 (THRAP3), DNAj homolog subfamily C member 3 (DNAJC3), Heme oxygenase 1 (HMOX1) and Aldose reductase (AKR1B1). GGH is a key enzyme of the metabolism of folic acid (Eisele *et al.*, 2006), which is essential for the production and maintenance of new cells for DNA and RNA synthesis as well as the prevention of changes to DNA (Kamen, 1997). THRAP3 is a nuclear receptor that plays a role in transcriptional coactivation (Ko *et al.,* 2000). THRAP3's and GGH's up-regulation by minoxidil suggests that RNA synthesis was increased; this would be expected if minoxidil was stimulating the increased secretion of paracrine regulators which stimulate keratinocyte growth. The protein DNAJC3 functions as an inhibitor of the protein kinase resource (PKR) (Austbø *et al.,* 2008). Kinases participate in signalling cascades that influence apoptosis (Franklin and McCubrey, 2000). DNAJC3 may have been up-regulated to defend against apoptosis.

HMOX1, which was also up-regulated by minoxidil, is a stress inducible protein, providing protection against oxidative stress (Slebos *et al.*, 2003). Oxidative stress creates a disturbance in the normal redox state of a cell and can cause toxic effects that damage all components of a cell, including its proteins, lipids and DNA (Otterbein *et al.,* 2000). AKR1B1 stimulates glucose metabolism and, similarly to HMOX1, functions as a stress inducible protein and is believed to have a protective role against steroidgenesis that, when accumulated, could affect cell growth or differentiation (Lefrancois-Martinez *et al.,* 2004), indicating that AKR1B1 has a benefit against the effects of the steroids produced by steroidgenesis. Steroidgenesis is the process during which desired forms of steroids are generated by transformation of other steroids. The androgens testosterone and 5alpha dihydrotestosterone (DHT) are products of

steroidgenesis and are of particular interest since male pattern baldness, androgenetic alopecia, is associated with a genetic sensitivity of the hair follicle to androgen (Randall., 2008). Other products of steroidgenesis include oestrogens and progesterone, corticoids and aldosterone. Steroidgenesis pathways are deeply complex. This could mean that the up-regulation of AKR1B1 potentially protects cells against the products of steroidgenesis, such as testosterone, which has been shown to inhibit hair growth in the presence of dermal papilla cells from the frontal bald scalp of the stumptailed macaque (Obana *et al.,* 1997). This seems less likely *in vivo* because most steroidogenesis takes place in endocrine organs, although the metabolisnm of testosterone to its more active metabolite can take place in dermal papilla cells (reviewed Randall 2008). Alternatively, male pattern hair loss is associated with ageing as well as androgens. Aging has also been associated with oxidative stress (Dröge, 2005), and thereforeDNAJC3 and AKR1B1 may be reducing this effect.

The five proteins that were significantly down-regulated included Fibronectin (FN1) (p=0.01) located in the plasma membrane, Mitochondrial carrier homolog 1 (MTCH1) (p=0.007), Actin related protein 2/3 complex subunit 4 (ARPC4) (p=0.0004), Collagen, type I, alpha 1 (CO1A1) (p=0.005), and Collagen alpha-2(I) chain (CO1A2) (p=0.007). FN1 protein induces apoptosis within the cell, whilst MTCH1 induces apoptosis only when over expressed (Sugahara *et al.,* 1994; Lamarca *et al.,* 2007). Down-regulation of these apoptotic-inducing proteins by minoxidil, in combination with the stimulation of increased production of DNAJc3 could suggest that minoxidil would inhibit/delay apoptosis *in vivo*. Indeed, one of the clinical effects of minoxidil is to prolong anagen, resulting in a larger hair (Messenger and Rundegren, 2004).

This involves delaying catagen which involves significant apoptosis (Botchkareva *et al.,* 2006).

The ARPC4 protein stimulates actin polymerisation in the cell, an essential function for maintaining cell shape (Otsubo *et al.,* 2004), although the mechanism by which it promotes this action remains unclear (Welch *et al.,* 1997). ARPC4 is stimulated by another protein: Wiskott Aldrich Syndrome-like (WASL) protein, which was significantly down-regulated in this study, although outside of the CAMPTF network. This could offer an explanation as to why ARPC4 was down-regulated by minoxidil. WASL is implicated in the transduction of signals from receptors on the cell surface to the actin cytoskeleton, and while this protein interacts with multiple proteins (Lyubimova *et al.,* 2010), no studies have examined its full functioning. Further investigations are required to establish in detail the functions and regulatory factors that modulate WASL and the possible inhibitory effect of minoxidil on WASL. The role of reduction in actin polymerisation is unclear, but could suggest that minoxidil is enabling the cells to move and be more dynamic.

Collagen CO1A1 and CO1A2 generally function as extracellular mechanical support for the structural organisation of cells. This could be important *in vivo* since the dermal papilla contains extensive extracellular matrix (Messenger *et al.,* 1991). Cultured dermal papilla cells do produce extracellular matrix proteins including collagen I and type III (Katsuoka *et al.,* 1988) and collagen type IV (Messenger *et al.,* 1991). CO1A1 and CO1A2 are both members of the group 1 collagens, which are fibrillar forming collagen. Fibrillar type 1 collagen has been reported to inhibit cell growth (Henriet *et al.,*

2000), therefore minoxidil's inhibition of CO1A1 & A2 again has the potential to assist maintaining anagen *in vivo*.

Incorporating the study of proteomics in the treatment of dermal papilla cells with minoxidil and identifying the specific intracellular proteins that have been influenced as a result, brings us closer to forming a more comprehensive understanding of the intricate mechanisms that stimulate hair growth. The findings indicate that minoxidil has both inhibitory and stimulatory effects within the protein profiles of dermal papilla cells, which appear to be relevant to its clinical effects on hair growth. However, there is no really clear evidence suggesting exactly how it initially works, i.e. an obvious specific mechanism resulting from opening K^+_{ATP} channels. Previous suggestions by Li *et al* (2001) implicated an adenosine-related mechanism. Using DNA microarray analysis Iino *et al* (2007) showed that adenosine stimulated a 2-fold increase in VEGF gene expression and up-regulated the expression of fibroblast growth factor-7 (FGF-7) in the dermal papilla cells. They suggested that minoxidil stimulates adenosine secretion by potassium channel opening, which in turn enables up-regulation of VEGF and FGF-7 gene expression, resulting in stimulation of hair follicle growth. This study did not detect VEGF or FGF-7 in the dermal papilla cells. Although VEGF and FGF-7 could potentially have been secreted into the medium during culture, but unfortunately time did not permit the examination of proteins secreted into the medium here. However, the results in Chapter 2 of this thesis are not in support of the proposals made by Iino and colleagues, as minoxidil stimulated hair growth in organ culture in the absence of a vascular supply.

The superiority of proteomics allows for novel investigations to be conducted on hair follicle growth that concentrate on specific protein regulation as an indicator of the effectiveness of a drug. Minoxidil would be expected to be changing the paracrine regulatory proteins secreted either as soluble factors or extracellular matrix factors, which would primarily influence the epithelial hair follicle cells. Future investigations could elucidate the mechanism of action of minoxidil by analysing the medium derived from cultured dermal papilla cells in the presence of potassium channel modulators, to ascertain the possible transference of growth factors into the medium. It was not possible to complete this aspect in the time available. This study first focused on the intracellular proteins, allowing for a more concentrated protein sample as the method had not been done previously at the University of Bradford. Furthermore, future investigations could delve into the effects of K_{ATP} channel blocker tolbutamide, or the combined treatment of minoxidil and tolbutamide to elucidate their effect on protein profiles in dermal papilla cells. This holds the potential of revealing a more authoritative account of the mechanism of action of potassium channel modulators.

Chapter 5

Overall discussion

5. Overall Discussion

Minoxidil is the main topical treatment for alopecia although it can be rather limited in its effectiveness (Messenger and Rundegren, 2004). It opens certain ATP sensitive potassium (K_{ATP}) channels which have been found in human hair follicles (Shorter *et al.*, 2008). K_{ATP} channels are composed of two subunit classes: sulfonylurea receptors (SUR), the site of drug interaction, and pore-forming subunits (Kir 6.x). The expression of both types of sub-units are necessary to form a functional K_{ATP} channel (Gribble *et al.*, 1997; Inagaki *et al.*, 1995a; Yamada *et al.*, 1997).

Previous investigations using human anagen hair follicles demonstrated the presence of several K_{ATP} channels (Shorter *et al.*, 2008). To form a comprehensive outline of the role of the potassium channels in the hair follicle, it was important to investigate the presence of these channels in both their anagen and telogen phases. Investigating the presence of K_{ATP} channels in a human telogen hair follicle is extremely challenging as generally only scalp hair follicles are available and these are in the anagen phase for the majority of the time (Randall and Ebling, 1991). The use of methods that induce the telogen phase in humans is not ethical.

The red deer hair follicle is a well-established model (Thomas *et al.*, 1994; Thornton *et al.*, 1996; Randall *et al.*, 2003) and is an ideal animal to investigate K_{ATP} channels in the telogen phase. The seasonal growth cycles mean that follicles in any given area are at the same stage of the hair cycle (Lincoln and Kay, 1971), the pelage follicles are large, unlike most of those in laboratory animals, and are readily available without ethical constraints. Pharmacological studies examining the responses of red deer follicles in organ

culture revealed that minoxidil and other K_{ATP} channel openers stimulated follicle growth; an effect inhibited by potassium channel closers (Davies *et al.*, 2005). Thereby, suggesting the presence of K_{ATP} channels in red deer hair follicles and associating them with an ability to regulate hair growth, at least *in vitro*.

A histological comparison of human and red deer hair follicles confirmed that deer hair follicles are larger in structure than that of the human scalp hair follicle, rendering the medulla visible in the deer hair follicle (Figures 2.7 and 2.8). However, the structure was on the whole similar, thereby reinforcing the deer hair follicle as a good model system for the research. Furthermore, molecular biological investigations in red deer anagen hair follicles revealed the expression of K_{ATP} channel subunit genes SUR1, SUR2B, Kir6.1 and Kir6.2, although SUR2A was not expressed (Figures 2.13, 2.15, 2.17 and 2.19). These results are similar to a study on human hair follicles (Shorter *et al.,* 2008) and also fit with the pharmacological stimulation of deer hair growth (Davies *et al.,* 2005). Also paralleling human hair follicles (Shorter *et al.*, 2008) was the presence of SUR2B and Kir6.1 proteins, in the dermal papilla and connective tissue sheath (Figure 2.21). Therefore, it is most probable that SUR2B forms a K_{ATP} channel with Kir6.1 in deer follicle dermal papilla while SUR1 can form a K_{ATP} channel with Kir6.2, as SUR1/Kir6.1 channels are not physiologically relevant (Babenko *et al.*, 1998a). This suggests the possible existence of two K_{ATP} channels in deer anagen hair follicles. The strong correlation in the expression of K_{ATP} channel sub-units in deer anagen follicles with those found in human follicles reinforces the practicality of the deer hair follicle model as a

system for understanding hair follicle biology and its use for the screening of new hair growth treatments.

When red deer telogen follicles (Figure 2.9) were isolated and the gene expression of the K_{ATP} channel subunits investigated, no K_{ATP} channel subunit expression was detected (Figures 2.23-2.26). The absence of gene expression in telogen follicles highlights the significance of K_{ATP} channels in the normal anagen processes. Several reports of clinical observations have suggested that minoxidil advances anagen (Price and Menefee, 1996; Messenger and Rundegren, 2004), indicating towards an active K^+_{ATP} channel sub-unit in telogen. The absence of K^+_{ATP} channels in the red deer telogen hair follicles in this thesis suggests that they are possibly expressed at the end of the telogen phase, when exogen takes place (Higgins *et al.,* 2009).

Minoxidil has been reported to have a specific affinity for SUR2B (Schwanstecher *et al.*, 1998) and has been shown to have a stimulatory effect on growth in cultured red deer (Davies *et al.*, 2005) and human scalp hair follicles (Han *et al.*, 2004; Shorter *et al.,* 2008). Minoxidil's effect on cultured human hair follicles has garnered conflicting results of stimulation, inhibition and no effect (Table 3.1). Comparisons drawn between these studies are limited due to the varying culture conditions, particularly because of the use of insulin in the culture medium, which aims to prolong anagen.

Therefore, prior to further investigations on K_{ATP} channel openers on human anagen follicles the role of insulin was examined. In the comparison carried out in this thesis, in the presence of insulin minoxidil had no effect, whereas, in the absence of insulin it had a significant stimulatory effect (Figure 3.4). The potassium channel blocker tolbutamide, shortened anagen in cultured

human hair follicles in the presence of insulin, while in the absence of insulin tolbutamide had no effect (Figure 3.7). Overall, it is clear that insulin in the medium affects follicular responses. Insulin advances the movement of ions across the plasma membrane (Irwin and Rippe, 2008), and the resultant alterations may lead to the opening of K_{ATP} channels, mirroring the probable main action of minoxidil. Alternatively, as insulin acts as a stimulant of glucose uptake into cells and storage (Cushman and Wardzala, 1980; Suzuki and Kono, 1980; Leney and Tavare, 2009), follicles may have achieved maximum growth already in insulin supplemented medium.

Tolbutamide's inhibitory effect in the presence of insulin could be due to the closing of the channels; whilst in the insulin-free medium, tolbutamide had no real effect, presumably as the channels were closed. The effects of insulin on hair follicles grown in organ culture are not yet fully understood and further research is necessary to bridge this gap. However, tolbutamide's inhibitory effect on anagen follicles could be harnessed to formulate clinical topical treatments that reduce hair growth, caused by disorders such as hirsutism and this merits further investigation.

Minoxidil only opens SUR2B channels; however, both the human (Shorter *et al.,* 2008) and deer hair follicles (Chapter 2) express both SUR1 and SUR2B K_{ATP} channel types. In red deer hair follicles NNC 55-0118, a drug which would only open SUR1 containing channels, also had a stimulatory effect on hair follicle growth (Davies *et al.*, 2005). The results presented in chapter 3 on human hair follicles, showed that another SUR1 opener drug, NNC55-9216 significantly prolonged anagen and increased hair follicle length in organ culture in the absence of insulin (Figure 3.13). This effect was inhibited by

tolbutamide in the absence of insulin (Figure 3.13). The combined treatment of minoxidil and NNC55-9216 produced a significantly greater stimulation of anagen and hair length than either drug alone (Figure 3.14). Therefore, opening SUR1 K_{ATP} channels in human hair follicles stimulates hair growth. These results suggest novel approaches for more effective pharmaceuticals to treat alopecia via SUR1 K_{ATP} channels, or perhaps in combination with minoxidil.

Minoxidil's mechanism of action after activation of K_{ATP} channels remains unclear. The presence SUR2B/Kir6.1 K_{ATP} channels in human dermal papillae (Shorter *et al.*, 2008) offers a target for minoxidil. This holds the potential of binding to the receptors and modifying the gene expression of factors acting on other cell types involved in hair follicle growth. Thereby, lending to the prospect that the dermal papilla is a target through which at least some K_{ATP} channel openers function.

The dermal papilla plays a crucial role in hair follicle activity (Reynolds and Jahoda 1991; Jahoda and Reynolds 1996; Rendl *et al.*, 2005; Richardson *et al.*, 2005; Waters *et al.*, 2007). The effect of minoxidil was not significant on dermal papilla cell proliferation, following 15 days in culture, paralleling findings by Katsuoka *et al* (1987). The potassium channel blocker, tolbutamide, had an inhibitory effect on total cell proliferation though not the pattern of growth (Figures 4.11 and 4.12). The same effect was noted in total cellular content using protein quantification and the viability assay MTT (Figures 4.13 and 4.14).

The study of proteomics lends to greater understanding of cell behaviour and identifies particular cell phenotypes. The effect of minoxidil on the protein

profile was investigated using the quantitative proteomic approach by labelling the cells with SILAC allowing measurement of quantitative differences in the levels of individual proteins after treatment with minoxidil. This was the first time that the SILAC method had been used at the University of Bradford and is one of the first attempts to use the proteomics approach for investigations in human cultured dermal papilla cells. The author carried out all the complete and time consuming processes in this investigation. The mass spectrometry analysis identified 941 proteins in cultured dermal papilla cells (Figure 4.14), from which 8 proteins were significantly up-regulated (Table 4.1) and another 9 were down-regulated (Table 4.2). The proteins were sorted into networks that related to their functions. This thesis focused on the proteins associated with cellular assembly, maintenance and protein trafficking functions (CAMPTF), due the essential role they play in cell survival (Figure 4.15). Within this network APP, CTSK and SNRPG proteins were up-regulated (Table 4.1; Figure 4.15). APP has a growth promoting factor, whilst CTSK was associated with prostaglandin synthesis, which has been known for inducing hair follicle growth and SNRPG was implicated in cellular growth and division (Sayer *et al.*, 2008; Johnstone and Albert, 2002). FN1, MTCH1, CO1A1, CO1A2 and ARPC4 proteins were down regulated in the CAMPTF network (Table 4.2; Figure 4.15). FN1 and MTCH1 were both found to be apoptotic proteins (Sugahar *et al.,* 1994; Lamarca *et al.*, 2007). CO1A1 and CO1A2 are both associated with cell growth inhibition (Henriet *et al.,* 2000). Thus, minoxidil altered proteins in cultured dermal papilla cells to increase cell synthesis activity and inhibit apoptosis, fitting with its effects *in vivo.*

The investigations in this thesis concur with the hypothesis that minoxidil has a stimulatory effect on hair growth by acting via K_{ATP} channels within hair follicles by detecting SUR2B genes in anagen, but not telogen deer hair follicles. The stimulatory effect of a selective SUR1 channel opener, NNC 55-9216, on human hair follicles and the identification of SUR1 gene expression in hair follicles also implicate SUR1 K_{ATP} channels in the regulation of hair growth. This and the combined effect of NNC 55-9216 with SUR2B channel opener minoxidil in organ culture calls for novel approaches for more effective pharmaceuticals to treat alopecia via SUR1 K_{ATP} channels, or in combination with minoxidil. Identification of proteins that were altered following treatment with minoxidil authenticates the crucial role of dermal papilla cells in the hair follicle and suggests it has anti-apoptotic effects, which may delay the onset of catagen, thereby extending anagen *in vivo*. They also support a role for promoting prostaglandin synthesis, an area of current interest due to eyelash growth stimulation as a side effect of prostaglandin analogues used for glaucoma (Wester *et al.*, 2010). Future investigations could extend these findings and focus on the proteomics of the media of cultured dermal papilla cells and also use DNA microarray techniques to investigate differences in gene expression. This should enhance our understanding of hair follicle biology and assist in the creation of more sophisticated therapeutic treatments that can promote hair growth and thereby relieve the widespread distress caused by hair disorders.

REFERENCES

Abell, E. (1988). "Histologic response to topically applied minoxidil in male pattern alopecia." Clin Dermatol **6**: 191-194.

Aguilar-Bryan, L., J. P. Clement, G. Gonzalez, K. Kunjilwar, A. P. Babenko and J. Bryan (1998). "Toward understanding the assembly and structure of K_{ATP} channels." Physiol Rev **78**(1): 227-245.

Aguilar-Bryan, L., C. G. Nichols, S. W. Wechsler, J. P. Clement, A. E. Boyd, G. Gonzalez, H. Herrera-Sosa, K. Nguy, J. Bryan and D. A. Nelson (1995). "Cloning of the beta cell high-affinity sulfonylurea receptor: a regulator of insulin secretion." Science **268**(5209): 423-426.

Allard, B. and M. Lazdunski (1993). "Pharmacological properties of ATP-sensitive K+ channels in mammalian skeletal muscle cells." Eur J Pharmacol **236**(3): 419-26.

Antcliff, J. F., S. Haider, P. Proks, M. S. Sansom and F. M. Ashcroft (2005). "Functional analysis of a structural model of the ATP-binding site of the KATP channel Kir6.2 subunit." Embo J **24**(2): 229-39.

Arranz-Marquez, E. and M. A. Teus (2008). "Prostanoids for the management of glaucoma." Expert Opin Drug Saf **7**(6): 801-8.

Ashcroft, F. M. (2006). "K(ATP) channels and insulin secretion: a key role in health and disease." Biochem Soc Trans **34**(Pt 2): 243-6.

Ashcroft, F. M. and F. M. Gribble (2000). "New windows on the mechanism of action of K(ATP) channel openers." Trends Pharmacol Sci **21**(11): 439-45.

Ashcroft, F. M., D. E. Harrison and S. J. H. Ashcroft (1984). "Glucose induces closure of single potassium channels in isolated rat pancreatic beta-cells." Nature **312**: 446-448.

Ashcroft, F. M. and P. Rorsman (1989). "Electophysiology of the pancreatic beta-cell." Prog Biophys Mol Biol **54**(2): 87-143.

Ashcroft, S. J. and F. M. Ashcroft (1990). "Properties and functions of ATP-sensitive K-channels." Cell Signal **2**(3): 197-214.

Ashford, M. L. J., N. C. Sturgess, N. J. Trout, N. J. Gardner and C. N. Hales (1988). "Adenosine-5'-triphosphate-sensitive ion channels in neonatal rat cultured central neurones." Pflugers Arch **412**: 297-304.

Auber, L. (1952). "The anatomy of follicles producing wool-fibres, with special reference to keratinization." <u>Transactions of the Royal Society of Edinburgh</u> **62**: 191-254.

Austbo, L., A. Kampmann, U. Muller-Ladner, E. Neumann, I. Olsaker and G. Skretting (2008). "Identification of differentially expressed genes in ileal Peyer's patch of scrapie-infected sheep using RNA arbitrarily primed PCR." <u>BMC Vet Res</u> **4**: 12.

Babenko, A. P., L. Aguilar-Bryan and J. Bryan (1998). "A view of sur/KIR6.X, KATP channels." <u>Annu Rev Physiol</u> **60**: 667-87.

Babenko, A. P., G. Gonzalez, L. Aguilar-Bryan and J. Bryan (1998). "Reconstituted human cardiac K_{ATP} channels: functional identity with the native channels from the sarcolemma og human ventricular cells." <u>Circ Res</u> **83**(11): 1132-1143.

Bantscheff, M., M. Schirle, G. Sweetman, J. Rick and B. Kuster (2007). "Quantitative mass spectrometry in proteomics: a critical review." <u>Anal Bioanal Chem</u> **389**(4): 1017-31.

Bardin, C. W. and M. B. Lipsett (1967). "Testosterone and androstenedione blood production rates in normal women and women with idiopathic hirsutism or polycystic ovaries." <u>J Clin Invest</u> **46**(5): 891-902.

Baukrowitz, T. and B. Fakler (2000). "K(ATP) channels: linker between phospholipid metabolism and excitability." <u>Biochem Pharmacol</u> **60**(6): 735-40.

Bernardi, H., M. Fosset and M. Lazdunski (1988). "Characterization, purification and affinity labeling of the brain [³H]glibenclamide-binding protein, a putative neuronal ATP-regulated K^+ channel." <u>Proc Natl Acad Sci USA</u> **85**: 9816-9820.

Berridge, M. J., M. D. Bootman and H. L. Roderick (2003). "Calcium signalling: dynamics, homeostasis and remodelling." <u>Nat Rev Mol Cell Biol</u> **4**(7): 517-29.

Blackstock, W. P. and M. P. Weir (1999). "Proteomics: quantitative and physical mapping of cellular proteins." <u>Trends Biotechnol</u> **17**(3): 121-7.

Blume, U., J. Ferracin, M. Verschoore, J. M. Czernielewski and H. Schaefer (1991). "Physiology of the vellus hair follicle: hair growth and sebum excretion." <u>Br J Dermatol</u> **124**(1): 21-8.

Botchkareva, N. V., G. Ahluwalia and D. Shander (2006). "Apoptosis in the hair follicle." <u>J Invest Dermatol</u> **126**(2): 258-64.

Bradfield, R. B. (1971). "Protein deprivation: comparative response of hair roots, serum protein, and urinary nitrogen." <u>Am J Clin Nutr</u> **24**(4): 405-10.

Buhl, A. E., S. J. Conrad, D. J. Waldon and M. N. Brunden (1993). "Potassium channel conductance as a control mechanism in hair follicles." J Invest Dermatol **101**(1 Suppl): 148S-152S.

Buhl, A. E., D. J. Waldon, T. T. Kawabe and J. M. Holland (1989). "Minoxidil stimulates mouse vibrissae follicles in organ culture." J Invest Dermatol **92**(3): 315-20.

Burton, J. L. and A. Marshall (1979). "Hypertrichosis due to minoxidil." Br J Dermatol **101**(5): 593-5.

Burton, J. L., W. H. Schutt and I. W. Caldwell (1975). "Hypertrichosis due to diazoxide." Br J Dermatol **93**(6): 707-11.

Cha, R. S. and W. G. Thilly (1995). Specificity, Efficiency and Fidelity of PCR. PCR Primer: A Laboratory Manual. C. W. Dieffenbach, and Dveksler, G.S. New York, Cold Spring Harbor Laboratory Press**:** 37-51.

Chamrad, D. C., G. Korting, K. Stuhler, H. E. Meyer, J. Klose and M. Bluggel (2004). "Evaluation of algorithms for protein identification from sequence databases using mass spectrometry data." Proteomics **4**(3): 619-28.

Charroux, B., L. Pellizzoni, R. A. Perkinson, A. Shevchenko, M. Mann and G. Dreyfuss (1999). "Gemin3: A novel DEAD box protein that interacts with SMN, the spinal muscular atrophy gene product, and is a component of gems." J Cell Biol **147**(6): 1181-94.

Chase, H. B. (1954). "Growth of the hair." Physiol Rev **34**(1): 113-26.

Chase, H. B., R. Rauch and V. W. Smith (1951). "Critical stages of hair development and pigmentation in the mouse." Physiol Zool **24**(1): 1-8.

Chiang, S. H., J. Hwang, M. Legendre, M. Zhang, A. Kimura and A. R. Saltiel (2003). "TCGAP, a multidomain Rho GTPase-activating protein involved in insulin-stimulated glucose transport." Embo J **22**(11): 2679-91.

Chutkow, W. A., M. C. Simon, M. M. Le Beau and C. F. Burant (1996). "Cloning, tissue expression, and chromosomal localization of SUR2, the putative drug-binding subunit of cardiac, skeletal muscle and vascular K_{ATP} channels." Diabetes **45**(10): 1439-1445.

Clapham, D. E. (2007). "Calcium signaling." Cell **131**(6): 1047-58.

Clement, J. P. t., K. Kunjilwar, G. Gonzalez, M. Schwanstecher, U. Panten, L. Aguilar-Bryan and J. Bryan (1997). "Association and stoichiometry of K(ATP) channel subunits." Neuron **18**(5): 827-38.

Cook, D. L. and C. N. Hales (1984). "Intracellular ATP directly blocks K^+ channels in pancreatic beta-cells." Nature **311**: 271-273.

Cook, D. L., L. S. Satin, M. L. Ashford and C. N. Hales (1988). "ATP-sensitive K+ channels in pancreatic beta-cells. Spare-channel hypothesis." Diabetes **37**(5): 495-8.

Couchman, J. R. (1986). "Rat hair follicle dermal papillae have an extracellular matrix containing basement membrane components." J Invest Dermatol **87**(6): 762-7.

Couchman, J. R., J. L. King and K. J. McCarthy (1990). "Distribution of two basement membrane proteoglycans through hair follicle development and the hair growth cycle in the rat." J Invest Dermatol **94**(1): 65-70.

Courtois, M., G. Loussouarn, S. Hourseau and J. F. Grollier (1996). "Periodicity in the growth and shedding of hair." Br J Dermatol **134**(1): 47-54.

Croft, N. J. (2002). Antler velvet is a novel model for the study of hair follicle morphogenesis. Department of Biomedical Sciences. Bradford, PhD thesis, Department of Biomedical Sciences, University of Bradford. **PhD:** 225.

Croft, N. J. and V. A. Randall (2003). The antler of the red deer (Cervus elaphus): an androgen target organ. Hair Science and Technology D. Van Neste**:** 69-74.

Cushman, S. W. and L. J. Wardzala (1980). "Potential mechanism of insulin action on glucose transport in the isolated rat adipose cell. Apparent translocation of intracellular transport systems to the plasma membrane." J Biol Chem **255**(10): 4758-62.

D'Hahan, N., H. Jacquet, C. Moreau, P. Catty and M. Vivaudou (1999). "A transmembrane domain of the sulfonylurea receptor mediates activation of ATP-sensitive K(+) channels by K(+) channel openers." Mol Pharmacol **56**(2): 308-15.

D'Hahan, N., C. Moreau, A. L. Prost, H. Jacquet, A. E. Alekseev, A. Terzic and M. Vivaudou (1999). "Pharmacological plasticity of cardiac ATP-sensitive potassium channels toward diazoxide revealed by ADP." Proc Natl Acad Sci U S A **96**(21): 12162-7.

Dabrowski, M., F. M. Ashcroft, R. Ashfield, P. Lebrun, B. Pirotte, J. Egebjerg, J. Bondo Hansen and P. Wahl (2002). "The novel diazoxide analog 3-isopropylamino-7-methoxy-4H-1,2,4-benzothiadiazine 1,1-dioxide is a selective Kir6.2/SUR1 channel opener." Diabetes **51**(6): 1896-906.

Davies, G. C. (2001). *In vivo* and *in vitro* models of hair growth for the assessment of potassium channel openers. Department of Biomedical Sciences. Bradford, University of Bradford. **PhD thesis:** 297.

Davies, G. C., M. J. Thornton, T. J. Jenner, Y. J. Chen, J. B. Hansen, R. D. Carr and V. A. Randall (2005). "Novel and established potassium channel openers stimulate

hair growth in vitro: implications for their modes of action in hair follicles." J Invest Dermatol **124**(4): 686-94.

Dawber, R. (2000). Update on minoxidil treatment of hair loss. Hair and its disorders: Biology, research and management. F. M. Camacho, Randall, V.A., and Price, V.H. London, Martin Dunitz**:** 169-173.

Ding, W. G., L. P. He, M. Omatsu-Kanbe and H. Kitasato (1996). "A possible role of the ATP-sensitive potassium ion channel in determining the duration of spike-bursts in mouse pancreatic beta-cells." Biochim Biophys Acta **1279**(2): 219-26.

Doyle, D. A., J. Morais Cabral, R. A. Pfuetzner, A. Kuo, J. M. Gulbris, S. L. Cohen, B. T. Chait and R. MacKinnon (1998). "The structure of the potassium channel: molecular basis of K$^+$ conduction and selectivity." Science **280**(5360): 69-77.

Droge, W. (2005). "Oxidative stress and ageing: is ageing a cysteine deficiency syndrome?" Philos Trans R Soc Lond B Biol Sci **360**(1464): 2355-72.

Dry, F. W. (1926). "The coat of the mouse (*Mus Musculus*)." Journal of Genetics **16**: 287-340.

Duvic, M., N. A. Lemak, V. Valero, S. R. Hymes, K. L. Farmer, G. N. Hortobagyi, R. J. Trancik, B. A. Bandstra and L. D. Compton (1996). "A randomized trial of minoxidil in chemotherapy-induced alopecia." J Am Acad Dermatol **35**(1): 74-8.

Ebling, F. J. G. (1985). "The mythological evolution of nudity." Journal of Human Evolution **14**: 33-41.

Edman, P. (1949). "method for the determination of the amino acid sequence of peptides." Arch. Biochem. Biophys **22**: 475-483.

Eisele, L. E., K. J. Chave, A. C. Lehning and T. J. Ryan (2006). "Characterization of Human gamma-glutamyl hydrolase in solution demonstrates that the enzyme is a non-dissociating homodimer." Biochim Biophys Acta **1764**(9): 1479-86.

Elliott, K., T. J. Stephenson and A. G. Messenger (1999). "Differences in hair follicle dermal papilla volume are due to extracellular matrix volume and cell number: implications for the control of hair follicle size and androgen responses." J Invest Dermatol **113**(6): 873-7.

Epstein, E. (2001). "Evidence-based treatment of alopecia areata." J Am Acad Dermatol **45**(4): 640-2.

Faivre, J. F. and I. Findlay (1990). "Action potential duration and activation of ATP-sensitive potassium current in isolated guinea-pig ventricular myocytes." Biochim Biophys Acta **1029**(1): 167-72.

Fiddes, J. C., F. Sanger, G. M. Air, B. G. Barrell, N. L. Brown, A. R. Coulson, C. A. Hutchison, P. M. Slocombe and M. Smith (1977). "Nucleotide-sequence of

bacteriophage OX174 DNA." Journal of Supramolecular Structure. Suppl **1**: 57-57.

Field, A. P. (2009). Discovering statistics using SPSS : (and sex and drugs and rock 'n' roll). London, SAGE.

Field, A. P. and G. Hole (2003). How to design and report experiments. London ; Thousand Oaks, Calif., Sage publications Ltd.

Flux, J. E. C. (1970). "Colour change of mountain hares (Lepus timidus scotius) in north-east Scotland." Zoology **162**: 345-58.

Forslind, B. (2000). Structure and function of the hair follicle. Hair and its disorders: biology, pathology and management. F. M. Camacho, Randall, V.A., and Price, V.H., Martin Dunitz Ltd**:** 3-15.

Franklin, R. A. and J. A. McCubrey (2000). "Kinases: positive and negative regulators of apoptosis." Leukemia **14**(12): 2019-34.

Franks, S. (1989). "Polycystic ovary syndrome: a changing perspective (review)." Clin Endocrinol (Oxf) **31**(1): 87-120.

Frater, R. and P. G. Whitmore (1973). "In vitro growth of postembryonic hair." J Invest Dermatol **61**(2): 72-81.

Fujita, A. and Y. Kurachi (2000). "Molecular aspects of ATP-sensitive K+ channels in the cardiovascular system and K+ channel openers." Pharmacol Ther **85**(1): 39-53.

Gier, B., P. Krippeit-Drews, T. Sheiko, L. Aguilar-Bryan, J. Bryan, M. Dufer and G. Drews (2009). "Suppression of KATP channel activity protects murine pancreatic beta cells against oxidative stress." J Clin Invest **119**(11): 3246-56.

Gilhar, A., Y. Ullmann, T. Berkutzki, B. Assy and R. S. Kalish (1998). "Autoimmune hair loss (alopecia areata) transferred by T lymphocytes to human scalp explants on SCID mice." J Clin Invest **101**(1): 62-7.

Girard, C. A., F. T. Wunderlich, K. Shimomura, S. Collins, S. Kaizik, P. Proks, F. Abdulkader, A. Clark, V. Ball, L. Zubcevic, L. Bentley, R. Clark, C. Church, A. Hugill, J. Galvanovskis, R. Cox, P. Rorsman, J. C. Bruning and F. M. Ashcroft (2009). "Expression of an activating mutation in the gene encoding the KATP channel subunit Kir6.2 in mouse pancreatic beta cells recapitulates neonatal diabetes." J Clin Invest **119**(1): 80-90.

Girman, C. J., T. Rhodes, F. R. Lilly, S. S. Guo, R. M. Siervogel, D. L. Patrick and W. C. Chumlea (1998). "Effects of self-perceived hair loss in a community sample of men." Dermatology **197**(3): 223-9.

Gobom, J., M. Schuerenberg, M. Mueller, D. Theiss, H. Lehrach and E. Nordhoff (2001). "Alpha-cyano-4-hydroxycinnamic acid affinity sample preparation. A protocol for MALDI-MS peptide analysis in proteomics." Anal Chem **73**(3): 434-8.

Godbout, R. and J. Squire (1993). "Amplification of a DEAD box protein gene in retinoblastoma cell lines." Proc Natl Acad Sci U S A **90**(16): 7578-82.
Goldberg, M. R. (1988). "Clinical pharmacology of pinacidil, a prototype for drugs that affect potassium channels." J Cardiovasc Pharmacol **12 Suppl 2**: S41-7.

Goodhart, C. B. (1960). "The evolutionary significance of human hair patterns and skin colouring." Advancement of Science **17**: 53-58.

Granai, C. O., H. Frederickson, W. Gajewski, A. Goodman, A. Goldstein and H. Baden (1991). "The use of minoxidil to attempt to prevent alopecia during chemotherapy for gynecologic malignancies." Eur J Gynaecol Oncol **12**(2): 129-32.

Gribble, F. M., R. Ashfield, C. Ammala and F. M. Ashcroft (1997). "Properties of cloned ATP-sensitive K+ currents expressed in Xenopus oocytes." J Physiol **498 (Pt 1)**: 87-98.

Gribble, F. M. and F. Reimann (2003). "Sulphonylurea action revisited: the post-cloning era." Diabetologia **46**(7): 875-91.

Gribble, F. M., S. J. Tucker, S. Seino and F. M. Ashcroft (1998). "Tissue specificity of sulphonylureas:studies on cloned cardiac and beta-cell K_{ATP} channels." Diabetes **47**(9): 1412-1418.

Gulec, A. T., N. Tanriverdi, C. Duru, Y. Saray and C. Akcali (2004). "The role of psychological factors in alopecia areata and the impact of the disease on the quality of life." Int J Dermatol **43**(5): 352-6.

Haider, S., J. F. Antcliff, P. Proks, M. S. Sansom and F. M. Ashcroft (2005). "Focus on Kir6.2: a key component of the ATP-sensitive potassium channel." J Mol Cell Cardiol **38**(6): 927-36.

Hamada, K. and V. A. Randall (2006). "Inhibitory autocrine factors produced by the mesenchyme-derived hair follicle dermal papilla may be a key to male pattern baldness." Br J Dermatol **154**(4): 609-18.

Hambrock, A., C. Loffler-Walz, U. Russ, U. Lange and U. Quast (2001). "Characterization of a mutant sulfonylurea receptor SUR2B with high affinity for sulfonylureas and openers: differences in the coupling to Kir6.x subtypes." Mol Pharmacol **60**(1): 190-9.

Hamilton, J. B. (1942). "Male hormone stimulation is a prerequisite and an incitant in common baldness." Am J Anat **71**: 451-481.

Hamilton, J. B. (1951). "Patterned loss of hair in man; types and incidence." Ann N Y Acad Sci **53**(3): 708-28.

Hamilton, J. B. (1958). Age, sex, and genetic factors in the regulation of hair growth in man: a comparison of Caucasian and Japanese populations. The biology of hair growth. W. Montagna, and Ellis, R.A., Academic Press, New York**:** 399-433.

Hamilton, J. B. (1960). "Effect of castration in adolescent and young adult males upon further changes in the proportions of bare and hairy scalp." J Clin Endocrinol Metab **20**: 1309-18.

Hammerstein, J. (1987). Cyproterone acetate-the European experience. In The cause and management of hirsutism : a practical approach to the control of unwanted hair. Carnforth, UK, Parthenon Publishing Group.

Han, J. H., O. S. Kwon, J. H. Chung, K. H. Cho, H. C. Eun and K. H. Kim (2004). "Effect of minoxidil on proliferation and apoptosis in dermal papilla cells of human hair follicle." J Dermatol Sci **34**(2): 91-8.

Hardy, M. H. (1992). "The secret life of the hair follicle." Trends Genet **8**(2): 55-61.

Heine, U., E. F. Munoz, K. C. Flanders, L. R. Ellingsworth, H. Y. Lam, N. L. Thompson, A. B. Roberts and M. B. Sporn (1987). "Role of transforming growth factor-beta in the development of the mouse embryo." J Cell Biol **105**(6 Pt 2): 2861-76.

Henriet, P., Z. D. Zhong, P. C. Brooks, K. I. Weinberg and Y. A. DeClerck (2000). "Contact with fibrillar collagen inhibits melanoma cell proliferation by up-regulating p27KIP1." Proc Natl Acad Sci U S A **97**(18): 10026-31.

Hibberts, N. A., Kato, S., Messenger, A.G., and Randall, V.A. (1996). "Dermal papilla cells from human hair follicles secrete factors (e.g. VEGF) mitogenic for endothelial cells." J Invest Dermatol **106**: 862.

Hibberts, N. A., A. G. Messenger and V. A. Randall (1996). "Dermal papilla cells derived from beard hair follicles secrete more stem cell factor (SCF) in culture than scalp cells or dermal fibroblasts." Biochem Biophys Res Commun **222**(2): 401-5.

Higgins, C. A., G. E. Westgate and C. A. B. Jahoda (2009). "From Telogen to Exogen: Mechanisms Underlying Formation and Subsequent Loss of the Hair Club Fiber." J Invest Dermatol **129**(9): 2100-2108.

Hoffmann, R., W. Eicheler, A. Huth, E. Wenzel and R. Happle (1996). "Cytokines and growth factors influence hair growth in vitro. Possible implications for the pathogenesis and treatment of alopecia areata." Arch Dermatol Res **288**(3): 153-6.

Holbrook, K. A. and S. I. Minami (1991). "Hair follicle embryogenesis in the human. Characterization of events in vivo and in vitro." Ann N Y Acad Sci **642**: 167-96.

Hordinsky, M. K. (2003). Alopecia areata. Disorders of hair growth: Diagnosis and treatment. E. A. Olsen, McGraw-Hill**: 239-274.

Hurley, H. J. (2001). The eccrine sweat glands: Structure and function. The biology of the skin. R. K. Freinkel, and Woodley, D.T., The Parthenon Publishing Group**: 47-76.

Ibrahim, L. and E. A. Wright (1982). "A quantitative study of hair growth using mouse and rat vibrissal follicles. I. Dermal papilla volume determines hair volume." J Embryol Exp Morphol **72**: 209-24.

Iino, M., R. Ehama, Y. Nakazawa, T. Iwabuchi, M. Ogo, M. Tajima and S. Arase (2007). "Adenosine Stimulates Fibroblast Growth Factor-7 Gene Expression Via Adenosine A2b Receptor Signaling in Dermal Papilla Cells." J Invest Dermatol.

Inagaki, N., T. Gonoi, J. P. Clement, N. Namba, J. Inazawa, G. Gonzalez and L. Aguilar-Bryan (1995). "Reconstitution of I_{KATP}: an inward rectifier subunit plus the sulfonylurea receptor." Science **270**(5239): 1166-1170.

Inagaki, N., T. Gonoi, J. P. Clement, C. Z. Wang, L. Aguilar-Bryan, J. Bryan and S. Seino (1996). "A family of sulfonylurea receptors determines the pharmacological properties of ATP-sensitive K^+ channels." Neuron **16**(5): 1011-1017.

Inagaki, N., T. Gonoi and S. Seino (1997). "Subunit stoichiometry of the pancreatic beta-cell ATP-sensitive K+ channel." FEBS Lett **409**(2): 232-6.

Inagaki, N., J. Inazawa and S. Seino (1995). "cDNA sequence, gene structure, and chromosomal localization of the human ATP-sensitive potassium channel, uKATP-1 gene (KCNJ8)." Genomics **30**(1): 102-104.

Inagaki, N., Y. Tsuura, N. Namba, K. Masuda, T. Gonoi, M. Horie, Y. Seino, T. Mizuta and S. Seino (1995). "Cloning and functional characterization of a novel ATP-sensitive potassium channel ubiquitously expressed in rat tissues, including pancreatic islets, pituitary, skeletal muscle, and heart." J Biol Chem **270**(11): 5691-5694.

Inoue, I., H. Nagase, K. Kishi and T. Higuti (1991). "ATP-sensitive K^+ channel in the mitochondrial inner membrane." Nature **352**: 244-247.

Inui, S., Y. Fukuzato, T. Nakajima, K. Yoshikawa and S. Itami (2002). "Androgen-inducible TGF-beta1 from balding dermal papilla cells inhibits epithelial cell growth: a clue to understand paradoxical effects of androgen on human hair growth." Faseb J **16**(14): 1967-9.

Inui, S., Y. Fukuzato, T. Nakajima, K. Yoshikawa and S. Itami (2003). "Identification of androgen-inducible TGF-beta1 derived from dermal papilla cells as a key mediator in androgenetic alopecia." J Investig Dermatol Symp Proc **8**(1): 69-71.

Irwin, R. S. and J. M. Rippe (2008). Irwin and Rippe's intensive care medicine. Philadelphia, Pa. ; London, Lippincott Williams & Wilkins.

Isomoto, S., C. Kondo, M. Yamada, S. Matsumoto, O. Higashiguchi, Y. Horio, Y. Matsuzawa and Y. Kurachi (1996). "A novel sulfonylurea receptor forms with BIR (Kir6.2) a smooth muscle type ATP-sensitive K$^+$ channel." J Biol Chem **271**(40): 24321-24324.

Jahangir, A. and A. Terzic (2005). "K(ATP) channel therapeutics at the bedside." J Mol Cell Cardiol **39**(1): 99-112.

Jahoda, C. and R. F. Oliver (1981). "The growth of vibrissa dermal papilla cells in vitro." Br J Dermatol **105**(6): 623-7.

Jahoda, C. A., K. A. Horne and R. F. Oliver (1984). "Induction of hair growth by implantation of cultured dermal papilla cells." Nature **311**(5986): 560-2.

Jahoda, C. A. and A. J. Reynolds (1996). "Dermal-epidermal interactions. Adult follicle-derived cell populations and hair growth." Dermatol Clin **14**(4): 573-83.

Jansen, V. A. A. and M. van Baalen (2006). "Altruism through beard chromodynamics." Nature **440**(7084): 663-6.

Johnstone, M. A. and D. M. Albert (2002). "Prostaglandin-induced hair growth." Surv Ophthalmol **47 Suppl 1**: S185-202.

Kamen, B. (1997). "Folate and antifolate pharmacology." Semin Oncol **24**(5 Suppl 18): S18-30-S18-39.

Karas, M., D. Bachmann, U. Bahr and F. Hillenkamp (1987). "Matrix-assisted ultraviolet laser desorption of non-volatile compounds." International Journal of Mass Spectrometry and Ion Processes **78**: 53-68.

Katsuoka, K., C. Mauch, H. Schell, O. P. Hornstein and T. Krieg (1988). "Collagen-type synthesis in human-hair papilla cells in culture." Arch Dermatol Res **280**(3): 140-4.

Katsuoka, K., H. Schell, O. P. Hornstein and B. Wessel (1987). "Epidermal growth factor and fibroblast growth factor accelerate proliferation of human hair bulb papilla cells and root sheath fibroblasts cultured in vitro." Br J Dermatol **116**(3): 464-5.

Kaufman, K. D., E. A. Olsen, D. Whiting, R. Savin, R. DeVillez, W. Bergfeld, V. H. Price, D. Van Neste, J. L. Roberts, M. Hordinsky, J. Shapiro, B. Binkowitz and G. J.

Gormley (1998). "Finasteride in the treatment of men with androgenetic alopecia. Finasteride Male Pattern Hair Loss Study Group." J Am Acad Dermatol **39**(4 Pt 1): 578-89.

Kawasaki, E. S. (1990). Amplification of RNA. PCR protocols: A guide to methods and applications. Innis, New York: Academic Press: 21-27.

Kligman, A. M. (1959). "The human hair cycle." J Invest Dermatol **33**: 307-16.

Kligman, A. M. (1959). "Neogenesis of human hair follicles." Ann N Y Acad Sci **83**: 507-11.

Ko, L., G. R. Cardona and W. W. Chin (2000). "Thyroid hormone receptor-binding protein, an LXXLL motif-containing protein, functions as a general coactivator." Proc Natl Acad Sci U S A **97**(11): 6212-7.

Koblenzer, P. J. and L. Baker (1968). "Hypertrichosis lanuginosa associated with diazoxide therapy in prepubertal children: a clinicopathologic study." Ann N Y Acad Sci **150**(2): 373-82.

Kollar, E. J. (1966). "An in vitro study of hair and vibrissae development in embryonic mouse skin." J Invest Dermatol **46**(3): 254-62.

Kondo, S., Y. Hozumi and K. Aso (1990). "Organ culture of human scalp hair follicles: effect of testosterone and oestrogen on hair growth." Arch Dermatol Res **282**(7): 442-5.

Kurata, S., H. Uno and B. L. Allen-Hoffmann (1996). "Effects of hypertrichotic agents on follicular and nonfollicular cells in vitro." Skin Pharmacol **9**(1): 3-8.

Kwon, O. S., J. K. Oh, M. H. Kim, S. H. Park, H. K. Pyo, K. H. Kim, K. H. Cho and H. C. Eun (2006). "Human hair growth ex vivo is correlated with in vivo hair growth: selective categorization of hair follicles for more reliable hair follicle organ culture." Arch Dermatol Res **297**(8): 367-71.

Lachgar, S., M. Charveron, N. Bouhaddioui, Y. Neveux, Y. Gall and J. L. Bonafe (1996). "Inhibitory effects of bFGF, VEGF and minoxidil on collagen synthesis by cultured hair dermal papilla cells." Arch Dermatol Res **288**(8): 469-73.

Lachgar, S., M. Charveron, Y. Gall and J. L. Bonafe (1998). "Minoxidil upregulates the expression of vascular endothelial growth factor in human hair dermal papilla cells." Br J Dermatol **138**(3): 407-11.

Lachgar, S., H. Moukadiri, F. Jonca, M. Charveron, N. Bouhaddioui, Y. Gall, J. L. Bonafe and J. Plouet (1996). "Vascular endothelial growth factor is an autocrine growth factor for hair dermal papilla cells." J Invest Dermatol **106**(1): 17-23.

Lamarca, V., A. Sanz-Clemente, R. Perez-Pe, M. J. Martinez-Lorenzo, N. Halaihel, P. Muniesa and J. A. Carrodeguas (2007). "Two isoforms of PSAP/MTCH1 share

two proapoptotic domains and multiple internal signals for import into the mitochondrial outer membrane." Am J Physiol Cell Physiol **293**(4): C1347-61.

Lawson, K. (2000). "Potassium channel openers as potential therapeutic weapons in ion channel disease." Kidney Int **57**(3): 838-45.

Lefrancois-Martinez, A. M., J. Bertherat, P. Val, C. Tournaire, N. Gallo-Payet, D. Hyndman, G. Veyssiere, X. Bertagna, C. Jean and A. Martinez (2004). "Decreased expression of cyclic adenosine monophosphate-regulated aldose reductase (AKR1B1) is associated with malignancy in human sporadic adrenocortical tumors." J Clin Endocrinol Metab **89**(6): 3010-9.

Leney, S. E. and J. M. Tavare (2009). "The molecular basis of insulin-stimulated glucose uptake: signalling, trafficking and potential drug targets." J Endocrinol **203**(1): 1-18.

Li, M., A. Marubayashi, Y. Nakaya, K. Fukui and S. Arase (2001). "Minoxidil-induced hair growth is mediated by adenosine in cultured dermal papilla cells: possible involvement of sulfonylurea receptor 2B as a target of minoxidil." J Invest Dermatol **117**(6): 1594-600.

Limas, C. J. and E. D. Freis (1973). "Minoxidil in severe hypertension with renal failure. Effect of its addition to conventional antihypertensive drugs." Am J Cardiol **31**(3): 355-61.

Lincoln, G. A. and R. N. B. Kay (1971). "The seasonal reproductive changes in the red deer stag (Cervus elaphus). ." Journal of Zoology **163**: 105-123.

Lucky, A. W., D. J. Piacquadio, C. M. Ditre, F. Dunlap, I. Kantor, A. G. Pandya, R. C. Savin and M. D. Tharp (2004). "A randomized, placebo-controlled trial of 5% and 2% topical minoxidil solutions in the treatment of female pattern hair loss." J Am Acad Dermatol **50**(4): 541-53.

Ludwig, E. (1977). "Classification of the types of androgenetic alopecia (common baldness) occurring in the female sex." Br J Dermatol **97**(3): 247-54.

Lyubimova, A., J. J. Garber, G. Upadhyay, A. Sharov, F. Anastasoaie, V. Yajnik, G. Cotsarelis, G. P. Dotto, V. Botchkarev and S. B. Snapper (2010). "Neural Wiskott-Aldrich syndrome protein modulates Wnt signaling and is required for hair follicle cycling in mice." J Clin Invest **120**(2): 446-56.

Madani, S. and J. Shapiro (2000). "Alopecia areata update." J Am Acad Dermatol **42**(4): 549-66.

Magerl, M., R. Paus, N. Farjo, S. Muller-Rover, E. M. Peters, K. Foitzik and D. J. Tobin (2004). "Limitations of human occipital scalp hair follicle organ culture for studying the effects of minoxidil as a hair growth enhancer." Exp Dermatol **13**(10): 635-42.

Marshall, W. A. and J. M. Tanner (1969). "Variations in pattern of pubertal changes in girls." <u>Arch Dis Child</u> **44**(235): 291-303.

Marshall, W. A. and J. M. Tanner (1970). "Variations in the pattern of pubertal changes in boys." <u>Arch Dis Child</u> **45**(239): 13-23.

Martin, K. A., R. J. Chang, D. A. Ehrmann, L. Ibanez, R. A. Lobo, R. L. Rosenfield, J. Shapiro, V. M. Montori and B. A. Swiglo (2008). "Evaluation and treatment of hirsutism in premenopausal women: an endocrine society clinical practice guideline." <u>J Clin Endocrinol Metab</u> **93**(4): 1105-20.

Martin, S. A., R. S. Rosenthal and K. Biemann (1987). "Fast atom bombardment mass spectrometry and tandem mass spectrometry of biologically active peptidoglycan monomers from Neisseria gonorrhoeae." <u>J Biol Chem</u> **262**(16): 7514-22.

McPherson, M. J. and S. G. Møller (2000). <u>PCR</u>. A. Bosher, BIOS Scientific Publishers Ltd.

Mehta, P. K., B. Mamdani, R. M. Shansky, S. D. Mahurkar and G. Dunea (1975). "Severe hypertension. Treatment with minoxidil." <u>Jama</u> **233**(3): 249-52.

Meisheri, K. D., G. A. Johnson and L. Puddington (1993). "Enzymatic and non-enzymatic sulfation mechanisms in the biological actions of minoxidil." <u>Biochem Pharmacol</u> **45**(2): 271-9.

Merrick, A. E., Hibberts, N.A., Kato, S., Messenger, A.G., Thornton, M.J., and Randall, V.A. (1999). "Both beard and scalp cultured dermal papilla cells express mRNA for, and secrete, VEGF but the levels are unaltered by testosterone *in vitro*." <u>J Invest Dermatol Sym Proc</u> **4**: 352.

Messenger, A. G. (1993). "The control of hair growth: an overview." <u>J Invest Dermatol</u> **101**(1 Suppl): 4S-9S.

Messenger, A. G., K. Elliott, A. Temple and V. A. Randall (1991). "Expression of basement membrane proteins and interstitial collagens in dermal papillae of human hair follicles." <u>J Invest Dermatol</u> **96**(1): 93-7.

Messenger, A. G. and J. Rundegren (2004). "Minoxidil: mechanisms of action on hair growth." <u>Br J Dermatol</u> **150**(2): 186-94.

Messenger, A. G. and N. B. Simpson (1997). Alopecia areata. <u>Diseases of the hair and scalp</u>. R. Dawber, Blackwell Science Ltd**:** 338-369.

Michelet, J. F., S. Commo, N. Billoni, Y. F. Mahe and B. A. Bernard (1997). "Activation of cytoprotective prostaglandin synthase-1 by minoxidil as a possible explanation for its hair growth-stimulating effect." <u>J Invest Dermatol</u> **108**(2): 205-9.

Milner, Y., J. Sudnik, M. Filippi, M. Kizoulis, M. Kashgarian and K. Stenn (2002). "Exogen, shedding phase of the hair growth cycle: characterization of a mouse model." J Invest Dermatol **119**(3): 639-44.

Montagna, W. and E. J. Van Scott (1958). The anatomy of the hair follicle. The biology of hair growth. W. Montagna, and Ellis, R.A., Academic Press, New York**:** 39-64.

Mosmann, T. (1983). "Rapid colorimetric assay for cellular growth and survival: application to proliferation and cytotoxicity assays." J Immunol Methods **65**(1-2): 55-63.

Muller, M., J. R. Jasmin, R. A. Monteil and R. Loubiere (1991). "Embryology of the hair follicle." Early Hum Dev **26**(3): 159-66.

Muller, S. A. and R. K. Winkelmann (1963). "Alopecia Areata. an Evaluation of 736 Patients." Arch Dermatol **88**: 290-7.

Myers, R. J. and J. B. Hamilton (1951). "Regeneration and rate of growth of hairs in man." Ann N Y Acad Sci **53**(3): 562-8.

Nesvizhskii, A. I. and R. Aebersold (2004). "Analysis, statistical validation and dissemination of large-scale proteomics datasets generated by tandem MS." Drug Discov Today **9**(4): 173-81.

Nichols, C. G. (2006). "K_{ATP} channels as molecular sensors of cellular metabolism." Nature **440**(7083): 470-6.

Nixon, A. J. (1993). "A method for determining the activity state of hair follicles." Biotech Histochem **68**(6): 316-25.

Noma, A. (1983). "ATP-regulated K^+ channel in cardiac muscle." Nature **305**: 147-148.

Norwood, O. T. (1975). "Male pattern baldness: classification and incidence." South Med J **68**(11): 1359-65.

Nutbrown, M. and V. A. Randall (1995). "Differences between connective tissue-epithelial junctions in human skin and the anagen hair follicle." J Invest Dermatol **104**(1): 90-4.

Nutbrown, M. and V. A. Randall (1996). Recognition of cellular differentiation in the human hair follicle at the light microscope level using SACPIC staining. Hair research for the next millenium. D. J. J. Van Neste, and Randall, V.A. , Elsevier Science B.V.**:** 161-166.

O'Farrell, P. H. (1975). "High resolution two-dimensional electrophoresis of proteins." J Biol Chem **250**(10): 4007-21.

Obana, N., C. Chang and H. Uno (1997). "Inhibition of hair growth by testosterone in the presence of dermal papilla cells from the frontal bald scalp of the postpubertal stumptailed macaque." Endocrinology **138**(1): 356-61.

Oliver, R. F. and C. A. B. Jahoda (1989). The dermal papilla and maintenance of hair growth. The biology of wool and hair. G. E. Rogers, Reis, P.J., Ward, K.A. and Marshall, R.C., Chapman & Hall, London**:** 51-67.

Olsen, E. A., E. R. DeLong and M. S. Weiner (1987). "Long-term follow-up of men with male pattern baldness treated with topical minoxidil." J Am Acad Dermatol **16**(3 Pt 2): 688-95.

Olsen, E. A., F. E. Dunlap, T. Funicella, J. A. Koperski, J. M. Swinehart, E. H. Tschen and R. J. Trancik (2002). "A randomized clinical trial of 5% topical minoxidil versus 2% topical minoxidil and placebo in the treatment of androgenetic alopecia in men." J Am Acad Dermatol **47**(3): 377-85.

Olsen, E. A. and M. S. Weiner (1987). "Topical minoxidil in male pattern baldness: effects of discontinuation of treatment." J Am Acad Dermatol **17**(1): 97-101.

Olsen, E. A., M. S. Weiner, I. A. Amara and E. R. DeLong (1990). "Five-year follow-up of men with androgenetic alopecia treated with topical minoxidil." J Am Acad Dermatol **22**(4): 643-6.

Olsen, E. A., M. S. Weiner, E. R. Delong and S. R. Pinnell (1985). "Topical minoxidil in early male pattern baldness." J Am Acad Dermatol **13**(2 Pt 1): 185-92.

Orentreich, N. (1969). "Scalp hair replacement in man: In: Montagna W, Dobson RL, editors. Hair Growth." Advances in Biology of Skin. **9**: 99-108.

Orentreich, N. and N. P. Durr (1982). "Biology of scalp hair growth." Clin Plast Surg **9**(2): 197-205.

Otomo, S. (2002). "[Hair growth effect of minoxidil]." Nippon Yakurigaku Zasshi **119**(3): 167-74.

Otsubo, T., K. Iwaya, Y. Mukai, Y. Mizokami, H. Serizawa, T. Matsuoka and K. Mukai (2004). "Involvement of Arp2/3 complex in the process of colorectal carcinogenesis." Mod Pathol **17**(4): 461-7.

Otterbein, L. E., F. H. Bach, J. Alam, M. Soares, H. Tao Lu, M. Wysk, R. J. Davis, R. A. Flavell and A. M. Choi (2000). "Carbon monoxide has anti-inflammatory effects involving the mitogen-activated protein kinase pathway." Nat Med **6**(4): 422-8.

Papadopoulos, A. J., R. A. Schwartz and C. K. Janniger (2000). "Alopecia areata. Pathogenesis, diagnosis, and therapy." Am J Clin Dermatol **1**(2): 101-5.

Paus, R. and G. Cotsarelis (1999). "The biology of hair follicles." N Engl J Med **341**(7): 491-7.

Paus, R., S. Muller-Rover, C. Van Der Veen, M. Maurer, S. Eichmuller, G. Ling, U. Hofmann, K. Foitzik, L. Mecklenburg and B. Handjiski (1999). "A comprehensive guide for the recognition and classification of distinct stages of hair follicle morphogenesis." J Invest Dermatol **113**(4): 523-32.

Philpott, M. (2000). The roles of growth factors in hair follicles: investigations using cultured hair follicles. Hair and its disorders: biology, pathology and management. F. M. Camacho, Randall, V.A., and Price, V.H., Martin Dunitz, London**:** 103-113.

Philpott, M., M. R. Green and T. Kealey (1989). "Studies on the biochemistry and morphology of freshly isolated and maintained rat hair follicles." J Cell Sci **93 (Pt 3)**: 409-18.

Philpott, M. P., M. R. Green and T. Kealey (1990). "Human hair growth in vitro." J Cell Sci **97 (Pt 3)**: 463-71.

Philpott, M. P., D. A. Sanders and T. Kealey (1994). "Effects of insulin and insulin-like growth factors on cultured human hair follicles: IGF-I at physiologic concentrations is an important regulator of hair follicle growth in vitro." J Invest Dermatol **102**(6): 857-61.

Philpott, M. P., D. A. Sanders and T. Kealey (1996). "Whole hair follicle culture." Dermatol Clin **14**(4): 595-607.

Philpott, M. P., G. E. Westgate and T. Kealey (1991). "An in vitro model for the study of human hair growth." Ann N Y Acad Sci **642**: 148-64; discussion 164-6.

Pierard, G. E. and M. de la Brassinne (1975). "Modulation of dermal cell activity during hair growth in the rat." J Cutan Pathol **2**(1): 35-41.

Pinkus, H. (1958). Embryology of hair. The biology of hair growth. W. Montagna, and Ellis, R.A., Academic Press, New York**:** 1-32.

Price, V. H. (2003). "Androgenetic alopecia in women." J Investig Dermatol Symp Proc **8**(1): 24-7.

Price, V. H. and E. Menefee (1996). Quantitative estimation of hair growth: comparative changes in weight and hair count with 5% and 2% minoxidil, placebo and no treatment. Hair research for the next Millenium. Proceedings of the 1st Tricontinental Meeting of Hair Research Societies, Brussels. D. Van Neste and V. A. Randall. Amsterdam, Elsevier Science BV**:** 67-71.

Price, V. H., E. Menefee and P. C. Strauss (1999). "Changes in hair weight and hair count in men with androgenetic alopecia, after application of 5% and 2%

topical minoxidil, placebo, or no treatment." J Am Acad Dermatol **41**(5 Pt 1): 717-21.

Quayle, J. M., M. T. Nelson and N. B. Standen (1997). "ATP-sensitive and inwardly rectifying potassium channels in smooth muscle." Physiol Rev **77**(4): 1165-232.

Randall, V. A. (1994). "Androgens and human hair growth." Clin Endocrinol (Oxf) **40**(4): 439-57.

Randall, V. A. (2001). "Is alopecia areata an autoimmune disease?" Lancet **358**(9297): 1922-4.

Randall, V. A. (2004). Androgens and hair: a biological paradox. Testosterone: action, deficiency, substitution. E. Nieschlag, and Behre, H.M., Cambridge University Press**:** 207-231.

Randall, V. A. (2005). Physiology and pathophysiology of androgenetic alopecia. Endocrinology. L. J. Degroot, and Jameson, J.L. Philadelphia, W B Saunders Co.**:** 3295-3309

Randall, V. A. (2007). "Hormonal regulation of hair follicles exhibits a biological paradox." Semin Cell Dev Biol.

Randall, V. A. (2008). "Androgens and hair growth." Dermatol Ther **21**(5): 314-28.

Randall, V. A. and F. J. Ebling (1991). "Seasonal changes in human hair growth." Br J Dermatol **124**(2): 146-51.

Randall, V. A., N. A. Hibberts, M. J. Thornton, K. Hamada, A. E. Merrick, S. Kato, T. J. Jenner, I. De Oliveira and A. G. Messenger (2000). "The hair follicle: a paradoxical androgen target organ." Horm Res **54**(5-6): 243-50.

Randall, V. A., J. P. Sundberg and M. P. Philpott (2003). "Animal and in vitro models for the study of hair follicles." J Investig Dermatol Symp Proc **8**(1): 39-45.

Randall, V. A., M. J. Thornton, K. Hamada, C. P. Redfern, M. Nutbrown, F. J. Ebling and A. G. Messenger (1991). "Androgens and the hair follicle. Cultured human dermal papilla cells as a model system." Ann N Y Acad Sci **642**: 355-75.

Rappsilber, J. and M. Mann (2002). "What does it mean to identify a protein in proteomics?" Trends Biochem Sci **27**(2): 74-8.

Reimann, F., P. Proks and F. M. Ashcroft (2001). "Effects of mitiglinide (S 21403) on Kir6.2/SUR1, Kir6.2/SUR2A and Kir6.2/SUR2B types of ATP-sensitive potassium channel." Br J Pharmacol **132**(7): 1542-8.

Rendl, M., L. Lewis and E. Fuchs (2005). "Molecular dissection of mesenchymal-epithelial interactions in the hair follicle." PLoS Biol **3**(11): e331.

Reynolds, A. J. and C. A. Jahoda (1991). "Hair follicle stem cells? A distinct germinative epidermal cell population is activated in vitro by the presence of hair dermal papilla cells." J Cell Sci **99 (Pt 2)**: 373-85.

Reynolds, A. J. and C. A. Jahoda (1991). "Inductive properties of hair follicle cells." Ann N Y Acad Sci **642**: 226-41; discussion 241-2.

Reynolds, E. L. (1951). "The appearance of adult patterns of body hair in man." Ann N Y Acad Sci **53**(3): 576-84.

Richardson, G. D., E. C. Arnott, C. J. Whitehouse, C. M. Lawrence, A. J. Reynolds, N. Hole and C. A. Jahoda (2005). "Plasticity of rodent and human hair follicle dermal cells: implications for cell therapy and tissue engineering." J Investig Dermatol Symp Proc **10**(3): 180-3.

Roepstorff, P. and J. Fohlman (1984). "Proposal for a common nomenclature for sequence ions in mass spectra of peptides." Biomed Mass Spectrom **11**(11): 601.

Rorsman, P. and G. Trube (1985). "Glucose dependent K+-channels in pancreatic beta-cells are regulated by intracellular ATP." Pflugers Arch **405**(4): 305-9.

Ross, E. K. and J. Shapiro (2005). "Management of hair loss." Dermatol Clin **23**(2): 227-43.

Rushan, X., H. Fei, M. Zhirong and W. Yu-Zhang (2007). "Identification of proteins involved in aggregation of human dermal papilla cells by proteomics." J Dermatol Sci **48**(3): 189-97.

Ryder, M. L. (1977). "Seasonal coat changes in grazing Red deer. (Ceruus elaphus)." J. Zool.Lond **181**: 137-143.

Saitoh, M., M. Uzuka and M. Sakamoto (1970). "Human hair cycle." J Invest Dermatol **54**(1): 65-81.

Sakura, H., C. Ammala, P. A. Smith, F. M. Gribble and F. M. Ashcroft (1995). "Cloning and functional expression of the cDNA encoding a novel ATP-sensitive potassium channel subunit expressed in pancreatic beta-cells, brain, heart and skeletal muscle." FEBS Lett **377**(3): 338-344.

Sanders, D. A., I. Fiddes, D. M. Thompson, M. P. Philpott, G. E. Westgate and T. Kealey (1996). "In the absence of streptomycin, minoxidil potentiates the mitogenic effects of fetal calf serum, insulin-like growth factor 1, and platelet-derived growth factor on NIH 3T3 fibroblasts in a K+ channel-dependent fashion." J Invest Dermatol **107**(2): 229-34.

Sayer, R., D. Robertson, D. J. Balfour, K. C. Breen and C. A. Stewart (2008). "The effect of stress on the expression of the amyloid precursor protein in rat brain." Neurosci Lett **431**(3): 197-200.

Schlake, T. (2007). "Determination of hair structure and shape." Semin Cell Dev Biol.

Schulze, D., M. Rapedius, T. Krauter and T. Baukrowitz (2003). "Long-chain acyl-CoA esters and phosphatidylinositol phosphates modulate ATP inhibition of KATP channels by the same mechanism." J Physiol **552**(Pt 2): 357-67.

Schwanstecher, M., C. Sieverding, H. Dorschner, I. Gross, L. Aguilar-Bryan, C. Schwanstecher and J. Bryan (1998). "Potassium channel openers require ATP to bind to and act through sulfonylurea receptors." Embo J **17**(19): 5529-35.

Seino, S. (1999). "ATP-sensitive potassium channels: a model of heteromultimeric potassium channel/receptor assemblies." Annu Rev Physiol **61**: 337-62.

Seino, S. and T. Miki (2003). "Physiological and pathophysiological roles of ATP-sensitive K+ channels." Prog Biophys Mol Biol **81**(2): 133-76.

Shapiro, J. and V. H. Price (1998). "Hair regrowth. Therapeutic agents." Dermatol Clin **16**(2): 341-56.

Sharma, V. K., G. Dawn and B. Kumar (1996). "Profile of alopecia areata in Northern India." Int J Dermatol **35**(1): 22-7.

Shevchenko, A., M. Wilm, O. Vorm and M. Mann (1996). "Mass spectrometric sequencing of proteins silver-stained polyacrylamide gels." Anal Chem **68**(5): 850-8.

Shorter, K., N. P. Farjo, S. M. Picksley and V. A. Randall (2008). "Human hair follicles contain two forms of ATP-sensitive potassium channels, only one of which is sensitive to minoxidil." Faseb J **22**(6): 1725-36.

Sica, D. A. (2004). "Minoxidil: an underused vasodilator for resistant or severe hypertension." J Clin Hypertens (Greenwich) **6**(5): 283-7.

Sinclair, R. D., C. C. Banfield and R. P. R. Dawber (1999). Androgenetic alopecia. Handbook of diseases of the hair and scalp, Blackwell Science Ltd**:** 49-63.

Slebos, D. J., S. W. Ryter and A. M. Choi (2003). "Heme oxygenase-1 and carbon monoxide in pulmonary medicine." Respir Res **4**: 7.

Soba, P., S. Eggert, K. Wagner, H. Zentgraf, K. Siehl, S. Kreger, A. Lower, A. Langer, G. Merdes, R. Paro, C. L. Masters, U. Muller, S. Kins and K. Beyreuther (2005). "Homo- and heterodimerization of APP family members promotes intercellular adhesion." Embo J **24**(20): 3624-34.

Solem, A., N. Zingler and A. M. Pyle (2006). "A DEAD protein that activates intron self-splicing without unwinding RNA." <u>Mol Cell</u> **24**(4): 611-7.

Spielman, A. I., X. N. Zeng, J. J. Leyden and G. Preti (1995). "Proteinaceous precursors of human axillary odor: isolation of two novel odor-binding proteins." <u>Experientia</u> **51**(1): 40-7.

Spruce, A. E., N. B. Standen and P. R. Stanfield (1985). "Voltage-dependent ATP-sensitive potassium channels of skeletal muscle membrane." <u>Nature</u> **316**: 736-738.

Standen, N. B., J. Quayle, N. Davies, J. Brayden, Y. Huang and T. Nelson (1989). "Hyperpolarizing vasodilators activate ATP-sensitive K^+ channels in arterial smooth muscle." <u>Science</u> **245**: 177-180.

Stanley, C. A. (2002). "Advances in diagnosis and treatment of hyperinsulinism in infants and children." <u>J Clin Endocrinol Metab</u> **87**(11): 4857-9.

Stenn, K. (2005). "Exogen is an active, separately controlled phase of the hair growth cycle." <u>J Am Acad Dermatol</u> **52**(2): 374-5.

Stenn, K. S., S. Parimoo and S. Prouty (1998). Growth of the hair follicle: a cycling and regenerating biological system. <u>Molecular basis of epithelial appendage morphogenesis</u>. C. M. Chuong, Landes, Austin**:** 111-130.

Stenn, K. S. and R. Paus (2001). "Controls of hair follicle cycling." <u>Physiol Rev</u> **81**(1): 449-494.

Sugahara, H., Y. Kanakura, T. Furitsu, K. Ishihara, K. Oritani, H. Ikeda, H. Kitayama, J. Ishikawa, K. Hashimoto, Y. Kanayama and et al. (1994). "Induction of programmed cell death in human hematopoietic cell lines by fibronectin via its interaction with very late antigen 5." <u>J Exp Med</u> **179**(6): 1757-66.

Suzuki, K. and T. Kono (1980). "Evidence that insulin causes translocation of glucose transport activity to the plasma membrane from an intracellular storage site." <u>Proc Natl Acad Sci U S A</u> **77**(5): 2542-5.

Tammi, R. and H. Maibach (1987). "Skin organ culture: why?" <u>Int J Dermatol</u> **26**(3): 150-60.

Thevenod, F., K. V. Chathadi, B. Jiang and U. Hopfer (1992). "ATP-sensitive K+ conductance in pancreatic zymogen granules: block by glyburide and activation by diazoxide." <u>J Membr Biol</u> **129**(3): 253-66.

Thomas, D. G., B. R. Brinklow, A. S. I. Loudon and V. A. Randall (1994). "Seasonal effects of prolactin and triidothyronine on hair follicle growth in red deer (Cervus elaphus) In: Milne JA (ed). Recent Developments in Deer Biology Aberdeen: Macaulay Land Use Research Institute."

Thornton, M. J., N. A. Hibberts, T. Street, B. R. Brinklow, A. S. Loudon and V. A. Randall (2001). "Androgen receptors are only present in mesenchyme-derived dermal papilla cells of red deer (Cervus elaphus) neck follicles when raised androgens induce a mane in the breeding season." J Endocrinol **168**(3): 401-8.

Thornton, M. J., S. Kato, N. A. Hibberts, B. R. Brinklow, A. S. Loudon and V. A. Randall (1996). "Ability to culture dermal papilla cells from red deer (Cervus elaphus) hair follicles with differing hormonal responses in vivo offers a new model for studying the control of hair follicle biology." J Exp Zool **275**(6): 452-8.

Thornton, M. J., D. G. Thomas, B. R. Brinklow, A. S. Loudon and V. A. Randall (1994). "Breeding season mane hair follicles from red deer (Cervus elaphus) stags are stimulated by testosterone in whole organ culture. In Milne JA (eds). Recent Developments in Deer Biology. Aberdeen: Macaulay Land Use Research Institute." p225–226.

Trotter, M. (1924). "The life cycles of hair in selected regions of the body." Am J Phys Anthrop **7**: 427-437.

Trube, G., P. Rorsman and T. Ohno-Shosaku (1986). "Opposite effects of tolbutamide and diazoxide on the ATP-dependent K+ channel in mouse pancreatic beta-cells." Pflugers Arch **407**(5): 493-499.

Van Scott, E. J. and T. M. Ekel (1958). "Geometric relationships between the matrix of the hair bulb and its dermal papilla in normal and alopecic scalp." J Invest Dermatol **31**(5): 281-7.

Venkatesh, N., S. T. Lamp and J. N. Weiss (1991). "Sulfonylureas, ATP-sensitive K+ channels, and cellular K+ loss during hypoxia, ischemia, and metabolic inhibition in mammalian ventricle." Circ Res **69**(3): 623-37.

Venter, J. C., M. D. Adams, E. W. Myers, P. W. Li, R. J. Mural, G. G. Sutton, H. O. Smith, M. Yandell, C. A. Evans, R. A. Holt, J. D. Gocayne, P. Amanatides, R. M. Ballew, D. H. Huson, J. R. Wortman, Q. Zhang, C. D. Kodira, X. H. Zheng, L. Chen, M. Skupski, G. Subramanian, P. D. Thomas, J. Zhang, G. L. Gabor Miklos, C. Nelson, S. Broder, A. G. Clark, J. Nadeau, V. A. McKusick, N. Zinder, A. J. Levine, R. J. Roberts, M. Simon, C. Slayman, M. Hunkapiller, R. Bolanos, A. Delcher, I. Dew, D. Fasulo, M. Flanigan, L. Florea, A. Halpern, S. Hannenhalli, S. Kravitz, S. Levy, C. Mobarry, K. Reinert, K. Remington, J. Abu-Threideh, E. Beasley, K. Biddick, V. Bonazzi, R. Brandon, M. Cargill, I. Chandramouliswaran, R. Charlab, K. Chaturvedi, Z. Deng, V. Di Francesco, P. Dunn, K. Eilbeck, C. Evangelista, A. E. Gabrielian, W. Gan, W. Ge, F. Gong, Z. Gu, P. Guan, T. J. Heiman, M. E. Higgins, R. R. Ji, Z. Ke, K. A. Ketchum, Z. Lai, Y. Lei, Z. Li, J. Li, Y. Liang, X. Lin, F. Lu, G. V. Merkulov, N. Milshina, H. M. Moore, A. K. Naik, V. A. Narayan, B. Neelam, D. Nusskern, D. B. Rusch, S. Salzberg, W. Shao, B. Shue, J. Sun, Z. Wang, A. Wang, X. Wang, J. Wang, M. Wei, R. Wides, C. Xiao, C. Yan, A. Yao, J. Ye, M. Zhan, W. Zhang, H. Zhang, Q. Zhao, L. Zheng, F. Zhong, W. Zhong, S. Zhu, S. Zhao, D. Gilbert, S. Baumhueter, G. Spier, C. Carter, A. Cravchik, T. Woodage, F. Ali, H. An, A. Awe, D. Baldwin, H. Baden, M. Barnstead, I. Barrow, K. Beeson, D. Busam, A. Carver, A.

Center, M. L. Cheng, L. Curry, S. Danaher, L. Davenport, R. Desilets, S. Dietz, K. Dodson, L. Doup, S. Ferriera, N. Garg, A. Glueck smann, B. Hart, J. Haynes, C. Haynes, C. Heiner, S. Hladun, D. Hostin, J. Houck, T. Howland, C. Ibegwam, J. Johnson, F. Kalush, L. Kline, S. Koduru, A. Love, F. Mann, D. May, S. McCawley, T. McIntosh, I. McMullen, M. Moy, L. Moy, B. Murphy, K. Nelson, C. Pfannkoch, E. Pratts, V. Puri, H. Qureshi, M. Reardon, R. Rodriguez, Y. H. Rogers, D. Romblad, B. Ruhfel, R. Scott, C. Sitter, M. Smallwood, E. Stewart, R. Strong, E. Suh, R. Thomas, N. N. Tint, S. Tse, C. Vech, G. Wang, J. Wetter, S. Williams, M. Williams, S. Windsor, E. Winn-Deen, K. Wolfe, J. Zaveri, K. Zaveri, J. F. Abril, R. Guigo, M. J. Campbell, K. V. Sjolander, B. Karlak, A. Kejariwal, H. Mi, B. Lazareva, T. Hatton, A. Narechania, K. Diemer, A. Muruganujan, N. Guo, S. Sato, V. Bafna, S. Istrail, R. Lippert, R. Schwartz, B. Walenz, S. Yooseph, D. Allen, A. Basu, J. Baxendale, L. Blick, M. Caminha, J. Carnes-Stine, P. Caulk, Y. H. Chiang, M. Coyne, C. Dahlke, A. Mays, M. Dombroski, M. Donnelly, D. Ely, S. Esparham, C. Fosler, H. Gire, S. Glanowski, K. Glasser, A. Glodek, M. Gorokhov, K. Graham, B. Gropman, M. Harris, J. Heil, S. Henderson, J. Hoover, D. Jennings, C. Jordan, J. Jordan, J. Kasha, L. Kagan, C. Kraft, A. Levitsky, M. Lewis, X. Liu, J. Lopez, D. Ma, W. Majoros, J. McDaniel, S. Murphy, M. Newman, T. Nguyen, N. Nguyen, M. Nodell, S. Pan, J. Peck, M. Peterson, W. Rowe, R. Sanders, J. Scott, M. Simpson, T. Smith, A. Sprague, T. Stockwell, R. Turner, E. Venter, M. Wang, M. Wen, D. Wu, M. Wu, A. Xia, A. Zandieh and X. Zhu (2001). "The sequence of the human genome." Science 291(5507): 1304-51.

Waldon, D. J., T. T. Kawabe, C. A. Baker, G. A. Johnson and A. E. Buhl (1993). "Enhanced in vitro hair growth at the air-liquid interface: minoxidil preserves the root sheath in cultured whisker follicles." In Vitro Cell Dev Biol Anim 29A(7): 555-61.

Wang, J., Z. Lu and J. L. Au (2006). "Protection against chemotherapy-induced alopecia." Pharm Res 23(11): 2505-14.

Wang, W. and G. Giebisch (1991). "Dual modulation of renal ATP-sensitive K+ channel by protein kinase A and C." Proc Natl Acad Sci USA 88: 9722-9725.

Waters, J. M., G. D. Richardson and C. A. Jahoda (2007). "Hair follicle stem cells." Semin Cell Dev Biol 18(2): 245-54.

Welch, M. D., A. H. DePace, S. Verma, A. Iwamatsu and T. J. Mitchison (1997). "The human Arp2/3 complex is composed of evolutionarily conserved subunits and is localized to cellular regions of dynamic actin filament assembly." J Cell Biol 138(2): 375-84.

Wester, S. T., W. W. Lee and W. Shi (2010). "Eyelash Growth from Application of Bimatoprost in Gel Suspension to the Base of the Eyelashes." Ophthalmology.
Westgate, G. E., W. T. Gibson, T. Kealey and M. P. Philpott (1993). "Prolonged maintenance of human hair follicles in vitro in a serum-free medium." Br J Dermatol 129(4): 372-9.

Weston, A. H. and G. Edwards (1992). "Recent progress in potassium channel opener pharmacology." Biochem Pharmacol 43(1): 47-54.

Whitehead, G. K. (1993). <u>The whitehead encyclopedia of deer</u> Swan Hill Press.

Wilkins, M. R., J. C. Sanchez, A. A. Gooley, R. D. Appel, I. Humphery-Smith, D. F. Hochstrasser and K. L. Williams (1996). "Progress with proteome projects: why all proteins expressed by a genome should be identified and how to do it." <u>Biotechnol Genet Eng Rev</u> **13**: 19-50.

Wu-Kuo, T. and C. M. Chuong (2000). Developmental biology of hair follicles and other skin appendages. <u>Hair and its disorders: biology, pathology and management</u>. F. M. Camacho, Randall, V.A., and Price, V.H., Martin Dunitz Ltd**:** 17-37.

Yamada, M., S. Isomoto, S. Matsumoto, C. Kondo, T. Shindo, Y. Horio and Y. Kurachi (1997). "Sulphonylurea receptor 2B and Kir6.1 form a sulphonylurea-sensitive but ATP-insensitive K^+ channel." <u>J Physiol</u> **499**(Pt 3): 715-720.

Young, J. Z. (1957). <u>The life of mammals</u>. Oxford, Clarendon Press.

Yunoki, T., N. Teramoto and Y. Ito (2003). "Functional involvement of sulphonylurea receptor (SUR) type 1 and 2B in the activity of pig urethral ATP-sensitive K+ channels." <u>Br J Pharmacol</u> **139**(3): 652-60.

Zappacosta, A. R. (1980). "Reversal of baldness in patient receiving minoxidil for hypertension." <u>N Engl J Med</u> **303**(25): 1480-1.

Zhang, H. L. and T. B. Bolton (1996). "Two types of ATP-sensitive potassium channels in rat portal vein smooth muscle cells." <u>Br J Pharmacol</u> **118**(1): 105-14.

Zheng, H. and E. H. Koo (2006). "The amyloid precursor protein: beyond amyloid." <u>Mol Neurodegener</u> **1**: 5.

Zins, G. R. (1988). "The history of the development of minoxidil." <u>Clin Dermatol</u> **6**(4): 132-47.

Zunkler, B. J., S. Lins, T. Ohno-Shosaku, G. Trube and U. Panten (1988). "Cytosolic ADP enhances the sensitivity to tolbutamide of ATP-dependent K+ channels from pancreatic B-cells." <u>FEBS Lett</u> **239**(2): 241-4.

APPENDICES

Appendix 1. Reagents for Bradford Protein Assay

The following were required for the quantification of protein in cell extracts:

(1) Bovine Serum Albumin (BSA) stock solution

- Sample Buffer 10 ml

  Glycerol (BDH Lab Supplies) 2.5 ml; ethylenedaiminetetraacetic acid (EDTA) (Sigma) 0.185 g; sodium dodecyl sulphate (SDS) (Sigma) 1.5 g; Tris (Sigma) 0.19 g; 25 ml distilled water)

- Bovine serum albumin (Sigma) 0.1 g (final concentration of 10 mg/ml)

(2) Protein Standards (Bovine Serum Albumin)

One ml of each standard solution was made over range of 0-2000μg/ml

- Blank: 1000 μl sample buffer
- 100 μg/ml: 990 μl sample buffer + 10 μl BSA stock
- 200 μg/ml: 980 μl sample buffer + 20 μl BSA stock
- 400 μg/ml: 960 μl sample buffer + 40 μl BSA stock
- 600 μg/ml: 940 μl sample buffer + 60 μl BSA stock
- 800 μg/ml: 920 μl sample buffer + 80 μl BSA stock
- 1000 μg/ml: 900 μl sample buffer + 100 μl BSA stock
- 2000 μg/ml: 800 μl sample buffer + 200 μl BSA stock

(3) Reagent A'

- Reagent A (D_c protein assay, Bio-Rad Labs) 2 ml
- Reagent S (D_c protein assay, Bio-Rad Labs) 40 μl

(4) Reagent B'

- Reagent B (D_c protein assay, Bio-Rad Labs, UK) 200 μl

Appendix 2. Reagents for SDS gel separation of proteins

The following are required for SDS Gel preparation and protein separation to be carried out:

(1) Lower Separating Gel

- High performance liquid chromatography grade water (HPLC) (Fisher Scientific) 3.3ml
- 30% Acrylamide (Sigma) 4ml
- 1.5 M Tris-Cl pH 8.8 (Sigma) 2.5 ml
- 10% Sodium dodecyl sulphate (SDS) (Sigma) 100 µl
- 10% Ammonium persulphate (APS) (100mg/ml) (Sigma) 100 µl
- Tetramethylethylenediamine (TEMED) (Sigma)4µl

(2) Upper Stacking Gel

- High performance liquid chromatography grade water (HPLC) (fisher scientific) 3.4ml
- 30% Acrylamide (Sigma)0.83ml
- 0.5 M Tris-Cl pH 6.8 (Sigma)0.63ml
- 10% Sodium dodecyl sulphate (SDS) (Sigma)50µl
- 10% Ammonium persulphate (APS) (100mg/ml) (Sigma)50µl
- Tetramethylethylenediamine (TEMED) (Sigma)5µl

(3) Sample loading dye composition: For 10ml

- Tris-base (Sigma)- 1.25 ml of 0.5M Tris HCl pH 6.8
- Glycerol (Sigma)- 2.5 ml
- Beta- mercaptoethanol (Sigma) 50 µl
- Sodium dodecyl sulphate (SDS) (Sigma) 2ml of 10% SDS
- Bromo-Phenol-Blue (BPB) (Sigma) Traces

(4) Electrophoresis Buffer

- Distilled water 450ml
- 10x electrode buffer 50ml

(5) 10x Electrode buffer pH 8.3

- Tris (Sigma) 15.15g

- Glycine (Sigma) 72g

- Sodium dodecyl sulphate (SDS) (Sigma)5g

- Distilled water 500ml

(6) Marker

(Invitrogen), Novex® Sharp Pre-stained Protein Standard

catalogue number : LC5800

The protein standard consists of 12 pre-stained protein bands that cover the range of 3.5-260 kDa when used in electrophoresis. The bands are spaced at convenient kDa weights: 260, 160, 110, 80, 60, 50, 40, 30, 20, 15, 10, and 3.5.